CRANFIELD UNIVERSITY

SIQI WANG

INTELLIGENT-BASED HYBRID-ELECTRIC PROPULSION SYSTEM FOR AERO VEHICLE

SCHOOL OF AEROSPACE, TRANSPORT AND MANUFACTURING
Aerospace

PhD
Academic Year: 2016-2020

Supervisor: Antonios Tsourdos, John Economou
March 2020

CRANFIELD UNIVERSITY

SCHOOL OF AEROSPACE, TRANSPORT AND MANUFACTURING
Aerospace

PhD

Academic Year 2016 - 2020

SIQI WANG

INTELLIGENT-BASED HYBRID-ELECTRIC PROPULSION SYSTEM FOR AERO VEHICLE

Supervisor: Antonios Tsourdos, John Economou
March 2020

This thesis is submitted in partial fulfilment of the requirements for the degree of PhD

ABSTRACT

To address the sustainability challenges for air transport, electrified aviation delivers promising benefits to the whole air transportation system. Focusing on reducing environmental impact and raising competitiveness, this thesis presents a research regarding the Distributed Series Hybrid-electric Propulsion System for aero vehicles, which involves study fields of system configuration design, component sizing and energy management strategies.

Based on the state-of-art of hybrid-electric aircraft and hybrid-electric propulsion systems, the study firstly improved the conventional series hybrid configuration by adopting distributed propulsion technology and more electric aircraft concept. These improvements can compensate for the drawbacks caused by the conventional series hybrid layout, so that the new designed propulsion system has the potential to reduce system weight and increase fuel economy.

After that, a comprehensive sizing method was particularly designed for the proposed system. The engine, as the primary power source, was firstly selected via the battery parametrisation criteria. Then, other components were selected according to a proposed sizing flowchart by using the genetic algorithm. System performance can also be demonstrated during the sizing process.

Finally, three different control methods had been applied to manage energy flows. The first supervisory controller is a deterministic rule-based controller, which was designed based on human experiences and can reduce 12% fuel consumption. The second is a battery-friendly fuzzy controller. It was particularly designed to improve the battery operating environment and can simultaneously achieve a 5% improvement on fuel economy compared to the rule-based. The third controller applied model predictive control algorithm, which can further improve the fuel efficiency by 4% and reveal the relationship between the fuel consumption and emissions.

Keywords: Hybrid-electric Aircraft, Hybrid-electric Propulsion System, Series Hybrid System, Sizing, Fuzzy Controller, MPC Controller, Energy Management

ACKNOWLEDGEMENTS

Foremost, I would like to express my sincere gratitude to my supervisors, Dr Economou and Prof Tsourdos, for their continuous support of my PhD study and research work. Their patience, enthusiasm and immense knowledge have provided me with great help throughout my research.

In addition, my deep thanks also go to Dr Savvaris, Prof Shin, and all my colleagues, for their assistance and concerns in my PhD research life. Especially grateful to Dr Xie, who is like an elderly sister guiding me in both my studies and life. Thanks to all my beloved friends, and thank you for their care and understanding. Because of you, my life became colourful. Thanks to all the staff in the Centre for Autonomous and Cyber-Physical Systems, Cranfield Student Association and Cranfield University.

Finally but not least, I would like to thank my father Jianguo Wang, and my mother Chengli Liu, for their support and encouragement. Your unconditional love will always be my energy.

TABLE OF CONTENTS

LIST OF FIGURES

LIST OF TABLES

LIST OF ABBREVIATIONS

AFIT	Air Force Institute of Technology
APF	Adaptive Power Follower
BLDC	Brushless Direct Current Motor
BSFC	Brake Specific Fuel Consumption
CI	Compression Ignition
CMF	Common-Core Multi-Fans
CO_2	Carbon Dioxide
DC	Direct Current
DIRECT	Divide Rectangle
DoD	Depth of Discharge
DP	Dynamic Programming
DRB	Deterministic Rule-Based
DSHEPS	Distributed Series Hybrid-Electric Propulsion System
ECMS	Equivalent Cost Minimization Strategy
EM	Electric Motor
FCR	Fuel Consumption Rate
FL	Fuzzy Logic
GA	Genetic Algorithm
HEPS	Hybrid-Electric Propulsion System
ICE	Internal Combustion Engine
Li	Lithium
Li-ion	Lithium-Ion
Li-Po	Lithium-Polymer
LP	Linear Programming
MEA	More Electric Aircraft
MF	Membership Function
MOO	Multi-Objective Optimization
MPC	Model Predictive Control
MSFL	Mamdani & Sugeno Fuzzy Logic
MVM	Mean Value Model
Ni-Cd	Nickel-Cadmium
Ni-MH	Nickel-Metal Hydride

NO_X	Nitrogen Oxide
NSGA-II	Non-Dominated Sorting Genetic Algorithm-II
PF	Power Follower
PMP	Pontryagin's Maximum Principle
PMSG	Permanent Magnet Synchronous Generator
PMSM	Permanent Magnet Synchronous Motor
RB	Rule-Based
RC	Resistor Capacitor
RPM	Revolutions Per Minute
QP	Quadratic Programming
SDP	Stochastic Dynamic Programming
SI	Spark-Ignition
SOC	State-Of-Charge
TeDP	Turbo-electric Distributed Propulsion
UAV	Unmanned Aerial Vehicle
VTOL	Vertical Take-Off and Landing
0-D	0-Degree

LIST OF NOMENCLATURES

β_k	Interaction coefficient between membership functions
δ_e	Engine throttle command
$\delta_{e,prc}$	Time for one engine process
η	Efficiency
η_{comb}	Combustion efficiency
η_g	Generator efficiency
η_{m_j}	The j_{th} motor efficiency
η_{th}	Thermal efficiency
η_W	Indicated efficiency
θ	Angle between the stator phase A and rotor
λ_{af}	Motor magnet mutual flux linkage
ρ	Air density
ρ_{gas}	Gas constant
σ	Width of Gaussian set
τ_e	Time constant
ω_e	Engine angular speed
ω_{e_max}	Engine maximum angular speed
ω_{e_min}	Engine minimum angular speed
ω_g	Generator angular speed
ω_m	Motor angular speed
ω_r	Motor angular speed of the stator electromagnetic field
$\mathcal{w}_f$	Weighting parameter for fuel consumption
$\mathcal{w}_i$	Weighting parameter for current
$\mathcal{w}_{NO_x}$	Weighting parameter for emissions
$\mathcal{w}_{SOC}$	Weighting parameter for SOC
$\boldsymbol{A}$	Coefficient matrix for states
A_W	Aircraft wing area
A_b	Battery exponential voltage coefficient
A_{aero}	Aircraft system property factor
Ah	Ah-throughput
a	Width of the bell-shaped fuzzy set

a_{nj}	Coefficient for the n-j th variable
$\boldsymbol{B}$	Coefficient matrix for inputs
B_b	Battery exponential capacity coefficient
B_d	Battery pre-exponential factor for battery degradation
b	Positive integer
b_n	Constant coefficient of output membership functions
C_b	Battery operating environment indicator
C_D	Drag coefficient
C_e	Centre position of engine's high-efficient operating area
C_g	Centre position of generator's high-efficient operating area
C_{full}	Full battery capacity
C_L	Lift coefficient
c	Locating centre of fuzzy sets
D	Distance
D_a	Aerodynamic drag
D_{avg}	Average drag
DoD	Depth of discharge
$d_{takeoff}$	Take-off distance
E	Battery open-circuit voltage of the battery
E_a	Activation energy
E_b	Battery energy
$E_{etaxiing}$	Required energy for electric taxiing
E_m	Motor energy
E_{safety}	Safety threshold of energy
E_0	Battery constant voltage
EF	Engine factor
e_{air}	Engine altitude-related coefficient
F_{total}	Sum of scaled fuel consumption rate
FCR	Scaled fuel consumption rate
f_f	Function of fuel consumption rate
f_{Line}	Function of the line
f_{NO_x}	Function of NOx rate

g	Gravity factor
HF	Hybridization factor
HF_{opt}	Optimal hybridization factor
$HF_{realtime}$	Realtime hybridization factor
i	Current
i^*	Filtered current
J_e	Engine inertia
J_m	Motor inertia
J_p	Performance indicator
j	Number of input membership functions
K	Battery polarization coefficient
L	Stator inductances
m	Aircraft weight
$\dot{m_{NO_x}}$	Engine NOx rate
$\dot{m_f}$	Engine fuel consumption rate
N	Prediction horizon
N_{cycle}	Number of cycles
N_m	Number of motors
N_{SOC}	SOC performance indication
n	Number of rules
O_e	Overlap rate of high-efficient areas
P	Power
P_b	Battery output power
P_{brake}	Engine braking power
P_{climb}	Power requirement for climbing
P_{comb}	Combustion power
P_{cruise}	Power requirement for cruising
P_e	Engine power
P_{e_max}	Engine maximum power
P_{e_min}	Engine minimum power
P_{e_opt}	Engine optimal power output
P_g	Generator power

P_f	Future power demand
P_{fri}	Engine friction power
P_{fuel}	Fuel power
$P_{landing}$	Power requirement for landing
P_m	Motor power
P_{m_max}	Motor maximum power
P_{m_min}	Motor minimum power
P_{m_j}	The jth motor power
P_{other}	Power requirement for other electric loads
P_{pole}	Number of pole pairs
P_{pro}	Power requirement for propulsion loads
P_{req}	Power requirement
P_{req_av}	Average value of power requirement
P_{req_max}	Maximum power requirement
P_{sum}	Sum of power
$P_{takeoff}$	Power requirement for take-off
Q	Battery capacity
Q_{loss}	Battery capacity loss
Q_{max}	Maximum battery capacity
$Q(t)$	Instantaneous battery capacity
R	Resistance
R_b	Battery internal resistance
R_e	Radius of engine's high-efficient operating area
R_g	Radius of generator's high-efficient operating area
R_u	Weighting vector of inputs
Roc	Rate of climb
RPM	Engine revolutions per minute
S	The scaled factor of the parameter
SOC	Battery SOC
SOC_{high}	High SOC threshold
SOC_{low}	Low SOC threshold
T	Absolute temperature

T_{avg}	Average thrust
T_e	Induced engine torque
$T_{e,idle}$	Engine idle torque
$T_{e,load}$	Engine torque of the load
$T_{e,ref}$	Requested engine torque
T_g	Generator torque
T_m	Motor torque
$T_{m,load}$	Requested motor torque
$T_{m,loss}$	Motor torque loss
t	Time
u	System input
$\underline{u}, \overline{u}$	Input upper and lower bound
V	Voltage
V_b	Battery voltage
V_{lhv}	Lower heating value
v	Velocity
$v_{liftoff}$	Velocity for lift-off
W_{sum}	Sum of weight
x	System state
$\underline{x}, \overline{x}$	State upper and lower bound
y	System output
$\underline{y}, \overline{y}$	Output upper and lower bound
y_n	The n_{th} Rule
z	Power law factor
$_{avg}$	Average value
$_b$	Battery
$_d$	d axis
$_e$	Engine
$_g$	Generator
$_m$	Motor
$_{opt}$	Optimal value
$_q$	q axis

1 INTRODUCTION

In recent years, public concern about the environment has risen markedly in response to clear evidence about the impact of humankind's activities. The UK Committee on Climate Change has recommended that the UK urgently embrace a low carbon future, leading the government to commit to net-zero greenhouse gas emissions by 2050 [1]. The aviation industry is responsible for around 12 percent of all transportation-caused carbon dioxide (CO_2) emissions, plus nitrous oxides (NO_X) emissions and condensation trails further exacerbate the impact of aviation on global warming [2]. At the 2019 Paris Air Show, seven of the world's largest aerospace companies recommitted to neutral carbon growth in aviation from 2020 [3, 4], along with the 2050 ACARE environmental goals [5, 6, 7]. Concretely, AIRBUS is working on some strategic programmes, focusing on the next-generation propulsion systems, complex aircraft systems and advanced aircraft structures. NASA is persistence making an effort on reducing aircraft fuel burn and emissions in the last decade abiding by their N+3 goals [8, 9].

Reducing emissions is a significant challenge for traditional aviation, especially due to that the root cause of the emission problem, the combustion engine, is hard to be replaced or achieve much better energy efficiency with present technologies. The next generation of aircraft, which is sustainable aviation, is awaited to reduce environmental impact with raising competitiveness. This is a pivotal moment for the aerospace industry, and a new era is underway enabled by low-emission propulsion.

1.1 Hybrid Aircraft

To realize sustainable aviation, different intelligent technologies spurred in the last decade for reducing aircraft emissions and improving fuel efficiency. Since aircraft's emissions mainly come from fuel burn, or more precisely, the amount of emissions is proportional to the fuel consumption, electric propulsion might be the most effective technique to address the aviation's sustainability [10]. Therefore, with different electrification degrees, hybrid-electric aircraft and pure-electric aircraft are proposed.

Hybrid-electric aircraft refers to the aircraft applying a Hybrid-Electric Propulsion System (HEPS) as the main propulsion system. It possesses characteristics of both pure-electric aircraft and combustion-engine aircraft. As a result, it is more powerful than pure-electric aircraft, and more efficient than traditional aircraft. Therefore, although hybrid-electric aircraft cannot realize the net-zero emission target, it is still a prospective technology which provides a possibility to reduce aircraft fuel consumption and improve emission simultaneously.

The concept of hybrid-electric aircraft was initially proposed as a compromise option to pure-electric aircraft. For the propulsion point of view, the pure-electric power system has many advantages, for example, it is very high-efficient and does not have emission or noise issues caused by the chemical reaction of fuel burning. However, the energy density of electrical storage devices, especially the battery pack, is very low and hard to be promoted in the foreseeable future [11]. The long refuelling-time also restricts electric power systems' performance for the high-power workload. Thus, the hybrid-electric power system applies a combustion engine as an auxiliary power source to compensate for the power short. Unlike pure-electric aircraft being affected by the limited storage capacity of the battery pack, hybrid-electric aircraft is longer-endurance and can handle high-power workload. In other words, this evolutionary combination would result in a potential win-win situation.

1.1.1 Powertrain Configuration

Hybrid-electric aircraft comes in many types. Based on system layouts, they can be categorized into series, parallel and series-parallel.

a) Series Configuration

Series configuration refers to a structure whose all components are arranged in series. As shown as Figure 1, a typical series hybrid system has three propulsion devices (an engine, a generator and an electric motor), one energy storage unit (a battery pack), a converter and few mechanical linkages. In a series hybrid, the engine firstly produces mechanical energy by burning the fuel, then the generator converts that into electricity. Depended on the current mission demand and battery State-Of-Charge (SOC), the generated electrical energy can either be transferred to the electric motor, or be stored in the battery pack. Finally, the electric motor converts electricity into mechanical energy to drive the propeller. Please note only the electric motor can provide energy to the propeller in the series hybrid. The motor is mechanically connected to the propeller, so that the motor should operate according to propulsion demands.

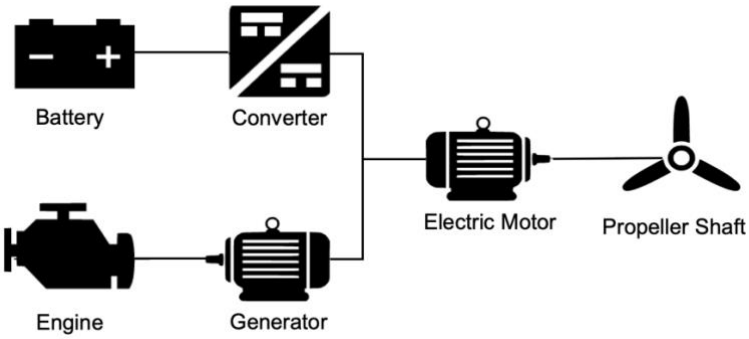

Figure 1 Series configuration.

There is one special characteristic of the series configuration, i.e. the engine is completely decoupled from the propeller. Namely, the engine does not need to operate along with mission demands, only the motor needs to follow the given operating instruction. Therefore, to some extent, the engine, generator and battery pack form an on-board power plant for the motor and propeller. As a result,

the major difficulty of the series hybrid-electric power system is the cooperation between the engine (and generator) and the battery pack.

There are many energy transformations happened inside the series hybrid-electric propulsion system, e.g. from thermal energy to mechanical energy etc. All energy conversions are illustrated in Figure 2. According to this figure, there are two repeated energy transformations. The first one is the charging and discharging process of the battery pack, which repeats the conversion between chemical energy and electrical energy many times. The second excess part refers to the transformation caused by the generator and motor. The generator converts the mechanical energy to electricity, and the motor performs reverse process. Apparently, the first repeated conversion cannot be avoided if the system selected a battery pack as the storage plant, but the second can be removed by a properly adjusted configuration.

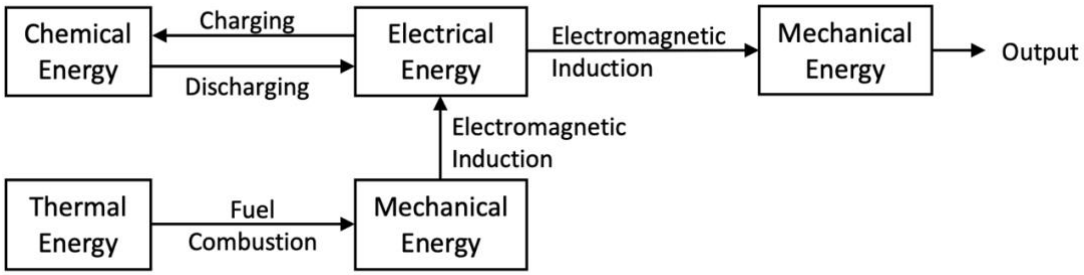

Figure 2 Energy transformations of the series hybrid-electric power system.

Some series hybrid-electric system performances could be predicted. At first, the fuel efficiency could be significantly increased due to the engine is decoupled to the propeller. Secondly, electricity connections and no need for clutch ease the installation. The series hybrid-electric system has few requirements for space. Furthermore, envisioning the future, if the energy density of any electrical energy storage devices reaches a very high value, the engine and generator can be disassembled and replaced. Therefore, the series hybrid has a great re-configurability.

As for drawbacks, the series hybrid-electric system may not perform as efficient as other hybrids. It applies a generator to generates electricity, and then converts

that back to mechanical energy. In other words, the engine's output, i.e. mechanical energy, has to be converted twice and cannot be transmitted to the propeller directly. Power losses during energy conversions. Therefore, the series hybrid suffers from poor system efficiency.

Overall, characteristics of the series hybrid are:

- Engine is decoupled from the propeller, high fuel efficiency;
- No clutch, no complex transmission, structure simple and easy to install;
- Repeated energy conversions, low system efficiency.

b) Parallel Configuration

Parallel configuration is a structure whose engine output can be directly transferred to the propeller. In parallel configuration, seeing Figure 3, the engine and motor are both connected to the propeller, so that they can transmit energy either simultaneously or individually. Therefore, the parallel configuration overcomes one of drawbacks of the series hybrid, i.e. the energy loss problem is alleviated to some extent.

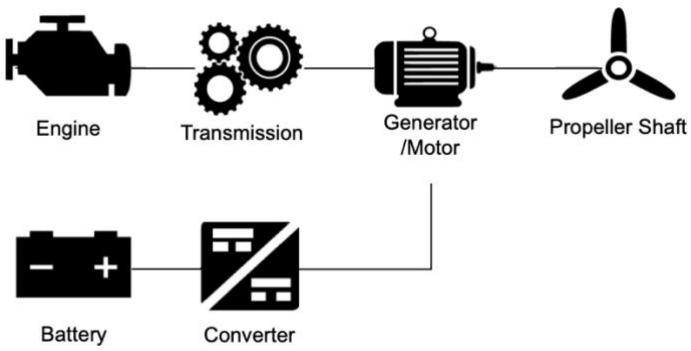

Figure 3 Parallel configuration.

Energy transformations inside the parallel hybrid-electric propulsion system are shown as Figure 4. The parallel configuration not only allows the engine to drive the motor and propeller simultaneously, but also permits the engine and motor to drive the propeller at same time. In a parallel hybrid system, the engine, motor

and batteries composite a power plant only for the propeller, that the generator in the series configuration is replaced by the motor. This replacement is feasible due to the electric motor could be used in reverse as a generator, and moreover, the weight of total system can be reduced by removing the generator. Another benefit of the parallel configuration is that, compared with the series configuration, a smaller electric motor is powerful enough to accomplish a same mission [11]. In parallel hybrids, the engine does not need to be rated to the highest power demand.

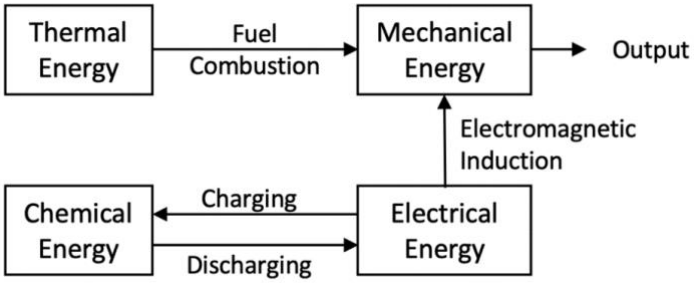

Figure 4 Energy transformations of the parallel hybrid-electric system.

Using less components increases the difficulty of the coordination amongst propulsion devices. The first specific performance is that every parallel hybrid system needs a customized mechanical coupling and transmission system to connect the engine, motor and propeller. The coupling and transmission system are compulsorily required, and always be costly and makes installation difficult. Secondly, due to the requested rotational speed of the engine is not always in its optimal speed range, the engine cannot operate at its most efficient point at most of the mission time. Therefore, the fuel efficiency of the parallel hybrid system might not be as good as that of the series.

Overall, characteristics of the parallel hybrid are:

- Engine is coupled to the propeller, low fuel efficiency;
- Needs mechanical couplings and transmissions, complex structures;
- Less energy loss, high system efficiency.

c) Series-parallel Configuration

The third type, series-parallel hybrid, possesses the most advanced structure by combining series and parallel configurations [12]. Shown as Figure 5, in a series-parallel hybrid system, both the engine and motor can provide energy for propulsion. The engine, generator and motor are connected by mechanical transmissions, e.g. a planetary gear, which may allow the engine and motor to operate in its most efficient region in order to improve the fuel efficiency. In general, the series-parallel hybrid always requires a complicated transmission system to coordinate the rotational speed of each component. It increases the difficulty of the system implementation and makes installation more difficult. Overall, the series-parallel configuration not only needs three propulsion devices (an engine, a generator and a motor) and one battery pack, but also requires complex mechanical transmissions. Therefore, it must be heavier than previous configurations.

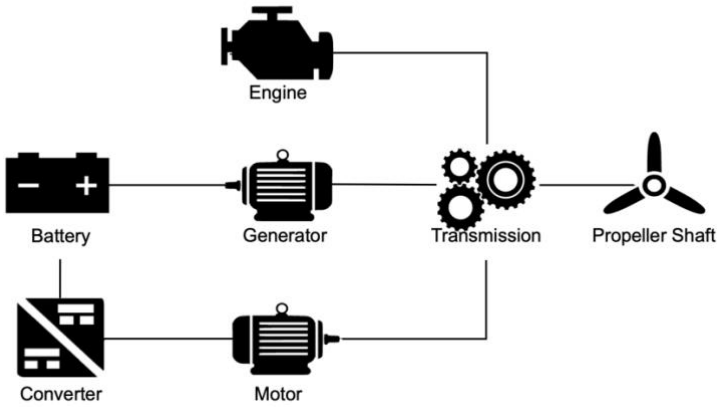

Figure 5 Series-parallel configuration.

Additionally, according to energy transformations shown by Figure 6, the series-parallel hybrid configuration still suffers from energy loss problems. Namely, it can be predicted that the system efficiency might be relatively low. Moreover, because the series-parallel configuration is complex, the system always requires a high-computational controller. Therefore, the series-parallel hybrid is mostly theoretical in literatures.

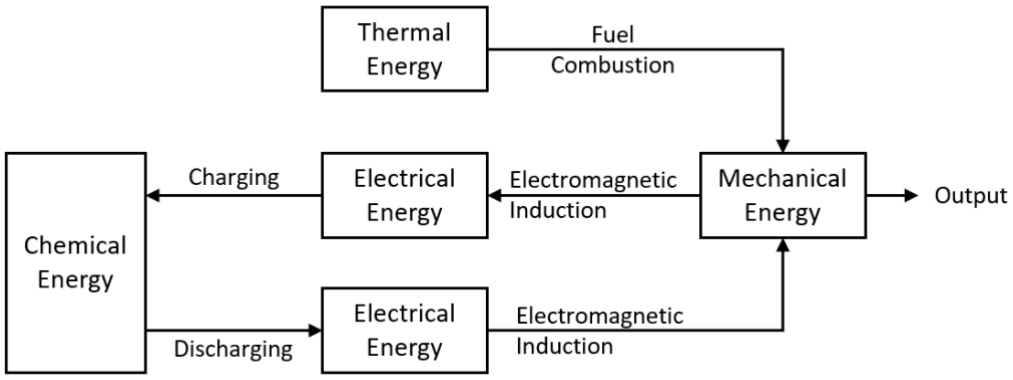

Figure 6 Energy transformations of the series-parallel hybrid-electric system.

Overall, characteristics of the series-parallel hybrid are:

- Engine is de-coupled to the propeller, high fuel efficiency;
- Needs mechanical coupling and transmission, structure complex;
- Repeated energy transformations, low system efficiency;
- Requires a complicate controller.

1.1.2 State-of-Art

Although different configurations lead to different performances, it is for sure that the HEPS provides an opportunity to aircraft to improve fuel efficiency and reduce emissions. As a result, various HEPSs have emerged as a promising research area in aerospace engineering [13].

The research of hybrid-electric aircraft started in the 21st century and grown rapidly in the past two decades. At present, there are some on-going projects regarding hybrid-electric aircraft leaded by NASA, AIRBUS, Boeing and some other institutions, which have obtained some achievements. According to the author's knowledge, both series and parallel configurations have been successfully applied on aircraft. Small-scale aircraft mostly adopts the parallel configuration, while the research in large-scale aircraft tends to focus on the series configuration instead.

Attempts started with small-scale aircraft. Hybrid-electric Unmanned Aerial Vehicles (UAV) emerged in the last decade. The Air Force Institute of Technology

(AFIT) started relative research from 2006, which completed a conceptual design and found that the clutch-start parallel configuration is the most practically realizable structure [14, 15]. The designed parallel hybrid-electric power system was formed by using a 1.3-HP (0.97kW) Honda G35 engine and a 1.6-HP (1.2kW) Fuji motor, and a flight test was performed smoothly [16, 17]. Later on, based on the AFIT's research, Queensland University developed another parallel hybrid-electric propulsion system using a 2kW piston engine and a 0.6kW brushless electric motor. According to the ground test result, it increased 6% fuel efficiency and significantly improved the aircraft performance [18, 19]. Some other relevant studies have been completed as well. In paper [20], Friedrich and Robertson presented a scaling approach for the combustion engine for a 20kg UAV, which used the engine's ideal operating line as the basis to select the engine. Sliwinski et al. [13], developed a retrofit design method for hybrid-electric aircraft by using the predicted flight range and endurance. It resulted in that for small-scale aircraft, promoting the mitigation of NO_X and CO_2 while providing adequate aircraft performance is a trade-off problem.

Some commercial hybrid-electric UAVs have been released by various companies. The first fuel-electric UAV is 'HYBRiX.20', developed from the company Quaternium. It incorporates an advanced technology with a fuel range-extender that can provide more than two-hour operational flight with maximum payload [21]. Another company, Skyfront, developed a series of hybrid-electric drones with their proprietary fuel-injected G2K hybrid gasoline-electric propulsion systems. Their 'Perimeter 8' UAV features an impressive 5.5kg payload capacity with one hour of endurance and a no-payload endurance of over 5 hours [22]. The Harris Aerial company also released a gas-electric hybrid drone, the 'Carrier H4 Hybrid'. It is a heavy-lift hybrid unmanned aircraft which has a maximum payload capacity of 15kg and allows for up to 2.5 hours of flight with 3kg payload [23]. The 'QL1200' drone, produced from Walkera, adopts a gasoline-electric power system to realize a 90-minute flight with a range of 43.2km. By using the designed hybrid-electric power system, the UAV achieved 3 times that of original flight-time and 2 times that of payload [24]. Compared with them, the ALTI company released a world's leading endurance Vertical Take-Off and Landing

(VTOL) unmanned air vehicle ‘ALTI REACH’, whose endurance is up to 20 hours by using a 70cc twin cylinder fuel-injected combustion engine, a 500W on-board generator and four powerful motors [25].

Figure 7 1) the Skyfront Perimeter8 UAV [22], 2) the ALTI REACH UAV [25].

The research of mid-scale demonstrators attracts much attention from 2005s. The ‘DA36 E-Star’ is the first hybrid-electric aircraft realized by a collaboration between Diamond Aircraft, European Aeronautic Defence and Space Company, and Siemens AG [26]. It applied a 70kW Siemens electric motor and a 30kW rotary engine as propulsors for the series HEPS, and its debut flight was successfully launched in June 2011 [27]. This aircraft can be considered as a milestone which proved the feasibility of replacing the traditional combustion power system with the hybrid-electric propulsion system. Its successor version, ‘DA36 E-star2’, used the same series hybrid-electric technology, but it is lighter 100kg, and showed a better performance and driveability. Another project ‘HYPSTAIR’ unveiled a most powerful series hybrid powertrain in 2016. The 200kW propulsor developed in the project can deliver the power equivalent to a typical general aviation piston engine [28].

Aircraft ‘Alatus’ and ‘EcoEagle’ are hybrid-electric aircraft using parallel hybrid configurations. The aircraft ‘Alatus’ is a proof-of-concept parallel hybrid electric conversion of a single-seat, ultralight Alatus-M motor glider developed by the University of Cambridge in 2010 [29]. It applied a 2.8kW internal combustion engine and a 12kW motor for the parallel HEPS. The two-seat aircraft ‘EcoEagle’, designed by Embry-Riddle Aeronautical University, utilized a 74.5kW internal combustion engine and a super-efficient 29.8kW gas motor to power the propeller,

and has been successfully tested in 2011 [30]. This propulsion system was designed based on the previous research accomplished by Flight Design, who developed a parallel HEPS by using a 115-HP (86kW) internal combustion engine and a 40-HP (30kW) electric motor [31]. However, none of them has the capability of on-board battery recharging. The aircraft 'SOUL' is the first ever to be able to recharge batteries during the flight. This plane was retrofitted from a light aircraft by combining an 8kW engine and a 12kW electric motor, and a flight test was commenced in 2014 [20]. Additionally, besides the hybrid-electric technology, other hybrid propulsion technologies are also implemented on midscale aircraft. For example, the fuel cell-electric hybrid aircraft – 'Antares DLR-H2' and 'E-Plane' (using series configurations), and the solar-electric hybrid aircraft 'Solar Impulse' (using series configuration).

As for largescale aircraft, due to the fossil fuel has a high power-density, the hybrid-electric propulsion technology was rarely discussed or considered by airliners at the beginning [20]. However, the achievements on midscale hybrid-electric aircraft admitted the scaling potential of the hybrid-electric propulsion system from the midscale to the largescale sector. In addition, along with the prosperity of hybrid-electric ground vehicles and the urgency of sustainable aviation, the proposal of large hybrid-electric aircraft appeared. The 'NXG-50' hybrid-electric aircraft is one of the first conceptual designs developed by the Georgia Institute of Technology. The design won the 2012-2013 Federal Aviation Administration Design Competition in the electric/hybrid-electric aircraft category, which has a potential with an expected reduction of 15% energy consumption [32]. Delft University of Technology also designed few large-scale hybrid-electric conceptual aircraft [33], and one of designs can achieve a 28% fuel reduction and a 14% reduction in global aircraft weight. As for practical projects, based on few attempts and simulations, NASA took the lead of constructing hybrid-electric aircraft, such as the 'STARC-ABL' project [34], and the 'N3-X Turbo-electric Distributed Propulsion' (TeDP) project [35]. The 'N3-X TeDP' project designed a series HEPS which hybridized a turboshaft engine with the distributed electric powertrain. The European aircraft manufacturer, AIRBUS, is teaming up with the German industrial conglomerate SIEMENS to develop hybrid planes as well.

Their on-going project, called ‘E-Fan X’, planned to use the parallel HEPS technology to construct a 100-passenger aircraft, as their first step in the long-term goal of developing the hybrid-electric regional airliner. Two other projects ‘SUGAR Volt’ and ‘SUGAR Freeze’, funded by Boeing and NASA, were aiming to design subsonic hybrid-electric aircraft [36]. The aircraft ‘SUGAR Volt’ adopted a parallel hybrid system and met NASA goals on fuel burn according to their 2014 report. The ‘SUGAR Freeze’ utilized the turboelectric hybrid technology that runs on liquid neutral gas for the propulsion [37]. Later, AIRBUS started a joint project DEAP [38, 39] in 2016, collaborated with Rolls-Royce and Cranfield University. Moreover, ESAero is continuous researching HEPS based on their previous ‘SCEPTOR’ project [40], the latest project ‘SBIR’ applied a gas generator and a superconducting motor to improve the aircraft performance [41]. It is noteworthy that many largescale aircraft projects usually apply turboelectric hybrid power systems. The turboelectric hybrid technique is a type of series HEPSs, it uses one or multiple turboshaft engines to generate electricity for electric motors and internal electrical grids. This is a highly-rewarded concept and technology [42], which increases the electrification degree so that can achieve a higher efficiency, less noise and become more environmentally friendly.

Overall, hybrid-electric aircraft is on the rise. For small and midsize aircraft, the relative research started with series hybrid technologies but mainly adopts the parallel hybrid-electric propulsion system at present, while largescale aircraft is more likely to use series hybrid configuration instead.

1.2 Research Gap

According to literatures, relevant research regarding hybrid-electric propulsion systems has obtained lots of achievements. However, most of prior research are designed for automobiles, only few of them are proposed for aircraft. Therefore, an aircraft-favoured hybrid-electric power system is urgently required. Concretely, to develop a good power system for aircraft, aircraft specifications, flight missions and hybrid-electric power system features should be all incorporated into the design process. The huge difference between the maximum and minimum power

requirements should also be considered, although it increases the difficulty of the design.

Commonly, there are two design targets for realizing sustainable aviation. Firstly, the degree of electrification should be further increased in order to obtain a higher fuel efficiency. On the other hand, considering the development of the battery technology, it is important to ensure that the designed propulsion system will still be competitive even if the battery power density has been significantly improved. In addition, the designed configuration should be simple and easy to install.

Since aircraft has a stricter safety standard, the requirement of each component of hybrid-electric aircraft may differ from that of automobiles. At first, the sizing process is an exclusive customization problem and needs to be specifically designed for the proposed system. Previous engineering applications always applied an iterative sizing procedure to select components, i.e. it firstly selects some devices as candidates and then validates the chosen result through a simple simulation, which is time consuming and inefficient. Therefore, an intelligent and thoughtful sizing method, which not only can select components for the hybrid-electric aircraft, but also can predict system performance simultaneously, is on demand.

The next contribution is the design of supervisory controllers. The supervisory controller is the primary part of the research. It can realize fuel and emission reduction, and reveal the relationship between different control objectives. Therefore, three different real-time controllers are planned for this study.

1) A deterministic ‘power follower’ rule-based controller. This controller is intended as a criterion for this study.
2) A battery longevity fuzzy controller. The battery pack is an essential part of the hybrid-electric power system, but it is easily damaged caused by outside operating environment. Thus, it is necessary to monitor and improve the operating circumstance of the battery pack in order to extend its lifetime. Due to the fuzzy control algorithm is adaptive and easy to be tuned, the battery longevity technology can be combined into the fuzzy logic control method to construct a new supervisory controller.

3) An intelligent real-time controller. Although many studies claimed that hybrid-electric propulsion system can reduce fuel consumption and emissions simultaneously, there is rare research studied emission performance. The relationship between these two research goals has not been clearly illustrated as well. Therefore, based on two given maps, the third controller is required to discuss the performance on the fuel economy and emission reduction.

1.3 Aims and Objectives

This study is aiming to design a high-efficient and low-emission hybrid-electric propulsion system for aero vehicles. As traditional hybrid-electric propulsion technologies, i.e. series or parallel HEPS, have respective drawbacks limiting their performance, a novel configuration is proposed in this study. After the determination of configuration, each component is intelligently selected by a well-developed sizing frame and the Genetic Algorithm (GA). Then, several supervisory controllers are designed for the power management problem of the proposed system. Except looking forward to better fuel efficiency, a highly adaptable configuration and lower emission rates are also expected. Therefore, this research involves four fields: system design, component selection, system modelling, and supervisory control.

1) **System design**: this study proposes a distributed series hybrid-electric configuration for aero vehicles. Firstly, it selected the series configuration as the basis due to its special advantages compared with other hybrids. After that, to further improve the conventional series HEPS's performance, both distributed propulsion technology and More Electric Aircraft (MEA) concept are integrated to construct a new configuration. The new structure has a potential to perform better with little compromises in other features.
2) **Component selection**: According to the designed configuration, an indirect engine sizing method and a genetic algorithm based sizing method are invented to find the most suitable components for the system. The engine is firstly determined based on batteries' parametrization criteria, then other components are selected by genetic algorithms. The GA-based sizing method divides the system into two parts. The first part applies a multi-objective

genetic algorithm to reduce the system weight and increase the fuel efficiency, while the second part uses a general GA algorithm to select motors.

3) **Modelling**: Different dynamic modelling methods have been applied for each component according to different subsystem's timescales characteristics. Main subsystems involve an internal combustion engine, electric motors, an electric generator, a battery pack and DC/DC converters.
4) **Supervisory control:** The supervisory controller of this study is responsible for intelligently managing different power flows in order to complete missions with the minimum fuel consumption and less emissions. To achieve these objectives, both the sophisticated rule-based control method and the optimization-based control algorithm have been applied to the system to ensure efficiencies are not out-weighted by higher weight or cost. Concretely, a deterministic rule-based controller, a fuzzy-based battery longevity controller and a MPC-based controller have been designed, and applied to the system to perform a standard flight mission profile respectively. All algorithms are validated by MATLAB simulations, and the performance is analyzed via comparisons.

1.4 Contributions

This research presents a study about a novel hybrid-electric propulsion system for aero vehicles. The study firstly designs a Distributed Series Hybrid-Electric Propulsion System (DSHEPS) based on the conventional series hybrid structure. Then, according to mission requirements, the whole system is sized by component's parametrizations by using the genetic algorithm. After that, various control algorithms are applied for the power management issue. The first controller is an adaptive power follower deterministic rule-based controller, which uses given thresholds of the battery SOC as references to adjust the engine. The second controller is proposed for improving the battery working environment in order to extend the battery's life. This controller is designed based on Mamdani and Sugeno fuzzy logic inference strategies, and uses batteries' parameters as the control input. The third is the Model Predictive Controller (MPC) based controller. It first formulates the power management problem into a nonlinear

optimization problem, and then uses the Dynamic Programming (DP) algorithm to find the result. All of three controllers are simulated by the SIMULINK models. The dynamic models of each component are developed based on experiential data. The main contributions of the study can be summarized as:

1) An innovative hybrid-electric configuration for aero vehicle. Because the power demands of different flight stages vary greatly, the conventional series hybrid configuration was improved for better adapting to flight missions. The new structure reduces the limitations of the series hybrid while retaining its advantages.
2) An indirect engine sizing method via battery SOC parametrization criteria. Five candidate engines were considered with different starting conditions for the electrical system, and the simulation result shows that by using the state-of-charge properties, it is possible to select an appropriate sizing of engine pack while carrying a suitable electric propulsion pack. By applying the rule-based control strategy, the system is able to reduce fuel consumption up to 12%.
3) A genetic algorithm based sizing framework. The proposed sizing framework divided the system into two parts. The first is the power source part, including an engine, a generator and a battery pack. This is a multi-objective optimization problem that solved by the Non-dominated Sorting Genetic Algorithm-II (NSGA-II). The second part consists of system loads, which is a single-objective problem so that a general genetic algorithm was applied to solve the problem. An extra archive was added into the NSGA-II to increase the selecting speed.
4) Due to the strict requirement of flight safety and the vulnerability of the battery pack, a Mamdani & Sugeno fuzzy battery longevity controller is designed for the DSHEPS. The controller firstly applied a Mamdani fuzzy inference system to evaluate the battery operating environment, and utilized the Sugeno fuzzy logic algorithm to obtain the control instructions for the engine. The controller fully considered batteries' operating variables and adjusted the working condition to a battery-friendly environment. According to simulation results, it

achieved a 5% improvement on the fuel economy compared with that of the deterministic rule-based controller.

5) For optimizing the fuel efficiency and emission rate, an MPC-based intelligent controller is proposed as well. The controller is a real-time controller, which succeeded in reducing both fuel consumption and emissions. The conflict between the fuel economy and emission rate was stressed within this approach. According to simulation results, the MPC-based controller can improve 5% fuel consumption, but 6% worse in emission performance than the rule-based controller due to these two objectives cannot be obtained at same time.

1.5 Thesis Layout

Overall, this research completed the design, sizing, modelling and energy management of a hybrid-electric propulsion system for the aero vehicle. In order to achieve a high-efficient and low-emission hybrid-electric power system, the study could be divided into three sub-objectives. The first goal is to improve the original series system configuration, i.e. design a system with the potential of obtaining higher fuel efficiency and lower emissions. The second target is to establish a comprehensive sizing frame particularly for the designed hybrid-electric propulsion system. The last objective is to design a supervisory controller to manage different energy flows. The entire thesis structure is illustrated in Figure 8. The content of each chapter:

Chapter 1 introduces the background of hybrid-electric aircraft and the ambition of the sustainable aviation. It presents various configurations and introduces the state-of-art of hybrid-electric aircraft and relative projects. The research gap, research aim and contribution of this research are also concluded.

Chapter 2 reviews the previous research about the hybrid-electric propulsion system, including the research field of system design, system sizing, modelling and different energy management methods.

Chapter 3 illustrates the novel distributed series hybrid-electric power system configuration. The design process, and the pros and cons of the system will be

analyzed respectively. The modelling methods of all subsystems, including the engine, electric motor and battery pack are also demonstrated.

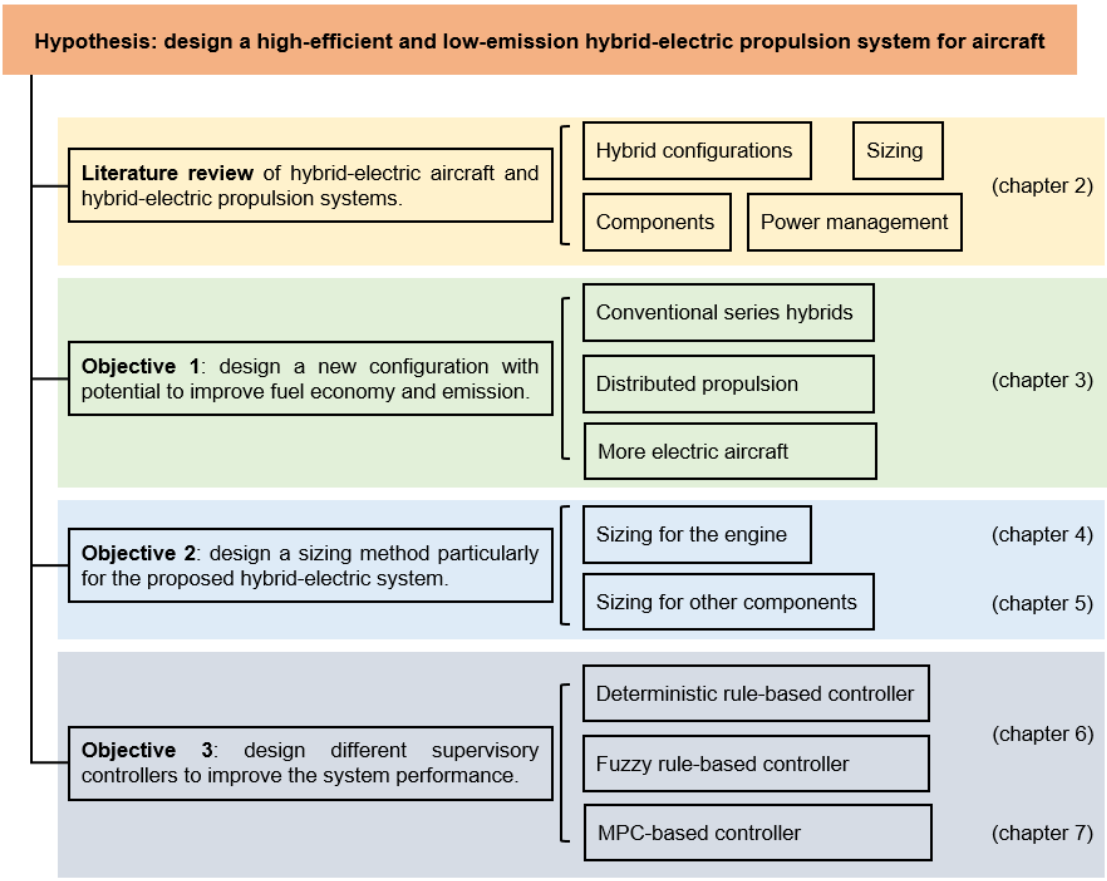

Figure 8 Thesis structure.

Chapter 4 presents a design process for the challenging problem of sizing the engine pack for the designed hybrid-electric power system. The indirect sizing approach via properties on the electrical part of the system is be illustrated in this chapter, which selects the engine based on battery criteria.

Chapter 5 introduces the genetic algorithm-based sizing method proposed for the designed hybrid-electric propulsion system. Based on the special configuration and characteristics, a two-step sizing method is proposed and illustrated in this section. By using the genetic algorithm, suitable components are selected and the system can achieve a 12% fuel consumption reduction.

Chapter 6 proposes two rule-based controllers. The first is an adaptive power follower rule-based controller, which controls the engine based on the battery

SOC. The second controller is a Mamdani & Sugeno Fuzzy Logic (MSFL) controller, which is designed for improving batteries' operating environment and extending the battery life. Simulation results and characteristics of each controller are presented and analyzed in this chapter. It finds that the MSFL controller can achieve a better fuel efficiency than the rule-based controller.

Chapter 7 introduces a nonlinear MPC-based power management strategy to simultaneously improve the fuel economy and emissions. By using the designed controller, an optimal operating trajectory of the engine could be determined. Compared to the results obtained by the deterministic rule-based controller and MSFL controller, the MPC-based controller shows the best performance on the fuel consumption, and is able to reduce NO_X emissions simultaneously.

Chapter 8 summarizes the whole research and concludes the study. Recommended future work is also presented.

***** Please note that Chapter 4 and Chapter 5 contain two published papers respectively. Chapter 4 is the paper "Indirect Engine Sizing via Distributed Hybrid-Electric Unmanned Aerial Vehicle State-Of-Charge-Based Parametrisation Criteria", which has been published in the IMechE journal. The second paper is "Design of a Distributed Hybrid-Electric Propulsion System for a Light Aircraft based on Genetic Algorithm", which is a conference paper that published at the AIAA propulsion and energy 2019 forum.

2 LITERATURE REVIEW

This chapter contains a literature review regarding hybrid-electric propulsion systems. The chapter structure is shown in Figure 9, it includes the information of system design, present sizing methodologies, subsystems and representative energy management technologies. In this chapter, each main component will be introduced respectively, and the advantages and disadvantages of each energy management approach will also be analysed.

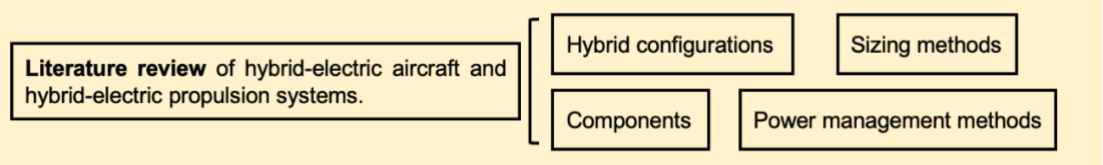

Figure 9 Chapter 2 structure.

2.1 System Design

The intuition of the hybrid-electric propulsion system is to develop a greener and more fuel-efficient powertrain by combining existing propulsion components. For a given vehicle, in addition to the external structure optimization, increasing system efficiency and fuel economy is a way to reduce the fuel consumption and emissions. At present, there are numerous proposed hybrid-electric propulsion systems. Series, parallel, series-parallel hybrid configurations all have been studied and some promising achievements have been obtained.

For hybrid-electric power systems, the configuration is one essential factor affecting system performance. Based on literatures, each kind of configuration

has its own unique characteristics, so that the system structure should be carefully designed based on design objectives and emphasises. Paper [43] compared series and parallel hybrid configurations, and found that the parallel architecture can provide a higher range than the series without considering distant future advancements. However, as mentioned in the previous chapter, the series hybrid structure decouples the engine and propeller, in which possesses the potential to achieve the highest fuel-economy compared to other configurations.

Figure 10 illustrates a general design process of a hybrid-electric propulsion system. It starts with design motivations, following by the determinations of the system configuration, components and control strategies, and finally verifies the performance.

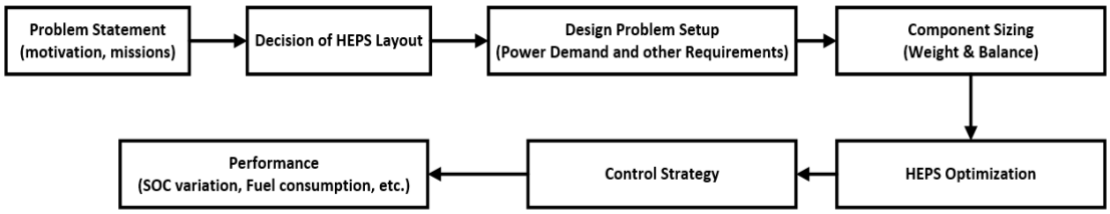

Figure 10 System design process.

Apparently, better fuel efficiency and lower emissions are motivations for constructing hybrid-electric aircraft. The powertrain layout is available in multiple choices. Previous research regarding hybrid-electric aircraft applies similar hybrid-electric propulsion systems to hybrid-electric automobiles. In other words, the propulsion systems of hybrid-electric cars are generally applicable for aircraft so that some research adopted same power systems. However, there are many obvious differences between the driving pattern of automobiles and aircraft. For example, there is no stopping during the flight, and the fluctuations of aircraft power requirements are bigger but smoother than that of cars. More importantly, aircraft requires a high-level safety and stability. Therefore, a customized hybrid-electric propulsion system, which is particularly designed for aircraft, is on-demand.

2.1.1 Sizing Method

After determining the system configuration, the sizing problem should be introduced in the sequence. For hybrid-electric vehicles, sizing refers to the component selection, i.e. the process for determining the specifications of each corresponding equipment, including its capacity, mass, volume and other parameters.

Sizing is a complex and challenging procedure, various choices and combinations can lead to different results. Therefore, all system components should be comprehensively selected. At present, the simplest sizing method is choosing devices by their power-to-weight ratio (or other specifications) [44, 45]. It is one of the most popular sizing methods for engineering applications. Simulation-based optimal sizing approaches are developed as well. Paper [46] presented a simulation-based method to size the external battery pack, and stated that the Ni-MH battery technology can provide the most suitable expansion possibility for that design. After that, Schoemann et al. proposed a complete parallel hybrid-electric aircraft design process, which is a quasi-static and back-facing process and can minimize the system mass [47].

Intelligent methodologies have been applied for the sizing problem subsequently. Paper [48, 49] used the Divide Rectangle (DIRECT) and the complex algorithm to optimize component's capacity of a parallel hybrid-electric vehicle. Galdi et al. developed a genetic algorithm-based sizing methodology that minimized emissions and the fuel consumption simultaneously by using a weighted cost function [50]. These single-objective optimization methods can obtain the optimal sizing result based on the designed cost function, but they cannot simultaneously show the system performance. As a result, extra simulations have to be carried out to examine the sizing result. Therefore, in recent years, some Multi-Objective Optimization (MOO) algorithms are studied for the sizing optimization problem. Murgovski et al. [51] proposed a novel convex optimization-based method for optimizing the battery pack capacity and energy management for a plug-in hybrid powertrain. Abdelkader et al. [52] minimized electricity cost and power loss within its sizing process by using a MOO genetic algorithm for a hybrid power supply

system. Meanwhile, Xie [53] realized a fuel consumption minimization during a retrofitting of a midscale aircraft, which achieved a fuel-burn reduction of up to 17.6%.

In general, similar to the configuration design, the component selection method should be specifically designed according to research targets. Requirements for subsystems of the series and parallel hybrid-electric systems vary widely. Thus, based on the given system configuration and mission demands, an exclusive sizing method is required in this study.

2.2 Subsystems

The basic configuration of a series hybrid-electric propulsion system is illustrated in Figure 11, which consists of an engine, a generator, a motor and a battery pack. This section will introduce each main component, including their categories, characteristics and modelling methods.

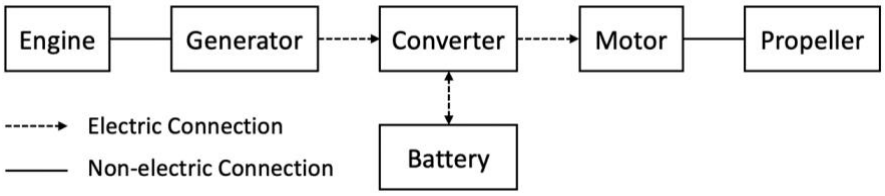

Figure 11 Basic series hybrid-electric configuration.

2.2.1 Internal Combustion Engine

The Internal Combustion Engine (ICE) is a prime propulsion component and has been widely used worldwide. It generates energy by burning the fuel, i.e. transforming chemical energy into mechanical energy. According to different combustion types, classifications of ICEs are shown in Figure 12 [54].

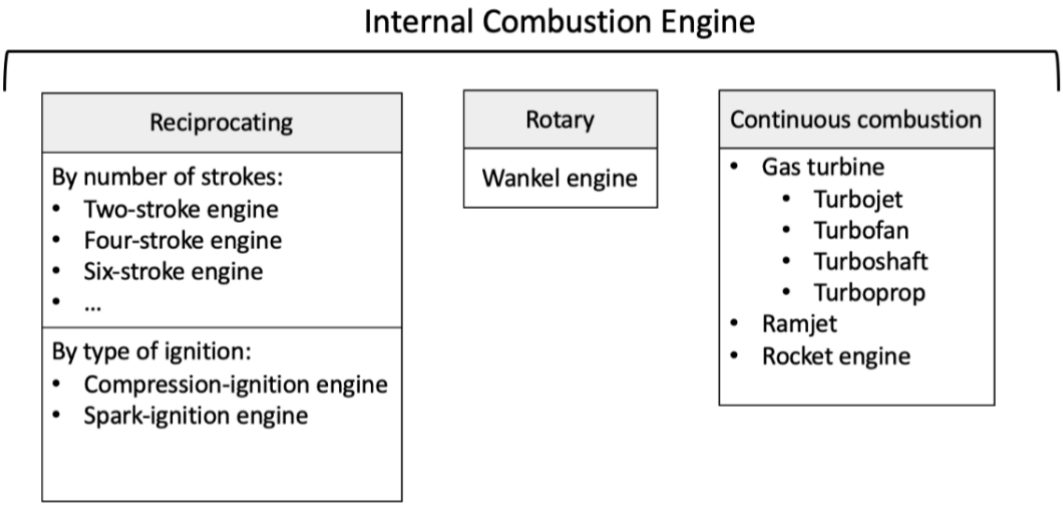

Figure 12 Internal combustion engine classifications [54].

Although there are many types of internal combustion engines, fuel combustion processes occurring in combustion chambers have many similarities. Directly speaking, the fuel burns in the chamber and generates thermal energy, which could be revealed by the thermal expansion, and then the expansion activity is transformed into other mechanical movements, such as rotation or other kinetic energy.

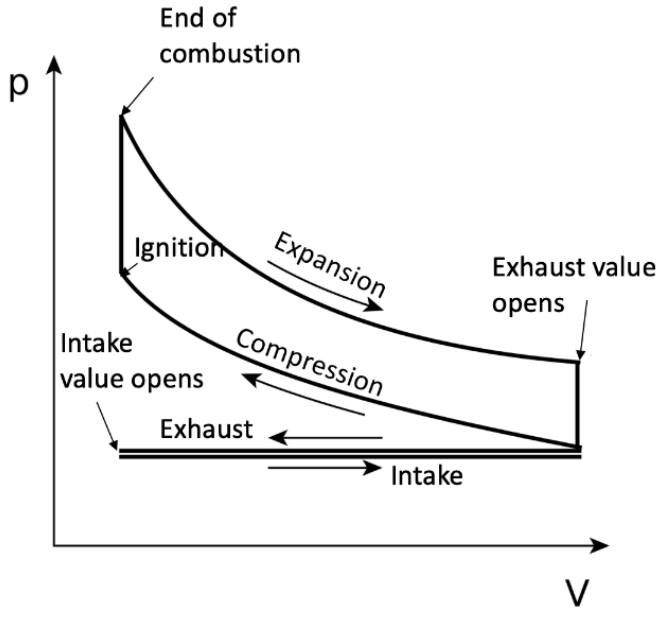

Figure 13 Otto Cycle [12].

For a typical Spark-Ignition (SI) engine, i.e. the petrol engine, the combustion process can be presented through an ideal thermodynamic process — the Otto cycle. An ideal Otto cycle is illustrated by the pressure-volume contour shown in Figure 13 [12]. According to the displayed cycle, the SI engine firstly absorbs a mixture of fuel and air, then compresses and ignites the mixture, i.e. converts chemical energy to thermal energy. After the combustion process, the working fluid expands, resulting in a volume increase, which symbolizes that thermal energy has been transformed into kinetic energy. After that, the engine ejects the combustion products and replaces them with a new charge of fuel and air. Thus, the Otto cycle can clearly display the operating process of the engine, and based on that, several modelling methods have been proposed.

- **Modelling Methods**

There are numerous methods of internal combustion engines modelling, for example, Willans line method, 0-Degree thermodynamic modelling method, and spark ignition engine modelling method. For this study, although some detailed modelling approaches with high complexity are able to perform ICEs' dynamic performance accurately, they may lack practicality and being inefficient for real applications and simulations. Therefore, few selected candidates of modelling methods are shown below.

1) Willans Line Method

The Willans line method, also known as the fuel rate extrapolation method, is a primary approach based on the linear relationship between the brake mean effective pressure and fuel consumption [55]. It is a quasi-static modelling method. Figure 14 shows an example [56] of the fuel consumption rate $\dot{m}_f$ (vertical axis) with respect to braking power P_{brake} (horizontal axis). The fuel consumption rate is extrapolated on the negative axis of the braking power, and the intercept of the negative axis is taken as the friction power P_{fri} of the engine. The friction power P_{fri} depends on the engine speed and displaced volume. According to the figure, in most range, the relationship between $\dot{m}_f$ and P_{brake} is linear so that it could be presented as:

$$P_{brake} = \eta_W \cdot V_{lhv} \cdot \dot{m}_f - P_{fri} \quad \textbf{(2-1)}$$

In the above equation, V_{lhv} is the lower heating value, η_W is the indicated efficiency which can be obtained by:

$$\eta_W = \frac{P_{brake}}{P_{fuel}} = \frac{P_{brake}}{P_{comb}} \cdot \frac{P_{comb}}{P_{fuel}} = \eta_{th} \cdot \eta_{comb} \quad \textbf{(2-2)}$$

where η_{th} is the thermal efficiency, and η_{comb} is the combustion efficiency. As a result, the fuel consumption rate is determined by above equations.

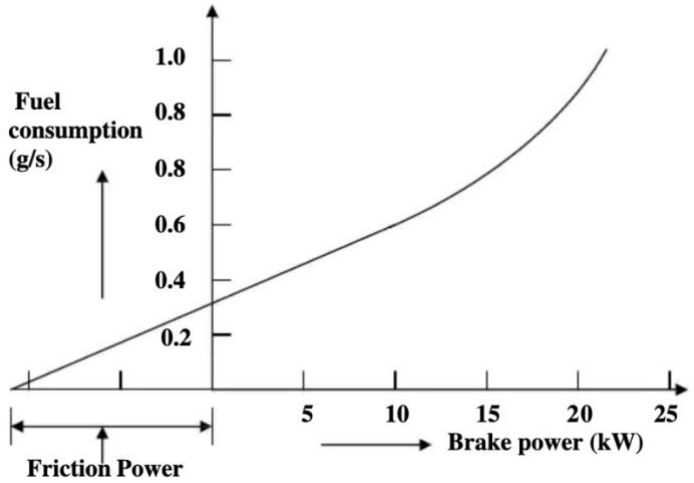

Figure 14 Willans line method [56].

In general, the Willans line modelling method is a simple approach that cannot show the influences of external conditions (pressure and temperature), nor can it describe the effects of engine speed and torque on the thermal efficiency. In addition, since for petrol engines, the air-fuel proportion is constant and the amount of intake air-fuel mixture varies with the required torque and power, the Willans line model is more suitable for Compression Ignition (CI) engines, i.e. diesel engines, rather than SI engines.

2) 0-Degree Thermodynamic Model

The 0-Degree (0-D) thermodynamic model is another modelling method for ICEs. It firstly calculates the pressure, temperature and mass inside the combustion chamber and determines the engine power output based on the engine shaft's

crank angle degree [57]. Then, assuming that the pressure and temperature are homogeneous in each cylinder, it uses three differential equations to describe the ICE operation process in every second. Three equations are the first law of thermodynamics for an open system, the perfect gas law, and the mass conservation equation respectively. The 0-D thermodynamic model can illustrate a precise fuel combustion procedure, including the volume changes, temperature changes, fuel consumption, emissions and other detailed information. However, it is too complicated for this study.

3) Spark Ignition Engine Model

The spark ignition engine model is a semi-empirical modelling method based on the engine two-zone model. Two zones contain burnt gases and fresh gases respectively. Under assumptions: 1) the mixture and pressure are homogeneous in each zone; 2) flame front propagation, the physical model of the spark ignition engine can be established by seven equations (the first law of thermodynamic, the perfect gas law, the mass conservation law, volume equation and other three equations). By solving these seven equations, all combustion parameters at each moment are able to be determined. Therefore, like the 0-D thermodynamic modelling method, the spark ignition engine model is also capable to simulate a detailed combustion process. However, it requires engine design variables and intrinsic parameters to determine an accurate model, which increases the difficulty of applications in engineering projects.

4) Mean Value Model

Mean Value Model (MVM) [58] is a widely used low-frequency engine modelling approach. Under the assumption that all processes and effects are spread throughout the engine cycle [59], the MVM method simplifies the engine combustion process and uses static look-up tables to describe the discrete cycles and sophisticated thermodynamics of the engine [60]. The model firstly calculates the engine instantaneous torque and fuel consumption based on the throttle command and operating speed, and uses rotational dynamics to represent transient response [61]. As a result, the MVM is able to show engine rotational dynamic performance, and predict fuel injection and pollutions. Therefore, the

MVM method is particularly suitable for problems which emphasize on engine performance (engine torque and speed), such as the engine speed control problem or fuel analysis problem [62, 63].

The MVM method can be further simplified by neglecting the inlet manifold dynamics and flow rate dynamics [60]. For example, it can use the first-order or second-order transfer function to characterize the torque response [64, 65], and utilizes a fuel-power function, which is derived from the steady-state experimental data, to determine the fuel consumption rate [66]. The simplified MVM modelling method possesses a less-complexity, but can still preserve a certain level of dynamics. However, this method cannot reflect the influence of the engine throttle, which is a common input of the engine control. Therefore, the study [60] developed another simplified MVM which can provide an insight into the inherent relationship between the throttle command and the torque output. It can provide just adequate information for the energy management problem of the hybrid-electric propulsion system.

2.2.2 Electric Motor & Generator

The Electric Motor (EM) is an electromagnetic device that converts electrical energy into mechanical energy according to the law of electromagnetic induction. A generator is mechanically identical to the electric motor, but operates in the reverse direction, converting mechanical energy into electrical energy [67]. The generator and motor have much in common. Thus, in some specific applications, motors are also used as generators to convert mechanical energy into electric power. General-purpose motors with standard dimensions and characteristics provide mechanical power for industrial use. They have various capacities and types. Based on the power source type and structural features, motors can be classified as shown in Figure 15.

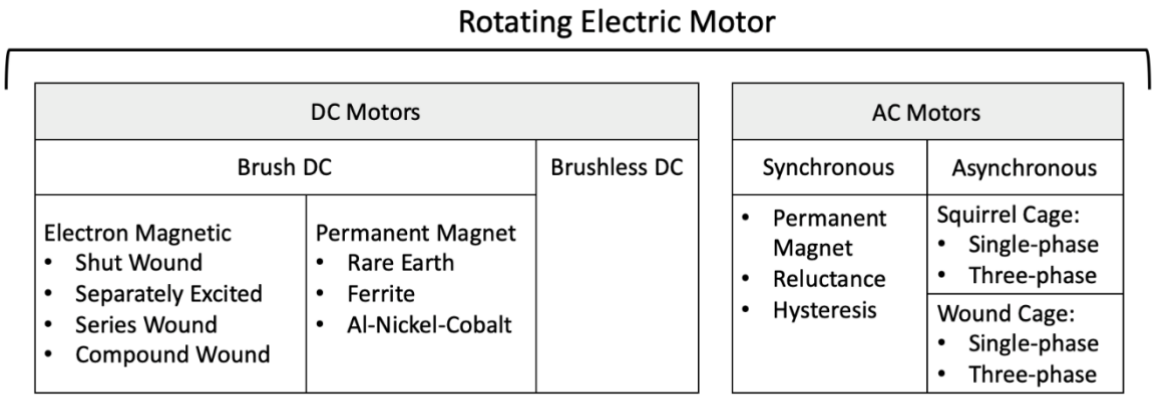

Figure 15 Electric motor classifications.

- **Modelling Methods**

There are several well-developed motor modelling methods. The quasi-static modelling approach, such as using efficiency maps to model the motor, is mostly used but cannot describe dynamic performance [60]. In this study, the Permanent Magnet Synchronous Motor/Generator (PMSM/PMSG) is selected as the propulsor of the system. For PMSMs (or PMSGs), the smooth air gap model, the position-independent model, the electrical conduction loss model and the linear magnetics model are all able to reflect motor behaviours. But amongst them, the $d-q$ model is one good choice.

The $d-q$ model is the most popular modelling method for PMSM [68, 69]. Unlike other approaches, the $d-q$ model simplifies the system dynamic by forcing all changing inductances to be constant, and calculates the rotor angular velocity, rotor angle and stator current based on the transition between the stator's abc frame and the rotor's $d-q$ frame. The energy loss can be achieved based on the motor steady-state behaviours.

2.2.3 Battery

The battery pack is another key element in the hybrid-electric propulsion system. It is a storage device which converts chemical energy into electricity and vice versa. At present, Lithium (Li) battery, including Lithium-ion (Li-ion) battery and Lithium-polymer (Li-Po) battery, is the most popular type of secondary batteries.

Compared with other batteries, Li batteries show great advantages – small size, light weight and high capacity. They have better dynamic properties, which can be charged faster, last longer, and can be formed into thin packages. Therefore, although Li-batteries are sensitive to environments, the strict size requirement makes them become the most applicable electrical storage unit for hybrid-electric power systems. Few advantages and limitations are summarized in Table 1 [70].

Table 1 Advantages and limitations of Lithium batteries [70].

Advantage	1) High specific energy and high load capabilities with power cells; 2) Long cycle and extend shelf-life; 3) High capacity, low internal resistance, good coulombic efficiency; 4) Simple charge algorithm, reasonably short charge times; 5) Low self-discharge; Maintenance-free.
Limitations	1) Requires protection circuit to prevent thermal runaway if stressed; 2) Sensitive to temperature; 3) Performance decreases at high or freezing temperature; 4) Transportation regulations required when shipping in large quantities; 5) Needs cell balancing, requires individual cells to be balanced.

There are not too many differences between the Li-ion and Li-Po battery. By using the same internal chemistry techniques, they have similar properties. The only difference between them is that Li-Po battery has a polymer cathode and a solid electrolyte, while Li-ion has a carbon cathode and a liquid electrolyte. In addition, Li-Po uses a microporous electrolyte rather than the traditional porous separator. Therefore, Li-Po is more advanced with less internal resistance and higher level of safety, but the price of Li-Po is higher than that of Li-ion battery.

- **Charge and Discharge Characteristics**

For lithium batteries, the charging process has two stages. The first stage is a constant-current charging process. If the battery voltage is lower than 4.2V per cell, the battery will be charged by a constant current. The second stage is the constant voltage charging stage. When the battery cell voltage reaches 4.2V, due to higher voltage may damage the lithium battery, the battery voltage will be fixed

at 4.2V, and the charging current will gradually decrease. After that, when the current drops to a certain value, the charging circuit will cut off, which indicates that the charging is completed [71]. Figure 16 [71] is an example of charge stages of lithium battery, the voltage curve and current curve are both illustrated. The charging process is a delicate procedure, extreme cold and high heat may reduce charge acceptance, so that the battery must be charged under a moderate temperature.

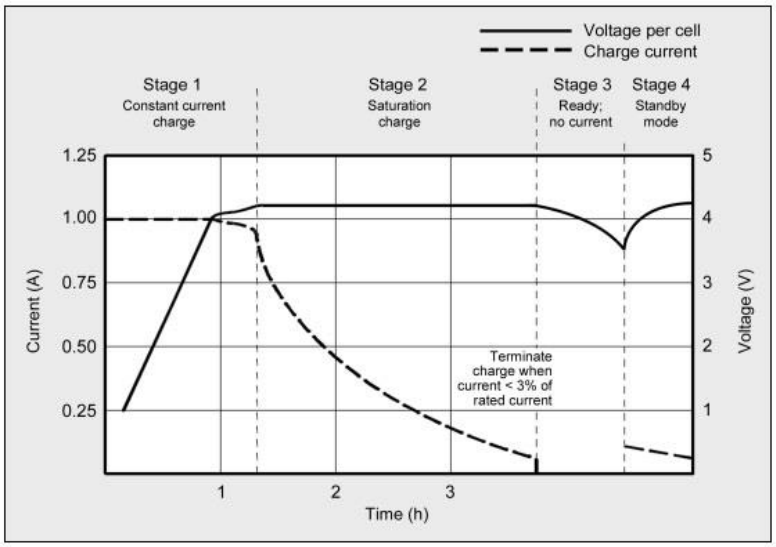

Figure 16 Charge stages of the lithium battery [71].

Lithium battery is capable of high loads, it can continuously deliver high power until the battery is exhausted. Figure 17 [71] shows an example of a voltage discharge curve of the Li battery with the graphite anode and the early coke version respectively. The voltage drops until to 2.5V during the discharging process. Please note that each battery pack has a factor indicating the continuous discharge rate, called the C rate. This parameter is a measurement at which Li battery is discharged relative to its maximum capacity.

In general, a battery prefers moderate current at a constant discharge rather than a pulsed or momentary high load. In addition, according to literature, researchers have found that heat can shorten the battery's life (especially above 35°C), and repetitive full discharges may also stress the battery [70, 71]. Concretely, there are many discharging parameters affecting the battery longevity, such as

temperature, current, depth of discharge, etc. A moderate current discharge and a cool environment are conducive to the health and life of the battery.

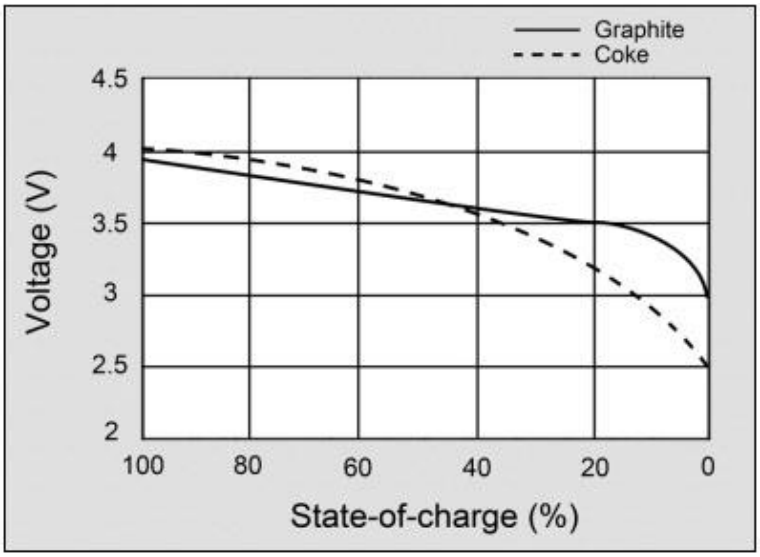

Figure 17 Voltage discharge curve of the lithium battery [71].

- **Modelling Methods**

The main objective for the battery modelling is to determine batteries' charge/discharge characteristics and its SOC. For hybrid-electric power systems, it is crucial to have an accurate battery model to predict batteries' remaining energy in order to coordinate different power sources. At present, there are three types of battery modelling methods: experimental, electrochemical and electric circuit-based. The experimental modelling method refers to using polynomial fittings or look-up tables to determine battery characteristics. All relative data is obtained by experiments. The second electrochemical method builds the model by describing the energy conversion process inside cells. This modelling approach has a very high complexity, so that it is good at the design level but not good for real-time prediction applications [72]. As for the electric circuit-based model, it employs an electric circuit to present the battery performance. This method can precisely present battery charge-discharge characteristics. The first-order Resistor Capacitor (RC) network [73], second-order RC network [74] or even third-order RC circuits [75] all have been developed for modelling the battery.

Shepherd model [76] is one of the experimental-based modelling methods. In contrast to the electric circuit-based model, the Shepherd model uses equations to describe the charge/discharge process. The relationship amongst the battery capacity, SOC, time, current density and other certain factors are expressed. The original Shepherd modelling method may cause an algebraic loop problem in the closed-loop simulation of modular models [72], but by replacing polarisation resistance with the polarisation voltage, the problem has been solved [77, 78]. Therefore, the Shepherd model can provide sufficient battery information for the energy management problem, only relying on a minimum of experimental data.

2.3 Energy Management

In addition to the configuration design and component selection, the energy management problem is the last research core regarding hybrid-electric propulsion systems. The energy management problem refers to the coordination problem among different power sources. Therefore, unlike conventional aircraft, the control structure of the hybrid-electric aircraft is a two-level controller, shown as Figure 18, in which the supervisory controller is responsible for power splitting and the low-level controller regulates each subsystem. In other words, the supervisory controller ensures the rationality and efficiency of the entire system, while the low-level controller guarantees the stable operation of each component.

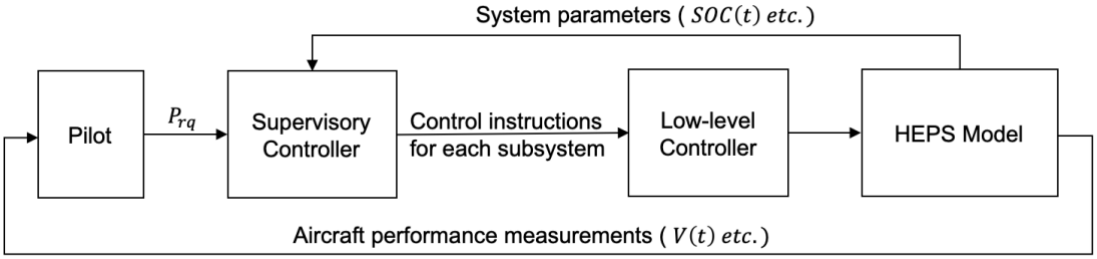

Figure 18 General control structure of the hybrid-electric propulsion system.

For series hybrid-electric propulsion systems, more precisely, the core issue inside the supervisory controller is how to distribute power flow between the engine and battery pack. The most ideal condition is that the system can accomplish the task by consuming the minimum fuel and producing the minimum

emissions. Overall, control strategies are essential for the performance of the hybrid-electric power system.

Different rules may trigger different system characteristics. How to design the supervisory controller is the most interesting topic in the research of hybrid-electric aircraft. Currently, there are two general trends to investigate the overall powertrain efficiency: Rule-Based (RB) control and optimization-based control [79]. A more detailed classification is listed in Figure 19.

Control Strategies for Hybrid-electric Propulsion Systems

Rule-Based (RB) Control Strategy		Optimization-Based Control Strategy	
Deterministic RB	**Fuzzy RB**	**Global Optimization (non-causal)**	**Real-Time Optimization (causal)**
Thermostat	Basic Fuzzy	Linear Programming	Equivalent Consumption Minimization Strategy
Power Follower (PF)	Adaptive Fuzzy	Genetic Algorithm (GA)	Model Predictive Control (MPC)
Adaptive PF	Predictive Fuzzy	Dynamic Programming (DP)	Pontryagin's Minimum Principle
Frequency-based		Stochastic DP	Neural Network
Points-tracking		Global ECMS	Robust Control
State Machine-Based		Game Theory	Extremum Seeking
		Convex Optimization	Reinforcement Learning
		Particle Swarm Optimization	

Figure 19 Energy management strategies for hybrid-electric propulsion systems.

2.3.1 Rule-based Control Strategies

Rule-based control strategies, or Heuristic control strategies, refer to the use of a series of logical statements to describe control instructions. These logical statements can be heuristics, intuition, human expertise, etc. [79]. Commonly, rule-based control methods only rely on the current states, while the priori or future knowledge of the mission is not considered. Therefore, rule-based controllers become the most applicable and adaptable methods, especially suitable for real-time implementations.

So far, different RB control rules have been proposed based on the 'load-levelling' theory. The load-levelling strategy is to shift the engine operating point to the most optimal point as much as possible during the mission. Thus, the engine Brake-Specific Fuel Consumption (BSFC) map, the engine emission map, the

motor efficiency map and battery efficiency map are the basis for the RB control strategies. Based on the applied algorithm, RB strategies can be further classified into deterministic rule-based controllers and fuzzy rule-based controllers.

- **Deterministic Rule-Based Control Strategy**

The information of some representative deterministic rule-based control strategies is summarized in Table 2. The earliest and simplest deterministic rule-based control strategy is Thermostat [80, 81], by which the engine can be switched on/off according to battery SOC values. Power Follower (PF) is a latter-proposed rule mentioned in many literatures [82, 83, 84]. It uses two trigger parameters - the power requirement and SOC, to regulate the engine. This is the most popular heuristic control strategy and applicable to all hybrid systems [79]. However, no consideration is given to the emission performance in rules of the power follower controller.

Then, the Adaptive Power Follower (APF) control strategy was developed, which is an improved rule that can reduce both energy usage and emissions simultaneously [85]. It uses a normalized cost function to compute the impact of all candidate operating points, and then selects the point with the minimum impact value as the final result. This method can take into account both the engine emission and the amount of the consumed fuel, and moreover, other variables can also be added into the cost function according to different mission targets. By simulating five different cycles, the APF controller proposed in paper [85] achieved a 22.7% reduction of NO_x but the energy consumption increased 1.4%. The fuel rate has been increased to reduce emissions, that is to say the energy management problem is a trade-off issue, and the design of weighting factors is important for the controller.

Table 2 Deterministic rule-based control strategies.

<table>
<tr><th>Methods</th><th>Description</th></tr>
<tr><td>Thermostat</td><td> 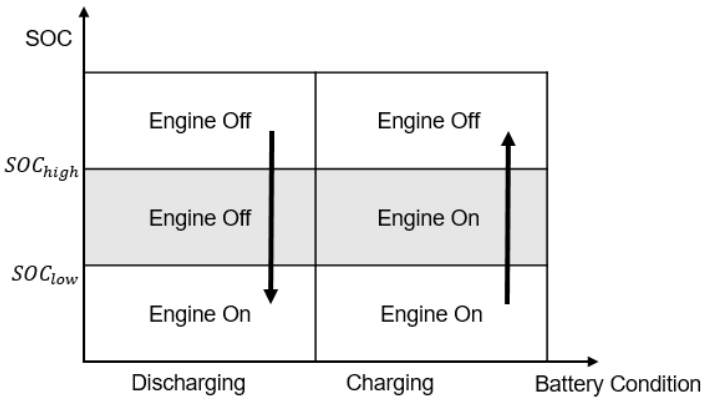
</td></tr>
<tr><td>PF</td><td> 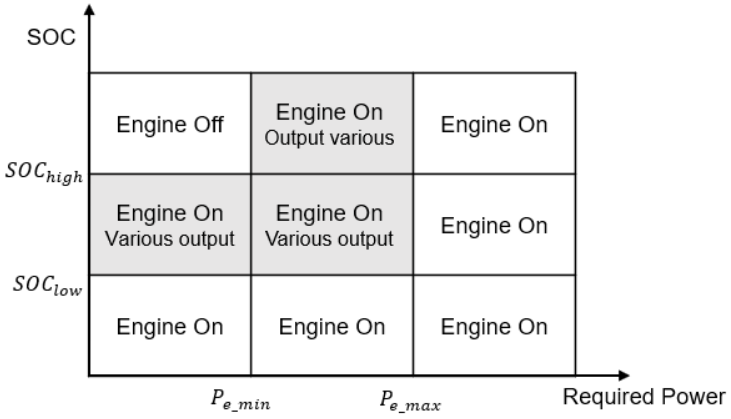
</td></tr>
<tr><td>APF</td><td>Multiple trigger parameters.
(Including SOC, power demand, emission, etc.)</td></tr>
<tr><td>State Machine</td><td>Four states:
<table>
<tr><th></th><th>Engine</th><th>Battery</th><th>Description</th></tr>
<tr><td>1</td><td>ON</td><td>Charging</td><td>Engine propels the system and charges battery;</td></tr>
<tr><td>2</td><td>ON</td><td>Discharging</td><td>Both engine and battery propel the system;</td></tr>
<tr><td>3</td><td>OFF</td><td>Discharging</td><td>Battery propels the system;</td></tr>
<tr><td>4</td><td>OFF</td><td>OFF</td><td>System OFF;</td></tr>
</table></td></tr>
</table>

The last control method, State Machine-based controller, was invented based on the state machine logic structure. State machine can guide the vehicle through its various operating modes and dynamic control strategies to specify the vehicle demands to each subsystems controller [86]. Generally, state machine is suitable for discrete inputs or abrupt inputs, while the hybrid-electric system is a continuous dynamic system. Therefore, the state machine-based controller is not very effective for the power management problem.

- **Fuzzy Rule-Based Control Strategies**

Fuzzy Logic (FL) control strategy is another heuristic method to solve the power management problem. It is a linguistic rule-based control approach and capable to translate expert knowledge and experience into corresponding rules [87]. Compared with other strategies, the fuzzy logic inference system uses membership functions and fuzzy rules to determine the output of the control. It applies a fuzzification on inputs, so that the FL controller can use membership degrees to infer the output rather than using precise values. As a result, the fuzzy logic controller can tolerate modelling errors, inaccurate measurements, component changes and other uncertainties, which enhances the degree of control freedom [79]. Additionally, fuzzy rules can be easily tuned, so that it is adaptive to different control purposes and can be formulated into suboptimal power splitting problems [88].

The fuzzy controller is good at the multi-domain, nonlinear and time-varying plant, which is exactly the type of the energy management problem. Therefore, the fuzzy rule-based control strategy is an effective control method and has been widely used in supervisory controllers. Early research followed the basic process of the fuzzy logic strategy, that firstly fuzzified inputs into membership degrees, then calculated outputs by given rules, and finally used the de-fuzzification to convert outputs into proportional control signals [89]. Paper [90, 91] presented a fuzzy controller which can improve all component operating efficiencies. The controller used the information of driver's power command, battery SOC and motor speed to determine the split ratio between different power plants and achieved a 6.8% and a 9.6% fuel reduction in an urban cycle and a highway cycle

respectively. Similarly, Baumann et al. [92] also applied the fuzzy logic theory to improve the system performance, which successfully achieved a 23%-35% improvement of the whole system efficiency. Lee and Sul [93] applied the fuzzy strategy aiming to reduce emissions. It used the acceleration pedal stroke and motor rotational speed to determine the best ratio of the torque command, and finally realized a 20% of NO_x emission reduction compared to a diesel engine vehicle in the dynamometer test. Another fuzzy controller, mentioned in paper [94], was proposed for improving fuel consumption and reducing pollutant emissions simultaneously. The simulation result showed that the system achieved a 20% and 5.7% fuel efficiency improvement on real and modal driving cycles respectively. The overall amount of emissions was also reduced by using the designed controller.

Fuzzy controllers have good adaptability. It can not only be easily adapted to different environments, but also be tuned by other optimization algorithms. In other words, conventional fuzzy controllers can be further enhanced if we integrate control parameters with optimization methods, current operating conditions (i.e. adaptive fuzzy controllers) and predictive upcoming scenarios (i.e. predictive fuzzy controllers). Membership Function (MF) shape and distribution slightly affect the performance [87]. Wang et al. [95] presented an optimized fuzzy controller for a hybrid-electric vehicle, whose membership functions were optimized by the genetic algorithm. The result proved that the optimized controller can realize a further improvement on the fuel economy, and the controller with a genetic-fuzzy logic was robust and easy to be implemented in real time. Additionally, on the basis of the work [62, 93], Langari and Won [96] proposed a driving situation identifier – Intelligent Energy Management Agent to improve the operation performance. It can recognize driving conditions and driver behaviors, including driving environments, driving styles and driving cycles, in order to further improve the system efficiency. Paper [97] and [98] also demonstrated a driving pattern recognition-based adaptive energy management approach, that can identify the real-time driving pattern by classifying the typical driving cycle. Zhang and Xiong [98] used the inferred driving pattern and predicted upcoming driving environment to generate control signals. The fuzzy logic-based driving

block identification module firstly classified the driving condition into three types, and based on the driving classification, the controller can apply three different control strategies on the system. Three strategies were developed for each driving condition respectively and optimized by the dynamic programming algorithm. The proposed controller improved the fuel efficiency by 1.5% compared with the original controller.

Furthermore, a prediction of upcoming can be integrated and adapted into fuzzy controllers. Hajimiri and Salmasi [99] proposed a predictive fuzzy controller based on the predicted future state of the vehicle, which obtained a better system performance on fuel consumption and emissions. The state of battery healthy has also been taken into the control rules, but the result showed that more fuel consumption and more emissions are the price to pay for the sake of the battery life. Moreover, an optimized predictive fuzzy controller has been proposed in the paper [100]. It initially predicted the traffic condition, and then determined the control strategy by an optimized fuzzy logic inference system, whose membership function is tuned by the genetic algorithm. The result showed that the proposed controller has successfully reduced power loss and increased fuel efficiency by about 20%.

Compared with the conventional fuzzy logic controller, the adaptive and predictive controllers are capable to achieve better fuel economy or emission reductions. However, adaptive and predictive controllers request higher level of abstractions that increase the computational burden [101]. In other words, these advanced control rules sacrifice the low-complexity and ease-implementation to obtain a better performance. Overall, the fuzzy controller is suitable for the energy management problem and can effectively obtain good results. But due to it is based on human expertise, the optimality of solutions cannot be always guaranteed.

2.3.2 Optimization-based Control Strategies

According to the literature, rule-based controllers can reduce fuel rate and emissions, but their capabilities are limited due to they are designed relying on human experiences. Thus, contending optimization-based controllers have been

developed for hybrid-electric propulsion systems. Supported by theoretical basis and according to given cost functions, these controllers are able to find the most optimal solution for systems. Furthermore, based on whether the control strategy involves future information, i.e. whether it can be applied in real-time, optimization-based control methods can fall into two classifications: causal (real-time) optimization and no-causal (global) optimization. Recent bibliometric reveals that optimization-based controllers grasp more attention in research with a percentage of 56.7% compared to rule-based approaches 32.9% [102].

- **Non-Causal (Global) Control Strategies**

Generally, a controller whose instant response depends on future values of inputs is called as a non-causal controller. For this study, the 'non-causal' refers to the optimization problem along with the complete mission profile. Moreover, since the non-causal control strategy requires future mission requirements, this kind of controller is also known as 'global optimization-based', for which the entire mission information is taken as the 'global information'.

As the non-causal optimization-based controller contains future samples, so that, to some extends, it is difficult to implement non-causal controllers in practical cases. In other words, unless the upcoming mission information is prior-known, the non-causal control algorithm is hard to be realized for actual applications. On the other hand, the non-causal optimization control method augments the computational load due to the calculation scale has been extended. This feature increases the optimality of the result, but limits the applicability for real-time utilizations. Therefore, non-causal controllers are always applied offline to assist or evaluate other control algorithms [102].

Linear Programming (LP) is a typical non-causal controller, which was firstly applied to hybrid-electric systems in the 1990s [103]. Many research endeavours applying LP to improve fuel economies [104, 105, 106]. The linear programming algorithm firstly simplifies the nonlinear hybrid-electric powertrain into a less-complex linearized model, then finds the near optimum result through several solvers. In paper [107], the original convex power management problem was converted into a discrete-time linear problem by neglecting power bus voltage

ripples and engine transients, and the controller successfully achieved an 8% fuel consumption reduction for a series hybrid-electric propulsion system. However, since some of hybrid-electric propulsion systems are too complex to be linearized, the performance obtained by linear programming is restricted [89].

Dynamic Programming (DP) is another most-studied non-causal control methods for the power management of hybrid-electric power systems. The technique is based on Bellman's Principle of Optimality [108], which solves the underlying problem sequentially by backwards calculating the optimal control of each state at every step [109]. Therefore, DP algorithm is good at multistage problems, and can guarantee the global optimality of the solution [110]. At present, numerous studies managed power flows by using DP to calculate the power splitting ratio between the combustion engine and the battery pack and have achieved good results [111, 112]. Few research utilized DP indirectly, for example [113, 114], that extracted the optimal solution of subsystems, such as the gear-shifting ratio, to assist the energy management. In general, dynamic programming is an effective method, but it requests future information and high computation loads. Thus, some research aiming to reduce the DP computational burden of the energy management problem have been proposed, and results revealed that the solution optimality might be sacrificed for lower computation [115, 116]. Therefore, broadly speaking, the dynamic programming optimization-based controller is able to determine an exclusively optimal solution for the problem, but is hard to solve practical real-time problems. Later, in order to further improve the adaptability of DP, the Stochastic Dynamic Programming (SDP) method was invented and applied to hybrid-electric vehicles [117]. Instead of being optimized over an entire mission, the split ratio was optimized over a family of random driving cycles, which reduced the amount of calculation and outperformed the conventional DP controller. More interestingly, the SDP optimization is not a real-time solution by nature, but the control values can be used for real-time implementations [118].

Inspired by the evolutionary mechanism, the metaheuristic control method – Genetic Algorithm (GA) has also been applied for the energy management

problem in some research. The algorithm initially postulates a set of chromosomes as the initial population, then evaluates the performance of each individual through a fitness function. After that, it selects individuals and creates a sequence of new population along with genetic operators — crossover and mutation, and repeats abovementioned procedures until one of the stopping criteria is met. Genetic algorithm is a common optimization approach and can handle different operational constraints. Paper [119] and [120, 121] proved the suitability of GA to hybrid-electric vehicles.

Convex optimization is another non-causal control method. Due to it has low computational complexity, convex optimization can optimize multiple issues at the same time. The algorithm was firstly applied by Murgovski [122, 51] and Elbert [123], to solve the sizing and power management problem of hybrid-electric vehicles. Then, Murgovski [124] further investigated the sizing optimization by adding a variable of the battery lifetime into the sizing process, and obtained a different optimal result from the former result. Later, Xie [60] extended that work to hybrid-electric aircraft. It firstly converted the energy management problem into a convex question, and then implemented two techniques – change of variables and equality relaxation, to convexify the concave constraints. The study testified that the convex optimization method is robust to the disturbance in power demand, and it can obtain optimal results under both charge-depleting and charge-sustaining environments. Therefore, in general, the convex optimization-based control strategy is able to solve both sizing and power splitting problems, and it can take less time than DP even in the presence of active constraints.

Many other non-causal control strategies, such as particle swarm optimization [125], game theory [126, 127], DIRECT [128] and Space Exploration Unimodal Region Elimination [129], have been implemented for the supervisory controller of hybrid-electric vehicles as well. They are different from each other, but they all can deliver a global optimal solution for the system.

- **Causal (Real-time) Control Strategies**

Generally, a controller whose output only depends on present and past inputs is called as a causal controller. Since they do not need future information, causal

control methods are also called as real-time control strategies, and they are practically realizable for most of applications. So far, numerous causal technologies have been introduced into hybrid-electric power systems and obtained good performance, a brief review is given in the sequel.

Pontryagin's Maximum Principle (PMP) is a classic causal control strategy, which is able to solve real-time constrained optimization problems under reasonable assumptions. There are two advantages of PMP controllers. The first is that it can convert a non-causal optimization problem into a corresponding Hamiltonian minimization, which simplifies the problem and enables that to be solvable in real-time [130]. Secondly, it can provide an analytical solution to the power management problem [131, 132]. Paper [133] demonstrated the global optimality of the PMP principle from a mathematical viewpoint under reasonable assumptions. PMP method provides a theoretical feasibility for real-time applications, however, the large computational cost still limits its practicality. Thus, the study described in the paper [134], used quadratic programming to reduce the computational cost.

For hybrid-electric systems, the most representative causal control method is the Equivalent Cost Minimization Strategy (ECMS). Pisu and Rizzoni [83] proved the capability of ECMS to yield a near optimal solution at lower computational loads. Paganelli et al. [135] applied ECMS to convert the on-board electric energy depletion into an equivalent fuel consumption by using equivalent factors, and predicted the future cost that can compensate for the consumed energy. There are two challenges in ECMS: 1) the estimation of the equivalent factor, 2) transient dynamics of power sources [89]. Literature found that equivalent factors affect the performance of the controller, so that some studies applied Hamilton-Jacobi-Bellman equation [136, 137], genetic algorithm [138] or other optimization technologies to find the most optimal equivalence factor to improve the result. There is one limitation amongst ECMS controllers that they cannot sustain the battery SOC due to that equivalence factors need to be evaluated off-line. To eliminate this drawback, adaptive-ECMS and predictive-ECMS control strategies were both developed. The adaptive ECMS can adjust the original factor based

on a penalty function of the current SOC value [139], while the predictive ECMS is based on the predicted future system behaviors [140].

Robust control and extremum seeking are two other real-time optimization methods. Robust control can handle systems with uncertain parameters, unknown models, disturbance inputs, inaccurate measurements and high-nonlinear dynamics. They can maintain high stability and robustness, but may cause heavy computational burdens and fail to obtain near-optimal solutions [83]. Extremum seeking is a model-free optimization control strategy. It uses the periodic excitation input to stimulate the system plant, then probes the gradient and seeks the minimum value at the zero-gradient locations [141]. Bizon's work [142] realized a 1% – 2.1% improvement of the energy efficiency by using the extremum seeking algorithm.

Model Predictive Control (MPC) is one popular intelligent optimal control strategy suitable for real-time applications. Basically, the MPC algorithm is a feedback law based on prediction, optimization and receding horizon implementation. Future control inputs and future plant responses are predicted and optimized at regular time intervals with respect to a performance index. The first element of the calculated optimal control sequence will input into the system. With a sound theoretical basis, if a reasonably accurate dynamic system model is available, the MPC strategy can solve large scale control problem with multi-variables. MPC can also handle constraints of control inputs and states no matter the plant model is linear or nonlinear. Numerous relevant researches focused on improving fuel efficiency. Based on the MPC methodology, paper [143] proposed three optimal controllers for a parallel hybrid-electric power system. The simulation result showed that the controller obtained 1% — 3% improvement on fuel consumption, and it also proved that the fuel rate can be further reduced by more information. In paper [144], Balaji designed a linear MPC controller to reduce fuel consumption. Compared with the result of dynamic programming, the execution time was shortened by 94-98%, but the fuel consumption is 17% —30% worse than that of DP. Furthermore, the paper [145] and [146] proposed two MPC-based control strategies – linear and nonlinear MPC controllers for a power-split

hybrid-electric power system. Since the nonlinear MPC controller obtained a better fuel efficiency than the linear one, the study proved that the short-horizon MPC algorithm is applicable for solving the real-time fuel minimization problem online in a nonlinear framework. Instead of emphasizing on fuel consumption, Cairano [147, 148] proposed a linear MPC-based controller to maximize the pointwise powertrain efficiency for a series hybrid-electric vehicle. Through experimental testing in city and highway cycles, engine operating points were concentrated in a small high-efficient area, and increased fuel economy by 5.7% and 4.6% compared with results of the load-following and load-leveling deterministic controllers respectively. After that, Cairano [149] developed a driver behavior predictive controller based on the stochastic MPC algorithm. The new controller can further improve engine efficiency by re-configuring for accommodating changes in driver behavior. As for the latest research, dual-loop nonlinear MPC frameworks have been established for hybrid-electric vehicles [150, 151]. Presented in paper [150], the controller firstly solved a low-sampling rate MPC problem to determine the long-term battery SOC variation for the entire predictive driving cycle, and then fed the SOC variation to the inner MPC loop in order to control the plug-in hybrid electric vehicle. Paper [151] presented another two-level MPC controller to split energy flows. The high-level controller calculated the travel time and battery energy, while the low-level determine the engine operating parameters based on the result from the high-level controller. The result showed that the proposed controller can reduce 8% – 39% fuel consumption and improve driving comfort simultaneously.

2.3.3 Summary

Non-causal optimization-based control strategies require future mission information to achieve a more optimized solution. However, also for this reason, non-causal methods request a large amount of calculation and are hardly to be applied for practical problems. Therefore, non-causal controllers are always utilized offline, and work as a benchmark to assist or assess other control algorithms. Causal control algorithms generate control instructions for the next step only based on current and past information that are universally applicable

for real-time implementations. However, causal optimization-based algorithms cannot guarantee the optimality of the result, and they may not able to meet system constrains if the controller is not designed properly.

Overall, different control strategies are suitable for different control goals. The control method should be selected based on objectives and circumstances. If the information of the entire task is available, non-causal optimization-based controllers may outperform other controllers. However, in practice, the future information is always not prior-known, so that real-time controllers are more promising for practical uses.

2.4 Conclusion

This section mainly contains a literature review of hybrid-electric power systems. It consists of three parts: system design, subsystems and control strategies. Firstly, it discussed the design process, where different configurations and common sizing methods are discussed. Then, it introduced subsystems and listed their feasible modelling methods. After that, it gave a review about control strategies applying to the energy management problem. Both rule-based and optimization-based methods have been discussed and some representative control algorithms are introduced in detail.

3 SYSTEM DESIGN AND MODELLING

A good hybrid-electric propulsion system consists of a well-designed configuration, appropriate components and an intelligent power management strategy. This chapter will present the design process and the modelling method for each component of the distributed series hybrid-electric propulsion system. The configuration of the proposed system will be firstly demonstrated, which is the first objective of this thesis as shown in Figure 20, followed by a feature analysis for the predicted system characteristics. After that, modelling methods of the engine, motor/generator and battery pack will be introduced individually.

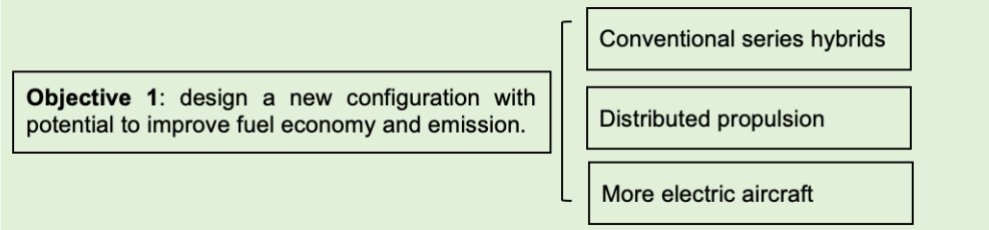

Figure 20 Chapter 3 structure.

3.1 System Design

As an indispensable means of transportation, aircraft brings many benefits to human life. With its continuous development, the raising awareness of negative aviation impacts inspired the research into sustainable aviation, thereby reducing aircraft fuel consumption and pollutant emissions. Commonly, hybrid aircraft has an opportunity to improve both above goals by applying multiple sources of energy. Therefore, this project proposed a new type of aircraft power system – Distributed Series Hybrid-Electric Propulsion System (DSHEPS).

For hybrid-electric propulsion systems, different configurations perform different characteristics. As the first proposed configuration, the structure of the series hybrid is the simplest compared to other hybrids. In addition, the series hybrid processes a most attractive advantage which effectively decouples the engine from the propulsion output. This characteristic allows the engine to keep operating in the high-efficient area no matter how much power is currently required. In other words, the series hybrid-electric propulsion system has the potential to obtain high fuel efficiency and being highly electrified. Therefore, the novel hybrid-electric propulsion system was designed based on the conventional series hybrid configuration.

Conventional series configurations have two main drawbacks: 1) energy loss; 2) heavy mass. Energy loss is caused by repeated energy conversions, and the system weight is burdened by an additional generator (please find the detailed explanation in chapter one). Therefore, two novel techniques are integrated into the original structure to improve its performance.

The first intelligent concept is the distributed propulsion technology, which uses multiple small motors and propellers to propel the aircraft. This propulsion layout can improve the aerodynamic property of wings and reduce the weight of the system [152]. Many small propellers distributed span-wise along the wing blow the wing during take-off and landing, which can effectively reduce the dynamic pressure over the wing and increase the lift. Moreover, this characteristic can reduce the wing area, and the smaller wing can further reduce cruise drag. Overall, the distributed propulsion technique benefits the system performance and reduces aircraft weight, which can compensate shortcomings of the series configuration.

The second modification is learned from the More Electric Aircraft concept [153, 154], which adds other electric loads into the main propulsion system. This integration simplifies the system and reduces the number of equipment on the aircraft, so that the usage rate of each component could be increased. To further improve the system efficiency, the electric taxiing proposal can also be adopted

into the new propulsion system. As a result, an example of flight stages of the designed hybrid-electric aircraft is shown in Figure 21.

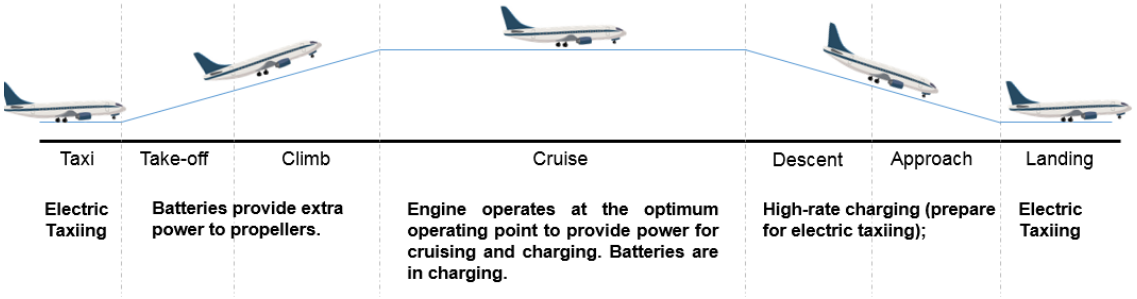

Figure 21 Flight stages of hybrid-electric aircraft.

Combining those two improvements can result in a rough system configuration, as illustrated in Figure 22. The left part consists of two power sources (the engine and the battery pack) and other electric loads of the aero vehicle. The right part of the system are motors and propulsors, whose number can be different values. This study initially applied six small motors and six propellers, but the number could be modified in the future. Based on the dynamic property of each component and the design proposal, a detailed system flowchart can be obtained which is shown in Figure 23.

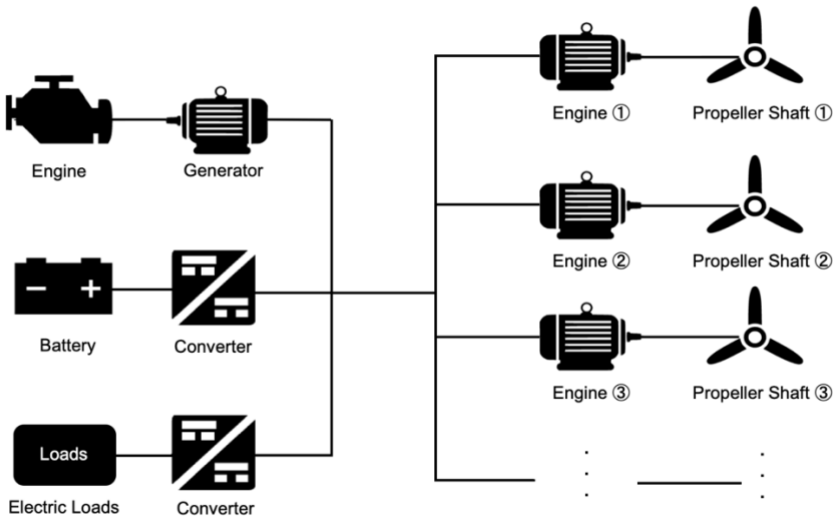

Figure 22 Distributed series hybrid-electric propulsion system.

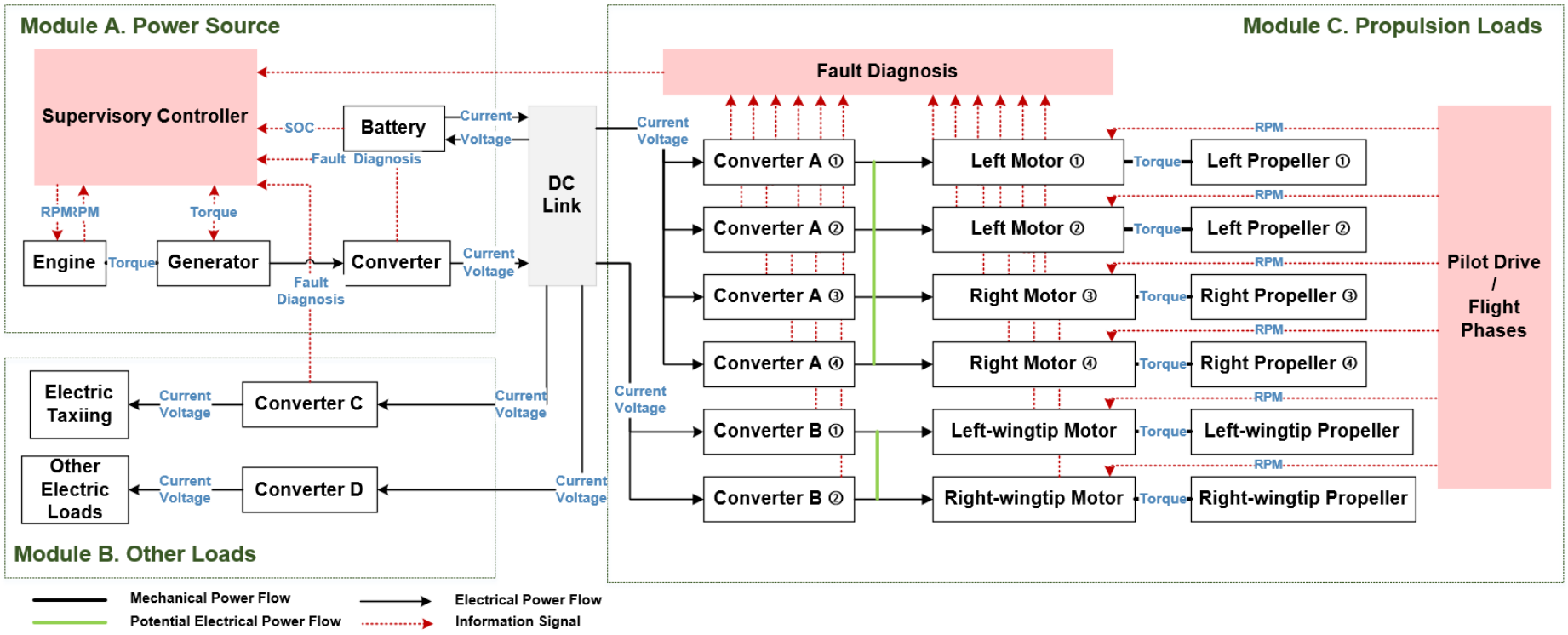

Figure 23 Schematic diagram of the designed distributed series hybrid-electric propulsion system.

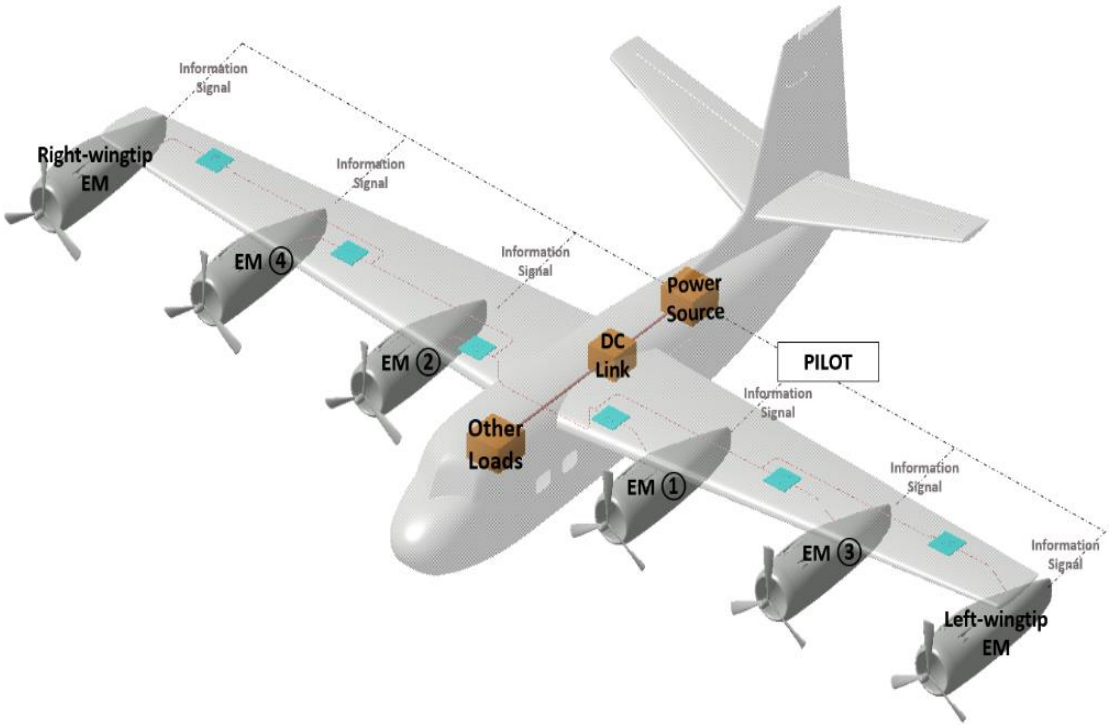

Figure 24 System layout.

The system can be divided into three parts. The first module is the power source module, which mainly provides energy to the other two parts. The module is composed of an engine, a generator, a battery pack and a converter. The engine produces energy by burning the fuel and the generator converts that energy into electricity. The engine and the generator are mechanically locked together, which can be considered as a power plant converting fuel into electrical energy. The battery pack is the storage unit of Module A. Because the battery pack can response quickly, the battery pack is a buffer between the engine-generator set and system loads. Hybrid-electric propulsion systems are usually equipped with a small engine, i.e. the maximum capacity is lower than the maximum power demand. Thus, when the power requirement is larger than the engine capacity, the battery pack discharges and supplies electricity to system loads in order to compensate for the shortfall. Vice versa, if the power requirement is lower than the engine-generator output, the excess electrical energy will charge the battery. Overall, the input of module A is fossil fuel and stored electrical energy, and the output is electricity. The primary supervisory controller in this part is used to coordinate the engine-generator and the battery pack.

The second part of the system is other electric loads. This module reveals the MEA technology, which integrates other electric loads into the entire system. Electric loads commonly refer to aircraft avionics, including communications, navigations, the display and other hundreds of functional systems. If the main propulsion system can power all electronic systems of aircraft, it is not necessary to allocate another electric system on aircraft. Therefore, it is worthy to combine the propulsion system with avionics together so that the number of system components and the total aircraft weight could be both reduced. Furthermore, the battery can also provide energy to support an electric taxiing. In which, if the remaining energy of the battery pack is capable to realize an electric taxiing after aircraft landing, the engine can be shut down earlier and applied an electric motor to drive the aircraft. This tentative plan is able to further reduce aircraft fuel consumption and increase system efficiency.

The third part is the propulsion load, which is responsible for propelling the aircraft. The module currently adopts a symmetrical structure assembling by six motors and six propellers. According to aerodynamic properties proposed in the literature, two motors at wingtips are different from other motors. Please note that both motors and propellers should be carefully selected, since their size can affect the aircraft aerodynamic properties. There are six converters in the diagram that corresponds to each motor respectively. These converters are always required in practice regardless if voltages are same or different. In addition, there are two integral parts in this module: the fault diagnosis and the pilot drive system. The fault diagnosis system monitors the operation of each motor and propeller. The pilot drive system is used for assigning instructions to each propeller to complete the mission. If one motor or propeller fails, the pilot drive function can re-calculate the mission and re-issue the command. Therefore, the proposed distributed series hybrid-electric propulsion system possesses re-configurability and higher flexibility to handle emergency situations. Please note that these two functional parts are crucial to the system, but they are not looked as part of this thesis work. Related work is recommended for future research.

In the long term, the designed system is still competitive compared with others. Firstly, the electrification degree of this configuration is relatively higher than other hybrids, so that the system is easy to install, and all components can be sparsely allocated. Secondly, since there is no complex mechanical transmission, the DSHEPS is ease-maintenance, that both the battery pack and the engine-generator set can be easily replaced. The next advantage of the system is its high flexibility. At present, the power-to-weight ratio of the battery is quite low. Thus, the engine is the main power source, while the battery pack acts as an auxiliary component and a buffer of the system. Assuming the battery technology can be significantly improved in the future, the emphasis can be shifted. If the battery is high powerful, the engine will operate as an auxiliary device and exist as the emergency power source in case of battery-failure conditions. Overall, the designed hybrid-electric power system has strong competitiveness and potential to achieve higher efficiency and lower emissions.

3.2 Modelling

The performance of the designed system is simulated by using MATLAB Simulink and Simscape system-based software packages. The modelling method of each main component are demonstrated in the sequence.

3.2.1 Internal Combustion Engine

The engine dynamic is displayed by a simplified mean value model [155]. The simplified MVM method is an experimental data-based modelling method, which cannot illustrate manifold dynamics but reserves the dynamic between the engine speed and throttle demand. In the simplified MVM, the engine torque can be obtained by:

$$T_{e,ref} = f(\delta_e, \omega_e, e_{air}) + T_{e,idle} \quad \textbf{(3-1)}$$

Where, $T_{e,ref}$ refers to the requested engine torque, $T_{e,idle}$ is the idle torque from idle speed controller, the term $f(\delta_e, \omega_e, e_{air})$ is an function which implies the relationship between the throttle command δ_e, the angular velocity ω_e and the

coefficient e_{air}. e_{air} is an altitude-related coefficient to compensate the engine loss caused by the variation of air density.

$$\dot{T}_e(t) = -\frac{1}{\tau_e}T_e(t) + \frac{1}{\tau_e}T_{e,ref}\left(t - \delta_{e,prc}\right) \quad \textbf{(3-2)}$$

The equation (3-2) shows the relationship between the requested torque $T_{e,ref}$ and the induced torque $T_e(t)$. The time constant τ_e is the time for intake fuel/air mixture, and $\delta_{e,prc}$ stands for the time period for one engine process.

The rotational dynamic of the engine can be governed by (3-3), where J_e is the inertia of the engine and $T_{e,load}$ is the torque of the load. In series hybrids, due to the engine and the generator coupled together, the load torque of the engine equals to the torque of the generator. Besides, the restriction of the engine speed should also be imposed on the output of rotational dynamics module.

$$\frac{d\omega_e}{dt} = (T_e - T_{e,load})/J_e \quad \textbf{(3-3)}$$

3.2.2 Electric Motor & Generator

Under three assumptions, the Permanent Magnet Synchronous Motor could be modeled by the $d-q$ model [69]. The $d-q$ model uses some differential equations and coordinate transformations to reveal the recursive mathematical logic of the PMPM operating process. For PMSMs, the stator uses three-phase current to stimulate magnet (abc frame), while the rotor uses a Direct Current (DC) current to do that ($d-q$ frame). Therefore, the $'abc' - 0 - 'd-q'$ transformation is important in the modelling.

At first, the dynamic behavior of the motor can be described by (3-4) and (3-5) based on the $d-q$ frame, where the subscript $_d$ and $_q$ refer to the $d-$ and $-q$ axis respectively.

$$V_d = R_s \cdot i_d + L_d \cdot \frac{di_d}{dt} - \omega_r \cdot L_q i_q \quad \textbf{(3-4)}$$

$$V_q = R_s \cdot i_q + L_q \cdot \frac{di_q}{dt} + \omega_r\left(L_q i_q + \lambda_{af}\right) \quad \textbf{(3-5)}$$

In above equations, V presents the stator voltage, i is the stator current and R refers to the resistance. The parameter L presents the stator inductances, ω_r is the angular speed of the stator electromagnetic field, and λ_{af} refers to the magnet mutual flux linkage. These two formulas could be rewritten to:

$$i_d = \int \left(\frac{V_d - R_s \cdot i_d + \omega_r \cdot L_q i_q}{L_d} \right) dt \quad \textbf{(3-6)}$$

$$i_q = \int \left(\frac{V_q - R_s \cdot i_q - \omega_r \cdot (L_q i_q + \lambda_{af})}{L_d} \right) dt \quad \textbf{(3-7)}$$

The rotational dynamic of the motor is shown by (3-8):

$$T_m = T_{m,load} + T_{m,loss} + J_m \frac{d\omega_m}{dt} \quad \textbf{(3-8)}$$

where, $T_{m,load}$ is the load torque requested by the propeller, $T_{m,loss}$ refers to the motor torque loss, J_m is the moment of inertia and ω_m represents the speed of motor. The motor torque loss $T_{m,loss}$, including friction loss and damping, is approximated by the efficiency map supplied by manufacturers [60]. There is an important relationship between the motor speed and the stator electromagnetic field speed as illustrated by Equation 3-9, where the parameter P_{pole} is the number of pole pairs.

$$\omega_r = \omega_m \cdot P_{pole} \quad \textbf{(3-9)}$$

Motor torque T_m is given by:

$$T_m = \frac{3}{2} P_{pole} [\lambda_{af} i_q + (L_d - L_q) i_d i_q] \quad \textbf{(3-10)}$$

Based on the equation (3-8) and (3-9), the angular velocity of the motor ω_m, and the angle θ between the stator phase A and the rotor could be obtained:

$$\omega_m = \int \left(\frac{T_m - T_{m,load} - T_{m,loss}}{J_m} \right) dt \quad \textbf{(3-11)}$$

$$\theta = \int \omega_r dt = P_{pole} \cdot \theta_m = P_{pole} \cdot \int \omega_m dt \quad \textbf{(3-12)}$$

The angle θ is an important parameter in the $'abc' - 0 - 'd - q'$ transformation, based on that, the voltage and current of each phase could be transformed into $d - q$ frame or vice versa. The transformation is shown as below.

$$\begin{bmatrix} i_a \\ i_b \\ i_c \end{bmatrix} = \begin{bmatrix} cos\theta & -\sin\theta \\ cos\left(\theta - \frac{2}{3}\pi\right) & -\sin\left(\theta - \frac{2}{3}\pi\right) \\ \cos(\theta + \frac{2}{3}\pi) & -\sin(\theta + \frac{2}{3}\pi) \end{bmatrix} \cdot \begin{bmatrix} i_d \\ i_q \end{bmatrix} \quad \textbf{(3-13)}$$

$$V_d = \frac{2}{3}[\cos\theta \cdot V_a + \cos\left(\theta - \frac{2}{3}\pi\right) \cdot V_b + \cos(\theta + \frac{2}{3}\pi) \cdot V_c] \quad \textbf{(3-14)}$$

$$V_q = -\frac{2}{3}[\sin\theta \cdot V_a + \sin\left(\theta - \frac{2}{3}\pi\right) \cdot V_b + \sin(\theta + \frac{2}{3}\pi) \cdot V_c] \quad \textbf{(3-15)}$$

Based on above equations, the motor dynamic in each second could be determined. Since the electric motor is able to be used as a generator, the modelling approach of the generator is same as that of the motor, the only difference is that $T_{m,load}$ is a negative value.

3.2.3 Battery

In this study, the battery model should be able to represent the charge/discharge curve of lithium batteries, especially the variation amongst the battery current, voltage and SOC. The modelling method, which was firstly proposed by Shepherd in 1965 [76] and then improved by Tremblay [77, 78], is applied for modelling the battery pack in this study. This battery modelling method neglects the RC circuit dynamics but can display the relationship between the battery open-circuit voltage and current.

The Shepherd model is a fitting process based on experimental data. Under four assumptions: 1) The anode and/or cathode have porous active materials; 2) The electrolyte resistance is constant through discharge; 3) The cell is discharged at a constant current; 4) The polarization is a linear function of the active material current density [76], the discharge performance of the battery pack could be predicted by the battery current:

$$E = E_0 - K \cdot \frac{Q}{Q - \int idt} \cdot i - K \cdot \frac{Q}{Q - \int idt} \cdot i^* + A_b e^{-B_b Q^{-1} \cdot \int idt} \quad \textbf{(3-16)}$$

and, the battery SOC is:

$$SOC = \frac{Q - \int idt}{Q} \quad \textbf{(3-17)}$$

In the equation (3-16), E is the open-circuit voltage of the battery, E_0 is the battery constant voltage, and K is the polarization coefficient. In addition, Q refers to the total capacity of the battery pack. As a result, the term $(Q - \int idt)$ calculates the instant battery capacity, where i is the battery current and $\int idt$ presents the actual discharged energy. The starred parameter i^* refers to the filtered current obtained by a low pass filter. It can not only solve the algebraic loop problem, but also reproduce a slow dynamic behavior of battery voltage for a step response [77]. The last term $A_b e^{-B_b Q^{-1} \cdot \int idt}$ gives an estimation of the initial potential drop, in which the parameter A_b is the exponential voltage coefficient and B_b is the exponential capacity coefficient. Both two parameters are empirical constants obtained from the discharge curve [76].

There is a difference between the discharging and charging process that the polarization resistance K will increase along with the charged energy $\int idt$ decreases. As a result, the charging performance could be described by:

$$E = E_0 - K \cdot \frac{Q}{Q - \int idt} \cdot i - K \cdot \frac{Q}{\int idt} \cdot i^* + A_b e^{-B_b Q^{-1} \cdot \int idt} \quad \textbf{(3-18)}$$

However, if the battery pack is fully charged, the current will decrease to zero and the term $\frac{Q}{\int idt}$ will become infinite. It is not practical and may cause a computational issue. Therefore, based on the shifting of the contribution of the polarisation resistance, the characteristic function of the battery charging could be updated to:

$$E = E_0 - K \cdot \frac{Q}{Q - \int idt} \cdot i - K \cdot \frac{Q}{(\int idt)^{-0.1Q}} \cdot i^* + A_b e^{-B_b Q^{-1} \cdot \int idt} \quad \textbf{(3-19)}$$

Then, the closed-circuit voltage is able to be determined by the current and the internal resistance R_b.

$$V_b = E - i \cdot R_b \quad \textbf{(3-20)}$$

3.3 Conclusion

This section presented the design process of the proposed distributed series hybrid electric propulsion system, as well as modelling methods of the engine, electric motor/generator and Li batteries. It started with the system design process, where emphasizing two improvements of the new proposed system. The detailed system flowchart and characteristic analysis are illustrated. Thereafter, this chapter presented different modelling methods for each main equipment. The dynamic characteristics of the internal combustion engine were achieved by a simplified MVM model, which mainly revealed the relationship between the engine throttle and engine torque. The electric motor/generator was modelled by the $d-q$ model. Based on the recursive mathematic logic, the model can show the electromagnetic dynamics. As for Li-batteries, the Shepherd model is applied to describe the charge/discharge characteristics. All models can respond quickly and be constructed by MATLAB.

4 ENGINE SIZING

Since the configuration has been determined, each component could be selected sequentially based on mission requirements and standards. This chapter will mainly talk about the sizing method for the engine, which is the first target in the second objective.

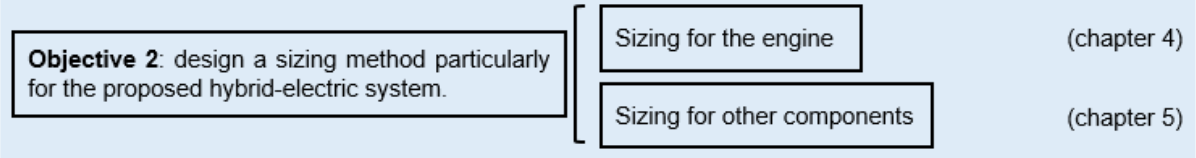

Figure 25 Chapter 4 structure.

Indirect Engine Sizing via Distributed Hybrid-Electric UAV State-of-Charge Based Parametrisation Criteria

Abstract

This paper presents a design process for the challenging problem of sizing the engine pack for a distributed series hybrid electric propulsion system of unmanned aircraft vehicle. Sizing the propulsion system for hybrid electric UAVs is a demanding problem because of the two different categories of propulsion, (the engine and the motor), and the electrical system characteristics. Furthermore, what adds to the difficulty is that the internal combustion engine does not directly drive the propellers, but it is connected to an electrical generator and therefore provides electrical power to the electric motors and propellers. Hence there is a clear distinction from the traditional engine solutions which are mechanically coupled to the propeller. This paper addresses this specific distinction and proposes an indirect solution based on properties on the electrical part

of the system. In particular, a novel parametric characterisation engine sizing approach is presented using the battery pack SOC during a realistic UAV flight scenario. Five candidate engine options were considered with different starting conditions for the electrical system. The results show that by using the SOC properties it is possible to select an appropriate size of engine pack while carrying a suitable electrical propulsion pack. However, the solutions are not unique and are appropriate for given design criteria clearly indicated in the paper.

4.1 Introduction

In the past couple of decades, the largest growth in commercial air transport have a big impact and changed the world in numerous ways, primarily by increasing the speed of travel, aiding growth in the international business, and making the world more connected. However, a conventional aircraft consumes a large amount of fuel during each flight and simultaneously emits greenhouse gases, noise, heat, and particulates. To prevent the exacerbation of aircraft negative impact on energy supply and environment, a higher fuel-efficiency and more environmental-friendly propulsion system is required. In general, there are three ways to improve aircraft performance: (a) optimization of the existing aircraft propulsion systems; (b) development of new propulsion components, and (c) a combination of existing propulsion subsystems into hybrid powertrains. Based on the third method, this paper presents a novel Distributed Series Hybrid Electric Propulsion System for an UAV.

At present, NASA, Airbus, Boeing, and many other companies are investing in hybrid-electric aircraft research to improve aviation performance. The most successfully tested hybrid-electric aircraft are UAVs and small-scale aircraft. Due to the fuel having higher power density than batteries', the fuel system contains more energy than an electric system for the same mass. Therefore, hybrid electric UAVs always can survive a longer flight. Hybrid UAVs emerged from 2010s, and to date, the one with the longest endurance is 'ALTI Transition', which offers up to 12 hours flight carrying no payload. University of Colorado Boulder [1], Queensland University of Technology [2], and U.S. Airforce Research Laboratory [3] all have researched this area. The other ongoing small hybrid aircraft project is 'AIRSTART', project in the UK, which is aiming to develop a parallel hybrid propulsion system to support routine small UAV operations beyond visual line of sight [4].

In terms of the hybrid-electric midscale demonstrators, several aircraft have been successfully tested. The ‘Alatus’ motor-glider, designed by Cambridge University, firstly realized a parallel hybrid electric power system. It utilises a 2.8kW internal combustion four-stroke leaf blower unit paralleled with a 12kW electric motor, and the first truncated flight took place in 2010. Embry-Riddle Aeronautical University, in association with Google, designed another hybrid plane ‘Eco-Eagle’. It also uses a parallel hybrid technology and was successfully tested in 2011 [5]. The first midscale series hybrid-electric aircraft is the ‘DA36 E-Star’ and its successor version, developed by Diamond Aircraft, EADS, and Siemens AG in 2013 [6]. The series system of ‘DA36 E-Star’ can provide 80kW power during take-off and 65kW continuous power during cruising. Later, Cambridge University developed another hybrid aircraft ‘SOUL’, which firstly realized the capability of on-board battery charging. It applies a parallel hybrid electric propulsion system and was successfully tested in 2014 [7].

Research in large-scale aircraft has increased over the recent years. The new series of aircraft from NASA is particularly designed using hybrid-electric propulsion systems. For example, the ‘N3-X’ Hybrid Wing Body Turboelectric Plane [8] and the ‘STARC-ABL’ Turboelectric Plane [9] utilise gas-turbine/electric hybrid propulsion systems; the ‘SCEPTOR X-57’ plane uses an engine/electric hybrid power system [10]; and the Subsonic Ultra Green Aircraft applies a liquefied natural gas fuel cell/electric hybrid propulsion system [11]. Meanwhile, Airbus, Rolls-Royce, and Siemens are working together to test the feasibility of a hybrid electric propulsion system in a relatively large aircraft, called ‘E-Fan X’ Plane, and the test flight is currently planned in 2020 [12].

As hybrid-electric aircraft is becoming increasingly more popular, new attempts to develop different hybrid aircraft are expected to increase. Therefore, the method for reasonable designing and sizing of hybrid electric propulsion system is also essential. Many optimal sizing works have been conducted in the literature. Most studies focus on single objective optimization, e.g. the paper [13] optimized the capacity of different components of a hybrid system using the loss of power supply probability and the ‘levelized’ cost of energy. A small number of studies focus on multi-objective optimization, which is able to optimize both system performance and other criteria [7, 14]. The paper [15] presents a method to optimize plant parameters and minimize the total fuel consumption simultaneously. However, none of the previous research discussed the relationship of battery’s performance and parameter sizing. In this

paper, we present a novel parametric engine sizing approach to size the engine pack for a hybrid-electric UAV. From simulation results, i.e. batteries pack SOC, the characteristics of five systems with different sized engines are obtained and analysed.

Therefore, based on a set flight scenario, a reasonable engine size region can be determined. The proposed sizing approach provides a new cognition of series hybrid-electric systems, especially focusing towards the relationship and synergy between fuel and electricity.

4.2 System Design

Within a simplified system design progress, as shown in Figure 26, the DSHEPS is designed. The system is basically derived from a conventional series HEPS configuration, integrated with the distributed propulsion concept and the more electric aircraft concept, the resulting system has improved fuel economics and emits fewer emissions.

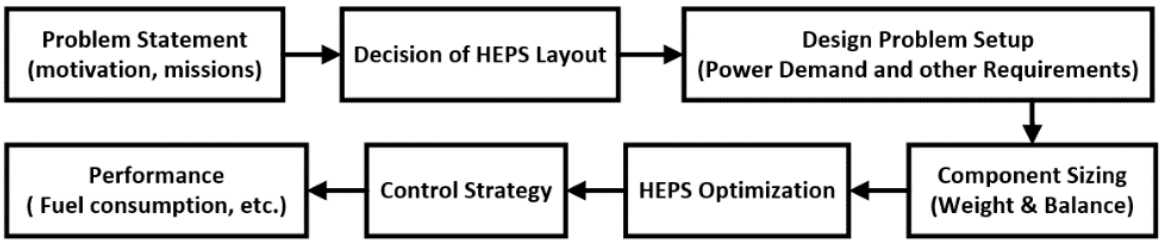

Figure 26 System design sequence.

In general, hybrid systems are categorized into series, parallel and complex hybrid. In particular, the series hybrid system has similar properties to a pure electric system, thus resulting in emission reduction. Furthermore, an additional important advantage of the series configuration is the decoupling between demand and supply. Engines can continuously operate at the most optimal operating point regardless of power requirement, which provides an enormous improvement on fuel efficiency. In addition, due to the high degree of electrification, mechanical linkages are not necessary so that all system components can be positioned at different locations within the UAV which increases subsystem level flexibility as shown in Figure 27.

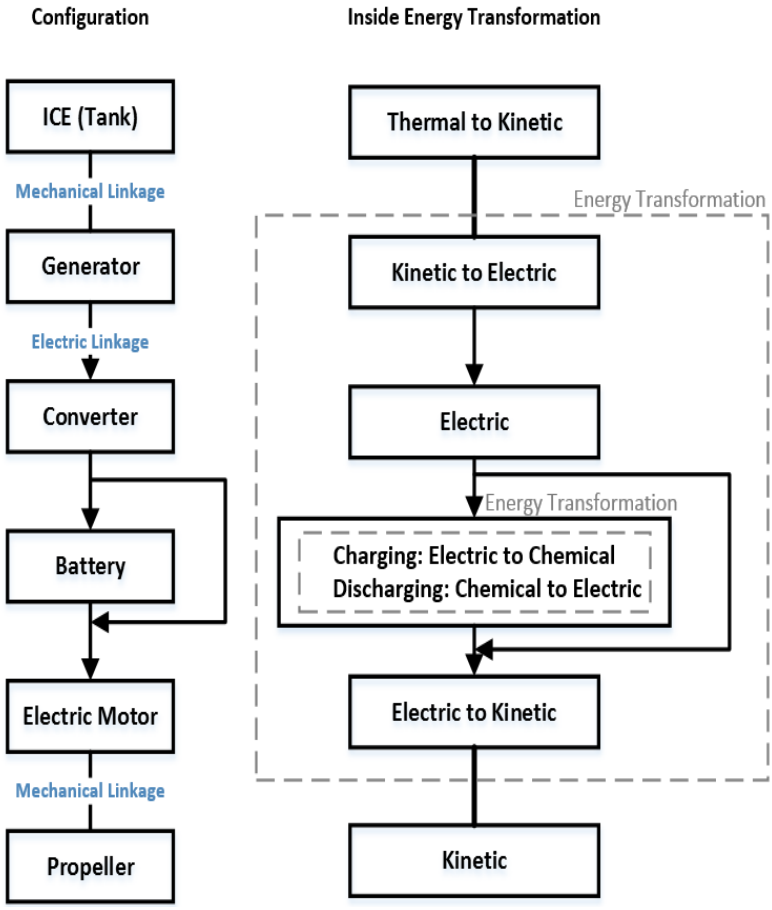

Figure 27 Series hybrid configuration and internal energy transformations.

However, series HEPSs have two persistent drawbacks: over-weight and inevitable energy loss. Normally this is because of the extra generator, battery and the large EM. Increasing the overall aircraft weight will consequently cost more fuel to complete the same mission. This is a challenge which needs solving. The other drawback is the energy conversion loss due to the multiple energy transformations, i.e. kinetic energy to electrical energy, electrical energy to chemical energy. Although the engine can operate at the high-efficiency area, it cannot be guaranteed that the series hybrid systems will have an increased efficiency. Therefore, in order to resolve these challenges, the distributed propulsion concept and the MEA concept are integrated.

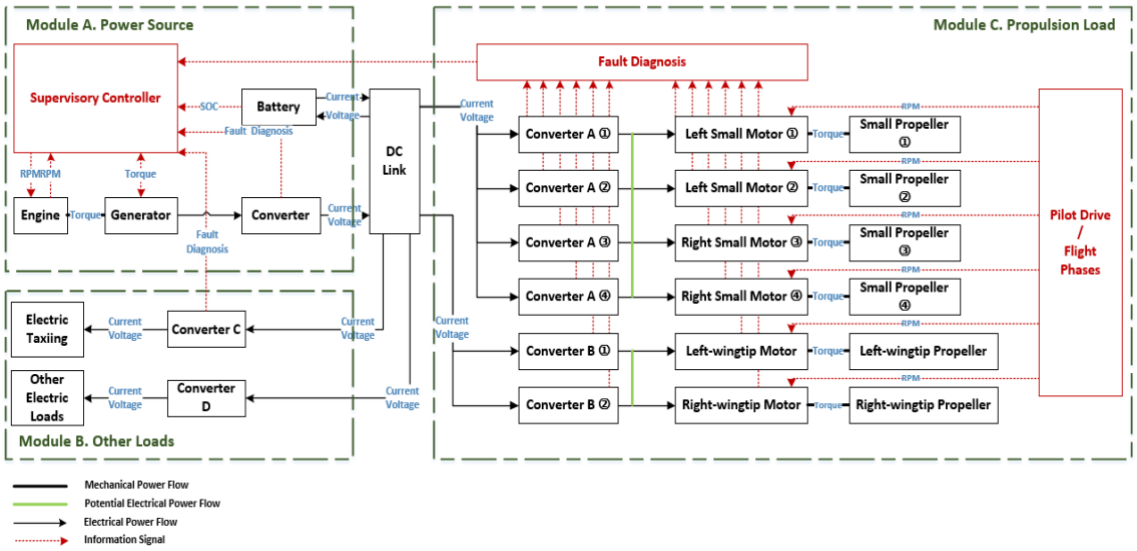

Figure 28 Distributed series hybrid-electric propulsion system.

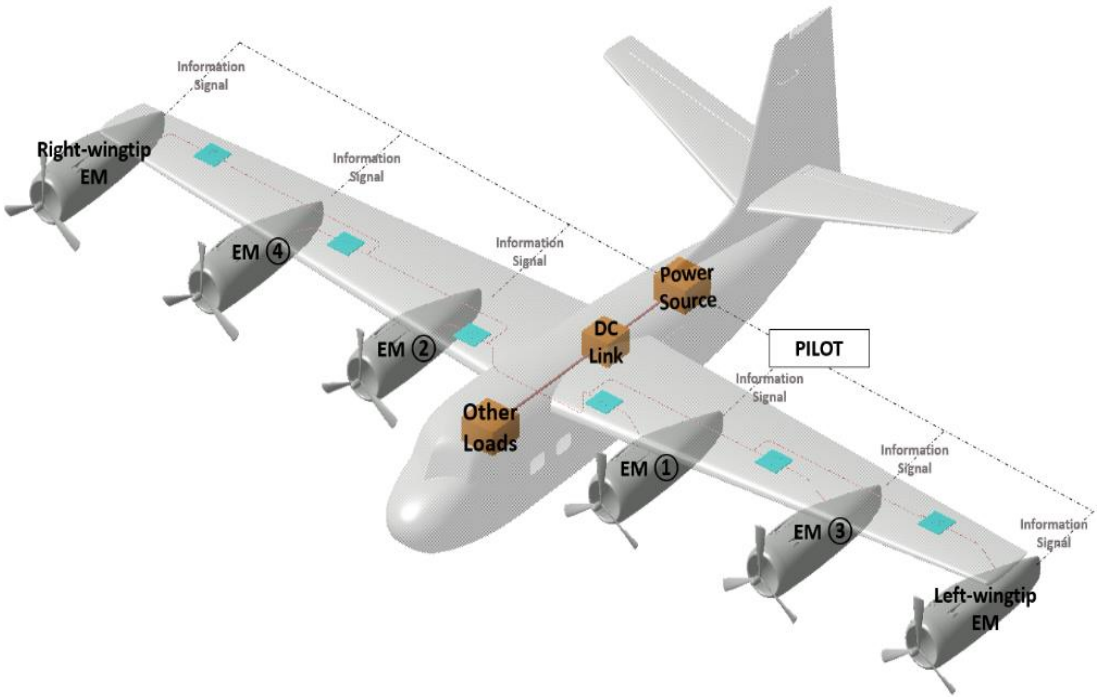

Figure 29 System layout.

The designed complete DSHEPS is shown in Figure 28 and Figure 29. For easier analysis, we divided the system into three parts: power source, propulsion load and other loads. The ‘power source’ consists of an engine, a generator, a converter, and batteries. All devices provide electricity to the loads or/and stores electricity in the batteries. The second part ‘propulsion load’ includes converters,

motors, and propellers. Motors are arranged symmetrically and connected to a corresponding propeller. Here, converters are not necessary if the rated voltage of motors are same as it of the main electric net (in this paper, the simulation neglects converters). The ‘other loads’ represents the auxiliary electric loads including an electric taxiing system, avionics systems etc.

According to the ‘propulsion load’ block shown in Figure 28, the designed system has six small motors instead of using a single motor. Applying multi small electric propulsion has many benefits. Firstly, it provides a robust propulsive control and enhances flight safety. Moreover, as engines are normally sized as large as twice the power demand for redundancy reasons. For example, a Boeing 737, 757, 767 and 777 can take off with one of two engines out. The distributed propulsion architecture reduces the excess weight from the extra engine since one extra small motor provides equal flight safety as one extra big engine in conventional aircraft. Additionally, the distributed propulsion concept increases the dynamic pressure over the wing and reduces aerodynamic drag [16-19], so that it can reduce the wing area, lighten the aircraft structure, and reduce power demand.

Similarly, inspired by the MEA concept [20-22], some improvements are made into the system. The most important improvement is the expanded electric network. Here, the engine not only provides propulsion power but also transports electric energy to all existing electric loads (flight control actuation, fuel pumping, etc.). This integration removes unnecessary electronic equipment, reduces system weight, eases the maintenance and improves system efficiency. The second improvement is the adoption of the electric taxiing concept. The electric taxiing system is more efficient and safer. Also, the engine can be turned off earlier, which can reduce engine’s operating time and reduce fuel consumption.

4.3 SOC-based Criteria for Aircraft Engine Sizing

As the system isolates the engine from the demand, the engine sizing becomes less challenging. To reassure safety, there are three engine requirements in this paper:

1. The engine can continuously provide power on a low fuel consumption rate.

2. Batteries can fill the gap between total power requirement and engine output.

3. Motors can provide enough torque and speed to propellers.

Table 3 UAV parameters [23].

Drag coefficient, C_D	0.067	Wing area, A_W	3.76 m^2
Lift coefficient, C_L	0.614	Air density, ρ	1.11 kg/m^3
Indicated airspeed, v	50 m/s	Lift to drag ratio	9.16
Maximum take-off mass, m	150 kg	Cruising altitude	1000 m

The properties of the example UAV are shown in Table 3 [23]. Based on this information, the power demand for cruising could be determined by the following equations. The aerodynamic drag D_a is depended on the drag coefficient C_D, the surface area over the air flows A_W, the density of the air ρ, and the square of the velocity v^2. Because the cruising altitude is approximately 1000m, the required power for cruising is about $P_{cruise} = 17kW$. Assuming the motor efficiency is 96% and the batteries efficiency is 98%, the required power for engine P_{req} could be determined. It is worth mentioning that, electronic system efficiencies have been used to calculate the power demand of the Module A (power source). This method ensures that the system would generate enough energy to complete the task or even produce surplus energy. Otherwise, there is a possibility that system cannot accomplish the mission, so that the battery pack may deplete quickly and cannot get charged in time.

$$D_a = \frac{1}{2} C_D A_W \rho v^2 \quad (N) \tag{4-1}$$

$$P_{cruise} = D_a v = \frac{1}{2} C_D A_W \rho v^3 \quad (N) \tag{4-2}$$

$$P_{req} = \frac{17\ Kw}{96\% * 96\% * 98\%} = 18.8\ kW \tag{4-3}$$

Therefore, the flight scenario and the engine power requirement are determined, as shown in Figure 27. Please note that the assumption of a constant thrust level leads to slight inaccuracies in the determination of the required energy.

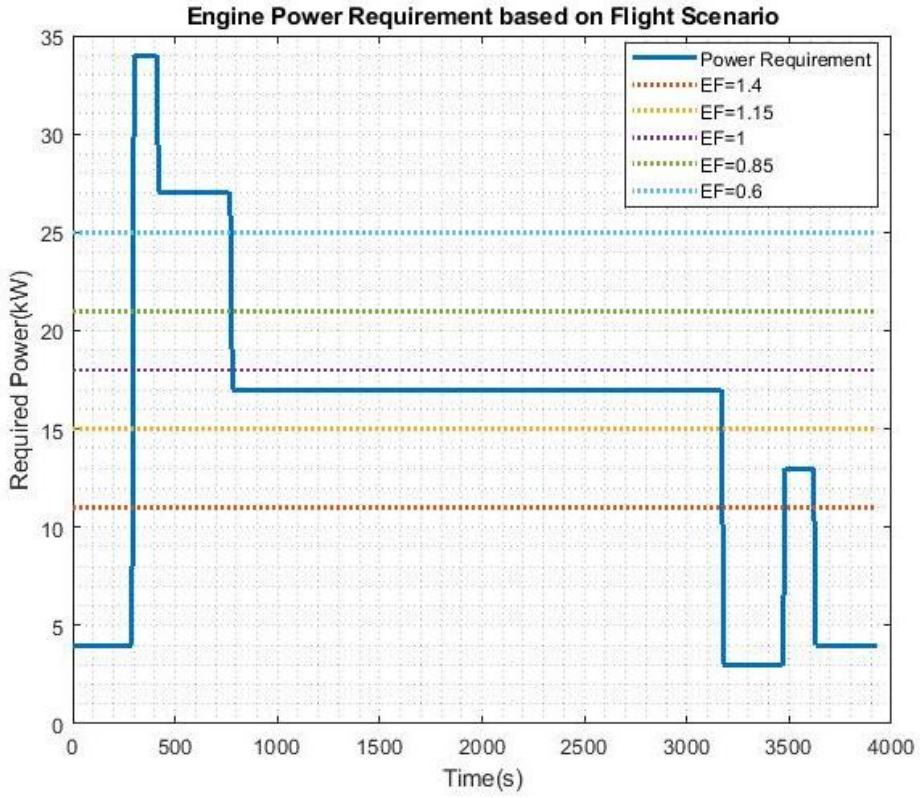

Figure 30 Power requirements of flight scenario and each engine's power.

To find an appropriate engine and observe the parametric variation, several engines have been simulated. These engines are selected based on a hybridization factor. The hybridization factor is a parameter mirroring the relationship between the sizes of the different power sources [24]. The first hybridization factor HF was introduced by Lukic and Emadi [25]:

$$HF = \frac{\left(P_{m\_max} - P_{e\_max}\right)}{P_{m\_max}} \quad \textbf{(4-4)}$$

P_{m_max} and P_{e_max} are the maximum power of motor and engine. The original hybridization factor HF shows the importance of the engine or the motor as part of the whole system. However, since the engine is always operating at its most efficient point, HF is difficult to clearly describe the proportion of electric energy and kinetic energy. Therefore, two other factors HF_{opt} and EF are developed for this paper, as shown in equation (4-5) and (4-6). P_{e_opt} is the engine output power at the most efficient area, and P_{req_av} is the average power of the mission

requirement. Engines are selected from $0.6EF$ to $1.4EF$, and the detailed information is represented in Table 4.

$$HF_{opt} = \frac{\left(P_{m\_max} - P_{e\_opt}\right)}{P_{m\_max}} \quad \textbf{(4-5)}$$

$$EF = \frac{P_{e\_opt}}{P_{req\_av}} \quad \textbf{(4-6)}$$

Table 4 Specifications of engines, motors, and batteries.

Engine type	Max power	Lowest-fuel-rate power	HF_{opt}	EF
RT300LCR	20kW @6500*RPM*	11*kW* @5000*RPM*	0.78	0.60
RT300XE	21kW @6500*RPM*	15*kW* @5250*RPM*	0.75	0.85
RT600JET-A1	38kW @6500*RPM*	19*kW* @4500*RPM*	0.62	1.05
RT600LCR	40kW @6500*RPM*	21*kW* @4750*RPM*	0.60	1.15
RT600XE	52kW @6500*RPM*	25*kW* @4750*RPM*	0.50	1.40
Motor type	Max continuous power	Max power	Efficiencies	
EMRAX228	42*kW*	100*kW*	96%	
Batteries	Capacity	Nominal voltage	Efficiencies	
Li-Po batteries	13*Ah*	296*V*	98%	

4.4 Simulation Result and Discussion

A key part of the design process is to explore the parametric variations prior to building a prototype UAV, thus reducing the design and development costs. Therefore, three simulations are processed for each selected engine with different initial SOC: $SOC_A(t=0) = 50\%$, $SOC_B(t=0) = 75\%$ and $SOC_C(t=0) = 100\%$. Engines has three fundamental operating modes: (a) the electric mode, (b) the ideal mode, and (c) the maximum power mode. Mode conversions are triggered by the SOC. In this paper, the high threshold is set as 80% and the low threshold is set at 20%. Namely, when the SOC is beyond 80%, the system

will switch into the electric mode; while if the SOC is below 20%, the system will switch into the maximum power mode. Moreover, this system incorporates a gap which results in obtaining an extra 10% SOC during the charging process. If the batteries were in the charging mode, the system will be switched back to the ideal mode at 90% SOC instead of 80%. This setting has dual purposes, which not only guarantees the power output, but also protects batteries.

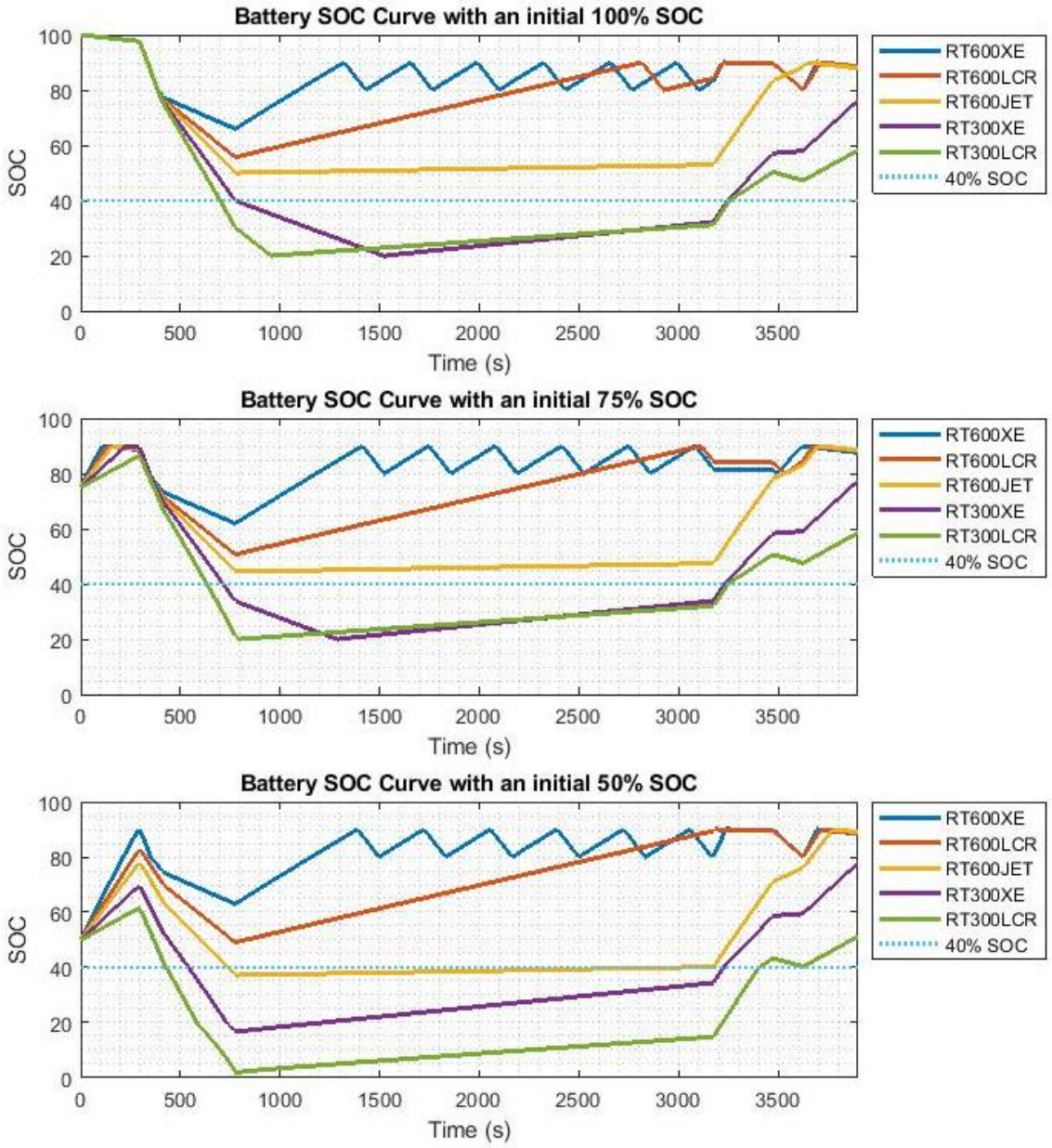

Figure 31 Batteries SOC curves.

Figure 31 shows the SOC curve of each simulation. When simulations start with a full SOC_c, all simulations began from the electrical mode. Gradually, when the SOC drops below 80%, the differences of various engines began to show up by the altered discharging rate. Amongst them, RT600XE is the most powerful engine and firstly recharged back to 80% SOC. Since its ideal power output is about 1.4 times of the average power demand, the SOC stays in 80%-90% area for most of the flight. RT600LCR engine recovers to 80% SOC as well but at a slower rate than RT600XE. RT600JET outputs just the right power as demanded at its ideal operating point. The SOC stays stable during the cruise mode. RT300XE and RT300LCR cannot provide enough power even for the average power demand for the specific UAV parameters. Their SOC dropped below 20% and jumped to maximum power mode. The fuel consumption rate during the maximum power mode is not as good as the ideal mode, but they are powerful to generate electricity and guaranteed that batteries are not fully depleted.

With an initial 75% SOC_B and 50% SOC_A, small engines can easily drop below 20% and trigger the maximum power operating mode. The SOC for RT300LCR was nearly 0 in its third simulation, which shows that although it was in maximum power mode, it cannot stop SOC decrease during a high-powerful requirement. In addition, it can be seen that RT600JET, RT600LCR and RT600XE have three similar SOC curve. For these three engines, no matter how much is the initial SOC, batteries have a similar performance. An alternative hybridization factor $HF_{realtime}$ is introduced to estimate the ratio of power which comes which relates to batteries power P_b and motor output P_m.

$$HF_{realtime} = 1 - \frac{P_b}{P_m} \quad \textbf{(4-7)}$$

While the system is running, the $HF_{realtime}$ is calculated to show the ‘‘degree of electrification’’ and the importance of electricity by second. These results are summarized in Figure 32 and Table 5.

Table 5 Simulation results.

		50% SOC_A (t=0)	75% SOC_B (t=0)	100% SOC_C (t=0)
RT600XE	**Electric Mode**	1305 s	1462 s	1648 s
	Ideal Mode	2595 s	2438 s	2252 s
	Max Power Mode	0	0	0
	Average $HF_{realtime}$	73%	77%	69%
RT600LCR	**Electric Mode**	631 s	851 s	1081 s
	Ideal Mode	3269 s	3049 s	2819 s
	Max Power Mode	0	0	0
	Average $HF_{realtime}$	85%	84%	77%
RT600JET	**Electric Mode**	124 s	382 s	642 s
	Ideal Mode	3776 s	3518 s	3258 s
	Max Power Mode	0	0	0
	Average $HF_{realtime}$	85%	84%	80%
RT300XE	**Electric Mode**	0	116 s	386 s
	Ideal Mode	1407 s	1840 s	1789 s
	Max Power Mode	2493 s	1944 s	1725 s
	Average $HF_{realtime}$	84%	80%	77%
RT300LCR	**Electric Mode**	0	0	386 s
	Ideal Mode	1078 s	1449 s	1215 s
	Max Power Mode	2822 s	2451 s	2299 s
	Average $HF_{realtime}$	80%	77%	73%

From the figure, it can be seen that RT600JET is operating at ideal conditions and its final SOC is the same as RT600LCR and RT600XE. RT600JET avoids the frequent mode conversions and can achieve a high SOC at the end of the

mission. Therefore, if the vehicle is not specially designed for an electric mode, it is not necessary to have a big engine.

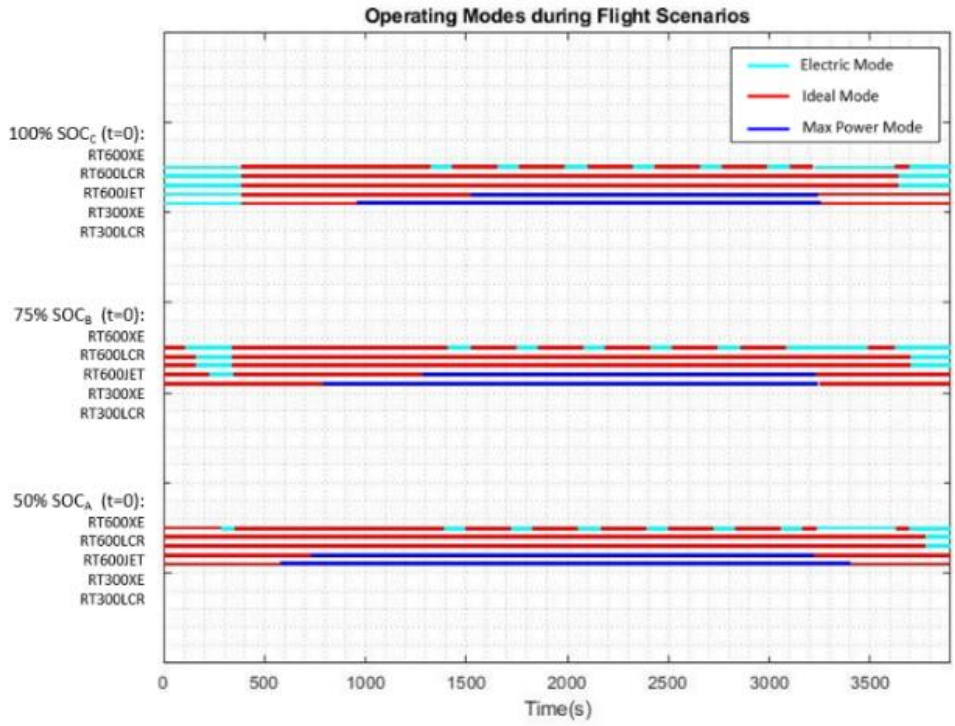

Figure 32 Operating modes missions.

In this thesis, electronic system efficiencies are assumed to be constant values that less than 98 percent. The energy losses of these electronic systems would affect system performance and increase the difficulty of control. As mentioned in this chapter before, the engine operating mode is adjusted mainly based on the battery SOC and current mission power requirements. Thus, the energy loss occurring in the battery pack leads to an increase in power demand of the engine, i.e. requiring the engine to generate more energy to meet mission demands and satisfy the battery SOC criteria. If the power demand of the engine is not increased appropriately, the battery pack will be discharged quickly that damages the battery and fails the mission. Regarding the generator/motor, low efficiency refers to that it generates less electricity or consumes more electrical energy than expected. Namely, if electronic system efficiencies have not been well considered, there will always be insufficient energy supply to the battery pack and motors. As a result, the battery pack would be discharged faster so that increases the

possibility of mission fails. However, the above conditions can be avoided by appropriate methods. In this study, due to efficiencies have been considered during the calculation of mission power demands, it guarantees that the system will generate enough energy by default.

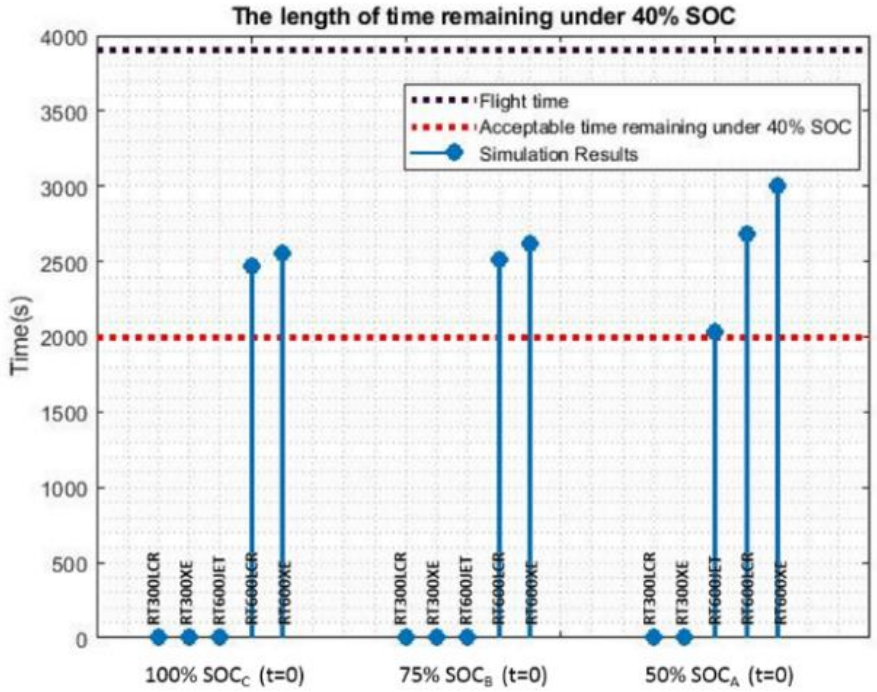

Figure 33 Length of time remaining under 40% SOC.

Figure 33 illustrates the length of time remaining under 40% SOC during each simulation. The value of the criterion (40%) is set up based on requirements of system performance and aircraft safety. Considering electronic system efficiencies and the huge difference amongst power demands at different flight stages, the criterion was increased by 20% from the original common low SOC threshold 20%. Please note that the criterion may have other values for some reasons. According to the figure, it can be observed that SOC of RT600XE and RT600LCR have not been to a value under 40%. The SOC of RT600JET was once under 40% SOC when $SOC_A(t = 0) = 50\%$. But from Figure 31, it can be determined that the SOC is around 40% and the lowest SOC value is about 38%. It has not dropped to the low boundary of 20% SOC. For the other two small engines, although the initial SOC is different, the length of time remaining under 40% SOC is similar. Because SOC_B and SOC_C tests have a charging procession

at the beginning of the flight, they performed similarly. However, due to the difference of the result of SOC_A and SOC_B is small, it can be deduced that the initial SOC has less influence for a system operating, engine size indeed influences the system performance. The HEPS requires an engine which can provide slightly higher energy than the average power demand at its lowest fuel consumption rate point.

4.5 Conclusion

The UAV simulations were repeated for three cases: SOC_A, SOC_B, SOC_C with initial battery pack state-of-charge $SOC_A(t = 0) = 50\%$, $SOC_B(t = 0) = 75\%$ and $SOC_C(t = 0) = 100\%$ respectively for the defined UAV mission flying scenario. For each one of the three state-of-charge five combustion power sizes (RT600XE, RT600LCR, RT600JET, RT300LCR, RT300XE) were simulated to explore if the SOC will enter the range of less than 40% which is considered the acceptance criterion.

From all the results presented the five different power pack options performed well however two did not meet the minimum SOC criterion: LT300LCR and RT300XE. Clearly using the proposed approach, the design team can select for different flight scenarios and range of engine packs (five in this case) the best option for a range of initial pre-flight battery pack SOC. The design sizing approach is effective because it links the combustion engine power pack operation and choice of size with the battery pack and also the power pack initial conditions.

The next step of research is to optimize the entire propulsion system design by using genetic algorithms. Each subsystem would be selected according to the total system weight and the estimated fuel consumption. Furthermore, a trade-off study of fuel efficiency and emissions will be conducted, and an intelligent controller with configurability will also be designed.

4.6 Reference

1 Koster J, Velazco A and Munz C, Hyperion UAV: An International Collaboration, 50th AIAA Aerospace Sciences Meeting including the New Horizons Forum and Aerospace Exposition, Aerospace Sciences Meetings, Nashville, 2012 Jan.

2 Glassock R, Hung J and Gonzalez L, Multimodal Hybrid Powerplant for Unmanned Aerial Systems Robotics, Twenty-Fourth Bristol International Unmanned Air Vehicle Systems Conference, Bristol, United Kingdom, 2009 Mar.

3 Ausserer J and Harmon F, Integration Validation and Testing of a Hybrid-Electric Propulsion System for a Small Remotely Piloted Aircraft, 10th International Energy Conversion Engineering Conference, Georgla, 2012.

4 Xie Y, Savvaris A and Tsourdos A, Modelling and control of a hybrid electric propulsion system for unmanned aerial vehicles, 2018 IEEE Aerospace Conference, Big Sky, MT, 2018.

5 Talbert T, The EcoEagle, National Aeronautics and Space Administration, 2012 Aug.

6 Siemens, Diamond Aircraft and EADS, World's first serial hybrid electric aircraft to fly at Le Bourget, Siemens, Diamond Aircraft and EADS, Munich, 2011.

7 Friedrich C and Robertson P.A, Hybrid-Electric Propulsion for Aircraft, Journal of Aircraft, 2015; 52: 176-189.

8 National Aeronautics and Space Administration, Overview of Subsonic Fixed Wing Project: Technical Challenges for Energy Efficient, Environmentally Compatible Subsonic Transport Aircraft, 3rd NASA Glenn Propulsion Control & Diagnostics Workshop, Cleveland OH, 2012.

9 Welstead J and Felder J.L, Conceptual Design of a Single-Aisle Turboelectric Commercial Transport with Fuselage Boundary Layer

Ingestion, 54th AIAA Aerospace Sciences Meeting, AIAA SciTech Forum, California, USA, 2016.

10 Moore M.D, Distributed Electric Propulsion (DEP) Aircraft, National Aeronautics and Space Administration, 2014.

11 Bradley M.K and Droney C.K, Subsonic Ultra Green Aircraft Research Phase II: N+4 Advanced Concept Development, National Aeronautics and Space Administration, California, 2012.

12 Siemens, Airbus and Rolls-Royce, Airbus, Rolls-Royce, and Siemens team up for electric future, London, 2017.

13 Yang H, Lu L and Zhou W, A novel optimization sizing model for hybrid solar-wind power generation system, Solar Energy, 2007; 81: 76-84.

14 Seeling-Hochmuth G.C, A combined optimisation concept for the design and operation strategy of hybrid-PV energy system, solar energy, 1997; 61(2): 77-87.

15 Zou Y, Sun F and Hu X, Combined Optimal Sizing and Control for a Hybrid Tracked Vehicle, Energies, 2012; 5: 4697-4710.

16 Deere K.A, Viken J.K and Viken S, Computational Analysis of a Wing Designed for the X-57 Distributed Electric Propulsion Aircraft, 35th AIAA Applied Aerodynamics Conference, AIAA AVIATION Forum, 2017.

17 Stoll A.M, Bevirt J and MooreM.D, Drag Reduction Through Distributed Electric Propulsion, 14th AIAA Aviation Technology, Integration, and Operations Conference, AIAA AVIATION Forum, 2014.

18 Papathakis K.V, NASA Armstrong Flight Research Center Distributed Electric Propulsion Portfolio, Safety and Certification Considerations, 2017.

19 Brelje B.J, Martins J.R.R.A, Development of a Conceptual Design Model for Aircraft Electric Propulsion with Efficient Gradients, Electric Aircraft Technologies Symposium (EATS) 2018 AIAA/IEEE, 2018.

20 Wheeler P.W, Clare J.C., Trentin A and Bozhko S, An overview of the more electrical aircraft. Proceedings of the Institution of Mechanical Engineers, Part G: Journal of Aerospace Engineering, 2013; 227: 578–585.

21 Naayagi R.T, A review of more electric aircraft technology, 2013 International Conference on Energy Efficient Technologies for Sustainability, Nagercoil, India, 2013.

22 Hafez A.A.A, Forsyth A, A Review of More-Electric Aircraft, 13th International Conference on Aerospace Sciences and Aviation Technology, 2009.

23 Dunne A, Aerodynamic Analysis and Optimization of the Aegis UAV, MSc Thesis, Cranfield, the United Kingdom, 2012.

24 Friedrich C and Robertson P.A, Design of Hybrid-Electric Propulsion Systems for Light Aircraft, 14th AIAA Aviation Technology, Integration, and Operations Conference, AIAA Aviation Forum, 2004.

25 Lukic S.M and Emadi A, Effects of drivetrain hybridization on fuel economy and dynamic performance of parallel hybrid electric vehicles, in IEEE Transactions on Vehicular Technology, 2004 Mar; 53(2): 385-389.

5 SYSTEM SIZING

In the previous chapters, the system configuration and the engine capacity have been determined. This chapter will mainly discuss about the sizing method for other components, which is the second target in the second objective. Please note that due to the data of candidate components is limited, this chapter selected a larger aero vehicle as the research objective and adjusted the value of the mission power demand proportionally. Specifically, according to the collected engine and motor information, the mission requirement in this chapter was scaled up in order to better demonstrate the designed sizing algorithm. The sizing method proposed in this chapter is universal and applicable to all similar problems, so that proportionally increasing mission demand would not affect research.

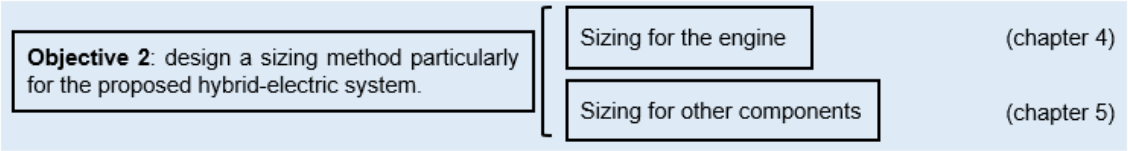

Figure 34 Chapter 5 structure.

Design of a Distributed Hybrid Electric Propulsion System for a Light Aircraft based on Genetic Algorithm

Abstract

Hybrid-electric aircraft is a new attempt for the sustainable aviation, which are environmentally friendly and highly efficient. This paper proposed an intelligent

sizing method for a novel hybrid-electric propulsion system for light aircraft. The sizing problem consists of two parts. The power source part applied a non-dominated sorting genetic algorithm to choose components and simultaneously minimized the system total weight and fuel consumption. The second part of the system used a conventional genetic algorithm to minimize the system weight and guarantee that selected motors can generate enough power for propulsion. By applying a simple deterministic energy management strategy, it is proved that the hybrid-electric system using selected components can achieve a 12% improvement in the fuel consumption reduction.

5.1 Introduction

Nowadays, the depletion of fossil fuels and anthropogenic climate change are two crises urged to be mitigated. As one of the root causes, the air transportation industry is reasonable to expect a technology revolution to reduce both fuel consumption and pollutant emissions. In 2011, ACARE developed the 'Flightpath 2050 Goals' aiming to continuously reduce the environmental impact and energy shortage problem in the face of continuing expansion in aviation demand [1]. Later, ICAO published a more detailed report on aircraft noise and emissions, which agreed on a comprehensive set of environmental aircraft design standards. At present, energy conservation and environmental protection are two key points of the aviation industry.

Up to now, some alternative fuels and low-carbon propulsion technologies have been invented, such as the pure-electric aircraft. Although using electricity is a promising solution, the pure-electric propulsion system cannot complete long-duration or high-powerful missions due to the limited storage capacity of the battery pack. Therefore, the hybrid-electric propulsion technique becomes a feasible and expected option for the next-generation aircraft. The research of hybrid-electric aircraft grows rapidly over the past two decades. Based on the type of hybrid propulsion systems, hybrid-electric aircraft is commonly categorized into three types: series, parallel and complex. Series hybrid owns the simplest configuration and is firstly successfully tested on the aircraft DA36 E-star. Parallel hybrid is invented later, but has a compacted structure and higher

fuel efficiency than series. Some hybrid-electric aircraft projects are summarized in Table 6 [2-11].

Table 6 Hybrid-electric aircraft projects [2-11].

Aircraft	Producer	Pax	Information
DA36 E-star	DA/EADS/Siemens	1	Series: wankel ICE,70kW EM
DA36 E-star 2	DA/EADS/Siemens	2	Series: 30kW ICE, 65kW EM
Alatus	Cambridge University	1	Parallel: 2.8kW ICE, 12kW EM
SOUL	Cambridge University	1	Parallel: 7.5-8kW ICE, 12kW EM
Eco-Eagle	Embry-Riddle Aeronautical Uni	2	Parallel: 74.5kW ICE, 29.8kW EM
AIRSTART	Airbus/ Cranfield Uni	-	Parallel: 24kW ICE, 42kW EM
DEAP	Airbus/Rolls-Royce/ Cranfield Uni	100	Turboelectric
E-fan X	Airbus/ Siemens	146	Turboelectric: turbofans, 2MW EM
Quad-Fan	BHL	180	Turboelectric
SUGAR	Boeing	154	Turboelectric
BW-11	Cranfield University	800	Turboelectric
Eco-150	ESAero	150	Turboelectric
STRAC-ABL	NASA	154	Partial Turboelectric
N3-X TeDP	NASA	300	Turboelectric

Since different hybrid systems have different features, various choices and combinations will direct to different performance, so that the entire design process is a complex and challenging procedure. Therefore, the hybrid-electric propulsion system should be specified designed for each aircraft. Regarding the selection of hybrid types, paper [12] compared the series and parallel hybrid, and found that, without considering distant future advancements, the parallel architecture can provide greater range performance than the series hybrid. As for component sizing, the simplest and popular method is selecting devices by their power-to-weight ratio and other characteristics [13,14], but some other intelligent sizing methods [15-17] have been proposed as well. For example, by using a multi-objective optimization algorithm, paper [16] minimized electricity cost and power loss during its sizing process for a wind/photovoltaic hybrid power supply system. Paper [17] minimized the fuel consumption and achieved a fuel-burn reduction of up to 17.6% by retrofitting of a midscale aircraft.

This paper mainly discusses a design process of an innovative hybrid-electric propulsion system, including the research field of the hybrid configuration and

components sizing. The paper starts with an introduction of the hybrid-electric aircraft, followed by a general description of the design process of the new propulsion system. In the third section, methods to improve a conventional series hybrid system are presented, and by combining two new techniques, the final system structure is determined. In the section four, requirements for each component are put forward. The optimization model, i.e. objective functions and constraints are demonstrated afterward. Section five mainly introduces candidates of each component, in where a comparison of internal combustion engines has been conducted to find the suitable engine type. After that, the sizing algorithm applied is introduced. As the problem is divided into two parts, two different types of genetic algorithms are used for each part respectively. Finally, the performance of the new system is validated at the end of the paper.

5.2 System Design

The test object of this study is a two-engine light aircraft, Tecnam P2006T [18], whose specifications are shown in Table 7. The estimated parameters, which are shown in the right column of the table, are calculated based on the plane performance.

Table 7 Tecnam P2006T specifications [18].

Parameters		Estimated Parameters	
Maximum cruise speed (km/h)	278	Wing area (m^2)	15
Stall speed (km/h)	102	Lift coefficient	0.342
Cruise altitude (m)	4267	Drag coefficient	0.023
Take-off distance (m)	394	Endurance (h)	4.25
Landing distance (m)	349	Wing loading (kg/m^2)	80
Rate of climb (m/s)	5.3		
Range (km)	1239		
Max take-off weight (kg)	1230		
Empty weight (kg)	819		

Table 8 Different hybrid configurations and their characteristics.

Type	Configuration	Characteristics
Series	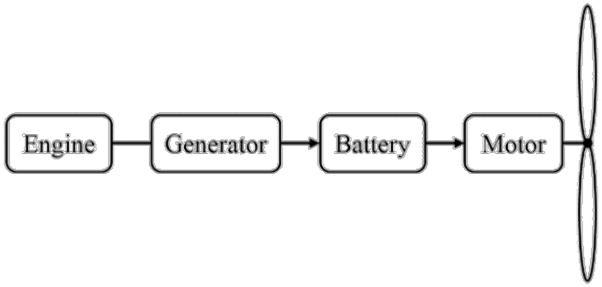	• All components are arranged in series; • Decouple engine from propeller; • Simple structure, no clutch or gearing; • Energy loss; • Heavy system.
Parallel	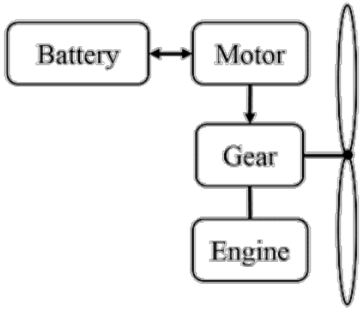	• Both engine and motor can propel; • Compacted and lighter structure; • Less energy loss; • Need gear; • Need mechanical linkages; • Maintenance difficult.
Complex	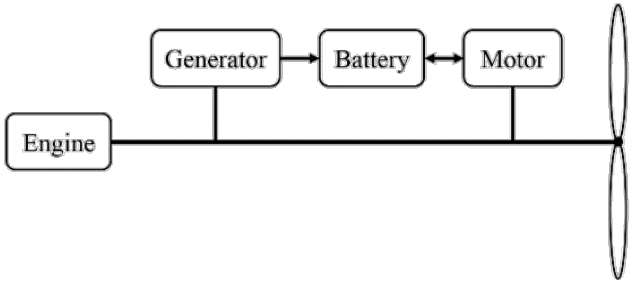	• Various configurations; • High efficiency; • Complicate management strategy; • Heavier computation; • Complex structure; • Maintenance difficult.

The first step for designing a hybrid-electric propulsion system is to define the configuration. As a reference, three hybrid configurations and their characteristics are shown in Table 8. Amongst them, the series hybrid configuration decouples the engine from the power demand, which provides an opportunity to allow the engine continuously operating in high-efficient or less-emission area. Parallel hybrid systems are higher efficient than series, due to the engine can straight propel the propeller without any energy transformations. The complex hybrid has various types and features. Due to the complex hybrid system mechanically links the engine to the propeller, the complex hybrid will be temporarily categorized into parallel in the rest of this paper.

Hybridization factor, *HF*, is a factor developed to examine hybrid-electric propulsion systems [19]. Showing by the equation (5-1), for both series and parallel hybrids, the denominator is the maximum power demand. Therefore, the engine capacity, P_{e_max}, becomes the only parameter to decide *HF*. A comparison can be conducted for a series and parallel system with a same *HF*. For example, assuming $HF = 0.5$, the engine and motor capacity for these two systems are shown in (5-2) and (5-3) respectively. When the instant mission power requirement is $0.5P_{req\_max}$ and the battery pack is depleted, the series hybrid-electric power system cannot work as efficient as the parallel. Parallel systems use engine to drive a propeller, while series systems firstly transform engine output to electricity and then use motor to drive the propeller. Since energy loss is unavoidable during energy conversions and the extra device, generator, heavies the entire system, the parallel hybrid system seems to be more efficient than other hybrids. However, when the power demand is still $0.5P_{req\_max}$ but the battery pack is not depleted, the performance may be different. The series hybrid-electric power system can arrange the engine to stably operate at its highest-efficient point, while the parallel hybrid has to regulate engine rotation speed according to mission demands since that is mechanically linked to the propeller. As a result, it is hard to define which category is better.

$$HF = \begin{cases} \dfrac{(P_{m\_max} - P_{e\_max})}{P_{m\_max}} & series \\ \dfrac{P_{m\_max}}{P_{m\_max} + P_{e\_max}} & parallel/complex \end{cases} \quad \textbf{(5-1)}$$

Series: $P_{e\_max} = \frac{1}{2} P_{req\_max}, \quad P_{m\_max} = P_{req\_max}$ **(5-2)**

Parallel: $P_{e\_max} = \frac{1}{2} P_{req\_max}, \quad P_{m\_max} = \frac{1}{2} P_{req\_max}$ **(5-3)**

This study selected the series hybrid configuration as a baseline since it has a unique decoupled structure. However, as mentioned before, series systems have drawbacks. To offset them, the technique of a common-core multi-fans (CMF) distributed propulsion system and more electric aircraft are integrated into the system configuration. Distributed propulsion refers to using multiple small propellers to blow the wing. Paper [20] proves that a distributed propulsion system has a better lift property for aircraft. The other technique MEA means an aircraft system transforms the engine output to electricity firstly and then use the generated electricity to power ailerons etc. The MEA concept removes redundant battery packs and increases the usage rate of each propulsion component. As a result, the configuration can be determined which is shown in Figure 35.

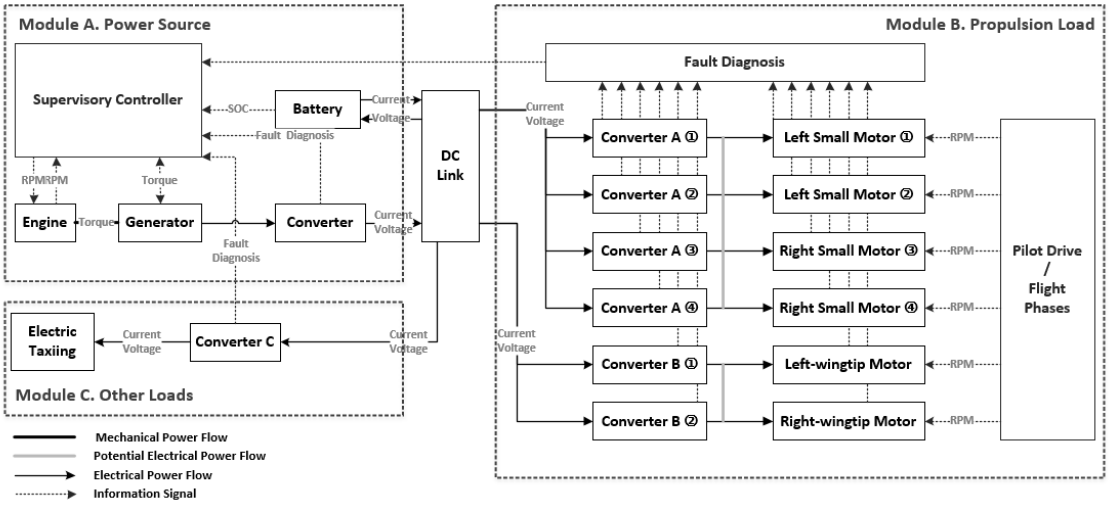

Figure 35 DSHEPS configuration.

The designed system is a distributed series hybrid-electric propulsion system with many advantages. At first, it is a series structure which allows the engine to run

isolated. The decoupled configuration not only benefits the engine performance but also increases the electrification degree of the whole propulsion system. Secondly, it can improve lift property by blowing more wind above the wing [21]. Furthermore, it can reduce engine size. Aircraft engines are always over-sized. For example, engines of a twin-engines aircraft must be sized as twice thrust as required in case of an engine-failure scenario. However, by applying multi-propulsors, other propulsors can generate more power to compensate the power short when one propulsor failure so that it is not necessary to over-size engines or other propulsors under this configuration.

For easily understanding, the system can be divided into three parts: power sources, other loads and propulsion loads. The first part is the power source of the entire system, which includes an engine, a generator, and a battery pack. The second part consists of outside electrical loads, such as an electric taxiing system. Electric taxiing refers to an aircraft uses a motor to directly drive wheels during taxiing stage instead of using propellers [22]. This new taxiing method is more efficient and allows the aircraft to switch off the engine earlier if the battery pack can provide enough energy for the taxiing. The third part contains all propulsors, mainly for energy output. It is a symmetric structure, i.e. all motors are placed symmetrically. Please note that motors will always need converters in practice regardless if voltages are different or otherwise.

5.3 Requirements of Sizing Problem

A typical flight mission consists of taxiing, taking-off, climbing, cruising, descending and landing flight stages. Amongst all stages, taking-off costs as twice much as cruise required which indicates the maximum power requirement of the mission. While the cruising, occupying most of the mission time, is the lowest power demand during the flight. Assuming cruising is steady without any acceleration in any direction, the minimum power requirement can be determined by the vertical and longitudinal equations. As a result, basic power requirements for the system are able to be defined. Following this method, a table of the sizing flowchart has been developed which is shown as Figure 36.

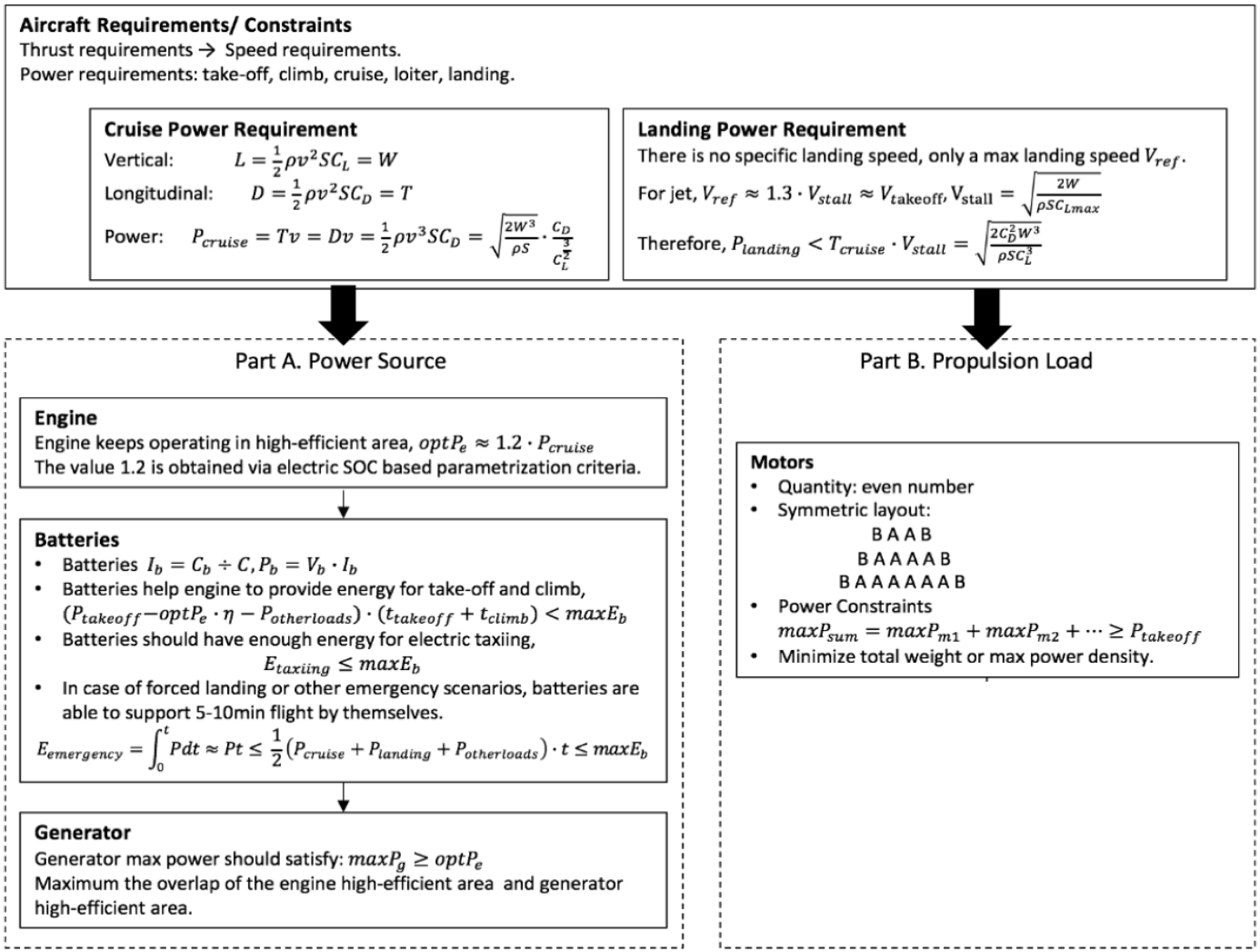

Figure 36 System sizing process.

Similarly, since the designed system is a decoupled configuration, the sizing process can be divided into two parts as well (power source and power loads).

- **Power Source**

Power source part includes an engine, a generator and a battery pack. In this part, the performance of the battery pack, i.e. whether charging or discharging, is decided by the engine operational condition. Namely, the battery pack operates passively, and its output should equal to the difference between the mission requirement and engine output. Therefore, the engine pack is the most important component of this part. To find a suitable engine, the author has proposed a new engine sizing method via state-of-charge based parametrization criteria. It found that the engine whose optimal output is around 1.2 times of the average value of power requirement $1.2P_{cruise}$, can lead to a better battery performance [23], which is expressed by the equation (5-6).

Because that the selected engine is not capable to generate enough power for high-powerful flight stages, such as take-off or climbing, the battery pack should provide the short of the required energy. Namely, the capacity of the battery pack must be larger than the difference between the highest power requirement and engine capacity, as seen in (5-9). In addition, if the battery pack has enough energy for electric taxiing, the engine can be switched off soon after a successful landing, which reduces the engine's operation time and decreases the amount of consumed fuel. Therefore, another criterion of the battery pack can be defined, i.e. (5-8), in which the remaining energy of the battery pack after landing, should be more than the electric taxiing demand. The last design consideration for the battery pack is an emergency scenario. In case of engine failure, the battery pack should be capable to support a 5-10 min flight for a forced landing. The equation (5-10) presents that requirement. As for the generator and engine, since they are tied tightly and work together, the generator's maximum capacity should be above the engine output, as shown as (5-7).

In summary, the objective functions of part A are:

$$min\, J_1 = W_{sum} \tag{5-4}$$

$$min\, J_2 = \int_0^t \dot{m}_f \tag{5-5}$$

While the constraints are:

$$opt\, P_e \geq 1.2 P_{cruise} \tag{5-6}$$

$$maxP_g \geq maxP_e \tag{5-7}$$

$$E_{etaxiing} \leq maxE_b \tag{5-8}$$

$$(P_{takeoff} - optP_e \cdot \eta_g - P_{other}) \cdot (t_{takeoff} + t_{climb}) < maxE_b \tag{5-9}$$

$$E_m = \int_0^t Pdt \approx Pt \leq \frac{1}{2}\left(P_{cruise} + P_{landing} + 2P_{other}\right) \cdot t \leq maxE_b \tag{5-10}$$

- **Propulsion Load**

Part B consists of motors and converters. The number of motors N_m should be an even number due to it is a symmetric configuration. However, the number of motors is not a fixed number. From the open-domain literature, the precise relationship between the number of motors and aircraft aerodynamic properties has not been clarified, so that it is difficult to say that using how many motors could benefit the aircraft performance. Unless the designed system conducts a wind tunnel test, it cannot straight say which kind of configuration is better than others. Therefore, this study invents a positive factor A_{aero} to indicate that distributed propulsion system outperforms than the conventional one. The factor is a constant number rating the distribution level. According to Figure 36, the objective function of part B can be written as to minimize the sum of the system weight and the designed factor. Due to the uncertainty of the factor A_{aero}, its maximum value has been scaled to half of the maximum weight.

$$min\, J_3 = W_{sum} + A_{aero} \tag{5-11}$$

$$max\ (sum\, P_m) = \sum_1^{N_m} max\, P_{m_n} \geq P_{takeoff} \tag{5-12}$$

- **Aircraft Performance**

Although the DSHEPS is a brand-new design, performance criteria of original aircraft cannot be sacrificed. In other words, the study should guarantee that the aircraft applying the designed system has the same or better properties, i.e.

$$Roc' \approx \frac{P_{climb} - P_{cruise}}{m \cdot g} \geq Roc \quad \textbf{(5-13)}$$

$$d'_{takeoff} \approx \frac{m \cdot V_{liftoff}^2}{2(T_{avg} - D_{avg})} \leq d_{takeoff} \quad \textbf{(5-14)}$$

5.4 System Components

Assuming cruise is steady and no acceleration, the power requirement for a common flight can be determined and calculations can be found in paper [17, 22]. Figure 37 shows the power demand for a typical flight. The power requirement for the cruise is $P_{cruise} = 60kW$ and the flight endurance is 60 min.

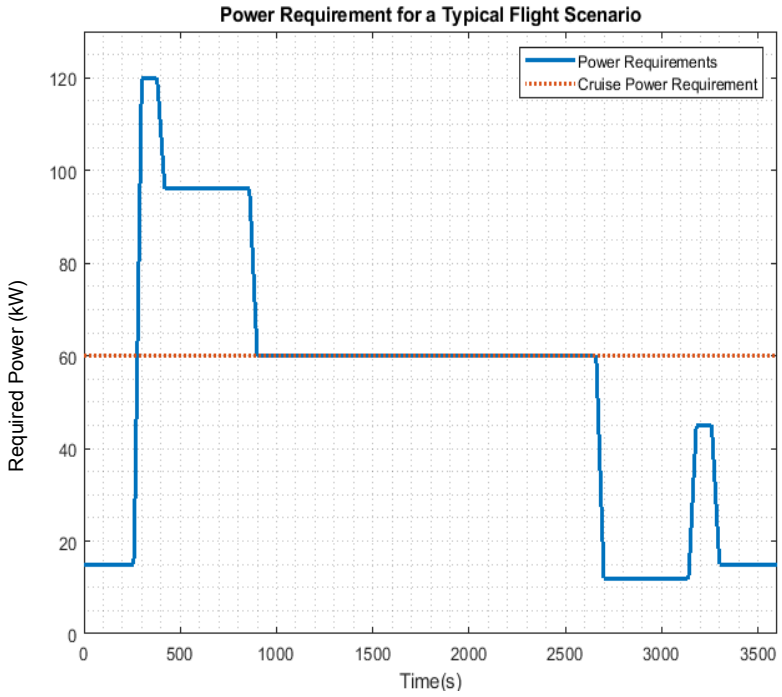

Figure 37 Mission requirement.

5.4.1 Engine

Common aero engines are internal combustion engines and gas turbines. ICEs can generate energy up to 2000kW, and gas turbines typically produce 100-400 MW. From the ideal propulsive efficiencies map in the book [23], when the Mach number is less than 0.3 (367km/h), the efficiency of ICE is higher than other propulsors'. Therefore, ICEs are more frequently applied in small, low-speed aircraft, especially for less than 400kW power demand.

About 80 different engines are selected as candidates, that all data is collected online shown by the designed figure [24-32]. Figure 38 displays the relationship between weight and capacity. There are six categories of engines, including 1-4 cylinder piston engines, rotary engines and turboshaft engines. From the figure, it can be found that the rotary engine has the best power-to-weight ratios, while the turboshaft engine shows great performance in the high powerful area. As for engines' volume and price, engines from three companies are elected. From Figure 39, the volume linearly increases with the increasing capacity, but the price (Lycoming engines) shows an exponential growth.

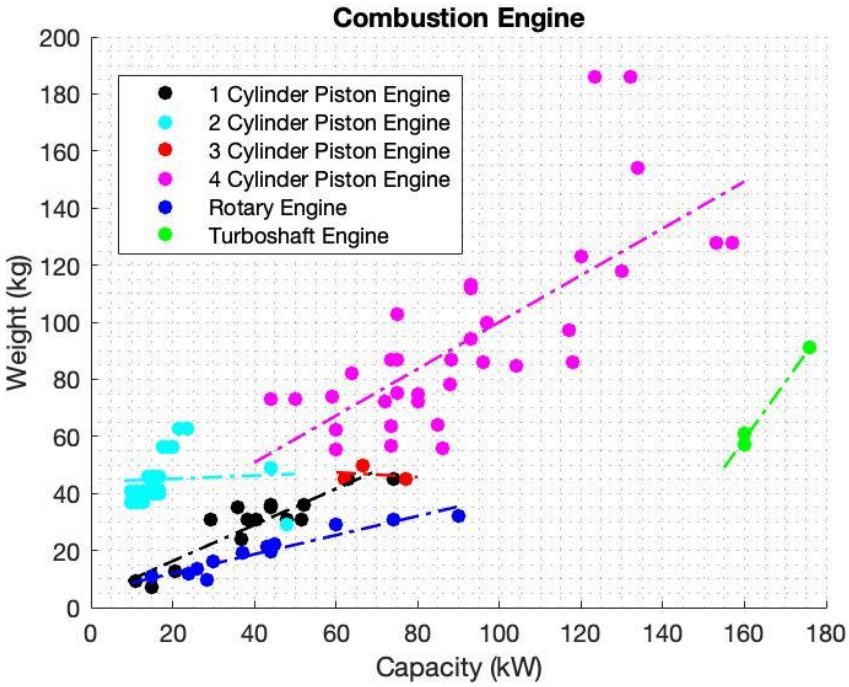

Figure 38 Weight-capacity figure of combustion engines.

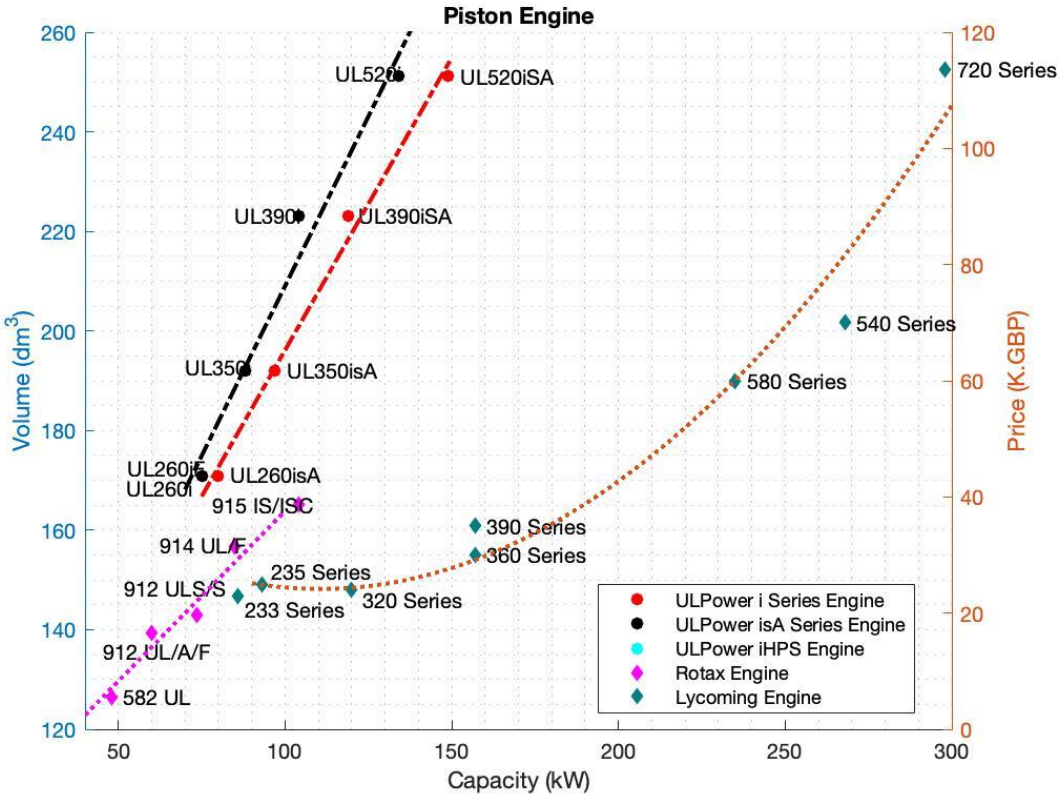

Figure 39 Volume-capacity figure of combustion engines.

5.4.2 Battery

The type, capacity, and normal voltage are essential variables for a battery pack. At present, common rechargeable batteries are Lead-acid, Nickel-Cadmium (Ni-Cd), Nickel-Metal Hydride (Ni-MH), Lithium-ion and Lithium-Po batteries. Their energy densities are shown in Table 9 [33]. Amongst them, Li batteries (Li-ion and Li-Po) are superior since they have higher energy-to-weight ratios and excellent performance. From literatures, Li batteries can charge faster, last longer and be packed in a thinner package. Li-ion and Li-Po utilize the same chemical reaction with different cathode and electrolyte to store the electrical energy. Compared with Li-ion, Li-Po is regarded as a more advanced tech which possesses slightly higher energy and thinner volume. Therefore, this study chose Li-Po batteries as the electrical energy storage device. Due to the voltage and capacity vary proportionally by adding or reducing the number of cells, the battery

pack's weight could be estimated by the energy-to-weight density and cell number. Therefore, the number of cells is the variable we need to determine.

Table 9 Batteries energy density [33].

	Lead-acid	Ni-Cd	Ni-MH	Li-ion	Li-Po
Energy density (Wh/kg)	33-42	30	100	100-265	100-265

5.4.3 Motor and Generator

Through the interaction between the magnetic field and current-carrying conductors, motors transform electric energy into mechanical energy, generators vice versa. Different classifications of motors are summarized in Figure 40. The permanent magnet synchronous motor and brushless direct current motor (BLDC) are two popular motors due to their output have less fluctuation. Based on the power-to-weight table of electric motors/electromotive generators in [34], some high power-to-weight density PMSMs and BLDCs are candidates.

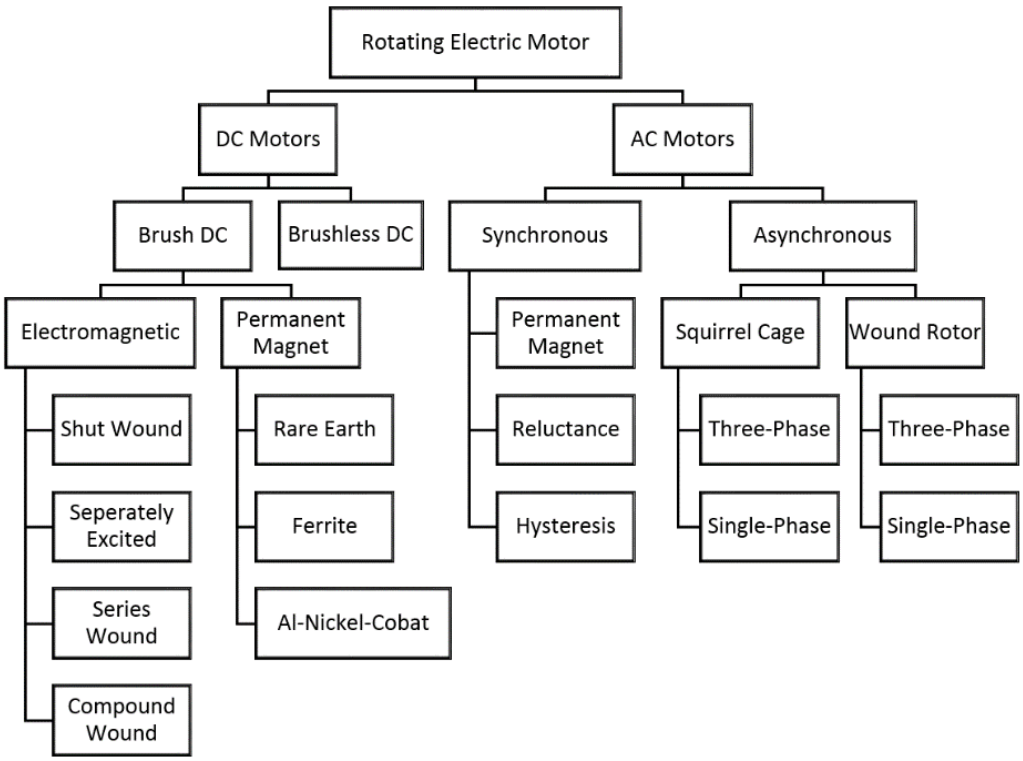

Figure 40 Electric motor categories.

5.5 Sizing Algorithm

- **Part A**

From the previous section, it can be known that there are two objectives of Part A: reduce weight and improve efficiency. In other words, the question in the Part A is a multi-objective optimization problem. Therefore, the fast non-dominated sorting algorithm-II (NSGA-II) [35] has been applied here to find a better component combination. The NSGA-II is a heuristic method based on Pareto ranking and crowding distance approaches. It firstly calculates objective values and sorts population according to the non-domination. The offspring population is mainly generated by high-ranking individuals with mutation and crossover behaviours. The pseudocode of NSGA-II is shown in Table 10.

Table 10 Pseudocode of NSGA-II.

Algorithm Pseudocode for Part A

Input: information of component candidates;

Initialization: randomly generate population ***P,*** and extract information;

Constraints handling: delete infeasible individuals and replaced by feasible ones;

for i = I : *NP* (or **while not Termination Condition**)

Select parent population;

Find the matched engine and generator based on overlap maps;

Crossover + Mutation → offspring *Q*, let $R = P \cup Q$

Constraints handling;

Evaluate the objective value: total weight and total fuel consumption for a typical flight scenario;

Non-dominated sorting and calculating crowding distance;

Tournament Selection → next generation *P;*

end

For the problem in Part A, an extra archive is added into the algorithm to find the best-matched engine and generator. This archive contains the information of the brake-specific fuel consumption map and efficiency map of each engine and generator. From these maps, the feasible and high-efficient operating area of each candidate could be roughly obtained. Therefore, if the best operating area of an engine and a generator is same, a group compositing by these two devices will have a very high efficiency that is good for the designed system. To better show the matching index, a new parameter O_e has been introduced. It is an overlap rate of the engine's and generator's high-efficient operating area. Assuming each high-efficient operating area is a circular whose centre is C_e, C_g with radius R_e, R_g respectively, the overlap rate could be estimated by:

$$O_e = \frac{R_e + R_g}{|C_e - C_g|} \quad \textbf{(5-15)}$$

Additionally, gears can change the Revolutions Per Minute (RPM) and torque. If there is a suitable gear connecting the engine and generator, the overlap rate may increase but the system will be heavier caused by the extra component. Therefore, depended on the variation of the overlap rate, the designed sizing will decide if a gearbox should be added into the system or not.

As a result, there are five genes in one chrome: the index of engine candidates, the index of generator candidates, the cell number of the battery pack, and engine operating point (RPM and torque) respectively. All components' specifications, such as the maximum power, weight, high-efficient operating area are imported according to the component index in each chrome. During the process, the generated population should satisfy all constraints, i.e. from (5-6) to (5-10), while infeasible chromes would be replaced by feasible ones. In this problem, the tournament method is used to select parent population, and O_e is calculated and recorded during the sorting process.

- **Part B**

The question of Part B is a single-objective problem so that it can use a conventional genetic algorithm to select the system component. The objective

function and constraint are shown in Section four. The flowchart of the applied genetic algorithm is shown in Figure 41.

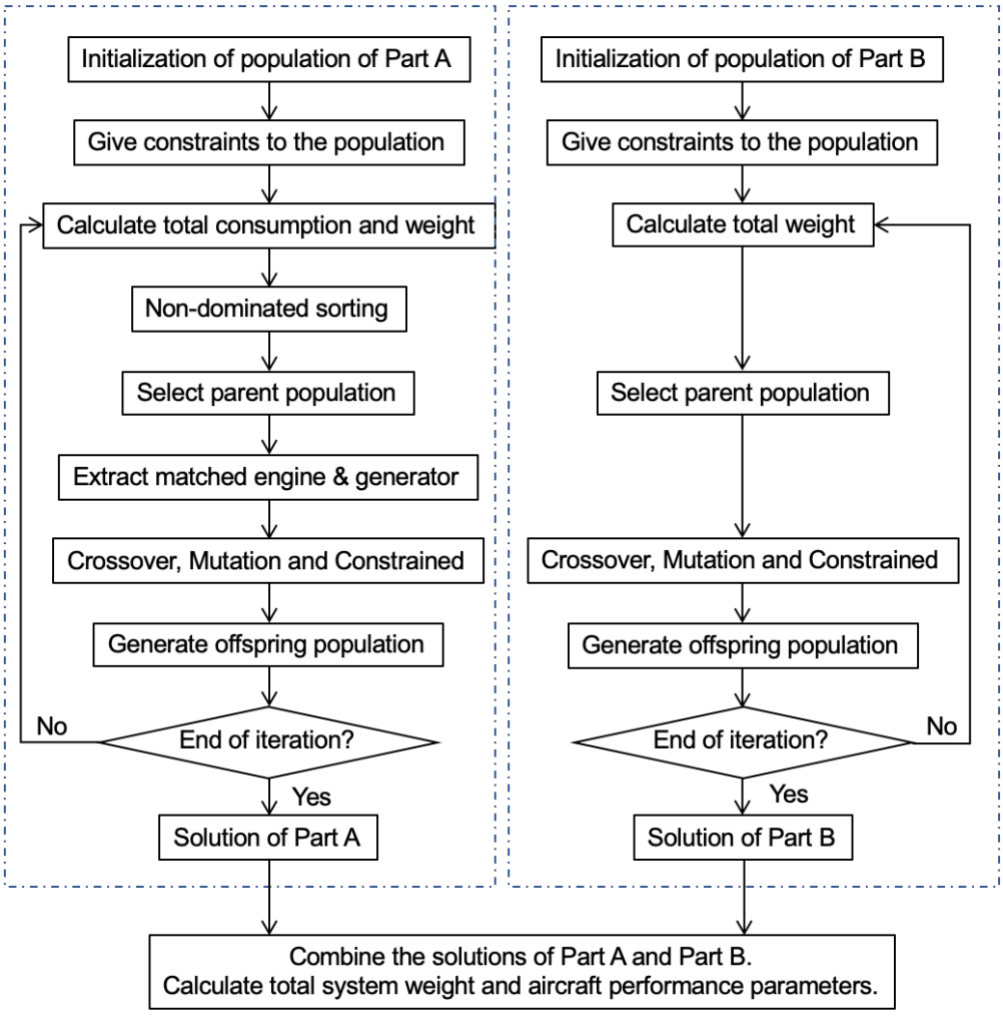

Figure 41 Flowchart of the sizing process.

- **Summary**

Part A and Part B are parallel problems. Two problems run separately and consequently deliver solutions to the final calculation. The result of Part A is a Pareto front, which is a series of non-dominated solutions with lower weight and low fuel consumption rate. Part B has only one objective, thus the result of Part B is a single solution. Combined results of Part A and Part B, a series of feasible solutions are determined.

$$FCR = \frac{BSFC\ @\ oprating\ \ point}{BSFC\ @\ the\ most - efficient\ point} \quad \textbf{(5-16)}$$

$$Fuel_{total} = \int_0^t FCR \quad \textbf{(5-17)}$$

$$d'_{takeoff} \approx \frac{m\ \cdot\ V_{liftoff}^2}{2(T_{avg} - D_{avg})} \leq d_{takeoff} \quad \textbf{(5-18)}$$

$$Roc \approx \frac{P_{climb} - P_{cruise}}{m \cdot g} \quad \textbf{(5-19)}$$

To examine the calculated solutions, some of the aircraft performances are estimated. The first and most important parameter is the total fuel consumption. Since engine candidates are from different companies, to achieve a fair comparison, it is more reasonable to use a Fuel Consumption Rate (FCR) for the comparison rather than using the total fuel consumption amount. The FCR mentioned here is the ratio of the brake-specific fuel consumption at the operating point to that at the most efficient operating point, shown as the equation (5-16). As a result of using this parameter, the total fuel consumption amount is the integrated FCR. The second important characteristic is the aircraft rate of climb. Here, the power requirement of the cruise mode is used to present the power overcoming drag. The last performance parameter is the take-off distance. Neglecting the rolling resistance and fraction, the take-off distance could be estimated by (5-14). Therefore, the comparison between the prototype and DSHPES aircraft is shown in the table.

From the table, it can be found that, firstly, the maximum propulsion power of the DSHEPS is much higher than that of the original propulsion system. Almost twice power could be generated by using the new hybrid-electric power system. As for each subsystem, the new engine capacity is a little smaller, but a high powerful generator and electric motors have been applied in the DSHEPS. Extra components guarantee sufficient power output to propel the aircraft but increase system weight. Thus, despite the high power-to-weight ratio of these subsystems,

the total weight of the new system is still heavier than the original one. Generally, it is difficult to obtain a lightweight HEPS using existing technologies.

Table 11 Comparison of conventional system and hybrid-electric system.

		P2006T [17]	DSHEPS
Max Propulsion Power		147kw	284 kw
System Power	Engine max power	147kw	135kw
	Generator power	0	75kw
	Motor power	0	284kw
	Battery capacity	0	7.5kwh
Weight	Engine weight	130kg	42kg
	Generator weight	0	20kg
	Motor weight	0	66kg
	Battery weight	10kg	28kg
	Total weight	140kg	156kg
Performance	Rate of climb	5.3 m/s	5.9 m/s
	Average FCR	4.1	3.6

However, the new system has better flight performance. According to the estimation results, the hybrid-electric system is able to increase the rate of climb and improve fuel efficiency. By using the variable FCR, the total fuel consumption could be increased by 12% with a simple rule-based controller. However, both of the Roc and FCR are calculated based on the original aircraft model. The advantage of distributed propulsion has not been reflected. Thus, the aircraft performance is potential to be further improved in practical applications. Therefore, it can be proved that the hybrid-electric propulsion technique is able to actually improve some performances of the aircraft.

5.6 Conclusion

This paper mainly proposed the sizing process about a distributed hybrid-electric aircraft. At first, based on an analysis of common hybrid propulsion technologies, it introduced a new hybrid-electric configuration improved by adopting the distributed propulsion and MEA concept. Then, with the proposed system configuration and mission power demand, the requirements for each component were determined, and a sizing flowchart was invented. Because of the system properties, different genetic algorithms have been applied to select different

components, and as a result, the new propulsion system can reduce fuel consumption by at least 12%.

5.7 Reference

[1] Advisory Council for Aviation Research and Innovation, "Protecting the environment and the energy supply," 2011. [Online], URL: https://www.acare4europe.org/sria/flightpath-2050-goals/protecting-environment-and-energy-supply-0

[2] C. Friedrich and P. A. Robertson, "Hybrid-Electric Propulsion for Aircraft," *Journal of Aircraft,* 2014.

doi: 10.2514/1.C032660

[3] J.B.Heywood, Internal Combustion Engine Fundamental, New York: McGraw-Hill, 1988.

[4] P.Pillay and K.Ramu, "Modelling of permanent magnet motor drives," in *Robotics and IECON'87 Conferences. International Society for Optics and Photonics*, 1987.

doi: 10.1109/41.9176

[5] National Aeronautics and Space Administration, "Overview of Subsonic Fixed Wing Project: Technical Challenges for Energy Efficient, Environmentally Compatible Subsonic Transport Aircraft," 3rd NASA Glenn Propulsion Control & Diagnostics Workshop, Cleveland OH, 2012.

[6] J. R. Welstead and J. L. Felder, "Conceptual Design of a Single-Aisle Turboelectric Commercial Transport with Fuselage," in *54th AIAA Aerospace Sciences Meeting*, 2016. doi: 10.2514/6.2016-1027

[7] M. D. Moore, "Distributed Electric Propulsion (DEP) Aircraft," National Aeronautics and Space Administration, 2014. URL: https://aero.larc.nasa.gov/files/2012/11/Distributed-Electric-Propulsion-Aircraft.pdf

[8] M. K. Bradley and C. K. Droney, "Subsonic Ultra Green Aircraft Research Phase II: N+4 Advanced Concept Development," National Aeronautics and Space Administration, California, 2012. URL: https://ntrs.nasa.gov/archive/nasa/casi.ntrs.nasa.gov/20120009038.pdf

[9] Siemens, Diamond Aircraft and EADS, "World's first serial hybrid electric aircraft to fly at Le Bourget," Siemens, Diamond Aircraft and EADS, Munich, 2011.

[10] Siemens, Airbus and Rolls-Royce, "Airbus, Rolls-Royce, and Siemens team up for electric future," London, 2017.

[11] P. Robertson, "Low Carbon Recreational Flying - The Hummingbird Electric Microlight".

[12] T. S. Dean, G. E. Wroblewski and P. J. Ansell, "Mission Analysis and Component-Level Sensitivity Study of Hybrid-Electric General Aviation Propulsion Systems," in *AIAA Aerospace Sciences Meeting*, Kissimmee, 2018.

doi: 10.2514/6.2018-1749

[13] C.Friedrich and P.A.Robertson, "Design of a Hybrid-Electric Propulsion System for Light Aircraft," in *AIAA Aviation Technology, Integration and Operation Conference*, Atlanta, 2014. doi: 10.2514/6.2014-3008

[14] J. Koster, C. Humbargar, E. Serani, A. Velazco, D. Hillery and L. Makepeace, "Hybrid Electric Integrated Optimized System Design of a Hybrid Propulsion System for Aircraft," in *9th AIAA Aerospace Sciences Meeting*, Orlando, 2011.

doi: 10.2514/6.2011-1011

[15] C. Pornet, C. Gologan, P. Vratny, A. Sertz, O. Schmitz and A. T. I. a. M. Hornung, "Methodology for Sizing and Performance Assessment of Hybrid Energy Aircraft," *Journal of Aircraft,* vol. 52, no. 1, January-February 2015.

doi: 10.2514/1.C032716

[16] A. Abdelkader, A. Rabeh, D. M. Ali and J. Mohamed, "Multi-objective genetic algorithm based sizing optimization of a stand-alone wind/PV power supply system with enhanced battery/supercapacitor hybrid energy storage," *Energy,* pp. 351-363, August 2018. doi: 10.1016/j.energy.2018.08.135

[17] Y. Xie, A. Savvaris and A. Tsourdos, "Sizing of hybrid electric propulsion system for retrofitting a mid-scale aircraft using non-dominated sorting genetic algorithm," *Aerospace Science and Technology,* no. 82-83, pp. 323-333, September 2018.

doi: 10.1016/j.ast.2018.09.022

[18] Tecnam, pt2006t, URL: https://www.tecnam.com/aircraft/p2006t/

[19] SM.Lukic and A.Emadi, "Effects of Drivetrain Hybridization on Fuel Economy and Dynamic Performance of Parallel Hybrid Electric Vehicles," vol. 53, no. 2, pp. 385-389, 2004.

doi: 10.1109/TVT.2004.823525

[20] J. Welstead and J. L. Felder, "Conceptual Design of a Single-Aisle Turboelectric Commercial Transport with Fuselage Boundary Layer Ingestion," *54th AIAA Aerospace Sciences Meeting,* 2016.

doi: 10.2514/6.2016-1027

[21] J. Hoelzen, Y. Liu, B. Bensmann, C. Winnefeld, A. Elham, J. Friedrichs and R. Hanke-Rauschenbach, "Conceptual Design of Operation Strategies for Hybrid Electric Aircraft," *Energies,* vol. 11, 2018.

doi: 10.3390/en11010217

[22] S.Wang, J.T.Economou and A.Tsourdos, " Indirect engine sizing via distributed hybrid-electric unmanned aerial vehicle state-of-charge-

based parametrisation criteria. Proceedings of the Institution of Mechanical Engineers, Part G: Journal of Aerospace Engineering.

doi: 10.1177/0954410019843722

[23] D. Howe, *Aircraft Conceptual Design Synthesis*, Wiley, 2014, p. 62.

[24] ROTRON, “Rotron Rotary Engines”, [Online]. Available: http://www.rotronuav.com/engines/rt-600. [Accessed 12 December 2018].

[25] ULPOWER, “ULPower Aero Engines,”. [Online]. Available: https://ulpower.com/en/engines. [Accessed 12 December 2018].

[26] ROTAX, “Rotax Products – Aero Engines,”. [Online]. Available: https://www.flyrotax.com/produkte/detail/rotax-912-ul-a-f.html. [Accessed 12 December 2018].

[27] LYCOMING, “Engines - Exceeding The Standard In General Aviation,”. [Online]. Available: https://www.lycoming.com/engines. [Accessed 12 December 2018].

[28] LIMBACH, “Engines drive us!”. [Online]. Available: https://limflug.de/en/products/engines.php. [Accessed 12 December 2018].

[29] PBS Aerospace, “Turbojet, Turboprop and Turboshaft Engines from PBS.” [Online]. Available: https://www.pbs.cz/en/our-business/aerospace/aircraftgines. [Accessed 12 December 2018].

[30] HIRTH, “Engines.” [Online]. Available: https://hirthengines.com/2-stroke-engines/. [Accessed 12 December 2018].

[31] Rolls-Royce, “M250 – Set you sights on the standard-bearer.” [Online]. Available: https://www.rolls-royce.com/products-and-services/civil-aerospace/helicopters/m250-turboshaft.aspx#/. [Accessed 12 December 2018].

[32] SAUER. [Online]. Available: http://www.sauer-flugmotorenbau.de/. [Accessed 12 December 2018].

[33] Wikipedia contributors, "Comparison of commercial battery types," 16 December 2018. [Online]. Available: https://en.wikipedia.org/w/index.php?title=Comparison_of_commercial_battery_types&oldid=873978689. [Accessed 7 January 2018].

[34] Wikipedia contributors, "Power-to-weight ratio," Wikipedia, The Free Encyclopedia., 1 January 2019. [Online]. Available: https://en.wikipedia.org/wiki/Power-to-weight_ratio. [Accessed 1 January 2019].

[35] K. Deb, A. Pratap, S. Agarwal and T. Meyarivan, "A fast and elitist multiobjective genetic algorithm: NSGA-II," in IEEE Transactions on Evolutionary Computation, vol. 6, no. 2, pp. 182-197, April 2002.

doi: 10.1109/4235.996017

6 RULE-BASED CONTROLLERS

Chapter 4 and 5 completed the system sizing that selected suitable components for the designed system. This chapter will introduce two rule-based controllers for the power management problem, which is the first two targets in the third objective.

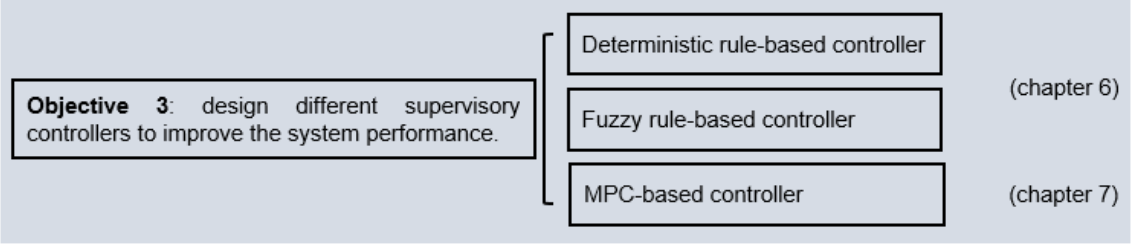

Figure 42 Chapter 6 structure.

Mamdani & Sugeno Fuzzy Battery Longevity for Distributed Series Hybrid Electric Aircraft

Abstract

During the energy revolution in transportation, the hybrid-electric propulsion system becomes a reasonable choice for the next generation of aircraft. Except for the system configuration and the selection of components, the control strategy is an essential part affecting the system performance. This paper proposed a battery longevity controller based on fuzzy logic strategies. The controller is particularly designed for hybrid aircraft due to the battery pack is sensible to

environment and may put the aircraft in danger scenarios without any warning. The controller firstly applies a Mamdani fuzzy inference system to evaluate the operating environment of the battery pack. Then, based on the evaluation result and the predicted future power requirement, a Sugeno fuzzy inference system is designed to obtain a control signal for the engine and generator. For better showing the performance, a deterministic rule-based controller is also developed to accomplish a comparison with the fuzzy controller. The result shows that the Mamdani & Sugeno fuzzy battery longevity controller performs better than the deterministic rule-based controller which can improve both the battery operating environment and fuel consumption.

6.1 Introduction

Hybrid aircraft is one of growing industries in recent years. Since the cooperation of two or more energy sources provides an opportunity of lowering system fuel consumption and emissions, the hybrid-electric technology has been successfully applied on light-aircraft and is attempting to be utilized on large commercial aircraft right now.

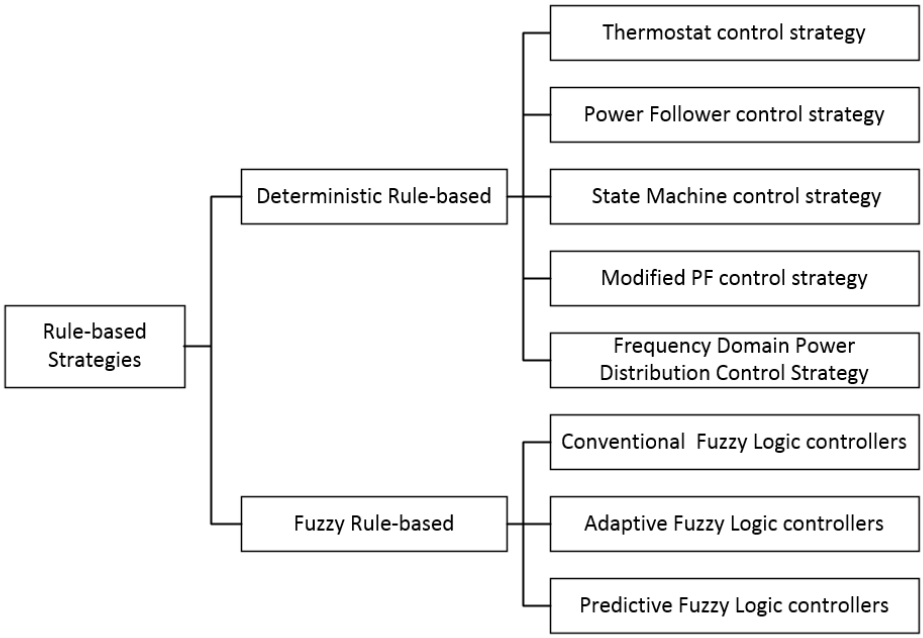

Figure 43 Classifications of rule-based control strategies.

Normally, a good hybrid-electric propulsion system refers to a system which can amplify the advantage and weaken the disadvantage of each component. This target is always realized by using an appropriate controller which can intelligently manage energy from different sources. Along with the popularity of the hybrid-electric vehicle market, various intelligent controllers have been developed. There are two categories of control strategies: rule-based (heuristic) control strategies and optimization-based control strategies [1-2]. Rule-based control strategies are a set of criteria defined based on heuristics, intuition and human experiences, which are simple and especially effective in the real-time control of hybrid systems [1]. The Deterministic Rule-Based (DRB) and fuzzy rule-based controllers are two classifications of rule-based control strategies.

In general, deterministic rule-based controllers heuristically split power demand to various power sources based on certain parameterizations and human experiences. The simplest control method is the thermostat strategy which refers to turning on/off the engine based on the remaining battery state-of-charge [3]. Improved on that, the power follower control strategy has been proposed, which adds the variable of power requirement into the control strategy so that the engine can adjust working status according to target performance. The state machine controller has also been developed in some research, but the result is not as desirable as others [4]. Although different controllers have minor differences, the central theme of all deterministic control strategies is ‘load leveling’.

The fuzzy rule-based control strategy is one other representative type of controllers which presents human inference processes. It translates expert knowledge and experience into corresponding rules [5]. For hybrid-electric aircraft, fuzzy controllers are very popular due to the hybrid-electric propulsion system is a nonlinear and time-varying plant. Paper [6,7] presented a fuzzy logic controller which is able to improve efficiencies of all components of the system. The study used the information of driver’s power command, battery SOC and motor speed to determine the split ratio between two power plants, and achieved a 6.8% fuel reduction in an urban cycle and a 9.6% fuel reduction in a highway cycle. The paper [8] developed a fuzzy controller to reduce emissions. It used the

information of the acceleration pedal stroke and the rotational speed to find the best ratio of torque command, and finally realized a 20% of NO_x emission reduction compared to a diesel engine vehicle. Paper [9] proposed a fuzzy controller for both improving fuel consumption and reducing pollutant emissions. Simulation results showed that the system achieved 20% and 5.7% fuel efficiency improvements on real and modal driving cycles respectively, and reduced overall amount of emissions. Similarly, paper [10] developed another fuzzy control strategy to improve each components' efficiency and it achieved a 23%-35% improvement of the system efficiency.

Fuzzy controllers have good adaptability. It not only can be easily tuned or adapted to different environments, but also can be integrated with other optimization approaches. Therefore, conventional fuzzy controllers will be further enhanced if control parameters are adaptive to optimization methods or current operating conditions, for example the driving environment, the driving style and the driving cycle. The paper [11] presented an optimized fuzzy controller, whose membership function is optimized by the genetic algorithm, to effectively improve the fuel economy of the hybrid electric vehicle. Additionally, on the basis of a torque distribution and a charge sustenance compensation strategy, paper [12,13] proposed a fuzzy logic-based driving situation identifier to obtain an enhanced operation. Similarly, the paper [14] used a Mamdani fuzzy logic inference to identify the driving pattern, and generated control signals based on the inferred driving pattern and the predicted upcoming driving environment. Due to it used the future information of the mission, it is a predictive fuzzy controller which is very popular in hybrid automobiles. The research in [15] has also proposed a predictive fuzzy controller, but it used the predicted future state of the vehicle to get a better system performance on the fuel consumption and emissions. Furthermore, an optimized predictive fuzzy controller has been proposed [16]. It initially predicted the traffic condition, and then determined the control result by using a fuzzy logic inference whose membership function have been tuned by the genetic algorithm. The simulation result showed that this new controller has successfully reduced the power loss and increased the fuel convertor efficiency by around 20%.

However, the objectives in most of researches are automobiles, only few hybrid-electric aircraft have been mentioned. Basically, there is no big difference between the hybrid-electric propulsion system of automobiles and other vehicles except they have different missions. However, due to the strict requirement of flight safety and the vulnerability of the battery pack, a distinguishing feature of the hybrid-electric aircraft is found, i.e. the system should monitor the condition of the battery pack all the time to avoid accidental damages and energy drops caused by unnoticed capacity fade. In other words, for hybrid-electric aircraft, the battery's condition is better to be well-considered and introduced into the control strategy. As a result, to obtain a superior hybrid electric propulsion system of aircraft, a battery longevity power management strategy is essential.

This paper presents a predictive fuzzy controller for an innovative distributed series hybrid-electric propulsion system for aircraft. The developed controller not only provides a healthy operating environment to the battery pack, but also improves the system fuel economy simultaneously. The paper starts with a review about present rule-based controllers for hybrid power systems, followed by a detailed description of the designed hybrid-electric propulsion system. In the third section, modelling methods and characteristics of each component are discussed, involving the battery ageing phenomena and an evaluation method of the battery operating condition. After that, a deterministic rule-based controller is introduced as the baseline of this study. The next section presents the designed fuzzy-based battery longevity controller. Each variable and membership functions are illustrated in detailed, and control rules are also demonstrated. Simulation results are presented in the last section, where the performance of the engine and the battery pack are analyzed respectively.

6.2 System Design

Based on the conventional series hybrid configuration, this paper proposes a novel Distributed Series Hybrid Electric Propulsion System for aircraft. This new structure improves propulsors' efficiency due to it adopts the distributed propulsion concept and integrates other electric loads into the main propulsion system. The complete system structure is shown in Figure 44.

There are three parts constituting the system. The first part contains two power sources, i.e. an engine and a battery pack, which are linked by a generator and a converter. The second part refers to the energy output. There are 6 aligned electric motors utilized to drive propellers. Applying multiple electric motors not only improves the aerodynamic properties of aircraft, but also mitigates the engine over-sized problem. Please note that the number of electric motors is initially designed as 6 to present a distributed propulsion configuration, and the number could be modified later for getting a better aerodynamic property. The third part of the system is the 'other electrical loads' part, where an electric taxiing system has been integrated in due to it has higher efficiency compared with the common propeller-driving taxiing [17]. Overall, the designed hybrid propulsion system is similar to an electric grid. The first part of the system indicates the energy source and the other two parts are electrical loads for different purposes. This configuration effectively streamlines the system structure and increases the utilization efficiency of each component. A more detailed description of the system could be found in paper [18].

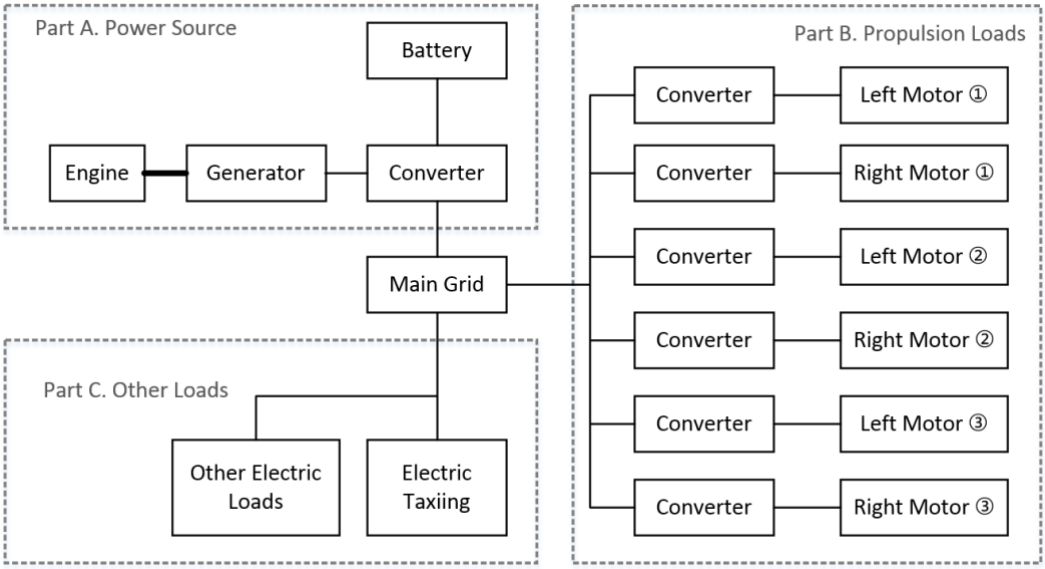

Figure 44 Distributed series hybrid-electric power system.

Apart from the special configuration, the selection of components is also crucial to the system performance. For example, using a bigger engine will increase the charging rate of the battery pack, which is good for SOC sustaining strategy, but

leads to a difficulty of protecting the battery pack from being overcharged and makes the system heavier. Therefore, each component should be carefully selected. The author has proposed an intelligent sizing method for the designed system based on the genetic algorithm, by which the system fuel efficiency and total mass could be both optimized [18,19].

6.3 Components and Modelling Methods

The simulation of this work is obtained by developing a detailed model using MATLAB Simulink and Simscape system-based software packages. Each component is composed of mathematical formulas to show performances.

6.3.1 Engine

The engine is the prime component of the hybrid propulsion system which can stably generate energy by burning fuels. According to Figure 44, the system decouples the power demand (electric motors and other loads) and the energy source (the engine and the battery pack) via the special configuration, so that the engine can operate isolatedly without considering current power requirement. Therefore, for the DSHEPS, the engine size is better to be determined via battery SOC parametrization criteria rather than the real-time power demand. In paper [18], it found that the engine with the capacity of 1.2 times of the average value of the mission power requirement can bring a better performance to the battery pack. Therefore, a rotary engine, ROTRON RT600LCR, is selected for this study. The specifications of RT600LCR is summarized in the Table 12 [20].

Table 12 RT600LCR Specifications [20].

Max Power	58HP @7500 RPM
Max Continuous Power	54HP @7500 RPM
Max Torque	43.55 lbs/ft @6500 RPM
Block Weight	21.2kg

There are plenty of modeling approach for the engine. One of the simplest modelling approaches is using performance maps to build the engine model

[21,22], such as the Willans line modelling method. The Willans modelling method uses a linear relationship of the brake mean effective pressure and the fuel consumption rate to reflect the engine performance [23]. This method is effective but cannot show engine's dynamic behaviours since the performance map is lack of dynamic response. Other modelling methods, for example, the spark ignition engine modelling method, the compression ignition engine modelling method and the mean value modelling method are precise and can accurately show engines' dynamic behaviors. In general, different modelling approaches suit to different problems. The modelling method should be selected depended on the purpose of the simulation. Therefore, in this study, a simplified mean value model [24] is applied. Based on the performance map, the mean value model reveals the relationship between the throttle with power, torque and brake specific fuel consumption respectively.

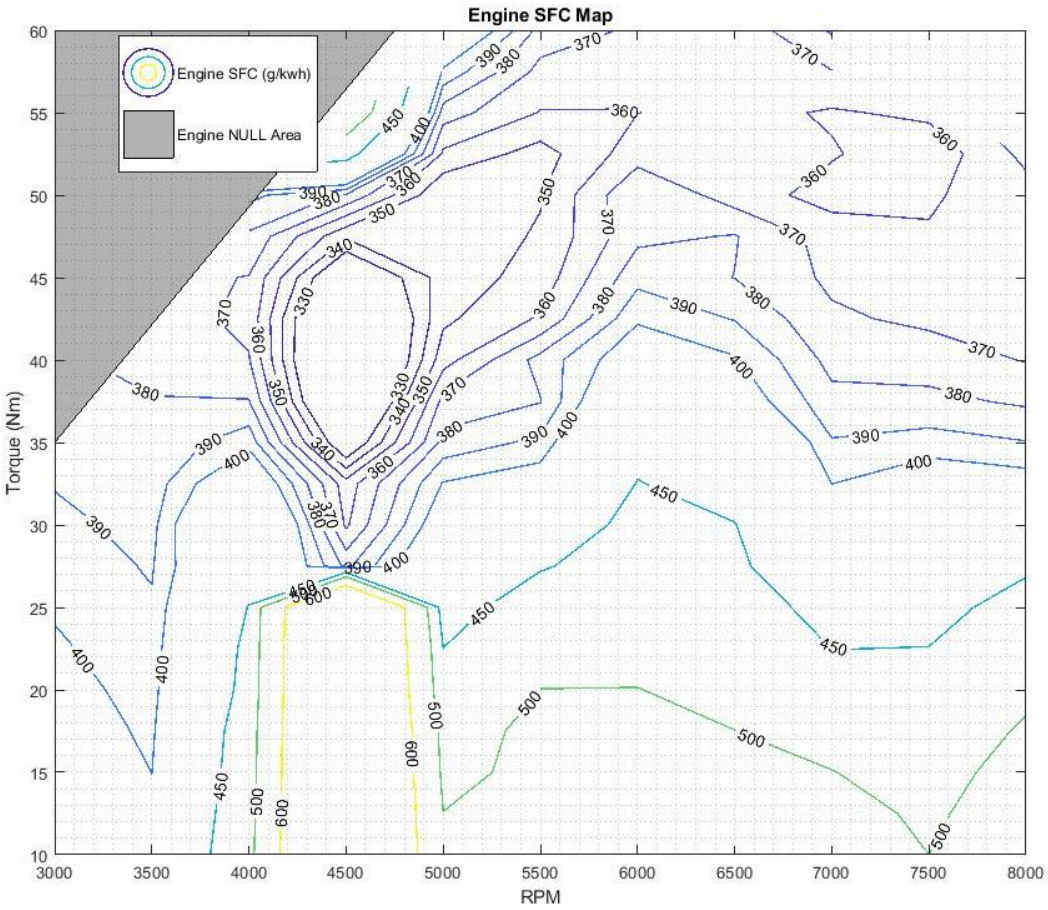

Figure 45 Engine BSFC map [25].

The engine Brake-Specific Fuel Consumption (BSFC) map is shown in Figure 45 [25]. BSFC is a commonly-used measurement of the fuel efficiency of the engine. It is the rate of fuel consumption divided by the power produced. Seen from the figure, the most efficient BSFC is about 330g/kwh with the engine speeds between 4300-4800RPM corresponding to 17-23kW power output. The second level of the engine high-efficient operating area is defined as the region where the BSFC is lower than 360g/kwh. It is a strip area with the speeds from 4100-7500RPM, and the highest power output is about 43kW shown by the contour line in the upper right corner. In general, if the engine can keep running in the restricted high-efficient area, the fuel economy of the whole system will be significantly improved. Specified to this problem, starting from a stationary state, the engine should operate in the most efficient area for most of the mission time. When the system requires higher power, the engine operating point should move to the high powerful area for a short period time to charge the battery pack until it has enough energy for the remaining mission. After that, the engine operating point could move back to the most-efficient point at an appropriate time. Overall, the problem for the engine of the hybrid system is to find a best timing for shifting the engine operating point.

6.3.2 Motor and Generator

The electric motor is another primary component in hybrid systems. It converts electrical energy into mechanical energy which realized electrical propulsion of aircraft. In addition, due to the designed hybrid-electric system generates energy by an engine and the engine outputs mechanical energy, it requires a generator to do a reverse energy transmission. The motor and generator have much in common, thus the motor is also used as a generator to convert mechanical energy into electricity. In this paper, a high power-to-weight ratio PMSM, EMRAX228 motor, is selected as the motor and generator. The motor's efficiency map is shown in the Figure 46 [26]. According to this figure, the contours of motor efficiencies are concentric circles, and most efficient area, with an efficiency of 96%, is at about the centre of all its operating range.

There are several modelling approaches for PMSMs. For example, simplifying the motor to a low-order transfer function or using a look-up table to represent its performance. This study uses a $d-q$ model to composite the PMSM [27,28]. The model applies the transformation between the stator's abc frame and the rotor's $d-q$ frame to calculate the rotor angular velocity, rotor angle and stator current of each phase to obtain three phase circuit.

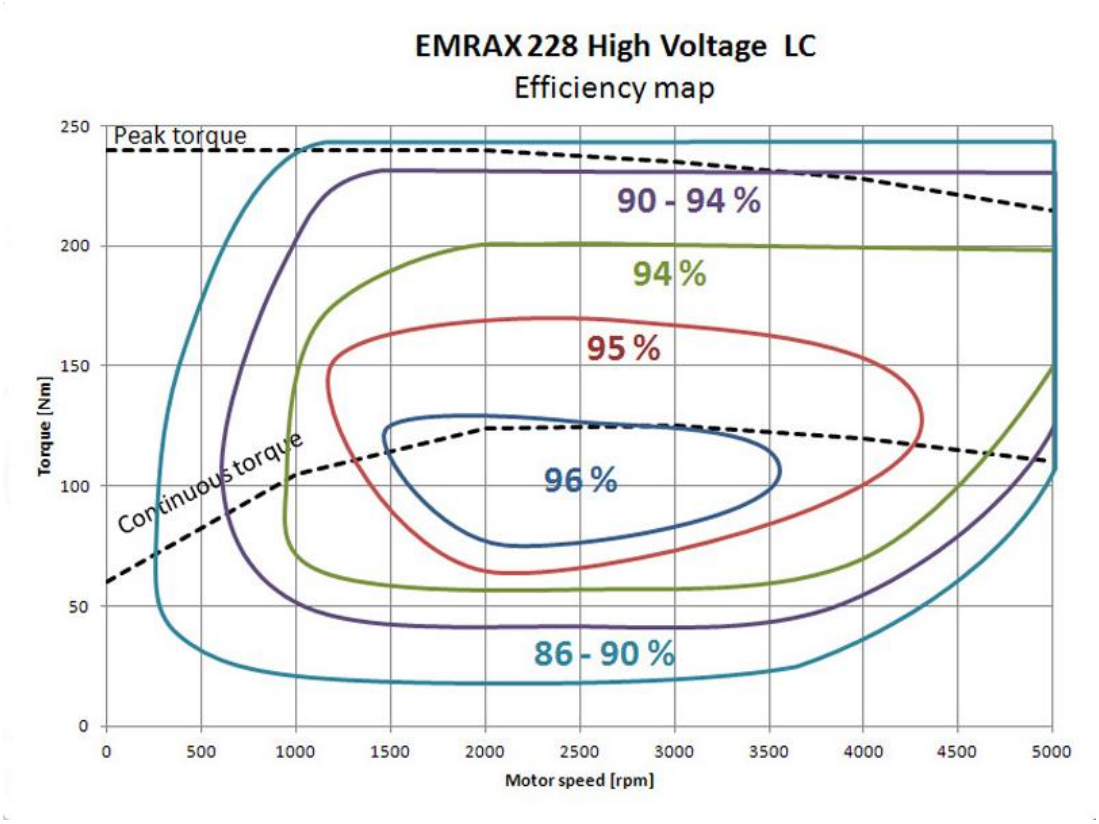

Figure 46 Electric motor efficiency map [26].

6.3.3 Battery

The battery pack is the substantial energy supplement for the hybrid-electric propulsion systems. It transfers or stores the energy based on the system demands, and responds rapidly without warm-up or start-up time. The capacity of the battery could be defined by the maximum difference between the power demand and the engine output, and the voltage is primarily designed as 296V.Compared with other batteries, the Lithium-ion (Li-ion) battery is outstanding due to its high power-to-weight ratio, no memory effect, longer

lifespan and lower self-discharge rate. Therefore, this work selected Li-ion as the storage component and uses the Shepherd model to predict the SOC at each moment [29]. The Shepherd modelling method summarized an empirical equation for Li-ion batteries' charging/discharging curves based on a huge amount of experimental data.

For achieving a better system performance, a long-term reliable and high energy-efficient battery is desired. In general, the Li-ion battery pack is sensible to the operation environment and improper operations. In addition, the efficiency of the battery pack, including the 'electrical efficiency' and 'columbic efficiency', all decrease over the lifetime of the battery, and the cell failure rate increases with the increased charging/discharging cycles. All above phenomena are caused by the battery ageing, also called as battery degradation, which is a major drawback on the battery's real usage. The battery ageing mainly reflects as increasing internal resistance and capacity fading, it occurs during the battery pack's whole life, no matter it is used or not. As a result, at present, the lifespan of the battery is around 15 years until the battery lost 20% of its initial capacity, i.e. the end-of-life of the battery is normally defined as the battery remains 80% of its capacity [30].

The battery degradation significantly affects the performance of the hybrid-electric propulsion system. Firstly, the lifespan of the battery pack influences the service life of the whole system. Although the battery pack could be easily replaced, the cost and adaption of a new battery pack is not less. Moreover, the abandoned battery pack pollutes the soil and is hard to be resolved. Secondly, the battery ageing affects the power management strategies, especially for the charging-sustaining control strategy. For example, a drop in useable capacity will represent a larger SOC variation in charge-sustaining operation for a given mission, i.e. a battery pack will show a larger SOC variation to complete a same task. In addition, the capacity loss reduces available flight range and decreases acceleration ability. Therefore, considering the capacity fading, the lowest SOC threshold should increase and all limitations regarding to the SOC are needed to be re-designed. However, estimating and modelling the battery ageing is a

challenging problem in the state-of-art. Battery ageing is hard to identify and quantify due to the diversity and the complexity of the phenomena [31]. Therefore, a battery longevity controller is proposed which is aiming to improve the battery operating environment and extend the battery lifespan.

- **Evaluation of Batteries' Operating Condition**

The battery degradation strongly depends on operating conditions and environment, relative variables such as time, working temperature, Depth of Discharge (DoD), discharge rate and charging stress [32-34]. The battery ageing is a completed progress. There are many prediction models have been developed for Li-batteries, such as the empirical equation (6-1) and (6-2) proposed by Wang et al. [34] and Bloom et al. [35]. In (6-1) and (6-2), Q_{loss} represents the percentage of capacity loss, B_d is the pre-exponential factor, E_a refers to the activation energy, ρ_{gas} is the gas constant, T means the absolute temperature, z is the power law factor, t is time and Ah is the Ah-throughput [34,35]. The value of the processed capacity is calculated by the number of cycles N_{cycle}, DoD and the full battery capacity C_{full}. All factors are obtained from experimental data, and values are different for different batteries. However, the result shows a similar trend by a same variation of these parameters. Therefore, summarized from previous research, a high-quality charging pattern of lithium-ion battery could be obtained, and key bullets are shown as below.

$$Q_{loss} = B_d \cdot exp\left(\frac{-E_a}{\rho_{gas} T}\right) t^z \ \ or \ \ B_d \cdot exp\left(\frac{-E_a}{\rho_{gas} T}\right) (Ah)^z \quad \textbf{(6-1)}$$

$$Ah = N_{cycle} \cdot DoD \cdot C_{full} \quad \textbf{(6-2)}$$

1) The capacity loss accumulates over time, i.e. the fading percentage increases respect to time.
2) Li-batteries perform poorly at extreme working temperature. The best operating temperature is between 15-35℃ [32].
3) The capacity degrades faster with high current. Namely, the fast charging/discharging, i.e. high charge/discharge rate, shortens the useful life of the battery pack.

4) Although the effect is minor compared with the first three parameters, long-term at high-DoD condition accelerates the capacity fade.

Therefore, to retard battery degradation, the hybrid-electric system requires a decision-making block to guarantee a healthy operating environment for the battery pack but also be capable to minimize the fuel consumption and emission. This paper proposed a battery-friendly controller which can intelligently manage power flow and extend the lifespan of the battery pack simultaneously. Due to the lack of the information of a precise battery ageing progress, a fuzzy logic controller seems to be one suitable control strategies. The controller firstly evaluates the battery operating environment, and then gives command to the engine and generator based on the evaluation result and predicted mission power requirement.

6.4 Deterministic Rule-Based Controller

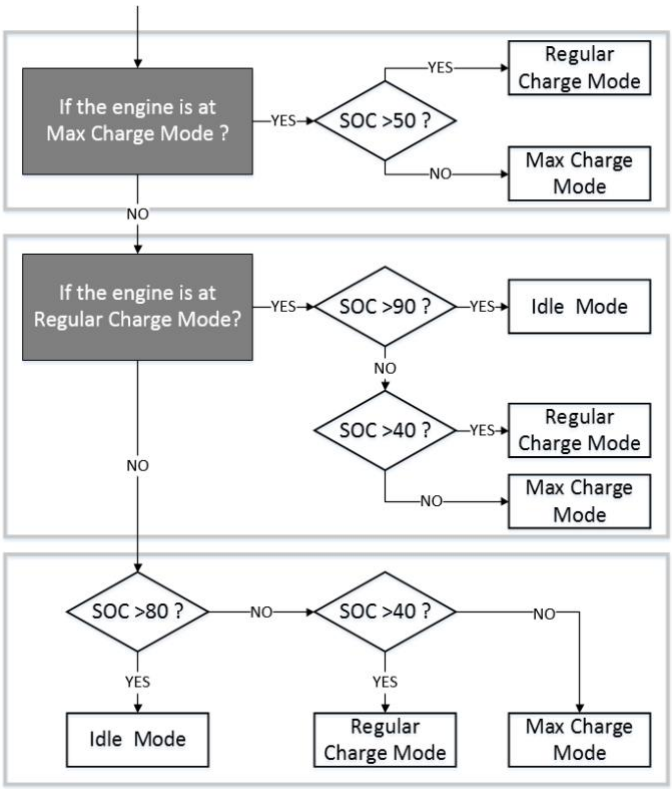

Figure 47 Flowchart of the DRB controller.

Before introducing the fuzzy controller, a basic deterministic rule-based controller is presented acting as a baseline for the new designed battery-friendly controller. The DRB controller here is a power follower controller, and the flowchart is shown in the Figure 47.

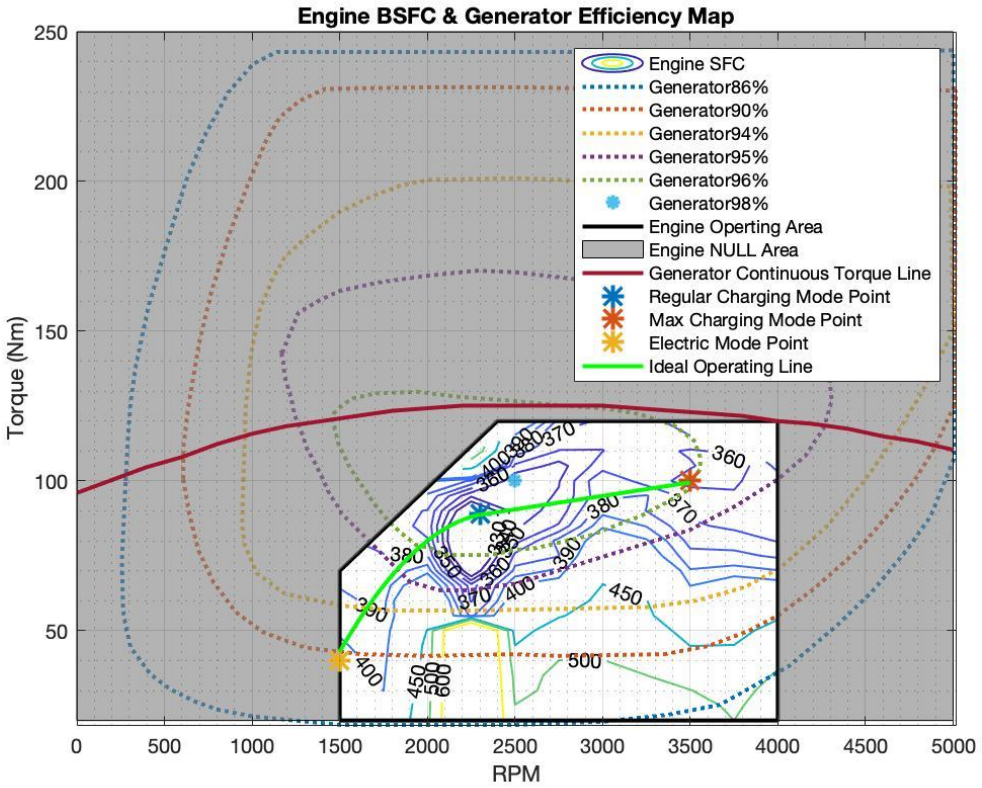

Figure 48 Engine and generator efficiency map.

In order to define appropriate operating modes, the engine efficiency map and motor efficiency map are put together to find good operating points, shown as Figure 48. Please note that because the system applies a gear box, the abscissa of the engine map is reduced to half and the ordinate of that is stretched to twice. From the figure, three feasible operating points are selected as main operating points which are (1500RPM, 10Nm), (4600RPM, 45Nm) and (7200RPM, 50Nm) corresponding to three operating modes respectively:

1) Max charge mode: highest power output with high efficiency, the operating point is (7200RPM, 50Nm);

2) Regular charge mode: moderate power output with best fuel efficiency, the operating point is (4600RPM, 45Nm);
3) Idle mode: low power output, the engine nearly to be idle, the operating point is (1500RPM, 10Nm).

Above three operating modes are designed for different specific scenarios. The max charge mode is a high powerful operating mode. The engine runs at the point (7200RPM, 50Nm) producing 37kW power output. Therefore, the engine will be switched to the max charge mode only when the battery SOC is below the given safety threshold. The next operating mode is the regular charge mode, whose engine operating point is at (4600RPM, 45Nm). This operating point is in the most efficient area, i.e. it refers to the ideal engine operating condition. Since the regular operating mode has the best fuel economy, the system will improve its fuel performance if the engine stays in this mode as long as possible. Therefore, except when the battery pack has an extreme SOC, the system could remain the second operating mode for most of the time. The third operating mode refers to the idle condition. Due to switching off the engine during the flight is not feasible and low-efficient, and the engine re-starting costs time, it is better to keep engine running during the whole flight. The engine can only be switched off after aircraft successfully landed. Therefore, the third mode is designed. The engine operating point is at (1500RPM, 10Nm), which is nearly idle with a low power output.

Based on the proposed operating modes, the rules of the controller can be determined. The controller firstly distinguishes the current engine operating mode. If the engine is at the max charge mode, the operating condition will be adjusted to the regular charge mode when the SOC is above 50%. Otherwise, the engine will stay at the max charge mode to charge the battery until it reaches the given limitation. Similarly, if current mode is the regular charge mode, the engine will change the operating mode based on two given SOC limitation 40% and 90% respectively. The engine will turn into the idle mode if the SOC reaches 90% and will turn into the max charge mode when the SOC is below 40%. Otherwise, if the engine is not in either the max charge mode or the regular mode,

thresholds of the SOC are 80% and 40%. The controller is a basic rule-based controller and each threshold is determined by author's experience.

6.5 Mamdani & Sugeno Fuzzy Logic Controller

To further enhance the performance of the system, this paper proposed a new fuzzy control strategy: Mamdani & Sugeno Fuzzy Logic (MSFL) controller, which can properly manage power flow and extend battery life. Namely, the controller monitors the current and SOC, and based on that, it can intelligently decide when the battery pack should be charged or discharged. Here, the fuzzy control strategy is selected due to the operating condition of the battery pack is easily assessed by expert knowledge and experience. In order to incorporate those well-defined rules within the UAV control architecture, it is critical to execute a transformation from a linguistic based rule-base command into a mathematical expression [36-37]. Considered all above conditions, the system requires two fuzzy inference systems to process the system, as shown in the Figure 49.

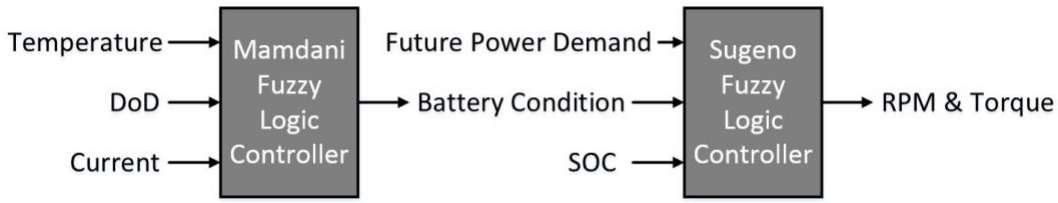

Figure 49 Fuzzy logic control structure.

6.5.1 Part 1 - Mamdani Fuzzy Logic Controller

The first inference system is designed to evaluate the operating environment of the battery pack. Due to that the real capacity fade is an extremely complicate progress, i.e. the percentage of the capacity fade is very hard to precisely defined, the assessment of the batteries' operating environment cannot be evaluated by a mathematical model. However, as mentioned in the last section, there are three main variables (working temperature, DoD and charge/discharge rate) affecting the health of the operating condition of the battery pack. Therefore, this study proposed a simple method that uses a fuzzy inference system to infer the operating condition.

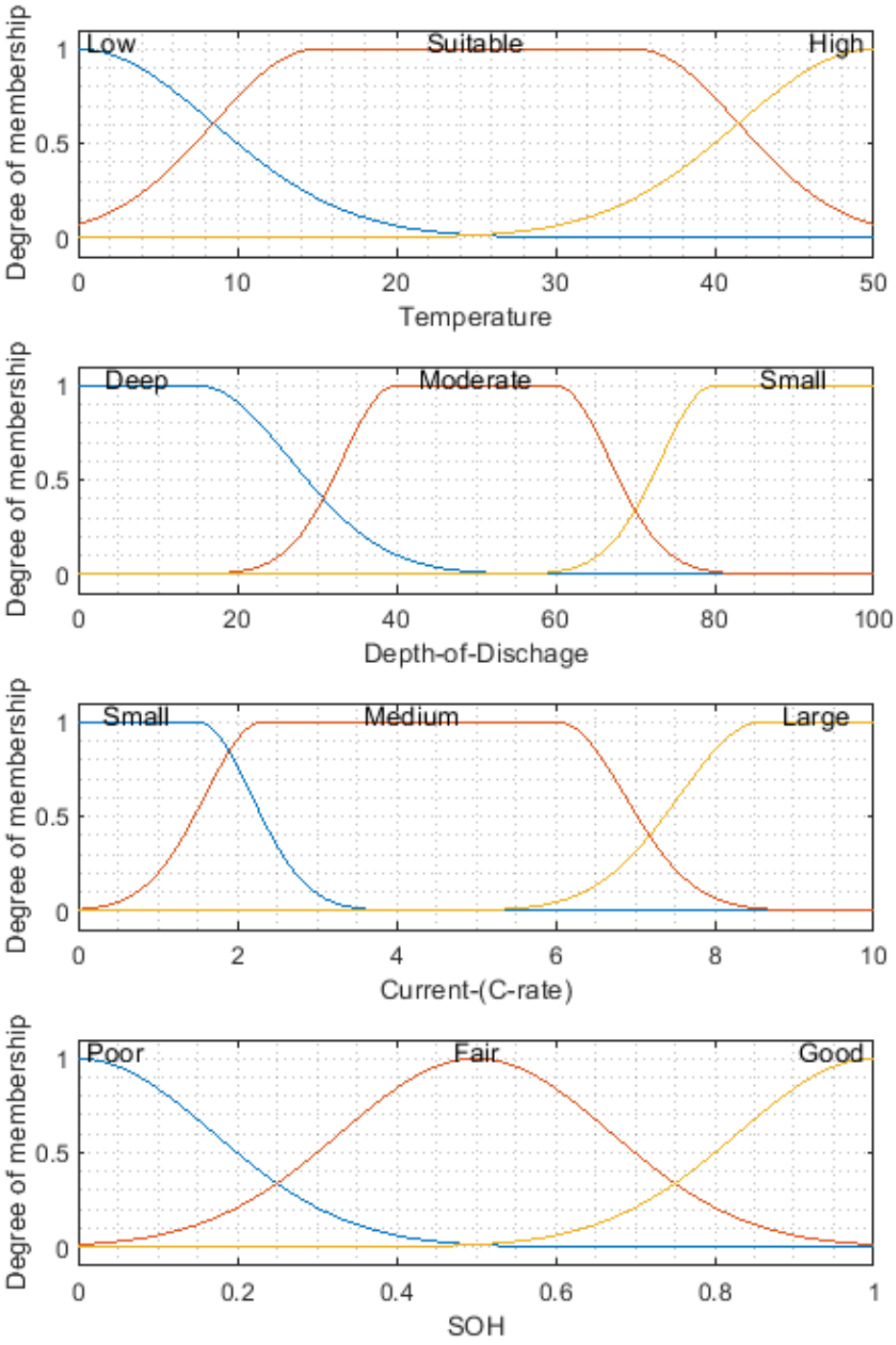

Figure 50 Membership functions for battery assessment system.

This inference process is obtained by using a Mamdani type fuzzy controller. The Mamdani fuzzy system is good at transforming human expertise to the control rules, which can perfectly convert the battery characteristics to evaluation standards. Based on literatures, it can be found that the best operating

temperature is around $15-35℃$, the suitable interval of DoD is between $40\%-60\%$, and charge/discharge with lower current benefits the battery health. Therefore, different membership functions are assigned to inputs and outputs respectively based on the battery operating properties, seen as Figure 50. The most 'suitable' operating temperature range and the 'moderate' DoD range are clear. Regarding the current, it is obvious that a small current is beneficial to the operation of the system. Therefore, based on the maximum estimated current value and considering the occasional huge current oscillations, the 'moderate' region is set to 2-6A. In addition, in order to ease optimization, Gaussian and generalized Bell-shaped membership functions are selected to depict fuzzy sets. Their normal equations are written as (6-3) and (6-4). In these functions, c refers to the locating centre of each curve, σ determines the width of the Gaussian curve, a is the width of the bell-shaped curve, and b is a positive integer influencing the slop of the curve.

$$GaussMF(x,\sigma,c) = exp\left(-\frac{(x-c)^2}{2\sigma^2}\right) \quad \textbf{(6-3)}$$

$$GbellMF(x,a,b,c) = \frac{1}{1+\left|\frac{x-c}{a}\right|^{2b}} \quad \textbf{(6-4)}$$

The output, battery operating condition, is described as an assigned output ranging from 0 to 1, where "0" corresponding to the poorest condition and "1" corresponding to the best operating condition. The fuzzy rules are listed as below:

- If the DoD is in the moderate area, i.e. 40%-60%, the fuzzy rules are:

Table 13 Rules for 40-60% DoD.

Temperature / Current	**Low**	**Suitable**	**High**
Small	Fair	Good	Good
Medium	Fair	Good	Fair
Large	Poor	Fair	Poor

- If the DoD is not in the moderate area, the fuzzy rules are:

Table 14 Rules for 0-40%& 60-100% DoD.

Temperature / Current	Low	Suitable	High
Small	Fair	Good	Fair
Medium	Poor	Good	Poor
Large	Poor	Fair	Poor

From above two tables, there is no difference between outputs under certain circumstances. When the temperature is 'suitable', the operating condition is assessed as "Good" no matter how DoD is. While the temperature is not in that range, some of outputs goes down to a lower level. This is because that the influence of DoD is minor compared to other two variables. Overall, the best operating condition for battery is that the battery pack is charged or discharged with a low current under a suitable outside temperature. The poorest condition is that charging/discharging the battery pack when it is deep discharged in an extremely high/cold environment.

6.5.2 Part 2 – Sugeno Fuzzy Logic Controller

The second fuzzy inference system is designed to generate a control signal for the entire system, i.e. the RPM and torque of Part A Power Source. Engine's optimal operating area is a given region between two high-efficient operating points shown in Figure 48. Due to the ideal engine output is restricted, the inference system for the system control signal is possible to achieve by a Sugeno type fuzzy inference [38,39].

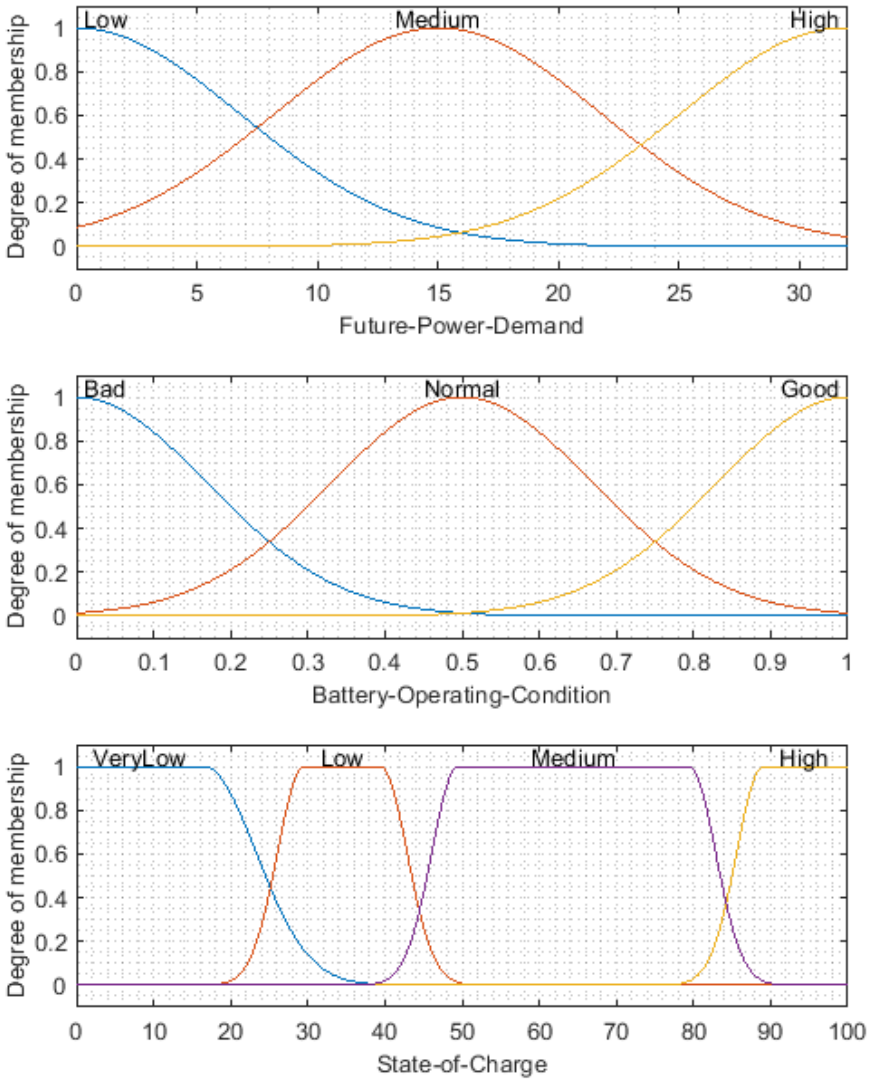

Figure 51 Membership functions for main controller.

Sugeno fuzzy logic system uses an analytical consequent equation as output, so that it can achieve a more accurate and efficient control instruction than using Mamdani fuzzy [40]. There are four input variables in this fuzzy controller, which can be of the form as $x = [P_f, C_b,\ SOC, RPM]'$. Here, P_f refers to the future power demand, C_b is the indicator of the battery operating environment, SOC means the state of charge of the battery pack and RPM refers to current RPM of the engine. Figure 51 gives membership functions for the future power demand, battery

operating condition and battery SOC. The membership function of RPM is not illustrated since it does not affect rules.

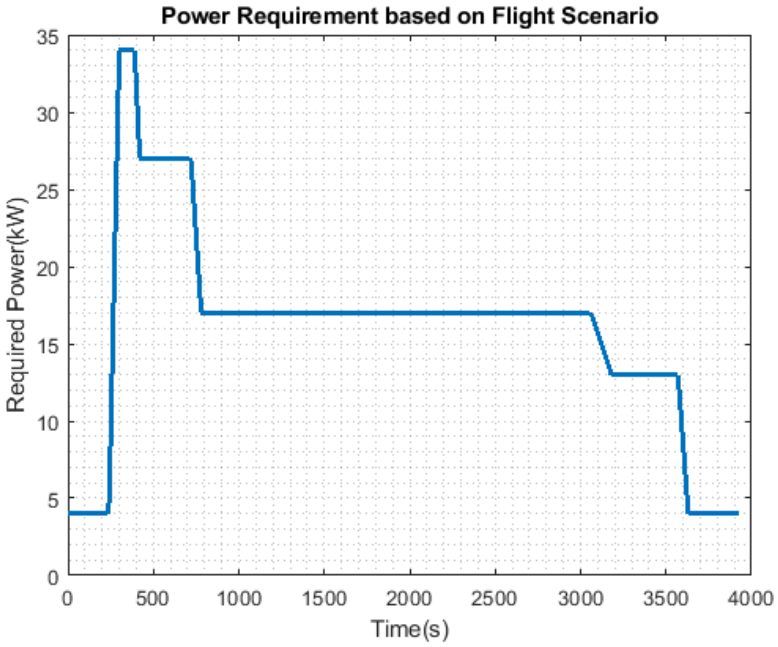

Figure 52 Power requirement for a typical flight

Different membership functions are designed for each variable. At first, the value of the variable P_f can be estimated by the mission power demand which is shown as Figure 52. The largest value of P_f should be equal to or less than the maximum value of required power, while the lowest value should be zero. This study uses an average value as the future power demand, see equation (6-5). It is the average value of the power requirement P_{req} in future 2min, 3min, 4min and 5min. There are three membership functions of the future power demand, which is shown in the Figure 51, representing mission accomplishment, cruising flight stage and take-off flight stage respectively.

$$P_f(t) = \frac{P_{req}(t+2min) + P_{req}(t+3min) + P_{req}(t+4min) + P_{req}(t+5min)}{4} \quad \textbf{(6-5)}$$

The second input variable is the battery operating condition. It is the result acquired from the first fuzzy controller whose range is [0 1], and it has been uniformly divided to three Gaussian membership functions. The third input is battery SOC in the range of [0 100]. There are four set crisps: very low, low, medium and high. The first 'very low' membership function indicates the safety threshold of the entire system E_{safety} and energy value $E_{etaxiing}$ that the energy electric taxiing required, i.e. equation (6-6). The safety threshold is 25% SOC in this study. Apart from the first, the rest of SOC are split into three membership functions. The 'middle' function occupies the SOC range from 50% to 80%, and the 'high' SOC refers to 90% SOC.

$$Very\ low = max\{E_{safety}, E_{etaxiing}\} \quad \textbf{(6-6)}$$

Regarding the fuzzy rules, the k_{th} rule level y_k of a Sugeno fuzzy system could be normally presented as a sum of decision variables with coefficients.

$$y_k = a_{k1}x_1 + a_{k2}x_2 + \cdots + a_{kj}x_j + b_k \quad \textbf{(6-7)}$$

Or a more general description is given by the following matrix:

$$\boldsymbol{A} = \begin{bmatrix} a_{11} & a_{12} \dots & a_{1j} \\ a_{21} & a_{22} \dots & a_{2j} \\ \vdots & \vdots & \vdots \\ a_{n1} & a_{n2} \dots & a_{nj} \end{bmatrix}, \boldsymbol{B} = \begin{bmatrix} b_1 \\ b_2 \\ \vdots \\ b_n \end{bmatrix}, \boldsymbol{Y} = \boldsymbol{A} \cdot \boldsymbol{X} + \boldsymbol{B} \text{ with } \boldsymbol{X} = \begin{bmatrix} x_1 \\ x_2 \\ \vdots \\ x_j \end{bmatrix} \quad \textbf{(6-8)}$$

In the above equations, n is the number of rules and j is the number of input variables. For this research question, to guarantee the engine can continuously work in the efficient area, the engine's operating condition is expected to be restricted to a low fuel consumption rate area, i.e. 4600-7000RPM. Therefore, three different expected control signals are proposed:

$$INCREASE: y = RPM(t+1) = 7000 \quad \textbf{(6-9)}$$

$$STEADY:\ y = RPM(t+1) = RPM(t) \quad \textbf{(6-10)}$$

$$DECREASE:\ y = RPM(t+1) = 4600 \quad \textbf{(6-11)}$$

These three equations refer to three output membership functions of this Sugeno inference system. The ‘increasing’ command aims to boost engine RPM and torque, which may increase the charging current or reduce the discharging current. The ‘decreasing’ command refers to an opposite condition, which reduces the engine output to decrease the charging current or increase current during discharging. The third sentence ‘steady’ means that the engine operating condition remains the same. Therefore, matrix $\boldsymbol{A}, \boldsymbol{B}, \boldsymbol{X}$ is

$$\boldsymbol{A} = \begin{bmatrix} 0\,0\,0\,0\,0\,0\,0\,0\,0\,0\,0\,0\,0\,0\,0\,0\,0\,0 \\ 0\,0\,0\,0\,0\,0\,0\,0\,0\,0\,0\,0\,0\,0\,0\,0\,0 \\ 0\,0\,0\,0\,0\,0\,0\,0\,0\,0\,0\,0\,0\,0\,0\,0\,0\,0 \\ 0\,0\,0\,1\,1\,0\,1\,0\,0\,0\,1\,1\,1\,1\,0\,1\,0\,0 \end{bmatrix}^T \tag{6-12}$$

$$\boldsymbol{B} = [7000,4600\ \ 4600,0,0,4600,0,4600,4600,7000,0,0,0,0,4600,0,4600,4600]^T$$

$$\boldsymbol{X} = \left[P_f, C_b, SOC, RPM\right]^T$$

The rules relating to the antecedent and consequent parts are shown as below. As for the torque of the engine, it is determined by a defined relationship regarding engine RPM, which is illustrated by the red line in Figure 48. This line is a smooth operation line linking two star-points. Ideally, the engine could operate at star points most of the time since they have the best fuel consumption rate. While at other times, the engine operates around the red line or be idling.

Following the design of system input, output and rules, the next step is the defuzzification. The defuzzification result of the Sugeno fuzzy inference system is a weighted mathematical average shown by the equation (6-15).

$$y^* = \frac{\sum_1^n M_k \cdot y_k}{\sum_1^n M_k} \tag{6-13}$$

Table 15 Fuzzy rules.

	IF	THEN
$Rule\ 1$	$SOC\ is\ Very\ Low\ AND\ P\ is \begin{cases} Low \\ Medium \\ High \end{cases} AND\ C_d\ is \begin{cases} Good \\ Normal \\ Bad \end{cases}$	$y_1 = INCREASE$
$Rule\ 2$	$SOC\ is\ High\ AND\ P\ is \begin{cases} Low \\ Medium \\ High \end{cases} AND\ C_d\ is \begin{cases} Good \\ Noemal \\ Bad \end{cases}$	$y_2 = DECREASE$
$Rule\ 3$	$SOC\ is\ Medium\ AND\ P\ is\ Low\ AND\ C_d\ is \begin{cases} Good \\ Noemal \\ Bad \end{cases}$	$y_3 = DECREASE$
$Rule\ 4$	$SOC\ is\ Medium\ AND\ P\ is\ High\ AND\ C_d\ is\ Good$	$y_4 = STEADY$
$Rule\ 5$	$SOC\ is\ Medium\ AND\ P\ is\ High\ AND\ C_d\ is\ Normal$	$y_5 = STEADY$
$Rule\ 6$	$SOC\ is\ Medium\ AND\ P\ is\ High\ AND\ C_d\ is\ Bad$	$y_6 = DECREASE$
$Rule\ 7$	$SOC\ is\ Medium\ AND\ P\ is\ Medium\ AND\ C_d\ is\ Good$	$y_7 = STEADY$
$Rule\ 8$	$SOC\ is\ Medium\ AND\ P\ is\ Medium\ AND\ C_d\ is\ Normal$	$y_8 = DECREASE$
$Rule\ 9$	$SOC\ is\ Medium\ AND\ P\ is\ Medium\ AND\ C_d\ is\ Bad$	$y_9 = DECREASE$
$Rule\ 10$	$SOC\ is\ Low\ AND\ P\ is\ High\ AND\ C_d\ is\ Good$	$y_{10} = INCREASE$
$Rule\ 11$	$SOC\ is\ Low\ AND\ P\ is\ High\ AND\ C_d\ is\ Normal$	$y_{11} = STEADY$
$Rule\ 12$	$SOC\ is\ Low\ AND\ P\ is\ High\ AND\ C_d\ is\ Bad$	$y_{12} = STEADY$
$Rule\ 13$	$SOC\ is\ Low\ AND\ P\ is\ Medium\ AND\ C_d\ is\ Good$	$y_{13} = STEADY$
$Rule\ 14$	$SOC\ is\ Low\ AND\ P\ is\ Medium\ AND\ C_d\ is\ Normal$	$y_{14} = STEADY$
$Rule\ 15$	$SOC\ is\ Low\ AND\ P\ is\ Medium\ AND\ C_d\ is\ Bad$	$y_{15} = DECREASE$
$Rule\ 16$	$SOC\ is\ Low\ AND\ P\ is\ Low\ AND\ C_d\ is\ Good$	$y_{16} = STEADY$
$Rule\ 17$	$SOC\ is\ Low\ AND\ P\ is\ Low\ AND\ C_d\ is\ Normal$	$y_{17} = DECREASE$
$Rule\ 18$	$SOC\ is\ Low\ AND\ P\ is\ Low\ AND\ C_d\ is\ Bad$	$y_{18} = DECREASE$

The rule strength M_k is the multi-variable interaction between the output membership functions under different inputs. Various fuzzy operations, i.e. interactions, could be selected, such as multiplication and maximum value. Here the operation max is selected as the fuzzy operation. Therefore, in this problem, the weight M_k of the k_{th} rule is obtained as the example:

$Rule\ k$: *if x_1 is in the fuzzy set 'MF_p' and x_2 is in the fuzzy set 'MF_q' and x_3 is in the fuzzy set 'MF_r' → the Kth rule.*

IF $\left(x_1\ is\ MF_p\right)$ *AND* $\left(x_2\ is\ MF_q\right)$ *AND* $(\ x_3\ is\ MF_r)$

THEN

$$\mu_1(k) = exp\left(-\frac{\left(x_1 - c_{MF_p}\right)^2}{2\sigma_{MF_p}^2}\right)$$

$$\mu_2(k) = exp\left(-\frac{\left(x_2 - c_{MF_q}\right)^2}{2\sigma_{MF_q}^2}\right)$$

$$\mu_3(k) = \frac{1}{1+\left|\frac{x_3 - c_{MF_r}}{a_{MF_r}}\right|^{2b_{MF_r}}}$$

$$M_k = max\{\mu_1(k), \mu_2(k), \mu_3(k)\}$$

$$= max\left\{ex\,p\left(-\frac{\left(x_1(k) - c_p\right)^2}{2\sigma_p^2}\right), ex\,p\left(-\frac{\left(x_1(k) - c_p\right)^2}{2\sigma_p^2}\right), \frac{1}{1+\left|\frac{x_3(k) - c_r}{a_r}\right|^{2br}}\right\} \quad \textbf{(6-14)}$$

$$y_k = a_{k1}x_1 + a_{k2}x_2 + a_{k3}x_3 + b_k$$

For a set of inputs, traversing all the rules to get $M_k\ and\ y_k$,

the final output is:

$$y^* = \frac{\sum_1^n max\{\mu_1(k), \mu_2(k), \mu_3(k)\} \cdot y_k}{\sum_1^n max\{\mu_1(k), \mu_2(k), \mu_3(k)\}}$$

The IF statement illustrates that each input variable is in which membership function (or fuzzy set) and will lead to the k_{th} rule (or result), that equals to that "if x_1 is MF_p, x_2 is MF_q and x_3 is MF_r, then k_{th} rule". For this rule, the degree of membership function for each input $\mu_1(k), \mu_2(k), \mu_3(k)$ is obtained by different membership curves. It is similar as Mamdani fuzzy inference process. After that,

the rule strength M_k is the maximum value of all degrees of membership function. In other words, the rule weight M_k is derived from rule antecedents, while the rule output level y_k is a linear consequent of input values calculated by a defined function and given constant coefficients. After traversing all the rules, i.e. calculating the rule strength and output level for each rule for a given set of inputs, the output could be obtained by the equation (6-14).

Normally, membership sets of both inputs and outputs offer a Boolean approach hence linear transition are more challenging between different rules. This would lead to an inference that no two or more rules can be selected at the same time. In our case crossovers are an advantage because there can be regions over the universe of discourse whereby two or more rules can activate at the same time instance.

6.6 Simulation Result and Discussion

Figure 52 shows the simulated mission task. Due to the fuzzy controller considered the operating environment of the battery pack, the engine and generator had a different performance compared to other controllers. Therefore, the DRB controller has been applied for the same mission as a baseline. The results are shown below.

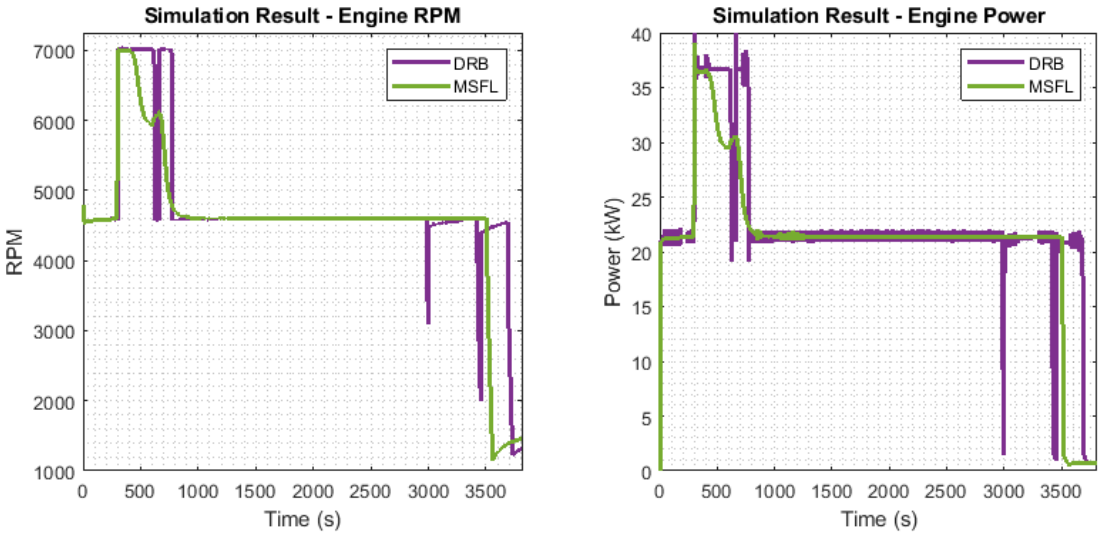

Figure 53 Simulation result of the engine.

The first figure illustrates RPM and torque of the engine. It is the performance of the generator as well since they are mechanically linked. From the figure, it can be seen that the trigger time of increasing engine RPM is similar due to the required power increases. After that, the fuzzy controller adjusts RPM to a lower value due to the mission requirement becomes less. For cruising flight stage, both of controllers control the engine to operate at its most-efficient point, i.e. the point (4600, 45). At the end of simulation, the results obtained by the rule-based controller has two big fluctuations while the performance of the fuzzy controller keep stable shortly and then reduces to an idle condition

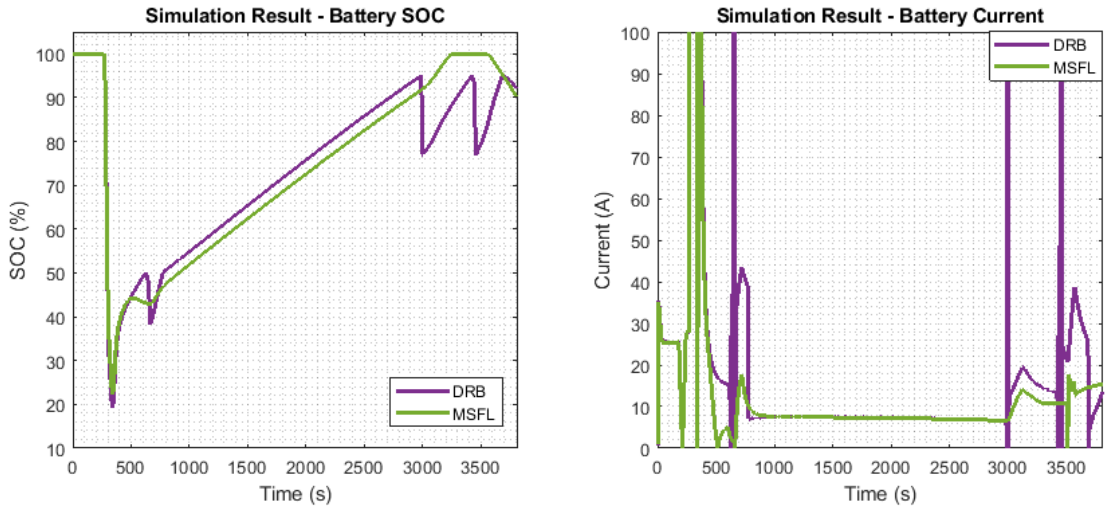

Figure 54 Simulation result of the battery pack.

To check the battery performance, another Figure 54 has been plotted. This figure shows the remaining SOC changes and the absolute value of the battery current with time. From the left figure, the fuzzy controller has a smoother result at the first fluctuation, while the performance of the rule-based controller has an extra concave. Then, the battery pack was charged by the same rate by two controllers, while the fuzzy system's SOC is a little lower than the other. In the last period of the simulation, the power requirement decreased so that it makes SOC reached 90%. The DRB controller adjusted the engine to the idle mode while the SOC of the fuzzy system reaches to 100%. As for the right figure, currents have huge fluctuations due to the mission and SOC changes. Compared with the DRB result, it can be found that the fuzzy system has a smaller current

with fewer oscillations. Therefore, the fuzzy controller indeed improved the battery operating environment.

The last figure illustrates the fuel consumption rate of each controller. The result of the fuzzy controller is smooth without small undulations. The total fuel consumptions are 718g and 764g for fuzzy and rule-based controller respectively. Therefore, the fuzzy controller improved 6% of fuel efficiency.

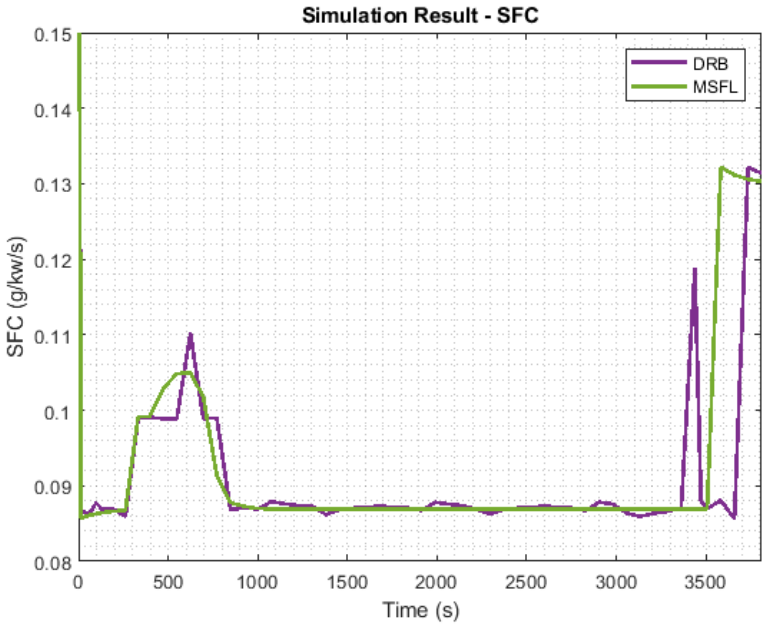

Figure 55 Simulation result of the fuel rate.

To better assess the system result, a performance function is proposed. Four relevant variables are scaled and added together as shown in the equation (6-15). S are scaled factors of each parameter, which are $S_{RPM} = 6600, S_{SOC} = 30, S_{SFC} = 500$ and $S_{current} = 760$ in this work. Please note that these scale numbers significantly affect the indication value of the total performance. They are designed by designers and could be modified. The first term of the equation, $\frac{R\dot{P}M}{S_{RPM}}$, indicates the rate of change of the RPM. A smooth change with low rate is better than a violent shock. The second term shows the SOC of the battery. It calculates the distance from the current SOC to the suitable range, i.e. 40%-60%. The next variable is the fuel consumption rate. As the lowest SFC of the engine, all SFCs minus 280g/kw/s to make it easier to being scaled. The last parameter is the

current of the battery pack. Since smaller c-rate is desired, the smaller current the better. As a result, the smaller the value of J_p refers to a better performance. The total performance value is shown in the Figure 56.

$$J_p = \frac{R\dot{P}M}{S_{RPM}} + \frac{min\{|SOC - 40|, |SOC - 60|\}}{S_{SOC}} + \frac{(SFC - 280)}{S_{SFC}} + \frac{|Current - 20|}{S_{current}} \quad \textbf{(6-15)}$$

From the figure, it can be seen that the largest value of performance indication is about 2.5 while the smallest is zero. Smaller value refers to better performance. Firstly, at the beginning of the mission, the MSFL's performance remained stable for the first flight stage, i.e. taxiing, while the DRB showed some fluctuations due to the unstable engine output. Afterwards, the mission came to the high-powerful take-off stage, both RPM and torque of the engine increased so that there is a pitch vibration occurring at 300s showed in both controllers' results. Then, interestingly, due to the mission consumed more electricity, the SOC and current size decreased so that the operating condition of battery was improved, which reduced the value of the total performance indication. Normally, ignoring several sharp tips, the performances are similar from 300 to 900s by two controllers. As for the cruise stage, the MSFL controller achieved the best performance in the whole mission, i.e. from 800 to 1900s. While in the same period, the DRB controller also performed great but the performance indication value oscillated frequently due to the engine torque was not stable. In addition, due to the battery pack was always charged during the cruise, the SOC and current size increased along with the plane flying, but the SFC still stayed at a low value due to the engine operating condition remained. The performances showed the same characteristics in the middle of the flight until the 3000s. There is one significant jump in the performance indicators of the DRB controller, which is caused by the engine was regulated into idle mode when the state-of-charge reached 90%. This movement affected both engine and battery, thus the J_p value oscillated significantly twice at the end of the simulation. From the figure, it can be found that switching the engine to idle mode when the SOC is over 90% is good for the whole system, which can reduce current and SOC to improve the battery operating environment. Overall, the MSFL controller achieved a stable and more

efficient performance than the DRB controller, but it is necessary to change engine operating mode when the SOC beyond 90%.

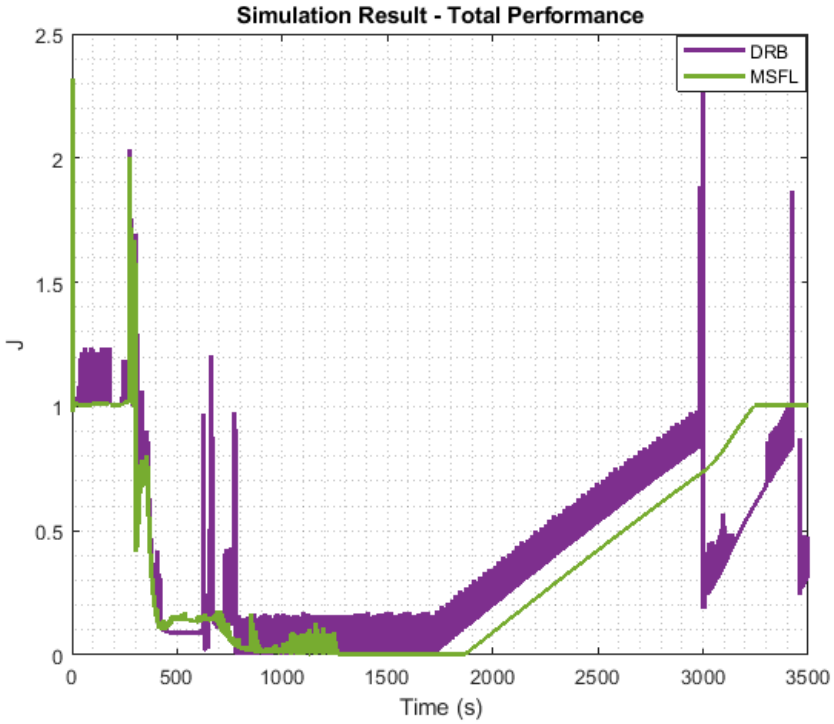

Figure 56 Simulation result of the total performance.

6.7 Conclusion

This paper has presented a novel battery-friendly fuzzy controller for a UAV distributed series hybrid-electric propulsion system. It firstly reviewed some of the current hybrid propulsion systems and the existing control strategies. Then, the designed distributed series hybrid system with its configuration is proposed. Based on the system structure, a basic analysis of important subsystems is conducted, where the modelling method for each device is introduced. Because the UAV battery pack is vulnerable to the outside environment the idea of a battery-friendly controller is generated. Since the battery ageing is a very complex process which is not easy to be described by simple equations, an expert-intelligent based system is suitable for this problem. Therefore, two fuzzy inference systems are designed to describe the battery operating condition and generate suitable control signals to drive the entire system. Lastly, a generic

mission has been simulated for the designed system with a deterministic controller. The performance and the difference between the two simulations are also compared and discussed. The proposed method has shown that the battery-friendly controller has achieved a 6% fuel consumption reduction while also having a smoother SOC and current performance. Therefore, the fuzzy controller improved both the battery operating profile and fuel consumption.

6.8 Reference

[1] F.R.Salmasi, “Control Strategies for Hybrid Electric Vehicles: Evolution, Classification, Comparison, and Future Trends,” *IEEE Transactions on vehicular technology,* vol. 56, no. 5, September 2007.

[2] S. G. Wirasingha and A. Emadi, “Classification and Review of Control Strategies for Plug-In Hybrid Electric Vehicles,” *IEEE Transactions on vehicular technology,* vol. 60, no. 1, January 2011.

[3] C. G. Hochgraf, M. J. Ryan and H. L. Wiegman, “Engine Control Strategy for a Series Hybrid Electric Vehicle Incorporating Load-Leveling and Computer Controlled Energy Management,” *SAE Technical Paper 960230,* 1996.

[4] A. M. Phillips, M. Jankovic and K. E. Bailey, “Vehicle system controller design for a hybrid electric vehicle,” in *IEEE International Conference on Control Applications*, Anchorage, AK, USA, 2000.

[5] S. H. Mahyiddin, M. R. Mohamed, Z. Mustaffa, A. C. Khor, M. H. Sulaiman, H. Ahmad and S. A. Rahman, “Fuzzy logic energy management system of series hybrid electric vehicle,” in *4th IET Clean Energy and Technology Conference*, Kuala Lumpur, 2016.

[6] N. Schouten, M. Salman and N. Kheir, “Fuzzy Logic Control for Parallel Hybrid Vehicles,” *IEEE Transactions on control systems technology,* vol. 10, no. 3, May 2002.

[7] N. J. Schouten, M. A. Salman and N. A. Kheir, “Energy management strategies for parallel hybrid vehicles using fuzzy logic,” *Control Engineering Practice,* vol. 11, no. 2, pp. 171-177, 2003.

[8] H-D. Lee and S.-K. Sul, “Fuzzy-logic-based torque control strategy for parallel-type hybrid electric vehicle,” *IEEE Transactions on Industrial Electronics,* vol. 45, no. 4, pp. 625-632, August 1998.

[9] M. Montazeri-Gh and M. Mahmoodi-k, “Development a new power management strategy for power split hybrid electric vehicles,” *Transportation Research Part D: Transport and Environment,* vol. 37, 2015.

[10] B. M. Baumann, G. Washington, B. C. Glenn and G. Rizzoni, “Mechatronic design and control of hybrid electric vehicles,” *IEEE/ASME Transactions on Mechatronics,* vol. 5, no. 1, pp. 58-72, March 2000.

[11] Y. Wang, Y. Zhang, J. Wu and N. Chen, “Energy management system based on fuzzy control approach for hybrid electric vehicle,” *Chinese Control and Decision Conference,* pp. 3382-3386, 2009.

[12] R. Langari and J.-S. Won, “Intelligent energy management agent for a parallel hybrid vehicle-part I: system architecture and design of the driving situation identification process,” *IEEE Transactions on Vehicular Technology,* vol. 54, no. 3, pp. 925-934, May 2005.

[13] J-S. Won and R. Langari, “Intelligent energy management agent for a parallel hybrid vehicle-part II: torque distribution, charge sustenance strategies, and performance results,” *IEEE Transactions on Vehicular Technology,* vol. 54, no. 3, May 2005.

[14] S.Zhang and R.Xiong, “Adaptive energy management of a plug-in hybrid electric vehicle based on driving pattern recognition and dynamic programming,” *Applied Energy,* vol. 155, pp. 68-78, 2015.

[15] M.H.Hajimiri and F.R.Salmasi, “A Fuzzy Energy Management Strategy for Series Hybrid Electric Vehicle with Predictive Control and Durability Extension of the Battery,” in *IEEE Conference on Electric and Hybrid Vehicles*, Pune, 2006.

[16] M.Montazeri-Gh and M.Mahmoodi-K, “Optimized predictive energy management of plug-in hybrid electric vehicle based on traffic condition,” *Journal of Cleaner Production,* vol. 139, pp. 935-948, July 2016.

[17] B. Sarlioglu and C. T. Morris, “More Electric Aircraft: Review, Challenges, and Opportunities for Commercial Transport Aircraft,” *IEEE Transactions on Transportation Electrification,* vol. 1, no. 1, pp. 54-64, June 2015.

[18] S.Wang, J.T.Economou and A.Tsourdos, “Indirect Engine Sizing via Distributed Hybrid-Electric UAV State-of-Charge Based Parametrisation Criteria”.

[19] S.Wang, J.T.Economou and A.Tsourdos, “Design of a Distributed Hybrid Electric Propulsion System for a Light Aircraft based on Genetic Algorithm,” *in AIAA Propulsion and Energy 2019 Forum*, Indianapolis, 2019.

[20] Rotron Technology, “Rotron RT600LCR,” [Online]. Available: http://www.rotronuav.com/engines/rt-600.

[21] G.Baumann and L.Rizzoni, “Unified modelling of hybrid electric vehicle drivetrains,” *IEEE/ASME Transactions on Mechatronics,* vol. 4, pp. 246-257.

[22] F.Cheli, F.L.Mapelli and R.Manigrasso, “Full energetic model of a plug-in hybrid electric vehicle,” *SPEEDAM - International Power Electronics,* pp. 733-738, 2008.

[23] J.B.Heywood, Internal Combustion Engine Fundamental, New York: McGraw-Hill, 1988.

[24] Y.Xie, A.Savvaris and A.Tsourdos, “Modelling and Control of a Hybrid Electric Propulsion System for Unmanned Aerial Vehicles,” *IEEE,* 2017.

[25] Y. Xie, A. Savvaris, A. Tsourdos, J. Laycock and A. Farmer, “Modelling and control of a hybrid electric propulsion system for unmanned aerial vehicles,” in *IEEE Aerospace Conference*, Big Sky, 2018.

[26] EMRAX , “EMRAX 228,” EMRAX INNOVATIVE E-MOTORS, [Online]. Available: https://emrax.com/products/emrax-228/. [Accessed 31 5 2019].

[27] P.Krause, Analysis of electric machinery, McGraw Hill, 1986.

[28] P.Pillay and K.Ramu, “Modelling of permanent magnet motor drives,” in *Robotics and IECON'87 Conferences. International Society for Optics and Photonics*, 1987.

[29] C. Shepherd, “Design of Primary and Secondary Cells: II. An Equation Describing Battery Discharge,” *Journal of The Electrochemical Society,* vol. 112, no. 7, pp. 657-664, 1965.

[30] L. Ahmadi, M. Fowler, S. B. Young, R. A. Fraser, B. Gaffney and S. B. Walker, “Energy efficiency of Li-ion battery packs re-used in stationary power applications,” *Sustainable Energy Technologies and Assessments,* vol. 8, 18 6 2014.

[31] A. Barre, B. Deguilhem, S. Grolleau, M. Gerard, F. Suard and D. Riu, “A review on lithium-ion battery ageing mechanisms and estimations for automotive applications,” *Journal of Power Sources,* pp. 680-689, 2013.

[32] N. Omar, M. A. Monem, Y. Firous, J. Salminen, J. Smekens, O. Hegazy, H. Gaulous, G. Mulder, P. V. d. Bossche, T. Coosemans and J. V. Mierlo, “Lithium iron phosphate based battery - Assessment of the aging parameters and development of cycle life model,” *Applied Energy,* pp. 1575-1585, 2014.

[33] Y. Gao, J. Jiang, C. Zhang, W. Zhang, Z. Ma and Y. Jiang, “Lithium-ion battery ageing mechanisms and life model under different charging stresses,” *Journal of Power Sources,* pp. 103-114, 2017.

[34] J. Wang, P. Liu, J. Hicks-Garner, E. Sherman, S. Soukiazian, M. Verbrugge, H. Tataria, J. Musser and P. Finamore, “Cycle-life model for graphite-LiFePO4 cells,” *Journal of Power Sources,* pp. 3942-3948, 2011.

[35] I. Bloom, B. Cole, J. Sohn, S. Jones, E. Polzin, V. Battaglia, G. Henriksen, C. Motloch, R. Richardson, T. Unkelhaeuser, D. Ingersoll and H. Case, “An accelerated calendar and cycle life study of Li-ion cells,” *Journal of Power Sources,* vol. 101, no. 2, pp. 238-247, 2001.

[36] E. H. Mamdani, “Application of fuzzy algorithms for control of simple dynamic plant,” vol. 121, no. 12, 1974.

[37] J. M. Mendel, “Fuzzy logic systems for engineering: a tutorial,” vol. 83, no. 3, 1995.

[38] T. Takagi and M. Sugeno, “Fuzzy identification of systems and its applications to modeling and control,” *IEEE Transactions on Systems, Man, and Cybernetics,* Vols. SMC-15, no. 1, pp. 116-132, Jan-Feb 1985.

[39] M. Sugeno and G. Kang, “Structure identification of fuzzy model,” *Fuzzy Sets and Systems,* vol. 28, no. 1, 1988.

[40] R.Babuška and H.B.Verbruggen, “An overview of fuzzy modeling for control,” *Control Engineering Practice,* vol. 4, no. 11, pp. 1593-1606, 1996.

7 OPTIMIZATION-BASED CONTROLLER

So far, the design process, sizing methods and rule-based controllers of the hybrid-electric propulsion system are presented in previous chapters. This chapter will introduce an optimization-based controller for the designed system, i.e. MPC-based controller, which is the third target in the third objective.

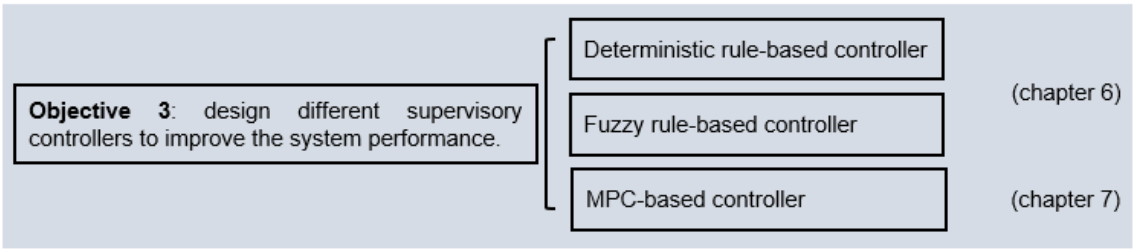

Figure 57 Chapter 7 structure.

An MPC-based Power Management Strategy for a Distributed Series Hybrid Electric Propulsion System of UAVs

Abstract

Reducing fuel consumption and emissions are always popular research targets for aircraft. At present, some hybrid-electric propulsion systems with different characteristics have been designed or even successfully applied for aircraft. On the basis of a distributed series hybrid electric propulsion system designed for a mid-scale unmanned aerial aircraft, this paper proposed a nonlinear Model Predictive Control based power management strategy to improve fuel economy and emissions. By using the MPC-based controller, an optimal operating

trajectory of the engine could be determined. Compared to the result of the power-follower deterministic controller and the battery longevity fuzzy controller, the MPC controller can achieve a good performance on the fuel consumption and NO_X emissions.

7.1 Introduction

With the maturity of the hybrid-electric vehicle industry, the environmentally friendly and high-efficient hybrid electric propulsion system has been widely recognized. As one of the main transportations, aircraft urgently needs an upgrade for propulsion systems to protect the environment and energy supply. According to the flightpath 2050 goals, aircraft is expected a 75% reduction in CO_2 emissions per passenger kilometer, a 90% reduction in NO_X emissions and an emission-free taxiing in the future 30 years [1]. For above targets, the hybrid-electric propulsion system might be one of the best replacements to the conventional combustion propulsion system. Compared to traditional aircraft, hybrid-electric aircraft has a potential to reduce fuel consumption and emissions due to its special configuration. Although there are plenty of types of hybrid systems, the core problem is how to manage two or more power flows properly.

Plenty of control strategies have been applied to find an optimal engine operating trajectory. There are two main classifications: rule-based and optimization-based control strategies [2]. Rule-based control strategies are designed based on the theme of ‘load-levelling’. Their simplicity and effectiveness make them recommended for the real-time energy management applications, but their results might be suboptimal. Optimization-based controllers obtain results by minimizing defined cost functions, and have causal (real-time) and non-causal (global) two categories. The non-causal controller is not applicable for real-time control problems since it requires past, present and future information [2]. The causal controller only considers current system variables so that it is good at real-time implementations. Typically, the real-time controller is necessary since it is not guaranteed that the future power requirement and other relative information could be obtained in advance. Therefore, a fast and robust causal optimization-based control strategy is on-demand for hybrid aircraft to perform unknown tasks.

Model Predictive Control is one typical optimal control strategy which is suitable for real-time optimization problems. It is a feedback law based on prediction, optimization and receding horizon implementation. Future control inputs and future plant responses are predicted using a system model and optimized at regular time intervals with respect to a performance index. With a sound theoretical basis and an accurate dynamic system model, MPC can solve large scale control problem with multi-variables, and can also handle constraints of control inputs and states no matter the plant model is linear or nonlinear.

The earliest application of the MPC algorithm for hybrid electric propulsion system is [3], which used that strategy to predict vehicle speed for a hybrid car in order to obtain a satisfactory control signal. Latter research shifted the focus to improve fuel economy. Based on the different level of navigation information, the paper [4] proposed three MPC optimal controllers for a parallel hybrid-electric system. The simulation results showed that it can achieve 1-3% improvement in fuel economy, and the fuel consumption can be further reduced with more information. In paper [5], Balaji developed a linear MPC to find the feasible solution for reducing fuel consumption based on a linearized system model. Compared with the dynamic programming solution, the execution time of the MPC algorithm improved 94-98%, but the fuel consumption was 17-30% worse than DP's. In paper [6-7], Borhan applied both linear and nonlinear MPC methodologies to improve the fuel economy of a power-split hybrid electric system. The research found that the nonlinear controller can achieve a better fuel economy than linear MPC, and it also proved that the short-horizon MPC is applicable to solve a real-time fuel minimization problem online in a nonlinear framework. Rather than focusing on fuel consumption, Cairano [8-9] initially proposed a linear MPC controller on maximizing the pointwise powertrain efficiency for a series hybrid-electric vehicle. By experimentally testing in city and highway cycles, the engine operating points were concentrated in the small high-efficient area which could be equivalent to 5.7% and 4.6% fuel economy improvements compared with the load-following and load-leveling deterministic controllers respectively. Furthermore, based on stochastic MPC, Cairano [10] also designed a driver behavior predictive controller. The new controller further

improved engine efficiency by accommodating changes in driver behavior. As for the latest research [11-12], two dual-loop nonlinear MPC frameworks have been established for hybrid electric vehicles. In paper [11], Johannes solved a low-sampling rate MPC problem for the entire predictive driving cycle to determine the long-term battery SOC variation for a plug-in hybrid electric vehicle. While, the paper [12] presented another two-level MPC strategy to control velocity and split energy flow. The high-level controller computed the travel time and battery energy, and the low-level determined engine parameters based on high-level controller's results. The simulation results showed that the proposed controller increased 8-39% fuel efficiency and improved driving comfort simultaneously.

This paper proposed an MPC-based power management method for the distributed series hybrid-electric aircraft. Hybrid-electric aircraft is different from other hybrid electric vehicles. The strict safety requirement and the huge difference in power requirement increase the difficulty of the energy coordination. The ideal controller is aiming to improve fuel consumption rate and emission rate simultaneously under a consideration of the battery longevity.

The paper starts with a brief review for hybrid propulsion systems, followed by the introduction of the designed system and its linearized plant model. The third section will illustrate the MPC algorithm and formulate the energy management problem into the optimization problem. The simulation result and performance analysis will be illustrated in the fourth section, where a power follower deterministic controller and a battery longevity controller are set as benchmarks. Finally, the conclusion and the future works are summarized in section five.

7.2 System Model

7.2.1 System Configuration and Control Scheme

By state-of-the-art, mainstream types of hybrid-electric aircraft is series or parallel hybrid configurations. The series configuration is more prevalent in the small-scale hybrid-electric aircraft due to its high simplicity and easy to install, while the parallel hybrid system is more common in mid-scale aircraft. Generally, the characteristic and performance of each hybrid system are determined by its

structure, components and control strategies. However, no matter the configuration is, hybrid-electric systems showed better fuel economy with varying growth degrees in literature. Based on the original series hybrid configuration, the author proposed a novel system whose structure is shown in Figure 58. According to the figure, the system has three interconnected parts: power source, propulsion loads and other loads. The propulsion loads and other loads parts are the energy consumers, while the power source part is responsible for the energy generation. System specifications are given in Table 16, more design details could be found in the paper [13,14].

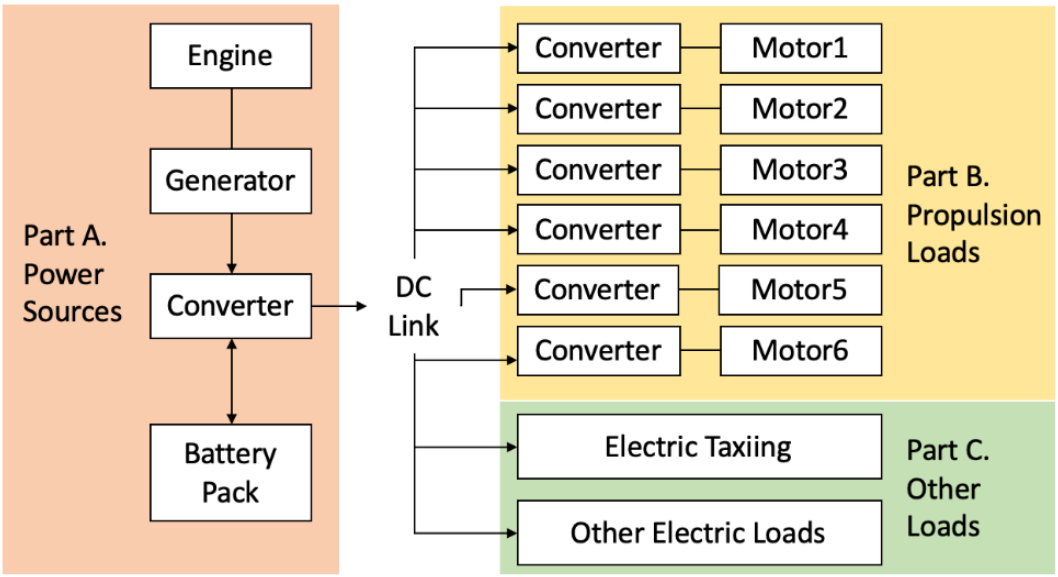

Figure 58 Distributed series hybrid-electric propulsion system.

For series hybrid-electric systems, the core question then refers to a coordination problem happened in the area of Part A, i.e. how much energy should be produced by the engine and the battery pack respectively in each second under a given mission. This problem is a constrained nonlinear dynamic optimization question. The most optimal result is finding a proper engine operating line which not only leads to a good performance on fuel consumption and emissions, but also can output enough power to complete the mission and guarantee the battery pack having enough remaining energy for emergency or other conditions simultaneously.

Table 16 System specifications.

Component	Specifications	
Engine	Maximum power	135 kW
Rotron RT600LCR	Maximum torque	60 Nm
Generator	Maximum power	75 kW
Emrax 228	Maximum torque	240 Nm
Battery	Capacity	7.5 kWh
	Voltage	296V

The entire control scheme of the designed system is illustrated in Figure 59. As the series hybrid decouples the power source and system loads, there are two parts of the supervisory controller. The power source supervisory controller is mainly to determine the instantaneous engine operating point, i.e. the engine rotation speed ω_e and torque T_e, and the propulsion loads controller regulates all motors by determining each motor's speed $\omega_{m_1} - \omega_{m_6}$ and torque $T_{m_1} - T_{m_6}$. Two controllers collaborate to give instructions to the low-level controller in order to allow all components to operate as commanded. This study only discusses the power source supervisory controller, as marked by the star in the figure.

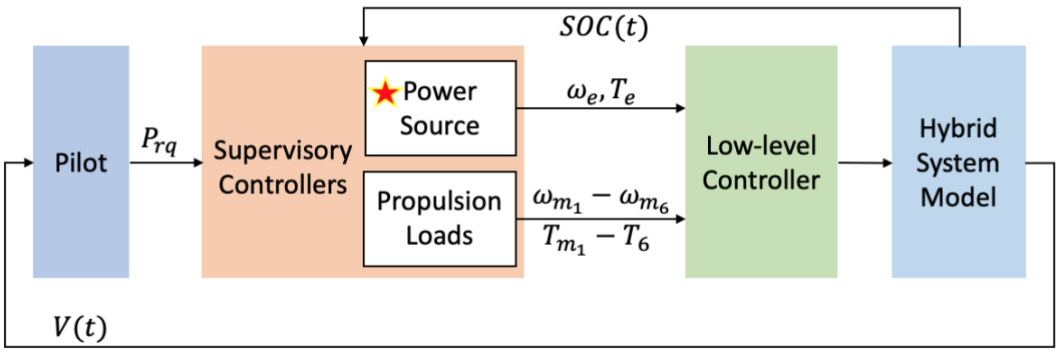

Figure 59 Control structure of the hybrid-electric propulsion system.

7.2.2 System Dynamic Model

According to the configuration, there is one engine, one generator, one converter and one battery pack installed in the power source part, which satisfies the following energy equation (7-1).

$$P_e \cdot \eta_g + P_b = P_{pro} + P_{other} = P_{req} \quad \textbf{(7-1)}$$

$$P_{pro} = \sum_{j=1}^{6} \frac{P_{m_j}}{\eta_{m_j}} \quad \textbf{(7-2)}$$

P_e and P_b are power outputs of the engine and the battery pack respectively, η_g is the generator efficiency. Please note that due to the generator is tightly locked to the engine, the generator output is presented by the engine output P_e instead. Moreover, for P_b, the positive value refers to a battery discharging and vice versa. The engine and the battery pack transfer energy to propulsion loads P_{pro} and other electric loads P_{other}, where P_{pro} could be calculated by motor power P_{m_j} and its efficiency η_{m_j} as equation (7-2), and the sum of them is the total power requirement P_{req}. The relationship is also illustrated by Figure 60.

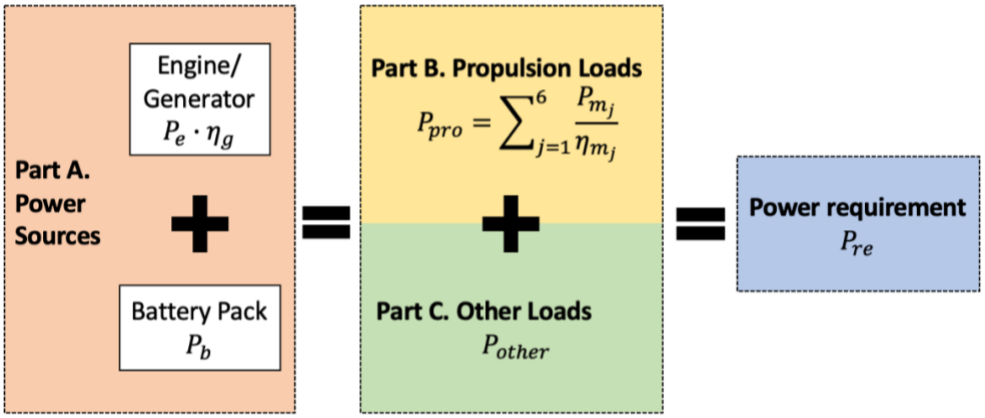

Figure 60 Energy flow of the hybrid-electric power system.

Straight to obtain engine's performance, the engine dynamic characteristic can be neglected. The engine output P_e is determined by its rotation speed ω_e and torque T_e. The fuel consumption rate $\dot{m}_f$ and emission rate $\dot{m_{NO_x}}$ could be looked-up from performance maps expressed by (7-4) and (7-5).

$$P_e = \omega_e \cdot T_e \quad \textbf{(7-3)}$$

$$\dot{m_f} = f_f(\omega_e, T_e) \quad \textbf{(7-4)}$$

$$\dot{m_{NO_x}} = f_{NO_x}(\omega_e, T_e) \quad \textbf{(7-5)}$$

The battery pack works as a buffer to smooth the energy transportation, which can provide energy to system loads and absorb extra energy from the engine. The instantaneous capacity of the battery pack $Q(t)$ is mainly presented by the parameter SOC, which is an indicator of its remaining energy showing as (7-6). The charge flow rate $\dot{Q}$ is the electric current $i(t)$ which has a relationship to battery voltage V_b and power output P_b as (7-8).

$$SOC = \frac{Q(t)}{Q_{max}} \quad \textbf{(7-6)}$$

$$\dot{Q} = -i(t) \quad \textbf{(7-7)}$$

$$P_b = V_b \cdot \ i(t) \quad \textbf{(7-8)}$$

Energy losses during system operations. However, the efficiency of the battery pack and the converter are assumed as 100% to simplify the calculation. In addition, the engine efficiency is not necessary for this study since here used an experimental look-up table to determine the performance which has already considered the energy loss. And for reality, the operating range of each component is limited [15], the system operating should satisfy all mechanical constrains of each component shown as below.

$$0 \leq SOC \leq 100\% \quad \textbf{(7-9)}$$

$$P_{e\_min} \leq P_e \leq P_{e\_max} \quad \textbf{(7-10)}$$

$$\omega_{e\_min} \leq \omega_e \leq \omega_{e\_max} \quad \textbf{(7-11)}$$

$$T_{e\_min} \leq T_e \leq T_{e\_max} \quad \textbf{(7-12)}$$

$$\omega_{g\_min} \leq \omega_g \leq \omega_{g\_max} \tag{7-13}$$

$$T_{\ g\_min} \leq T_g \leq T_{g\_max} \tag{7-14}$$

7.3 Nonlinear MPC

7.3.1 Standard Nonlinear MPC

Based on above system characteristics, the power management problem can be easily incorporated into the offline nonlinear MPC optimization strategy. The MPC algorithm contains the process of prediction, optimization and receding horizon implementation. It first predicts the system output along a future time horizon, then calculates a future control sequence to minimize a performance index subjected to constraints, after that the first element of the control sequence is applied to the system, and the process is repeated at the next time interval by moving the prediction horizon one step forward [6]. Nonlinear MPC is more complex than the linear problem for real-time implementations, while the nonlinear controller may improve the result [7]. The general nonlinear MPC algorithm is expressed as the below general form [16]:

$$\min J(k) = \sum_{i=0}^{N-1} \left[\|y(k+i|k)\|_{P_y}^2 + \|u(k+i|k)\|_{R_u}^2 \right] \tag{7-15}$$

Subject to the discrete system dynamics:

$$\begin{aligned} \boldsymbol{x}(k+1) &= A\boldsymbol{x}(k) + B_u\boldsymbol{u}(k) + B_v\boldsymbol{v_r}(k) \\ \boldsymbol{y}(k) &= C\boldsymbol{x}(k) + D\boldsymbol{u}(k) \end{aligned} \tag{7-16}$$

And the linear constraints:

$$\begin{aligned} \underline{\boldsymbol{u}} \leq \boldsymbol{u}(k) \leq \overline{\boldsymbol{u}} \\ \underline{\boldsymbol{x}} \leq \boldsymbol{x}(k) \leq \overline{\boldsymbol{x}} \\ \underline{\boldsymbol{y}} \leq \boldsymbol{y}(k) \leq \overline{\boldsymbol{y}} \end{aligned} \tag{7-17}$$

where J is a quadratic cost function of system input $\boldsymbol{u}(k)$ and output $\boldsymbol{y}(k)$, while $\boldsymbol{v_r}(k)$ is the measured input and $\boldsymbol{x}(k)$ is the vector of system state. In the cost function, N is the prediction horizon, P_y and R_u refer to constant positive weighting matrices, and $(k+i|k)$ indicates the parameter is at time $k+i$ that are predicted at time k. The model state and input vectors are often stacked by:

$$\boldsymbol{u}(k) = \begin{bmatrix} u(k|k) \\ u(k+1|k) \\ \vdots \\ u(k+N-1|k) \end{bmatrix}, \boldsymbol{x}(k) = \begin{bmatrix} x(k+1|k) \\ x(k+2|k) \\ \vdots \\ x(k+N|k) \end{bmatrix} \quad \textbf{(7-18)}$$

with upper bounds $\overline{\boldsymbol{u}}$, $\overline{\boldsymbol{x}}$ and lower bounds $\underline{\boldsymbol{u}}$,$\underline{\boldsymbol{x}}$. The stability and disturbance rejection properties for this algorithm are discussed in the literature [17]. Based on the objective function and constraints derived above, the optimization of the finite horizon cost subject to constraints requires the solution of a quadratic optimization problem.

7.3.2 Optimization Problem Formulation

Based on the above system properties, the optimization problem can be executed. At first, summarizing previous component information, the energy relationship hiding in the system is written by the equation (7-19).

$$P_b = V_b \cdot i = -V_b \cdot \dot{SOC} \cdot Q_{max}$$

$$P_e = \omega_e \cdot T_e \quad \textbf{(7-19)}$$

$$P_e \cdot \eta_g + P_b = (\omega_e \cdot T_e) \cdot \eta_g - V_b \cdot \dot{SOC} \cdot Q_{max} = P_{req}$$

As the study is aiming to improve the fuel economy and pollutant emissions, the basic cost function could be writing as (7-20). Furthermore, considering improving the operating environment of the battery pack, lower current and moderate SOC are desired. Therefore, the cost function could be extended to a weighted sum of fuel consumption, exhaust emissions, battery current and SOC (shown by (7-21)).

$$\min J_1 = \int_0^t (w_f \left\| \dot{m}_f(t) \right\|^2 + w_{NO_x} \left\| \dot{m_{NO_x}}(t) \right\|^2) \, dt \quad \textbf{(7-20)}$$

$$\min J_2 = \int_0^t (w_f \|\dot{m}_f(t)\|^2 + w_{NO_x} \|\dot{m_{NO_x}}(t)\|^2 + w_i \|i(t)\|^2 + w_{SOC} \|N_{SOC}(t)\|^2)\, dt \quad \textbf{(7-21)}$$

Variable $w_f, w_{NO_x}, w_i, w_{SOC}$ are weighting parameters for each objective, whose value could be regulated for different objectives. A new indicator N_{SOC} is invented to describe weather the instant SOC is in the moderate range from 40% to 80%.

$$N_{SOC}(t) = max\ \{|SOC(t) - 40|, |SOC(t) - 80|\} \quad \textbf{(7-22)}$$

Except for the performance indication which can be straight obtained by internal system parameters, such as i and N_{SOC}, the instantaneous fuel consumption rate and emission rate are obtained by look-up tables according to current engine rotation speed ω_e and torque T_e. Therefore, before formulating the problem into the standard MPC algorithm, the engine brake specific fuel consumption map, illustrated by Figure 61, is firstly analysed.

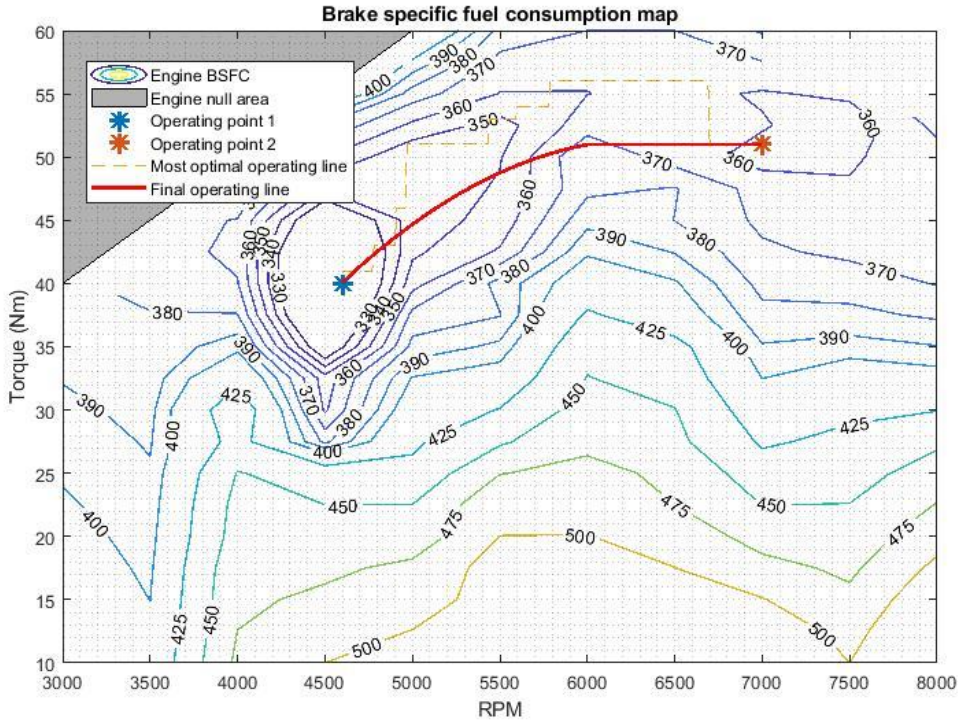

Figure 61 Engine BSFC map.

The figure shows the experimental fuel consumption performance of the engine RT600. In other literature, the fuel consumption can be calculated by using an average rate or some linear fitting equations. However, they may not show system fuel characteristics very detailed since the real fuel map is too complicated that cannot be perfect represented by fitting functions. Therefore, this study proposed a better demonstration method to present engine performance. The new method is achieved by restricting the engine operating area to a special operating line with the highest fuel efficiency in advance. Except for reducing the complicity of the fuel consumption performance, this method also confirms a relationship between engine speed and torque. Based on the calculated line, if one of three variables (engine speed, engine torque and engine power) is known, the other two variables will be then determined. This determination reduces the degree of freedom to one, while the degree of freedom of the original problem is two – engine speed and torque. Namely, a feasible and high-efficient operating line of the engine is necessary for the supervisory controller.

According to the figure, there are two high-efficient operating areas at (4600RPM, 40Nm) and (7000RPM, 51Nm) respectively in the map which could be nominated as engine main operating points. Based on the hybrid operating modes and components sizing methods mentioned in paper [13-14], the engine operating point (4600RPM, 40Nm) could be set for the main operating point while the point (7000RPM, 51Nm) is specially designed for high-power requirements. In addition, based on the limited experimental engine BSFC map, a most-optimal operating line for the transition process between two points could be defined in advance. The desired line allows the engine transits from a lower speed to a higher speed with a high fuel economy. Calculated by a basic genetic algorithm, the transition line is obtained shown by an orange dotted line in Figure 61. However, this result is not applicable for real operations since the torque of the dotted line goes up firstly then fall to a lower value from 4600 RPM to 7000 RPM. Compromised for the engine performance, a final engine operating line is defined which is shown by the red line in the figure. The engine torque smoothly increases to 51Nm at around 6000RPM then keeps being stable until to the speed at 7000RPM. From

the complex fuel map, the final operating line cannot obtain the best fuel consumption rate at each speed, but it is still acceptable since the total fuel consumption of the red line is just 1.1% higher than that of the orange dotted line.

$$\dot{m}_f = f_f(\omega_e, T_e) \quad \textbf{(7-23)}$$

$$T_e = f_{line}(\omega_e) \quad \textbf{(7-24)}$$

As for the engine emission, experimental performance result is lacked. Instead of using an accurate emission quantity which is hard to achieve, a simplified map is utilized in this study. The engine utilized in this paper is a Wankel engine, which is a spark ignition engine using aviation gasoline. The map shows the heavy pollutant area of NO_x and CO_2 respectively, which is shown in Figure 62 [18].

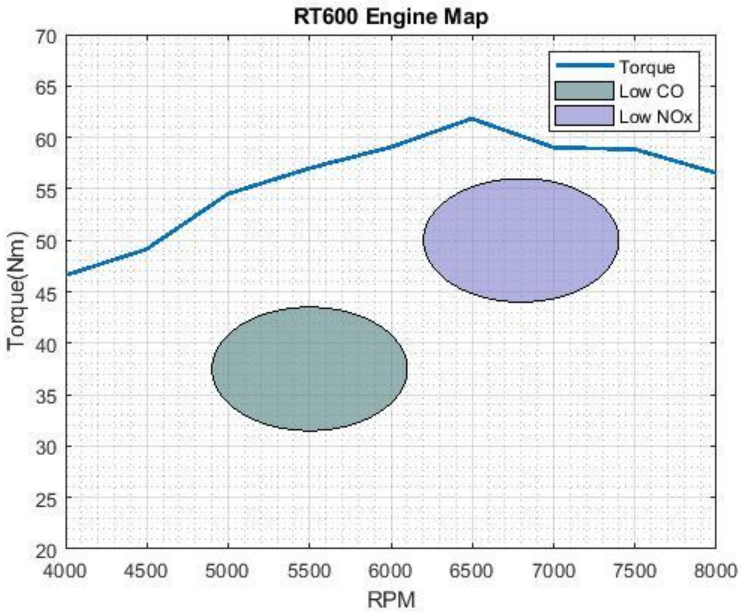

Figure 62 Emission map of the SI engine [18].

The prediction horizon is another important parameter for MPC algorithm. In this thesis, the prediction horizon was initially set to a 60s interval. In order to calculate the engine torque by Dynamic Programming, the prediction horizon consisted of six 10-second small intervals. During each part, the engine RPM and torque are considered constant. Consequently, the prediction horizon included six engine operating points corresponding to the future 60 seconds.

So far, the problem can be formulated in the MPC algorithm. The engine power output P_e is the system input. The battery pack's remaining capacity, as an important clue in the coordination amongst energy sources, is the state variable of the system model. Then, for the first cost function (7-20), the discretized model of the system becomes to:

Input, output and states:

$$x = SOC, u = P_e\ (or\ \omega_e), v_r = P_{re}, y = P_e\ (or\ \omega_e)$$

System dynamics:

$$\boldsymbol{x}(k+1) = A\boldsymbol{x}(k) + B_u\boldsymbol{u}(k) + B_v\boldsymbol{v_r}(k)$$

$$A = 1\ ;\ B_u = \frac{-\eta_g}{V_b \cdot Q_{max}};\ B_v = \frac{1}{V_b \cdot Q_{max}};$$

Outputs:

$$\boldsymbol{y}(k) = C\boldsymbol{x}(k) + D\boldsymbol{u}(k) \qquad \textbf{(7-25)}$$

$$C = 0; D = 1;$$

Cost function:

$$\min J = \int_0^t (w_f \left\| \dot{m_f}(t) \right\|^2 + w_{NO_x} \left\| \dot{m_{NO_x}}(t) \right\|^2)\, dt$$

$$\begin{bmatrix} \dot{m}_f \\ \dot{m_{NO_x}} \end{bmatrix} = \begin{bmatrix} f_f(\boldsymbol{y}(k)) \\ f_{NO_x}(\boldsymbol{y}(k)) \end{bmatrix} \cdot\ \boldsymbol{y}(k)$$

Mechanical constraints are listed by (7-9) to (7-14). As for the extended cost function, i.e. (7-21), battery current and remaining capacity are performance indications as well. Thus, the system would be:

Input, output and states:

$$x = \begin{bmatrix} SOC \\ i \end{bmatrix}, u = P_e\ (or\ \omega_e), v_r = P_{re}, y = \begin{bmatrix} P_e\ (or\ \omega_e) \\ SOC \\ i \end{bmatrix} \qquad \textbf{(7-26)}$$

System dynamics:

$$\boldsymbol{x}(k+1) = A\boldsymbol{x}(k) + B_u\boldsymbol{u}(k) + B_v\boldsymbol{v_r}(k)$$

$$A = \begin{bmatrix}1\\0\end{bmatrix};\ B_u = \begin{bmatrix}\frac{-\eta_g}{V_b \cdot Q_{max}}\\ \frac{-\eta_g}{V_b}\end{bmatrix};\ B_v = \begin{bmatrix}\frac{1}{V_b \cdot Q_{max}}\\ \frac{1}{V_b}\end{bmatrix};$$

Outputs:

$$\boldsymbol{y}(k) = C\boldsymbol{x}(k) + D\boldsymbol{u}(k)$$

$$C = \begin{bmatrix}0 & 0\\ 1 & 0\\ 0 & 1\end{bmatrix}; D = \begin{bmatrix}1\\0\\0\end{bmatrix};$$

Cost function:

$$\min J = \int_0^t (w_f \left\|\dot{m_f}(t)\right\|^2 + w_{NO_x}\left\|\dot{m_{NO_x}}(t)\right\|^2 + w_i\|N_i(t)\|^2 + w_{SOC}\|N_{SOC}(t)\|^2)\,dt$$

$$\begin{bmatrix}\dot{m}_f\\ \dot{m_{NO_x}}\\ SOC\\ i\end{bmatrix} = \begin{bmatrix}f_f(\boldsymbol{y}(k))\\ f_{NO_x}(\boldsymbol{y}(k))\\ 0 & 0 & 1 & 0\\ 0 & 0 & 0 & 1\end{bmatrix} \cdot\ \boldsymbol{y}(k)$$

This study will investigate both systems. The result of the first model will be compared with the results of the deterministic rule-based controller and the battery longevity fuzzy controller proposed in the paper [19], and then another comparison between systems using different cost functions will be performed.

7.3.3 Minimum Optimization Algorithm

In order to solve the above minimum optimization problem, many approaches have been applied in literature [20]. If only a limited prediction horizon is available, both Dynamic Programming (DP) method and Quadratic Programming (QP) method are popular with the MPC structure using a receding horizon. However, considering the optimization problem mentioned in the previous section is a discrete-time nonlinear dynamic system, DP is the suitable solver and has been applied in this study.

Dynamic programming was proposed by American mathematician Richard Bellman in the mid-1950s [21]. The method was initially designed for multi-level decision-making process optimization problems, i.e. the optimal control problems of discrete-time systems, and was extended for continuous-time systems later. Based on the theoretical basis—Bellman's optimality principle, DP breaks the decision problem into smaller sub-problems and establishes corresponding recursive optimization calculation formulas to obtain optimal control results. Bellman's equation shows the optimal problem of discrete-time systems by a recursive form by writing as:

$$J_{k,N}\left[x^*(k-1), u^*(k-1), u^*_{0,N-1}\right] = \max_{u(k-1)}\left\{j_k[x^*(k-1), u(k-1)] + J_{k+1,N}\left[x^*(k), u^*_{k,N-1}\right]\right\} \quad \textbf{(7-27)}$$

$$\dots\ k = 1, 2, \dots, N$$

Same as equations in previous sections, $u(k), x(k)$ are input and state at k_{th} sampling instant, and $u_{0,N}: u(0), u(1), \dots, u(N)$, and the upper label $*$ means the optimal input or system state. As for performance cost function, $J_{k+1,N}\left[x(k), u_{k,N-1}\right]$ refers to the cost from k_{th} to N_{th} time. Bellman's equation provides a step-by-step basis formula showing the relationship between the cost function in one period to the next period. The energy management problem then can be split into an integrated stage cost and an approximated minimum cost function from the end of the prediction horizon to the end of the mission cycle.

Combining the formulated MPC problem, the DP problem can be written as：

Input, output and states:

$$x = P_{sum}, u = P_e$$

Cost function:

$$J = \int_0^t (w_f \left\| m_f^{\cdot}(t) \right\|^2 + w_{NO_x} \left\| m_{NO_x}^{\cdot}(t) \right\|^2)\, dt \quad \textbf{(7-28)}$$

$$\begin{bmatrix} \dot{m}_f \\ \dot{m_{NO_x}} \end{bmatrix} = \begin{bmatrix} f_f(\boldsymbol{y}(k)) \\ f_{NO_x}(\boldsymbol{y}(k)) \end{bmatrix} \cdot \boldsymbol{u}(k)$$

Constraints:

$$0 \leq SOC \leq 100\%$$

$$P_{e\_min} \leq P_e \leq P_{e\_max}$$

$$\omega_{e\_min} \leq \omega_e \leq \omega_{e\_max}$$

In the above equations, P_{sum} is the sum of generated power in last K_{th} steps. Since this DP problem solves the most optimal input (engine power output, speed and torque) for the designed hybrid-electric propulsion system, the value of battery SOC should satisfied constraints. Meanwhile, please notice that the engine output cannot be zero due to that it is not wise to switch off the engine during the flight.

7.4 Simulation Result

A standard mission was used for this study. It includes a taxing, take-off, climbing, cruising, descending and landing flight stages, and the power requirement is shown as below.

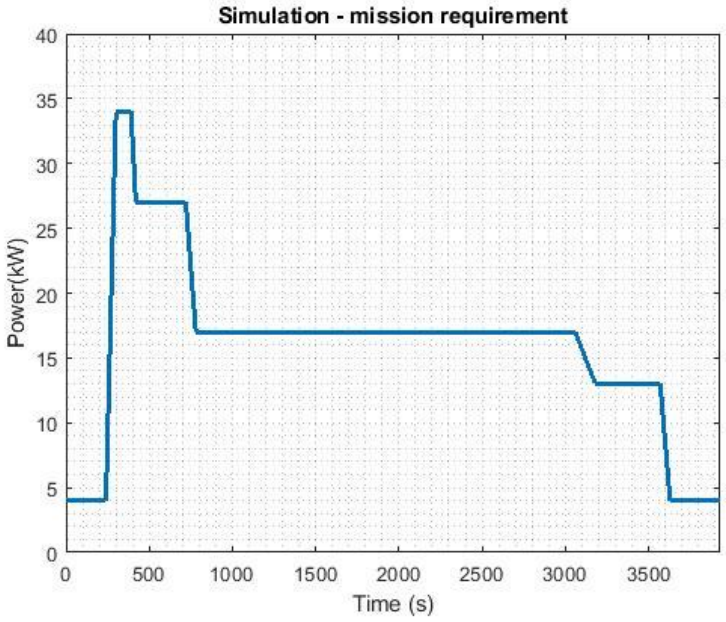

Figure 63 Power requirement.

7.4.1 Basis MPC

At first, the problem illustrated in (7-25**)** is simulated by using DP method, whose results are shown below. Figure 64 shows the engine power output in every second. The violet line shows the simulation result achieved by a determinate rule-based controller, and the green line shows the result obtained by the Mamdani & Sugeno Fuzzy Logic controller mentioned in paper [19]. Compared with the other two methods, the MPC controller's result is showing by the blue line. From the figure, it can be seen that engine operating conditions were the same during the mission except the period from 300s-800s. The engine remained operating at the most optimal operating point (4600RPM, 40Nm), for taxiing and cruise flight stage. This is because the optimal engine output is just above the mission demand for cruising, where the engine can provide enough power for propulsion and remaining at high efficiency simultaneously.

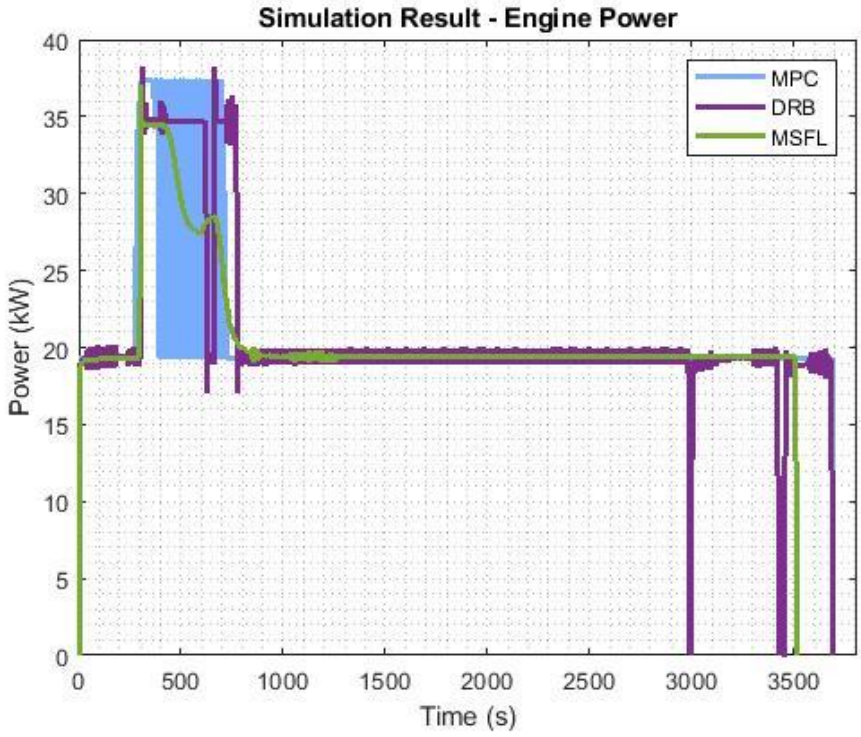

Figure 64 Simulation result of the engine.

As for take-off and climbing stages, results showed significant differences. Firstly, as shown by the blue line, the engine operating point varied frequently between two points (4600RPM, 40Nm) and (7000RPM, 51Nm). This performance is not

good for engine's real operation, but it can keep the battery SOC stays at a safety region. As shown in Figure 65, the minimal value of SOC is about 56% while the SOC of DRB and MSFL dropped to 20% at 350s. Namely, the MPC controller has a better predictive ability so that it can increase engine output immediately before a big drop of the SOC.

The fuel consumption at each moment is shown in Figure 66. The curve illustrated in that figure has the same shape as that of engine power performance. Calculated the total value of consumed fuel during the whole mission, the MPC controller costed lower fuel than others. Although the engine operating condition violent oscillated, the result by the MPC controller consumed 4.46% lower than that by the DRB controller, while the MSFL controller improved 4.24% fuel economy than the DRB controller.

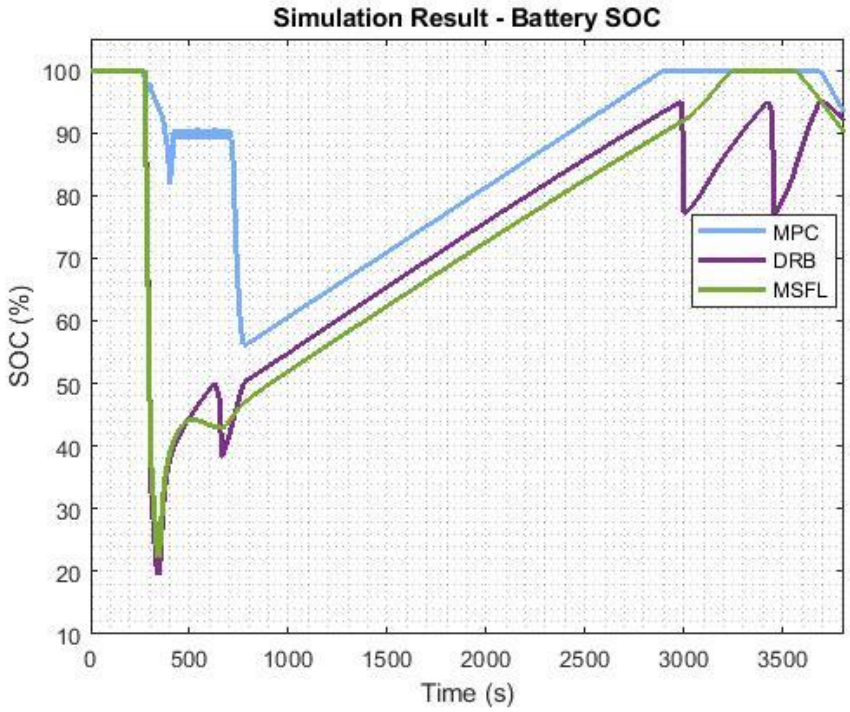

Figure 65 Simulation result of the battery.

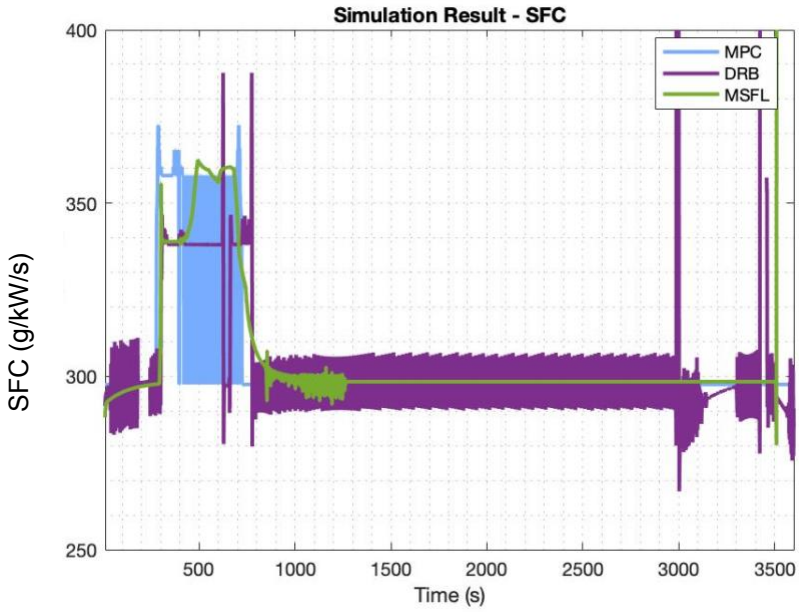

Figure 66 Simulation result of the engine fuel consumption.

The emission is also considered in the design of the MPC controller. For checking the emission performance, a simplified NOx map has been used in this study, which is shown in Figure 67. Different ovals present different emission level. The darkest, i.e. the central oval, illustrated the area with lowest NOx emission output (level 1). While, the lighter colour represents the heavier emission. The green line shows the maximum torque according to different engine RPM.

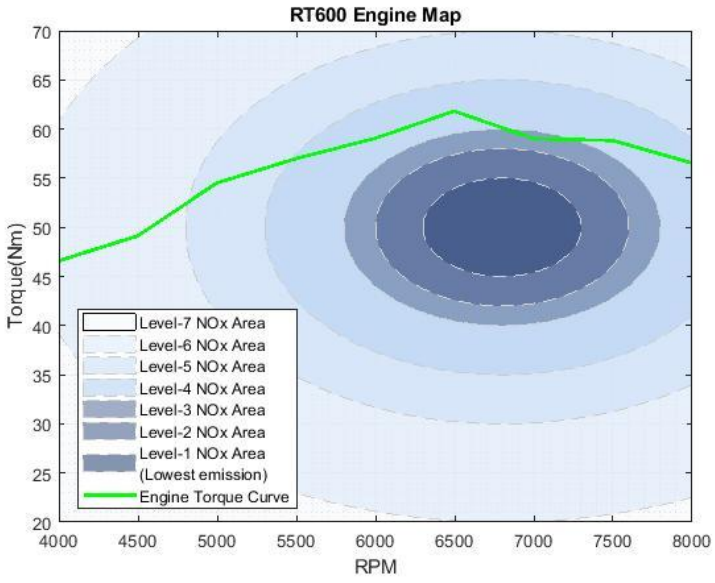

Figure 67 Engine map on NOx emission.

Figure 68 is the simulation result for NOx emission. From the figure, it can be seen that results obtained by three controllers have many similarities. The reason for this could be conducted. Since the designed hybrid electric propulsion system is a series hybrid configuration, namely the engine is decoupled to the motor, the engine can always operate along a same given operating line no matter what kind of controller is applied. Due to three controllers are designed based on the same engine operating line, the engine operating points are limited to the points on that given line. In other words, the performance of emission or other characteristics may have many similarities. The only difference amongst the results of three controllers is the timing of engine operating point's shifting.

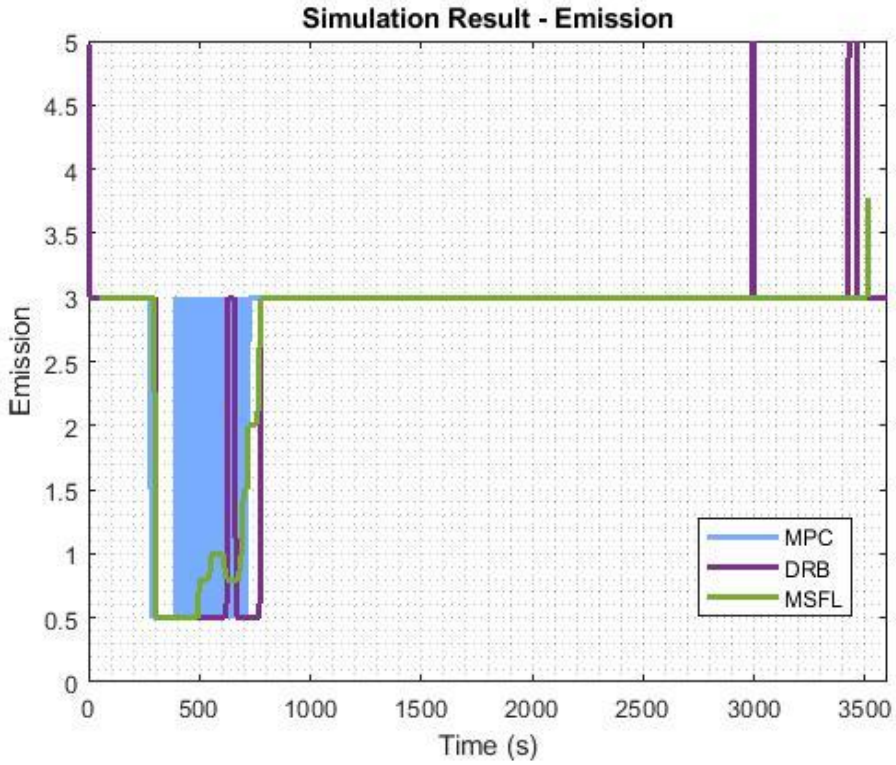

Figure 68 Simulation result of the emission NOx.

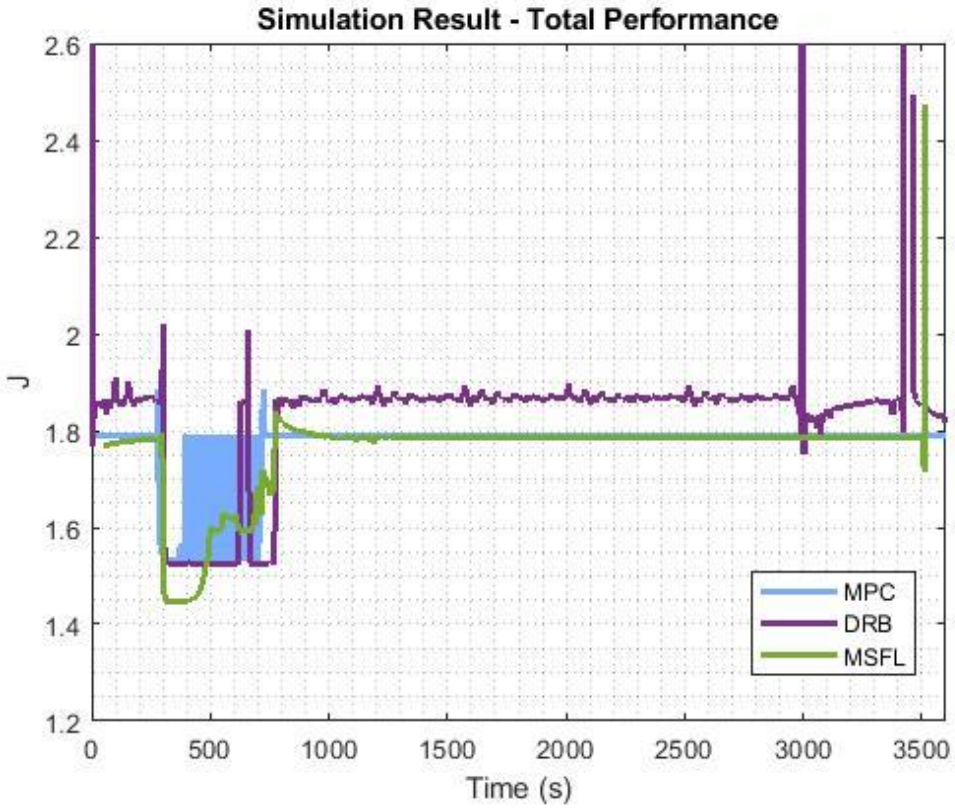

Figure 69 Simulation result of the total performance.

According to the emission map, the amount of NOx is lower in the high-power output area. However, the brake specific fuel consumption map (Figure 61) shows that the fuel economy is not the best in the high-power area. Therefore, the power management for the hybrid propulsion system is a trade-off problem. Depended on the cost function, the system may perform differently. In this study, by using weighting values $w_f = 2, w_{NO_x} = 1$, emission amounts are shown by Figure 68. Amongst three controllers, the system generated minimal NOx by using the DRB controller. The result of the MSFL and the MPC controller are similar, which produced 5.71% and 5.33% more emissions than the DRB controller.

To better address controllers' performance, the cost function shown in (7-29), is applied to the results obtained by the DRB and MSFL controllers. Two factors $\dot{m_f}(t)$ and $\dot{m_{NO_x}}(t)$ are scaled respectively to simplify the comparison and the result is shown as Figure 69. From the result, the MPC controller has the best

performance, but the result of the MSFL controller is only 0.1% worse than the MPC, while the DRB controller is 1.6% worse than the MSFL controller.

$$min\, J_1 = \int_0^t (2 * \left\|\dot{m}_f(t)\right\|^2 + 1 * \left\|\dot{m_{NO_x}}(t)\right\|^2)\, dt \qquad \textbf{(7-29)}$$

7.4.2 Effect of Cost Functions

Different cost functions will lead to different performances. Therefore, the second cost function proposed in the third section has been applied to the system as well, and the simulation results are shown as below comparing with the results by using the first cost function. To make the contrast more obvious, a different prediction horizon has been used for these two simulations.

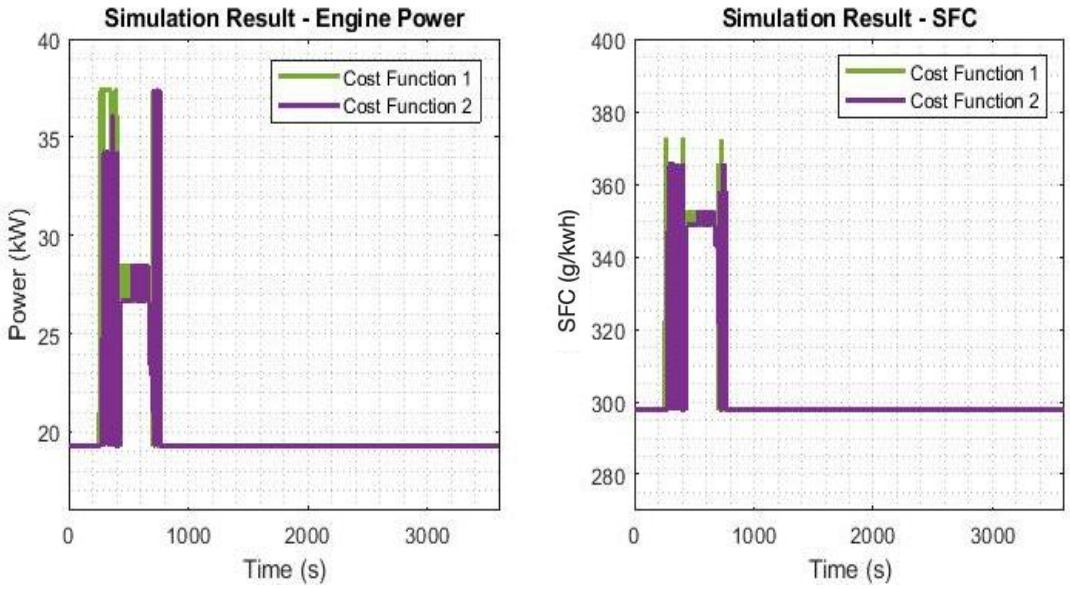

Figure 70 Simulation result of the engine.

At first, there is a little difference in the engine's performance. According to Figure 69, by using the second cost function (7-26), the engine generated less power than that by using the first function. Therefore, the battery SOC in the second system dropped deeply and fast from 300s-800s, and the minimal value of SOC is about 10%.

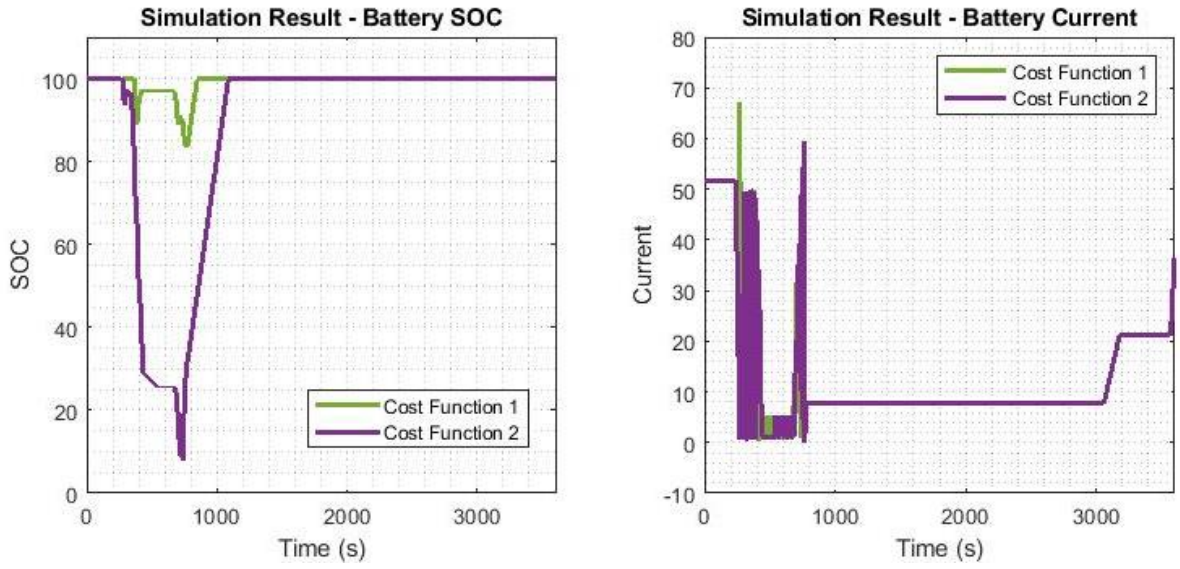

Figure 71 Simulation result of the battery.

As for emissions, there are almost no differences between them. The total NOx emission amount in the first simulation is 1.45% less than the second result.

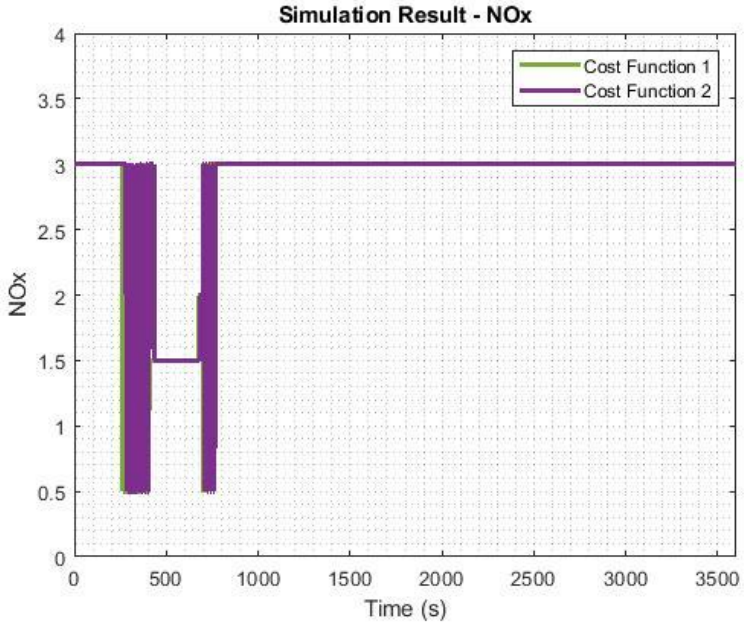

Figure 72 Simulation result of the NOx emission.

Figure 73 shows the value of the cost function 2 (equation (7-29)) with weight factors $w_f = 2, w_{NO_x} = 1, w_i = 1, w_{SOC} = 1$. The value varied from 1 to 3.5, and the lowest value is determined at 1000s. According to the figure, the value

obtained by the second simulation is lower than the other during the most period of missions. The second system's cost is 1.26% better than the first.

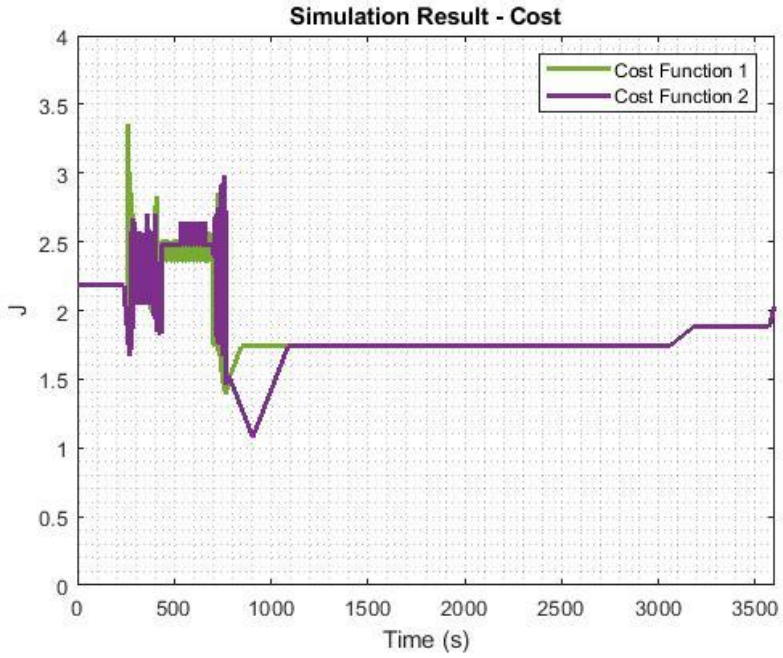

Figure 73 Simulation result of the total performance.

7.5 Conclusion

This paper proposed an MPC-based controller for the designed hybrid propulsion system. The study first analysed the power management problem and formulated it into the MPC method. There are two proposed cost functions, the first is only regarding fuel economy and emission, while the second considers batteries' performance, i.e. SOC and current. As the problem is nonlinear, the dynamic programming algorithm is used for solving the minimal optimization problem. Based on a standard flight mission, some simulations are conducted. The simulation result calculated by using the first cost function was compared to the result of a deterministic rule-based controller and a fuzzy controller. The MPC controller can improve 4.46% fuel efficiency than the rule-based controller, and 0.4% emission rate than the fuzzy controller. Meanwhile, the MPC controller with the second cost function has been applied to the system as well, and the result was compared with the MPC controller using the first cost function. Based on simulation results, it can be found that different weighting factors may affect

system performance. Therefore, a trade-off study regarding fuel consumption, emission, and battery performance will be the next research focus.

7.6 Reference

[1] European Union, "Flight Path 2050," Brussels, 2011.

[2] F. R. Salmasi, "Control Strategies for Hybrid Electric Vehicles: Evolution, Classification, Comparison, and Future Trends," *IEEE Transactions on Vehicular Technology,* vol. 56, no. 5, pp. 2393-2404, September 2007.

[3] E. Finkeldei and M. Back, "Implementing an MPC Algorithm in a Vehicle with a Hybrid Powertrain using Telematics as a Sensor for Powertrain Control," in *IFAC Proceedings Volumes*, Italy, 2004.

[4] L. Johannesson, M. Asbogard and B. Egardt, "Assessing the Potential of Predictive Control for Hybrid Vehicle Powertrains Using Stochastic Dynamic Programming," *IEEE Transactions on Intelligent Transportation Systems,* vol. 8, no. 1, pp. 71-83, March 2007.

[5] B. Sampathnarayanan, L. Serrao, S. Onori, G. Rizzoni and S. Yurkovich, "Model Predictive Control as an Energy Management Strategy for Hybrid Electric Vehicles," in *Dynamic Systems and Control Conference*, Hollywood, 2009.

[6] H. Borhan, A. Vahidi, A. M. Phillips, M. L. Kuang, I. V. Kolmanovsky and S. D. Cairano, "Predictive energy management of a power-split hybrid electric vehicle," in *2009 American Control Conference*, St. Louis, 2009.

[7] H. Borhan, A. Vahidi, A. M. Phillips, M. L. Kuang, I. V. Kolmanovsky and S. D. Cairano, "MPC-Based Energy Management of a Power-Split Hybrid Electric Vehicle," *IEEE Transactions on Control Systems Technology,* vol. 20, no. 3, pp. 593-603, May 2012.

[8] S. D. Cairano, W. Liang, I. V. Kolmanovsky, M. L. Kuang and A. M. Phillips, "Engine power smoothing energy management strategy for a series hybrid

electric vehicle," in *Proceedings of the 2011 American Control Conference*, San Francisco, 2011.

[9] S. D. Cairano, W. Liang, I. V. Kolmanovsky, M. L. Kuang and A. M. Phillips, "Power Smoothing Energy Management and Its Application to a Series Hybrid Powertrain," *IEEE Transactions on Control Systems Technology,* vol. 21, no. 6, pp. 2091-2103, November 2013.

[10] S. D. Cairano, D. Bernardini, A. Bemporad and I. V. Kolmanovsky, "Stochastic MPC With Learning for Driver-Predictive Vehicle Control and its Application to HEV Energy Management," *IEEE Transactions on Control Systems Technology,* vol. 22, no. 3, pp. 1018-1031, May 2014.

[11] J. Buerger, S. East and M. Cannon, "Fast Dual-Loop Nonlinear Receding Horizon Control for Energy Management in Hybrid Electric Vehicles," *IEEE Transactions on Control Systems Technology,* vol. 27, no. 3, pp. 1060-1070, May 2019.

[12] S. Uebel, N. Murgovski, B. Bäker and J. Sjöberg, "A Two-Level MPC for Energy Management Including Velocity Control of Hybrid Electric Vehicles," *IEEE Transactions on Vehicular Technology,* vol. 68, no. 6, pp. 5494-5505, June 2019.

[13] S. Wang, J. Economou and A. Tsourdos, "Indirect engine sizing via distributed hybrid-electric unmanned aerial vehicle state-of-charge-based parametrisation criteria," *Proceedings of the Institution of Mechanical Engineers, Part G: Journal of Aerospace Engineering,* vol. 233, no. 14, p. 5360–5368, 2019.

[14] S. Wang, J. Economou and A. Tsourdos, "Design of a Distributed Hybrid Electric Propulsion System for a Light Aircraft based on genetic algorithm," in *AIAA Propulsion and Energy 2019 Forum*, Indianapolis, 2019.

[15] M. Koot, J. T. B. A. Kessels, B. d. Jager, W. P. M. H. Heemels, P. P. J. v. d. Bosch and M. Steinbuch, "Energy Management Strategies for Vehicular

Electric Power Systems," *IEEE Transactions on Vehicular Technology,* vol. 54, no. 3, pp. 771-782, May 2005.

[16] J. M. Maciejowski, Predictive Control with Constraints, Prentice Hall, 2002.

[17] S. Oliveira, "Model Predictive Control for Constrained Nonlinear Systems," CaltechTHESIS, 1996.

[18] V. H. Johnson, K. B. Wipke and D. J. Rausen, "HEV Control Strategy for Real-Time Optimization of Fuel Economy and Emissions," *SAE Technical Paper 2000-01-1543,* 2000.

[19] S. Wang, J. T. Economous and A. Tsourdos, "Mamdani & Sugeno Fuzzy Battery Longevity for Distributed Series Hybrid electric Aircraft". Pending.

[20] S. Kermani, S. Delprat, T. M. Guerra, R. Trigui and B. Jeanneret, "Predictive energy management for hybrid vehicle," *Control Engineering Practice,* vol. 20, pp. 408-420, 12 January 2012.

[21] R. E. Bellman, "An Introduction to the Theory of Dynamic Programming," RAND Corporation, Santa Monica, 1953.

8 CONCLUSION

Responding to the call for sustainable aviation, this research proposed a distributed series hybrid-electric propulsion system for aero vehicles to improve the fuel economy and reduce emissions. The study started from the configuration design, followed by the system sizing and supervisory control. Simulation results showed that the designed hybrid-electric propulsion system can effectively reduce fuel consumption and emissions at varying degrees.

8.1 Conclusion

The first objective of this research is to determine the configuration of the aircraft propulsion system. The conventional series hybrid is a good structure, since it is high-electrified and decouples the engine from the propeller. However, the series configuration needs a generator to convert the mechanical energy into electricity. This extra device increases the system weight and exacerbates the energy loss caused by repeated energy conversions. Therefore, two intelligent techniques have been adopted into the conventional series hybrid system. The first technique of distributed propulsion applies multiple small propulsors to propel the aircraft, which can increase the system efficiency and reduce the system weight. Another more electric aircraft concept expands the original propulsion system and includes the avionic system into the propulsion system. This integration not only improves the efficiency and usage rate of each component, but also can remove the unnecessary equipment so that reduce the number of devices. Overall, these two modifications provide a possibility to improve the property of the conventional series hybrid system, and based on that, the configuration of the distributed series hybrid-electric propulsion system was determined.

Based on the defined system configuration, the component selection can be proceeded. Most of engineering applications select components by their power-to-weight ratio, which costs time and requires extra simulations to validate the selection result. Therefore, this research developed an intelligent sizing method. It firstly chose the engine based on the performance between the engine and battery pack, which found that the engine whose output at the most efficient point is about 1.2 times of the average value of the power requirement is the most suitable engine for the given mission. Then, other equipment was selected according to a proposed comprehensive sizing table by using genetic algorithm. The system divided the system into two parts, and applied the NSGA-II and traditional genetic algorithm to each part respectively. Moreover, the designed intelligent sizing method can illustrate the system performance simultaneously, that proved that a 12% improvement in fuel consumption can be expected by applying a rule-based controller with selected components.

The last objective in this research is to design a real-time supervisory controller to coordinate different power flows inside the proposed hybrid-electric system. At present, various control algorithms are applicable for the power management problem. Amongst them, three control methods are selected in this study. The first controller is a deterministic rule-based controller. It is basically a power follower controller, which regulates the engine operating condition according to the power requirement and the battery SOC. The second controller was designed by the fuzzy logic algorithm. It is a battery longevity controller which can monitor and improve the battery operating environment. Simulation result showed that the MSFL can effectively improve the battery circumstance as well as increase the fuel efficiency. The third controller was developed to discuss the relationship between fuel and emissions. Based on a rough emission map and a detailed BSFC map, an MPC-based controller was proposed to manage two power sources. The result showed that two objectives, i.e. improving fuel efficiency and reducing emissions, cannot be achieved at same time. However, since three controllers can effectively limit the engine operating area into a restricted region

with high efficiency, all of controllers significantly increased the fuel efficiency with different emissions variations. Overall, the coordination among the emission reduction, fuel reduction and battery operating environment improvement is a trade-off problem. Different emphasis will lead to different performance.

8.2 Future Works

The thesis completed the design of the distributed series hybrid-electric propulsion system. The improved fuel economy performance was validated by the numerical simulation tests. The areas of future work are recommended:

1. Analysis the relationship between the fuel consumption, emissions and battery operating environment: Based on the result of this study, it is clear that three goals of improving fuel efficiency, emissions and battery operating environment cannot be obtained at same time. Thus, the power management problem is a trade-off study, and the optimization result can be shifted by different emphasis. Namely, if the value of weighting factor on fuel increases, the reduction of the fuel consumption will be greater than the reduction of the other two objectives. Vice versa, if the value of weighting factor on emissions or other properties increases, the reduction of that characteristic will be greater than others. Therefore, a study amongst three control objectives should be processed. How to define the goals by detailed values, and how to balance them is a quite interesting topic.

2. The layout and management of motors: As mentioned in the design process, multiple small motors are utilized in the system. However, to realize the designed system in practical applications, a study of the aerodynamic properties of the aircraft with distributed propulsion is required. The layout and capacity of each motor should be carefully selected and allocated based on the aerodynamic study. Furthermore, a power management strategy for motors is required as well.

3. The establishment of the fault diagnose and re-configuration. The designed system has a potential to handle emergencies, such as motor failure. If one

motor stops work, other motors can increase output to compensate for the shortcoming. Therefore, a system which can diagnose the fault and re-configure the mission is required for the system. The system should be able to solve different urgent conditions, re-assign commands to each component under different circumstance.

REFERENCES

[1] Committee on Climate Change, “Net Zero – The UK’s contribution to stopping global warming,” UK, 2019.

[2] Air Transport Action Group, “FACTS & FIGURES,” October 2018. [Online]. Available: https://www.atag.org/facts-figures.html.

[3] Air Transport Action Group, “Air Transport Action Group (ATAG) environmental goals supported by IATA and at Government levels through ICAO and UNFCCC,” Paris, 2019.

[4] Advisory Council for Aeronautics Research and Innovation, “European Aeronautics: A version for 2020; Meeting Society's Needs and Winning global Leadership,” 2001.

[5] European Commission, “Flightpath 2050 Europe’s Vision for Aviation,” Luxembourg, 2011.

[6] International Civil Aviation Organization, “On Board a Sustainable Future - Environmental Report,” 2016.

[7] Advisory Council for Aeronautics Research and Innovation in Europe, “Flightpath 2050 Europe's Vision for Aviation,” European Commission, 2011.

[8] R.Wahls, “N+3 Technologies and Concepts,” 2010.

[9] F.Collier, “Concepts and technologies for Green Aviation,” Green Engineering Masters Forum, 2009.

[10] National Aeronautics and Space Administration, “Visions of the Future: Hybrid Electric Aircraft Propulsion,” Cheryl Bowman, 2016.

[11] C.C.Chan, “The State of the Art of Electric, Hybrid, and Fuel Cell Vehicles,” *Proceedings of the IEEE,* vol. 95, no. 4, pp. 704-718, April 2007.

[12] I.Husain, “Electric and Hybrid Vehicles Design Fundamentals,” CRC Press, 2003, p. 243.

[13] J.Sliwinski, A.Gardi, M.Marino and R.Sabatini, “Hybrid-electric propulsion integration in unmanned aircraft,” *Energy,* vol. 140, no. 2, pp. 1407-1416, 2017.

[14] R.M.Hiserote and F.G.Harmon, “Analysis of Hybrid-Electric Propulsion System Designs for Small Unmanned Aircraft Systems,” in *8th Annual International Energy Conversion Engineering Conference*, Nashville, 2010.

[15] F.G.Harmon, A.A.Frank and J.Chattot, “Conceptual Design and Simulation of a Small Hybrid-Electric Unmanned Aerial Vehicle,” *Journal of Aircraft,* vol. 43, no. 5, pp. 1490-1498.

[16] M.P.Molesworth, “Rapid Prototype Development of a Remotely Piloted Aircraft Powered by a Hybrid-Electric Propulsion System,” AFIT Scholar, Air Force Institute of Technology, 2012.

[17] J.K.Ausserer and F.G.Harmon, “Integration, Validation, and Testing of a Hybrid-Electric Propulsion System for a Small Remotely Piloted Aircraft,” in *10th International Energy Conversion Engineering Conference*, Atlanta, 2012.

[18] J.Y.Hung and L.F.Gonzalez, “On parallel hybrid-electric propulsion system for unmanned aerial vehicles,” *Progress in Aerospace Sciences,* vol. 51, pp. 1-17, 2012.

[19] R.Glassock, J.Y.Hung, L.F.Gonzalez and R.A.Walker, “Design, modelling and measurement of a hybrid powerplant for unmanned aerial systems,” in *5th Australasian Congress on Applied Mechanics*, Brisbane, 2007.

[20] C.Friedrich and P.A.Robertson, “Hybrid-Electric Propulsion for Aircraft,” *Journal of Aircraft,* vol. 52, no. 1, pp. 176-189, 2015.

[21] Quaternium, “THE FIRST PETROL-ELECTRIC MULTICOPTER,” Quaternium, [Online]. Available: https://www.quaternium.com/uav/hybrix-20/.

[22] Skyfront, “THE PERIMETER DRONE,” 2020. [Online]. Available: https://skyfront.com/.

[23] HARRIS AERIAL, “CARRIER H4 HYBRID,” [Online]. Available: https://www.harrisaerial.com/carrier-h4-hybrid-drone/.

[24] Walkera, “QL1200,” Walkera, January 2020. [Online]. Available: https://www.walkera.com/index.php/Goods/info/id/49.html.

[25] ALTI, “ALTI Reach,” ALTI, [Online]. Available: https://www.altiuas.com/reach/.

[26] Diamond Aircraft, “Diamond Aircraft proudly presents the world’s first serial hybrid electric aircraft “DA36 E-Star”,” Diamond Aircraft Industries GmbH, [Online]. Available: http://www.diamond-air.at/en/media-center/press-releases/news/article/diamond-aircraft-proudly-presents-the-worlds-first-serial-hybrid-electric-aircraft-da36-e-star/. [Accessed 15 December 2018].

[27] W.Wittmann, “Flying with Siemens Integrated Drive System,” SIEMENS, June 2013. [Online]. Available: https:// www.siemens.com/press/en/pressrelease/?press=/en/pressrelease/2013/industry/drive-technologies/idt2013064084.htm.

[28] HYPSTAIR, “Most powerful hybrid electric powertrain powers up,” 2016. [Online]. Available: http://www.hypstair.eu/most-powerful-hybrid-electric-powertrain-powers-up/.

[29] D.Sigler, “Launching on a Leaf Blower and a Hacker,” CAFE, 2010. [Online]. Available: http://cafe.foundation/blog/launing-on-a-leaf-blower-and-a-hacker.

[30] M.Cotter, “Embry-Riddle Students Make History With "Eco Eagle" Hybrid Propulsion Aircraft,” 16 September 2011. [Online]. Available: http://inhabitat.com/embry-riddle-students-make-history-with-eco-eagle-hybrid-propulsion-aircraft/.

[31] J.Paur, “Hybrid Power Comes to Aviation,” WIRED, July 2009. [Online]. Available: http://www.wired.com/2009/07/hybrid-aviation/.

[32] T.Banning, G.Bristow, C.Level, L.Sollmann, J.Calderon-Fernandez and etc., “NXG-50,” 2013.

[33] Journalistic platform TU Delft, “Hybrid plane: Prius in the sky,” Delft University of Technology, 2017. [Online]. Available: https://www.delta.tudelft.nl/article/hybrid-plane-prius-sky.

[34] J.R.Welstead and J.L.Felder, “Conceptual Design of a Single-Aisle Turboelectric Commercial Transport with Fuselage Boundary Layer Ingestion,” in *54th AIAA Aerospace Sciences Meeting*, San Diego, California, 2016.

[35] NASA, “Hybrid Wing Body Goes Hybrid,” August 2017. [Online]. Available: https://www.nasa.gov/content/hybrid-wing-body-goes-hybrid.

[36] M.K.Bradley and C.K.Droney, “Subsonic Ultra Green Aircraft Research Phase II: N+4 Advanced Concept Development,” in *SAE 2013 AeroTech Congress Exhibit*, 2013.

[37] A.Webster, “Boeing's SUGAR Freeze plane concept runs on cryogenically frozen liquid natural gas,” May 2012. [Online]. Available: https://www.theverge.com/2012/3/21/2890091/boeing-sugar-freeze-cryogenically-frozen-natural-gas.

[38] Airbus Group Limited, “Distributed Electrical Aerospace Propulsion (DEAP),” 2017. [Online]. Available: http://gtr.rcuk.ac.uk/projects?ref=101286.

[39] R.Gardner, “Into the DEAP,” *SAE Vehicle Electrification.*

[40] NASA, “SCEPTOR Distributed Electric Propulsion Aircraft,” May 2016. [Online]. Available: https://sbir.nasa.gov/success-stories/sceptor-distributed-electric-propulsion-aircraft.

[41] B.Schiltgen, A.R.Gibson, M.Green and J.Freeman, “More Electric Aircraft: "Tube and Wing" Hybrid Electric Distributed Propulsion with Superconducting and Conventional Electric Machines,” in *SAE 2013 AeroTech Congress & Exhibition*, 2013.

[42] N.Madavan, R.D.Rosario and A.L.Jankovsky, “Hybrid-Electric and Distributed Propulsion Technologies for Large Commercial Transports: A NASA Perspective,” in *IEEE Energy Conversion Congress and Exposition*, Montreal, 2015.

[43] T.S.Dean, G.E.Wroblewski and P.J.Ansell, “Mission Analysis and Component-Level Sensitivity Study of Hybrid-Electric General Aviation Propulsion Systems,” in *AIAA Aerospace Sciences Meeting*, Kissimmee, 2018.

[44] C.Friedrich and P.A.Robertson, “Design of a Hybrid-Electric Propulsion System for Light Aircraft,” in *AIAA Aviation Technology, Integration and Operation Conference*, Atlanta, 2014.

[45] J.Koster, C.Humbargar, E.Serani, A.Velazco, D.Hillery and L.Makepeace, “Hybrid Electric Integrated Optimized System Design of a Hybrid Propulsion System for Aircraft,” in *9th AIAA Aerospace Sciences Meeting*, Orlando, 2011.

[46] E.Tara, S.Shahidinejad, S.Filizadeh and E.Bibeau, “Battery Storage Sizing in a Retrofitted Plug-in Hybrid Electric Vehicle,” *IEEE Transactions on Vehicular Technology,* vol. 59, no. 6, pp. 2786-2794, July 2010.

[47] J.Schoemann and M.Hornung, “Modeling of Hybrid-Electric Propulsion Systems for Small Unmanned Aerial Vehicles,” in *12th AIAA Aviation Technology, Integration, and Operations (ATIO) Conference and 14th AIAA/ISSMO Multidisciplinary Analysis and Optimization Conference*, Indianapolis, 2012.

[48] D.Assanis, G.Delagrammatikas, Z. R.Fellini, J.Liedtke, N.Michelena, P.Papalambros, D.Reyes, D.Rosenbaum, A.Sales and M.Sasena, “Optimization Approach to Hybrid Electric Propulsion System Design,” *Mechanics of Structures and Machines,* vol. 27, no. 4, pp. 393-421, 1999.

[49] R.Fellini, N.Michelena, P.Papalambros and M.Sasena, “Optimal design of automotive hybrid powertrain systems,” in *Proceedings First International Symposium on Environmentally Conscious Design and Inverse Manufacturing*, Tokyo, 1999.

[50] V.Galdi, L.Ippolito, A.Piccolo and A.Vaccaro, “A genetic-based methodology for hybrid electric vehicles sizing,” *Soft Computing,* vol. 5, no. 6, pp. 451-457, December 2001.

[51] N.Murgovski, L.Johannesson, J.Sjöberg and B.Egardt, “ Component sizing of a plug-in hybrid electric powertrain via convex optimization,” *Mechatronics,* vol. 22, no. 1, pp. 106-120, 2012.

[52] A.Abdelkader, A.Rabeh, D.M.Ali and J.Mohamed, “Multi-objective genetic algorithm based sizing optimization of a stand-alone wind/PV power supply system with enhanced battery/supercapacitor hybrid energy storage,” *Energy,* pp. 351-363, August 2018.

[53] Y.Xie, A.Savvaris and A.Tsourdos, “Sizing of hybrid electric propulsion system for retrofitting a mid-scale aircraft using non-dominated sorting genetic algorithm,” *Aerospace Science and Technology,* no. 82-83, pp. 323-333, September 2018.

[54] Wikipedia contributors, “Internal combustion engine,” January 2020. [Online]. Available: https://en.wikipedia.org/w/index.php?title=Internal_combustion_engine&oldid=933934613.

[55] J.B.Heywood, Internal Combustion Engine Fundamental, New York: McGraw-Hill, 1988.

[56] S.R.Kumbhar, S.S.Satpute and S.D.Yadav, I C Engine Testing, Lap Lambert Academic Publishing GmbH KG, 2012.

[57] A.Kerimnes, “Internal Combustion Engine Modelling”.

[58] R.W.Weeks and J.J.Moskwa, “Automotive engine modelling for real-time control using matlab/simulink,” *SAE Technical Paper,* 1995.

[59] J.R.Wagner, D.M.Dawson and L.Zeyu, “Nonlinear air-to-fuel ratio and engine speed control for hybrid vehicles,” *IEEE Transactions on Vehicular Technology,* vol. 52, no. 1, pp. 184-195, January 2003.

[60] Y.Xie, “Design and Energy Management of Aircraft Hybrid-electric Propulsion System,” Cranfield University, 2017.

[61] F.G.Harmon, “Neural network control of a parallel hybrid-electric propulsion system for a small unmanned aerial vehicle,” 2005.

[62] L.Guzzella and C.H.Onder, Introduction to modelling and control of internal combustion engine systems, Springer, 2010.

[63] S.Menon and C.Cadou, “Experimental and computational investigations of small internal combustion engine performance,” in *Fifth US Combustion Meeting*, San Diego, 2007.

[64] F.U.Syed, “Modeling and Control Methods for Improving Drivability, Power Management and Fuel Economy in a Hybrid Electric Vehicle,” 2008.

[65] S.Maganti, “Control and Model of Power Split Hybrid Electric Car,” 2008.

[66] M.D.Rippl, “Analysis for Aircraft Utilizing Hybrid-Electric Propulsion Systems,” 2011.

[67] Wikipedia contributors, “Electric motor,” Wikipedia, The Free Encyclopedia, January 2020. [Online]. Available: https://en.wikipedia.org/w/index.php?title=Electric_motor&oldid=935557766.

[68] P.Krause, Analysis of electric machinery, McGraw Hill, 1986.

[69] P.Pillay, “Modelling of Permanent Magnet Motor Drives,” *IEEE Transactions on Industrial Electronics,* vol. 35, no. 1, 11 1988.

[70] Battery University, “BU-204: How do Lithium Batteries Work?,” 2018. [Online]. Available: https://batteryuniversity.com/learn/article/lithium_based_batteries. [Accessed 17 01 2020].

[71] Battery University, “BU-409 Charging Lithium-ion,” 2017. [Online]. Available: http://batteryuniversity.com/learn/article/charging_lithium_ion_batteries.

[72] A.A.Hussein, “Experimental modeling and analysis of lithium-ion battery temperature dependence,” in *2015 IEEE Applied Power Electronics Conference and Exposition*, Charlotte, 2015.

[73] J.Jaguemont., L.Boulon and Y.Dubé, “Characterization and Modeling of a Hybrid-Electric-Vehicle Lithium-Ion Battery Pack at Low Temperatures,” *IEEE Transactions on Vehicular Technology,* vol. 65, no. 1, pp. 1-14, 2016.

[74] Y.Hu and S.Yurkovich, “Linear parameter varying battery model identification using subspace methods,” *Journal of Power Sources,* vol. 196, no. 5, pp. 2913-2923, 2011.

[75] D.Andre, M.Meiler, K.Steiner, H.Walz, T.Soczka-Guth and D.U.Sauer, “Characterization of high-power lithium-ion batteries by electrochemical impedance spectroscopy. II: Modelling,” *Journal of Power Sources,* vol. 196, no. 12, pp. 5349-5356, 2011.

[76] C.M.Shepherd, “Design of Primary and Secondary Cells II . An Equation Describing Battery Discharge,” *Journal of The Electrochemical Society,* vol. 112, no. 7, pp. 657-664, 1965.

[77] O.Tremblay, L.Dessaint and A.Dekkiche, “A Generic Battery Model for the Dynamic Simulation of Hybrid Electric Vehicles,” in *2007 IEEE Vehicle Power and Propulsion Conference*, Arlington, 2007.

[78] O.Tremblay and L.Dessaint, “Experimental Validation of a Battery Dynamic Model for EV Applications,” *World Electric Vehicle Journal,* vol. 3, pp. 289-298, 2009.

[79] F.R.Salmasi, “Control Strategies for Hybrid Electric Vehicles: Evolution, Classification, Comparison, and Future Trends,” *IEEE Transactions on Vehicular Technology,* vol. 56, no. 5, pp. 2393-2404, 2007.

[80] C.G.Hochgraf, M.J.Ryan and H.L.Wiegman, “Engine Control Strategy for a Series Hybrid Electric Vehicle Incorporating Load-Leveling and Computer Controlled Energy Management,” *SAE Technical Paper 960230,* 1996.

[81] C.Anderson and E.Pettit, “TheEffects of APU Characteristics on the Design of Hybrid Control Strategies for Hybrid Electric Vehicles,” *SAE Technical Paper 950493,* 1995.

[82] N.Jalil, N.A.Kheir and M.Salma, “A rule-based energy management strategy for a series hybrid vehicle,” in *Proceedings of the 1997 American Control Conference*, 689-693, 1997.

[83] P.Pisu and G.Rizzoni, “A Comparative Study Of Supervisory Control Strategies for Hybrid Electric Vehicles,” *IEEE Transactions on Control Systems Technology,* vol. 15, no. 3, pp. 506-518, 2007.

[84] S.Barsali, C.Miulli and A.Possenti, “A control strategy to minimize fuel consumption of series hybrid electric vehicles,” *IEEE Transactions on Energy Conversion,* vol. 19, no. 1, pp. 187-195, 2004.

[85] V.H.Johnson, K.B.Wipke and D.J.Rausen, “HEV Control Strategy for Real-Time Optimization of Fuel Economy and Emissions,” *SAE Technical Paper 2000-01-1543,* 2000.

[86] A.M.Phillips, M.Jankovic and K.E.Bailey, “Vehicle system controller design for a hybrid electric vehicle,” in *Proceedings of the 2000 IEEE International Conference on Control Applications*, Anchorage, 2000.

[87] S.H.Mahyiddin, M.R.Mohamed, Z.Mustaffa, A.C.Khor, M.H.Sulaiman, H.Ahmad and S.A.Rahman, “Fuzzy logic energy management system of series hybrid electric vehicle,” in *4th IET Clean Energy and Technology Conference*, Kuala Lumpur, 2016.

[88] K.Ç.Bayindir, M.A.Gözüküçük and A.Teke, “A comprehensive overview of hybrid electric vehicle: Powertrain configurations, powertrain control techniques and electronic control units,” *Energy Conversion and Management,* vol. 52, no. 2, pp. 1305-1313, 2011.

[89] A.M.Ali and D.Söffker, “Towards Optimal Power Management of Hybrid Electric Vehicles in Real-Time: A Review on Methods, Challenges, and State-Of-The-Art Solutions,” *Energies,* vol. 11, no. 3, p. 476, 2018.

[90] N.J.Schouten, M.A.Salman and N.A.Kheir, “Fuzzy Logic Control for Parallel Hybrid Vehicles,” *IEEE Transactions on control systems technology,* vol. 10, no. 3, May 2002.

[91] N.J.Schouten, M.A.Salman and N.A.Kheir, “Energy management strategies for parallel hybrid vehicles using fuzzy logic,” *Control Engineering Practice,* vol. 11, no. 2, pp. 171-177, 2003.

[92] B.M.Baumann, G.Washington, B.C.Glenn and G.Rizzoni, “Mechatronic design and control of hybrid electric vehicles,” *IEEE/ASME Transactions on Mechatronics,* vol. 5, no. 1, pp. 58-72, March 2000.

[93] H-D.Lee and S-K.Sul, “Fuzzy-logic-based torque control strategy for parallel-type hybrid electric vehicle,” *IEEE Transactions on Industrial Electronics,* vol. 45, no. 4, pp. 625-632, August 1998.

[94] M.Montazeri-Gh and M.Mahmoodi-k, “Development a new power management strategy for power split hybrid electric vehicles,” *Transportation Research Part D: Transport and Environment,* vol. 37, 2015.

[95] Y.Wang, Y.Zhang, J.Wu and N.Chen, “Energy management system based on fuzzy control approach for hybrid electric vehicle,” *Chinese Control and Decision Conference,* pp. 3382-3386, 2009.

[96] R.Langari and J-S.Won, “Intelligent energy management agent for a parallel hybrid vehicle-part I: system architecture and design of the driving situation identification process,” *IEEE Transactions on Vehicular Technology,* vol. 54, no. 3, pp. 925-934, May 2005.

[97] J-S.Won and R.Langari, “Intelligent energy management agent for a parallel hybrid vehicle-part II: torque distribution, charge sustenance strategies, and performance results,” *IEEE Transactions on Vehicular Technology,* vol. 54, no. 3, May 2005.

[98] S.Zhang and R.Xiong, “Adaptive energy management of a plug-in hybrid electric vehicle based on driving pattern recognition and dynamic programming,” *Applied Energy,* vol. 155, pp. 68-78, 2015.

[99] M.H.Hajimiri and F.R.Salmasi, “A Fuzzy Energy Management Strategy for Series Hybrid Electric Vehicle with Predictive Control and Durability Extension of the Battery,” in *IEEE Conference on Electric and Hybrid Vehicles*, Pune, 2006.

[100] M.Montazeri-Gh and M.Mahmoodi-K, “Optimized predictive energy management of plug-in hybrid electric vehicle based on traffic condition,” *Journal of Cleaner Production,* vol. 139, pp. 935-948, July 2016.

[101] S.G.Wirasingha and A.Emadi, “Classification and Review of Control Strategies for Plug-In Hybrid Electric Vehicles,” *IEEE Transactions on Vehicular Technology,* vol. 60, no. 1, pp. 111-122, January 2011.

[102] P.Zhang, F.Yan and C.Du, “A comprehensive analysis of energy management strategies for hybrid electric vehicles based on bibliometrics,” *Renewable and Sustainable Energy Reviews,* vol. 48, pp. 88-104, 2015.

[103] R.Chedid and Y.Saliba, “Optimization and Control of Autonomous Renewable Energy Systems,” *International Journal of Energy Research,* vol. 20, pp. 609-624, 1996.

[104] G.Wu, K.Boriboonsomsin and M.J.Barth, “Development and Evaluation of an Intelligent Energy-Management Strategy for Plug-in Hybrid Electric Vehicles,” *IEEE Transactions on Intelligent Transportation Systems,* vol. 15, no. 3, pp. 1091-1100, June 2014.

[105] S.Delprat, J.Lauber, T.M.Guerra and J.Rimaux, “Control of a parallel hybrid powertrain: optimal control,” *IEEE Transactions on Vehicular Technology,* vol. 53, no. 3, pp. 872-881, May 2004.

[106] G.Steinmauer and L.D.Re, “Optimal control of dual power sources,” in *Proceedings of the 2001 IEEE International Conference on Control Applications (CCA'01)*, Mexico, 2001.

[107] E.D.Tate and S.P.Boyd, “Finding Ultimate Limits of Performance for Hybrid Electric Vehicles,” *SAE Technical Paper,* 2000.

[108] R.Bellman, “Dynamic Programming and Lagrange Multipliers,” vol. 42, no. 10, pp. 767-769, 1956.

[109] R.Wegmann, V.Döge, J.Becker and D.U.Sauer, “Optimized operation of hybrid battery systems for electric vehicles using deterministic and stochastic dynamic programming,” *Journal of Energy Storage,* vol. 14, no. 1, pp. 22-38, 2017.

[110] P.Elbert, S.Ebbesen and L.Guzzella, “Implementation of Dynamic Programming for n-Dimensional Optimal Control Problems With Final State Constraints,” *IEEE Transactions on Control Systems Technology,* vol. 21, no. 3, pp. 924-931, May 2013.

[111] M.Oprean, V.Ionescu, N.Mocanu, S.Beloiu and C.Stanciu, “Dynamic programming applied to hybrid vehicle control,” in *Proceedings of the International Conference on Electric Drives (ICED '88)*, 1988.

[112] A.Brahma, Y.Guezennec and G.Rizzoni, “Optimal energy management in series hybrid electric vehicles,” in *Proceedings of the 2000 American Control Conference. ACC*, Chicago, 2000.

[113] C.C.Lin, H.Peng, J.W.Grizzle and J-M.Kang, “Power management strategy for a parallel hybrid electric truck,” *IEEE Transactions on Control Systems Technology,* vol. 11, no. 6, pp. 839-849, Nov. 2003.

[114] D.Bianchi, L.Rolando, L.Serrao, S.Onori, G.Rizzoni, N.Al-Khayat, T-M.Hsieh and P.Kang, “A Rule-Based Strategy for a Series/Parallel Hybrid Electric Vehicle: An Approach Based on Dynamic Programming,” in *Proceedings of the ASME 2010 Dynamic Systems and Control Conference, ASME 2010 Dynamic Systems and Control Conference*, Massachusetts, 2010.

[115] A.Boyali and L.Güvenç, “Real-time controller design for a parallel hybrid electric vehicle using neuro-dynamic programming method,” in *2010 IEEE International Conference on Systems, Man and Cybernetics*, Istanbul, 2010.

[116] W.Li, G.Xu and Y.Xu, “Online learning control for hybrid electric vehicle,” *Chinese Journal of Mechanical Engineering,* vol. 25, no. 1, pp. 98-106, January 2012.

[117] C-C.Lin, H.Peng and J.W.Grizzle, “A stochastic control strategy for hybrid electric vehicles,” in *Proceedings of the 2004 American Control Conference*, Boston, 2004.

[118] S.J.Moura, H.K.Fathy, D.S.Callaway and J.L.Stein, “A Stochastic Optimal Control Approach for Power Management in Plug-in Hybrid Electric

Vehicles," *IEEE Transactions on Control Systems Technology,* vol. 19, no. 3, pp. 545-555, May 2011.

[119] M.Montazeri-Gh, A.Poursamad and B.Ghalichi, "Application of genetic algorithm for optimization of control strategy in parallel hybrid electric vehicles," *Journal of the Franklin Institute,* vol. 343, no. 4-5, pp. 420-435, 2006.

[120] C.Bertram, D.Buecherl, A.Thanheiser and H.Herzog, "Multi-objective optimization of a parallel hybrid electric drive train," Chicago, 2011.

[121] A.Piccolo, L.Ippolito, V.Galdi and A.Vaccaro, "Optimisation of energy flow management in hybrid electric vehicles via genetic algorithms," in *2001 IEEE/ASME International Conference on Advanced Intelligent Mechatronics*, Italy, 2001.

[122] N.Murgovski, L.Johannesson and J.Sjöberg, "Convex modeling of energy buffers in power control applications," vol. 45, no. 30, pp. 92-99, 2012.

[123] P.Elbert, T.Nüesch, A.Ritter, N.Murgovski and L.Guzzella, "Engine On/Off Control for the Energy Management of a Serial Hybrid Electric Bus via Convex Optimization," *IEEE Transactions on Vehicular Technology,* vol. 63, no. 8, pp. 3549-3559, 2014.

[124] N.Murgovski, L.Johannesson and B.Egardt, "Optimal Battery Dimensioning and Control of a CVT PHEV Powertrain," *IEEE Transactions on Vehicular Technology,* vol. 63, no. 5, pp. 2151-2161, June 2014.

[125] Z.Chen, R.Xiong and J.Cao, "Particle swarm optimization-based optimal power management of plug-in hybrid electric vehicles considering uncertain driving conditions," *Energy,* vol. 96, pp. 197-208, 2016.

[126] C.Dextreit and I.V.Kolmanovsky, “Game Theory Controller for Hybrid Electric Vehicles,” *IEEE Transactions on Control Systems Technology,* vol. 22, no. 2, pp. 652-663, March 2014.

[127] H.Yin, C.Zhao, M.Li, C.Ma and M.Chow, “A Game Theory Approach to Energy Management of An Engine–Generator/Battery/Ultracapacitor Hybrid Energy System,” *IEEE Transactions on Industrial Electronics,* vol. 63, no. 7, pp. 4266-4277, July 2016.

[128] A.Panday and H.O.Bansal, “Fuel efficiency optimization of input-split hybrid electric vehicle using DIRECT algorithm,” in *9th International Conference on Industrial and Information Systems (ICIIS)*, 2014.

[129] A.Younis, L.Zhou and Z.Dong, “Application of the new SEUMRE global optimisation tool in high efficiency EV/PHEV/EREV electric mode operations,” *International Journal of Electric and Hybrid Vehicles,* vol. 3, pp. 176 - 190, 2011.

[130] H.P.Geering, Optimal Control with Engineering Applications, Berlin: Springer, 2007.

[131] L.Serrao, S.Onori, A.Sciarretta, Y.Guezennec and G.Rizzoni, “Optimal energy management of hybrid electric vehicles including battery ageing,” in *Proceedings of the 2011 American Control Conference*, San Francisco, 2011.

[132] M.Ghasemi and X.Song, “A Computationally Efficient Optimal Power Management for Power Split Hybrid Vehicle Based on Pontryagin’s Minimum Principle,” in *Proceedings of the ASME 2017 Dynamic Systems and Control Conference*, 2017.

[133] N.Kim, S.Cha and H.Peng, “Optimal Control of Hybrid Electric Vehicles Based on Pontryagin's Minimum Principle,” *IEEE Transactions on Control Systems Technology,* vol. 19, no. 5, pp. 1279-1287, September 2011.

[134] M.Koot, J.T.Kessels, B.Jager, W.P.Heemels, P.P.Bosch and M.Steinbuch, “Energy Management Strategies for Vehicular Electric Power Systems,” *IEEE Transactions on Vehicular Technology,* vol. 54, no. 3, pp. 771-782, May 2005.

[135] G.Paganelli, S.Delprat, T.M.Guerra, J.Rimaux and J.J.Santin, “Equivalent consumption minimization strategy for parallel hybrid powertrains,” in *Vehicular Technology Conference, IEEE 55th Vehicular Technology Conference*, Birmingham, Alabama, 2002.

[136] C.Zhang and A.Vahidi, “Route Preview in Energy Management of Plug-in Hybrid Vehicles,” *IEEE Transactions on Control Systems Technology,* vol. 20, no. 2, pp. 546-553, 2012.

[137] D.Sinoquet, G.Rousseau and Y.Milhau, “Design optimization and optimal control for hybrid vehicles,” *Optimization and Engineering,* vol. 12, no. 1-2, pp. 199-213, March 2011.

[138] J.Park and J.H.Park, “Development of equivalent fuel consumption minimization strategy for hybrid electric vehicles,” *International Journal of Automotive Technology,* vol. 13, no. 5, pp. 835-843, August 2012.

[139] G.Paganelli, G.Ercole, A.Brahma, Y.Guezennec and G.Rizzoni, “General supervisory control policy for the energy optimization of charge-sustaining hybrid electric vehicles,” *JSAE Review,* vol. 22, no. 4, pp. 511-518, 2001.

[140] C.Sun, F.Sun and H.He, “Investigating adaptive-ECMS with velocity forecast ability for hybrid electric vehicles,” *Applied Energy,* vol. 185, no. 2, pp. 1644-1653, 2017.

[141] M.Krstić and H-H.Wang, “Stability of extremum seeking feedback for general nonlinear dynamic systems,” *Automatica,* vol. 36, no. 4, pp. 595-601, 2000.

[142] N.Bizon, “Energy optimization of fuel cell system by using global extremum seeking algorithm,” *Applied Energy,* vol. 206, pp. 458-474, 2017.

[143] L.Johannesson, M.Asbogard and B.Egardt, “Assessing the Potential of Predictive Control for Hybrid Vehicle Powertrains Using Stochastic Dynamic Programming,” *IEEE Transactions on Intelligent Transportation Systems,* vol. 8, no. 1, pp. 71-83, March 2007.

[144] B.Sampathnarayanan, L.Serrao, S.Onori, G.Rizzoni and S.Yurkovich, “Model Predictive Control as an Energy Management Strategy for Hybrid Electric Vehicles,” in *Dynamic Systems and Control Conference*, Hollywood, 2009.

[145] H.Borhan, A.Vahidi, A.M.Phillips, M.L.Kuang, I.V.Kolmanovsky and S.D.Cairano, “Predictive energy management of a power-split hybrid electric vehicle,” in *2009 American Control Conference*, St. Louis, 2009.

[146] H.Borhan, A.Vahidi, A.M.Phillips, M.L.Kuang, I.V.Kolmanovsky and S.D.Cairano, “MPC-Based Energy Management of a Power-Split Hybrid Electric Vehicle,” *IEEE Transactions on Control Systems Technology,* vol. 20, no. 3, pp. 593-603, May 2012.

[147] S.D.Cairano, W.Liang, I.V.Kolmanovsky, M.Kuang and A.M.Phillips, “Engine power smoothing energy management strategy for a series hybrid electric vehicle,” in *Proceedings of the 2011 American Control Conference*, San Francisco, 2011.

[148] S.D.Cairano, W.Liang, I.V.Kolmanovsky, M.Kuang and A.M.Phillips, “Power Smoothing Energy Management and Its Application to a Series Hybrid Powertrain,” *IEEE Transactions on Control Systems Technology,* vol. 21, no. 6, pp. 2091-2103, November 2013.

[149] S.D.Cairano, D.Bernardini, A.Bemporad and I.V.Kolmanovsky, “Stochastic MPC With Learning for Driver-Predictive Vehicle Control and its Application to HEV Energy Management,” *IEEE Transactions on Control Systems Technology,* vol. 22, no. 3, pp. 1018-1031, May 2014.

[150] J.Buerger, S.East and M.Cannon, “Fast Dual-Loop Nonlinear Receding Horizon Control for Energy Management in Hybrid Electric Vehicles,” *IEEE Transactions on Control Systems Technology,* vol. 27, no. 3, pp. 1060-1070, May 2019.

[151] S.Uebel, N.Murgovski, B.Bäker and J.Sjöberg, “A Two-Level MPC for Energy Management Including Velocity Control of Hybrid Electric Vehicles,” *IEEE Transactions on Vehicular Technology,* vol. 68, no. 6, pp. 5494-5505, June 2019.

[152] A.M.Stoll, J.Bevirt, M.D.Moore, W.J.Fredericks and N.K.Borer, “Drag Reduction Through Distributed Electric Propulsion,” in *14th AIAA Aviation Technology, Integration, and Operations Conference, AIAA AVIATION Forum*, 2014.

[153] J.A.Rosero, J.A.Ortega, E.Aldabas and L.Romeral, “Moving towards a more electric aircraft,” *IEEE Aerospace and Electronic Systems Magazine,* vol. 22, no. 3, pp. 3-9, March 2007.

[154] A.A.AbdElhafez and A.J.Forsyth, “A Review of More-Electric Aircraft,” in *IEEE Colloquium on Electrical Machines & System for the More Electric Aircraft*, 2009.

[155] Y.Xie, A.Savvaris and A.Tsourdos, “Modelling and Control of a Hybrid Electric Propulsion System for Unmanned Aerial Vehicles,” *IEEE,* 2017.

APPENDIX

This is the published version of the paper ‘Indirect Engine Sizing via Distributed Hybrid-Electric UAV State-of-Charge Based Parametrisation Criteria’, which is the Chapter 4 of this thesis.

Original Article

Institution of MECHANICAL ENGINEERS
Journal of AEROSPACE ENGINEERING

Proc IMechE Part G:
J Aerospace Engineering
0(0) 1–9

DOI: 10.1177/0954410019843722
journals.sagepub.com/home/pig
SAGE

Indirect engine sizing via distributed hybrid-electric unmanned aerial vehicle state-of-charge-based parametrisation criteria

S Wang[1], JT Economou[2] and A Tsourdos[1]

Abstract

This paper presents a design process for the challenging problem of sizing the engine pack for a distributed series hybrid-electric propulsion system of unmanned aircraft vehicle. Sizing the propulsion system for hybrid-electric unmanned aerial vehicles is a demanding problem because of the two different categories of propulsion (the engine and the motor), and the electrical system characteristics. Furthermore, what adds to the difficulty is that the internal combustion engine does not directly drive the propellers, but it is connected to an electrical generator and therefore provides electrical power to the electric motors and propellers. Hence there is a clear distinction from the traditional engine solutions which are mechanically coupled to the propeller. This paper addresses this specific distinction and proposes an indirect solution based on properties on the electrical part of the system. In particular, a novel parametric characterisation engine sizing approach is presented using the battery pack state-of-charge during a realistic unmanned aerial vehicle flight scenario. Five candidate engine options were considered with different starting conditions for the electrical system. The results show that by using the state-of-charge properties it is possible to select an appropriate size of engine pack while carrying a suitable electrical propulsion pack. However, the solutions are not unique and are appropriate for given design criteria clearly indicated in the paper.

Keywords

Hybrid unmanned aerial vehicle, hybrid system design, series hybrid, distributed hybrid system

Date received: 18 October 2018; accepted: 18 March 2019

Introduction

In the past couple of decades, the largest growth in commercial air transport have a big impact and changed the world in numerous ways, primarily by increasing the speed of travel, aiding growth in the international business, and making the world more connected. However, a conventional aircraft consumes a large amount of fuel during each flight and simultaneously emits greenhouse gases, noise, heat and particulates. To prevent the deterioration of aircraft negative impact on energy supply and environment, a higher fuel-efficiency and more environmental-friendly propulsion system is required. In general, there are three ways to improve aircraft performance: (a) optimisation of the existing aircraft propulsion systems; (b) development of new propulsion components and (c) a combination of existing propulsion subsystems into hybrid powertrains. Based on the third method, this paper presents a novel distributed series hybrid-electric propulsion system (DSHEPS) for an unmanned aerial vehicle (UAV).

At present, NASA, Airbus, Boeing and many other companies are investing in hybrid-electric aircraft research to improve aviation performance. The most successfully tested hybrid-electric aircraft are UAVs and small-scale aircraft. Due to the fuel having higher power density than batteries', the fuel system contains more energy than an electric system for the same mass. Therefore, hybrid-electric UAVs always can survive a longer flight. Hybrid UAVs emerged from 2010s, and to date, the one with the longest

[1]School of Aerospace, Transport, and Manufacturing, Cranfield University, UK
[2]Cranfield Defence and Security, Aeromechanical Systems Group Centre for Defence Engineering, The Defence Academy of the United Kingdom, Cranfield University, Shrivenham, UK

Corresponding author:
John Economou, Cranfield Defence and Security, Aeromechanical Systems Group Centre for Defence Engineering, The Defence Academy of the United Kingdom, Cranfield University, Shrivenham, UK.
Email: j.t.economou@cranfield.ac.uk

endurance is ALTI Transition, which offers up to 12 h flight carrying no payload. University of Colorado Boulder,[1] Queensland University of Technology[2] and U.S. Airforce Research Laboratory[3] all have researched this area. The other ongoing small hybrid aircraft project is AIRSTART, project in the UK, which is aiming to develop a parallel hybrid propulsion system to support routine small UAV operations beyond visual line of sight.[4]

In terms of the hybrid-electric midscale demonstrators, several aircraft have been successfully tested. Alatus motor-glider, designed by Cambridge University, firstly realised a parallel hybrid-electric power system. It utilises a 2.8 kW internal combustion four-stroke leaf blower unit paralleled with a 12 kW electric motor, and the first truncated flight took place in 2010. Embry-Riddle Aeronautical University, in association with Google, designed another hybrid plane 'Eco-Eagle.' It also uses a parallel hybrid technology and was successfully tested in 2011.[5] The first midscale series hybrid aircraft are the DA36 E-Star and its successor version, developed by Diamond Aircraft (DA), EADS and Siemens AG in 2013.[6] The series system of DA36 E-Star can provide 80 kW power during take-off and 65 kW continuous power during cruising. Later, Cambridge University developed another hybrid aircraft 'SOUL,' which firstly realised the capability of on-board battery charging. It applies a parallel hybrid-electric propulsion system and was successfully tested in 2014.[7]

Research in large-scale aircraft has increased over the recent years. The new series of aircraft from NASA are particularly designed using hybrid-electric propulsion systems. For example, the N3-X Hybrid Wing Body Turboelectric Plane[8] and the STARC-ABL Turboelectric Plane[9] utilise gas-turbine/electric hybrid propulsion systems; the SCEPTOR X-57 plane uses an engine/electric hybrid power system;[10] and the Subsonic Ultra Green Aircraft applies a liquefied natural gas fuel cell/electric hybrid propulsion system.[11] Meanwhile, Airbus, Rolls-Royce and Siemens are working together to test the feasibility of a hybrid-electric propulsion system in a relatively large aircraft, called E-Fan X Plane, and the test flight is currently planned in 2020.[12]

As hybrid-electric aircraft are becoming increasingly more popular, new attempts to develop different hybrid aircraft are expected to increase. Therefore, the method for reasonable designing and sizing of hybrid-electric propulsion system (HEPS) is also essential. Many optimal sizing works have been conducted in the literature. Most studies focus on single objective optimisation, e.g. the paper[13] optimised the capacity of different components of a hybrid system using the loss of power supply probability and the 'levelised' cost of energy. A small number of studies focuses on multi-objective optimisation, which is able to optimise both system performance and other criteria.[7,14] The paper[15] presents a method to optimise plant parameters and minimise the total fuel consumption simultaneously. However, none of the previous research discussed the relationship of battery's performance and parameter sizing. In this paper, we present a novel parametric engine sizing approach to size the engine pack for a hybrid-electric UAV. From simulation results, i.e. batteries pack SOC, the characteristics of five systems with different sized engines are obtained and analysed. Therefore, based on a set flight scenario, a reasonable engine size region can be determined. The proposed design sizing approach provides a new cognition of series hybrid-electric systems, especially focusing towards the relationship and synergy between fuel and electricity.

DSHEPS design process

Within a simplified system design progress, as shown in Figure 1, the DSHEPS is designed. The system is basically derived from a conventional series HEPS configuration, integrated with the distributed propulsion (DP) concept and the more electric aircraft (MEA) concept, the resulting system has improved fuel economics and emits fewer emissions.

In general, hybrid systems are categorised into series, parallel and complex hybrid. In particular, the series hybrid system has similar properties as that of a pure electric system, thus resulting in emission reduction. Furthermore, an additional important advantage of the series configuration is the decoupling between demand and supply. Engines can continuously operate at the most optimal operating point regardless of power requirement, which provides an enormous improvement on fuel efficiency. In addition, due to the high degree of electrification, mechanical linkages are not necessary so that all system components can be positioned at different locations within the UAV, which increases subsystem level flexibility as shown in Figure 2.

However, series HEPSs have two persistent drawbacks: overweight and inevitable energy loss. Normally, this is because of the extra generator, battery and large EM. Increasing the overall aircraft weight will consequently cost more fuel to complete the same mission. This is a challenge that needs solving. The other drawback is the energy conversion loss due to the multiple energy transformations, i.e. kinetic energy to electrical energy, electrical energy to chemical energy. Although the engine can operate at the high-efficiency area, it cannot be guaranteed that the series hybrid systems will have an increased efficiency. Therefore, in order to resolve these challenges, the DP concept and the MEA concept are integrated.

The designed complete DSHEPS is shown in Figures 3 and 4. For easier analysis, we divided the system into three parts: power source, propulsion load and other loads. The 'power source' consists of an engine, a generator, a converter and batteries. All devices provide electricity to the loads or/and

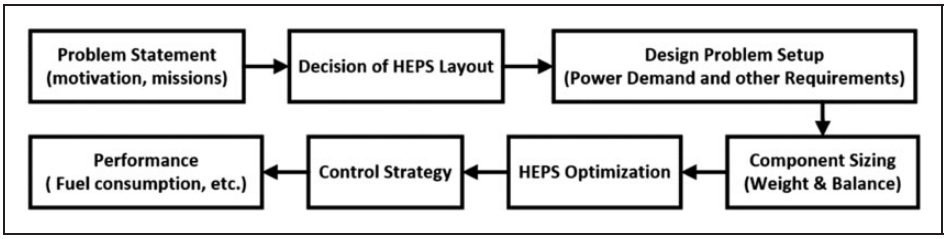

Figure 1. System design sequence.
HEPS: hybrid-electric propulsion system.

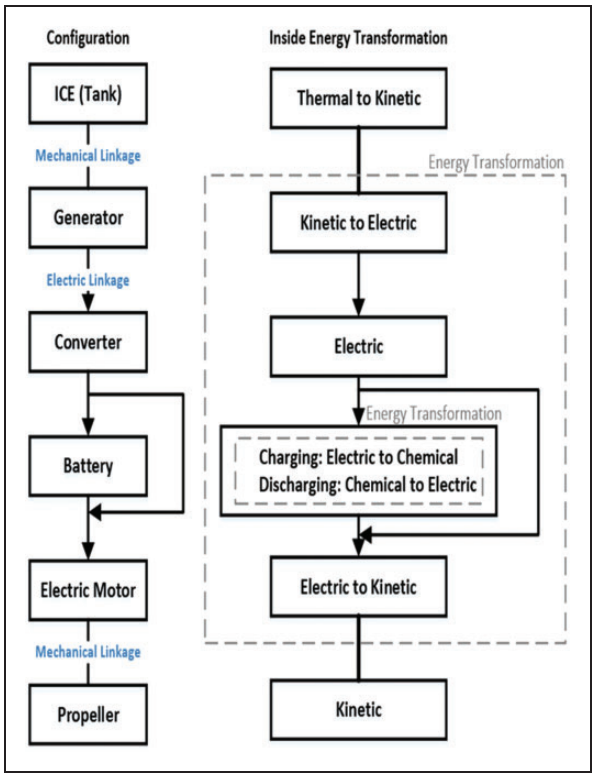

Figure 2. Series propulsion system configuration and internal energy transformation.

stores electricity in the batteries. The second part 'propulsion load' includes converters, motors and propellers. Motors are arranged symmetrically and connected to a corresponding propeller. Here, converters are not necessary if the rated voltage of motors are the same as it of the main electric net (in this paper, the simulation neglects converters). The 'other loads' represents the auxiliary electric loads including an electric taxiing system, avionics systems, etc.

According to the 'propulsion load' block shown in Figure 3, the designed system has six small motors instead of using a single motor. Applying multi-small-electric propulsion has many benefits. Firstly, it provides a robust propulsive control and enhances flight safety when an EM might stop operating safely. Moreover, as engines are normally sized as large as twice the power demand for redundancy reasons. For example, a Boeing 737, 757, 767 and 777 can take off with one of two engines out. The DP architecture reduces the excess weight from the extra engine since one extra small motor provides equal flight safety as one extra big engine in conventional aircraft. Additionally, DP concept increases the dynamic pressure over the wing and reduces aerodynamic drag,[16–19] so that it can reduce the wing area, lighten the aircraft structure and reduce power demand.

Similarly, inspired by the MEA concept,[20–22] some improvements are made into the system. The most important improvement is the expanded electric network. Here, the engine not only provides propulsion power but also transports electric energy to all existing electric loads (flight control actuation, fuel pumping, etc.). This integration removes unnecessary electronic equipment, reduces system weight, eases the maintenance and improves system efficiency. The second improvement is the adoption of the electric taxiing concept. The electric taxiing system is more efficient and safe. Also, the engine can be turned off earlier, which can reduce engine's operating time and reduce fuel consumption.

SOC-based criteria for aircraft engine sizing

As the system isolates the engine from the demand, the engine sizing becomes less challenging. To reassure safety, there are three requirements in this paper:

1. The engine can continuously generate power on a low fuel consumption rate.
2. Batteries can fill the gap between total power requirement and engine output.
3. Motors can provide enough torque and speed to propellers.

The properties of the example UAV are shown in Table 1.[23] Based on this information, the power demand for cruising could be determined by the following equations. The aerodynamic drag D is depended on the drag coefficient C_D, the surface area over the air flows A, the density of the air ρ and the square of the velocity v^2. Because the cruising altitude is approximately 1000 m, the required power for cruising is about $P = 17\,\text{kW}$. Assuming the motor efficiency is 98% and the batteries efficiency is 99%,

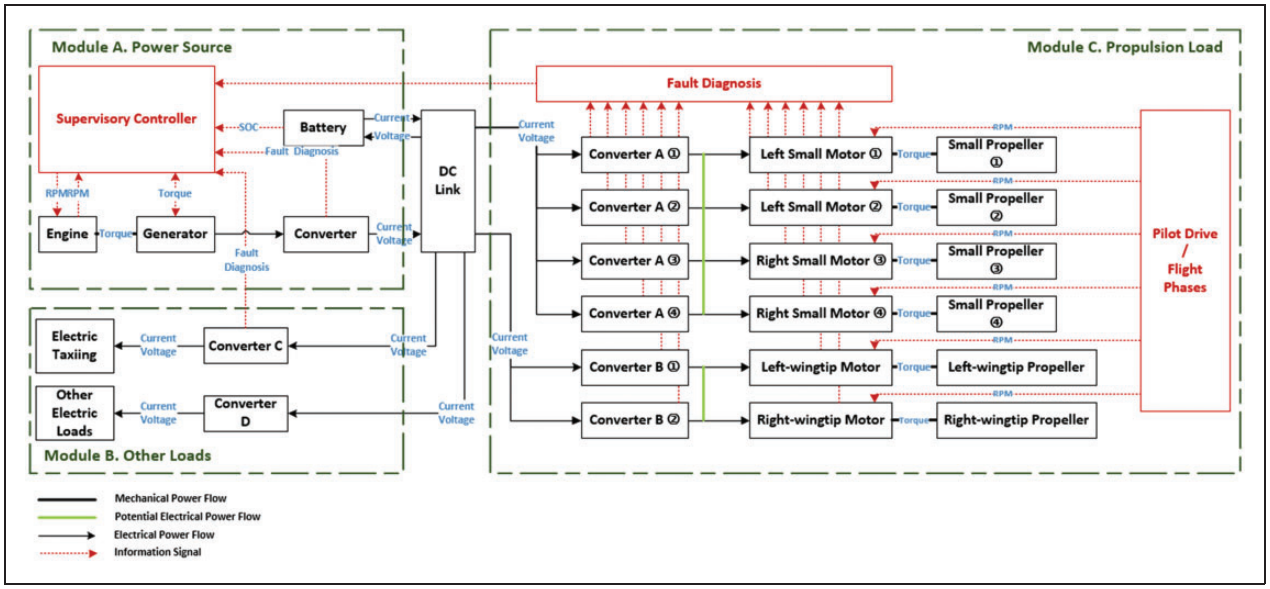

Figure 3. The complete distributed series hybrid electric propulsion system.

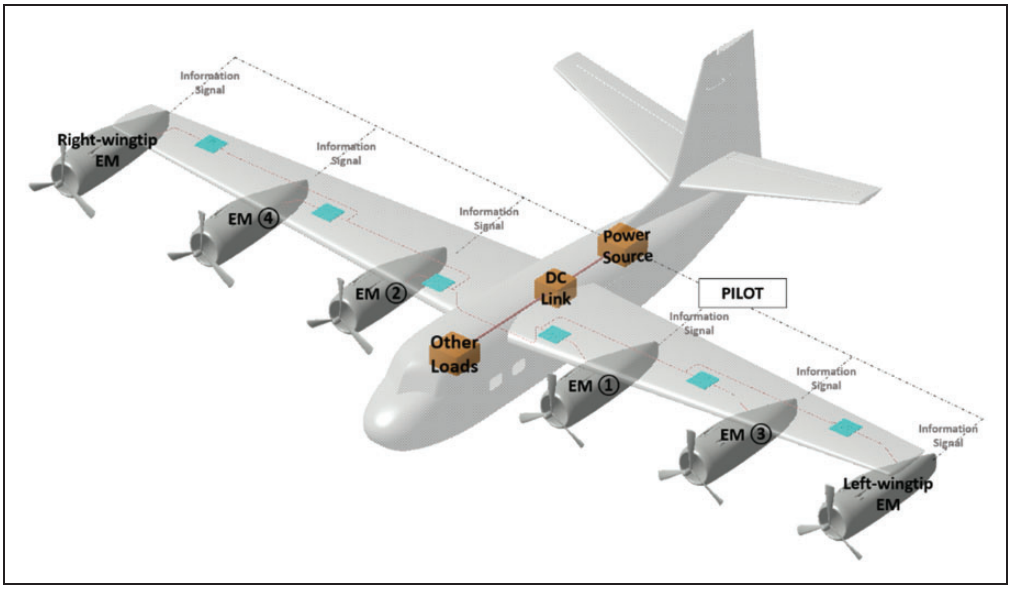

Figure 4. The complete distributed series hybrid propulsion system layout.

the required power for engine P_{req} could be determined

$$D = \frac{1}{2} C_D A \rho v^2 \quad \text{(N)} \tag{1}$$

$$P = Dv = \frac{1}{2} C_D A \rho v^3 \quad \text{(N)} \tag{2}$$

$$P_{req} = \frac{17\,\text{kW}}{98\% * 98\% * 99\%} \approx 18\,\text{kW} \tag{3}$$

Therefore, the flight scenario and the engine power requirement are both determined, as shown in Figure 5. Please note that the assumption of a constant thrust level leads to slight inaccuracies in the determination of the required energy.

Table 1. Example UAV parameters.

Drag coefficient, C_D	0.067	Wing area, A	3.76 m^2
Lift coefficient, C_L	0.614	Air density, ρ	1.1 kg/m^3
Indicated airspeed, v	50 m/s	Lift to drag ratio	9.16
Maximum take-off mass, m	150 kg	Cruising altitude	1000 m

To find an appropriate engine and observe the parametric variation, several engines have been simulated. These engines are selected based on a hybridisation

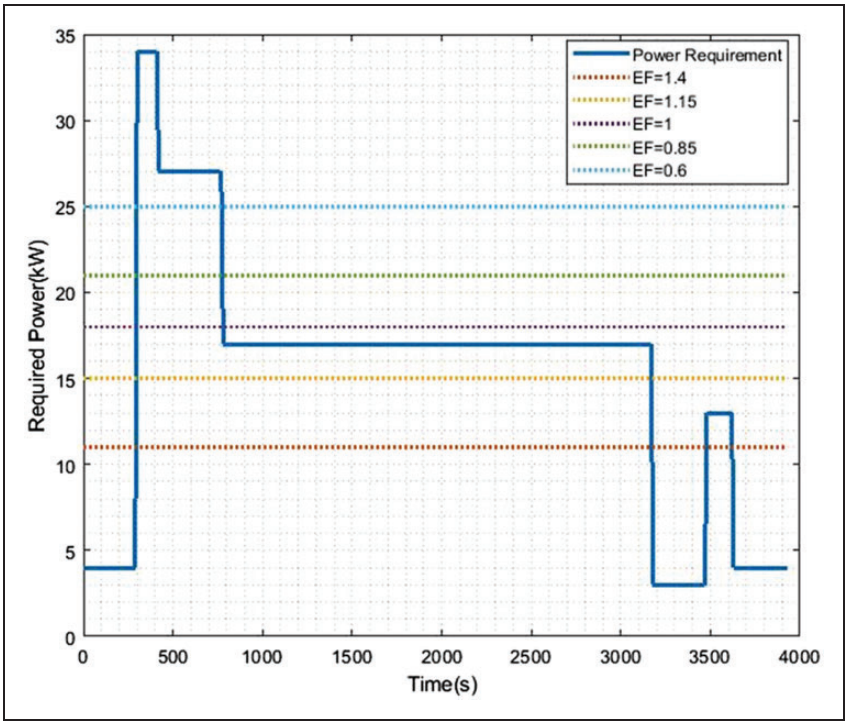

Figure 5. The power requirement of flight scenario and the ideal power of each engine.

Table 2. Specifications of engines, motors and batteries.

Engine type	Max continuous power	Lowest fuel-rate power	HF_{opt}	EF
RT300LCR	20 kW at 6500 r/min	11 kW at 5000 r/min	0.89	0.60
RT300XE	21 kW at 6500 r/min	15 kW at 5250 r/min	0.85	0.85
RT600JET-A1	38 kW at 6500 r/min	19 kW at 4500 r/min	0.81	1.00
RT600LCR	40 kW at 6500 r/min	21 kW at 4750 r/min	0.79	1.15
RT600XE	52 kW at 6500 r/min	25 kW at 4750 r/min	0.75	1.40
Motor type	Max continuous power	Max power	Efficiencies	
EMRAX228	42 kW	100 kW	96%	
Batteries	Capacity	Nominal voltage	Efficiencies	
Li-Po batteries	13 Ah	296 V	98%	

factor. The hybridisation factor is a parameter mirroring the relationship between the sizes of the different power sources.[24] The first hybridisation factor HF was introduced by Lukic and Emadi[25]

$$HF = \frac{(P_{EM\_max} - P_{E\_max})}{P_{EM\_max}} \tag{4}$$

P_{EM_max} and P_{E_max} are the maximum power of motor and engine. The original hybridisation factor HF shows the importance of the engine or the motor as part of the whole system. However, since the engine is always operating at its most efficient point, HF is difficult to clearly describe the proportion of electric energy and kinetic energy. Therefore, two other factors HF_{opt} and EF are developed in this paper, as shown in equations (5) and (6). P_{E_opt} is the engine output power at the most efficient area, and P_{req_av} is the average power of the mission requirement. Engines are selected from $0.6EF$ to $1.4EF$, and the detailed information is represented in Table 2.

$$HF_{opt} = \frac{(P_{EM\_max} - P_{E\_opt})}{P_{EM\_max}} \tag{5}$$

$$EF = \frac{P_{E\_opt}}{P_{req\_av}} \tag{6}$$

Simulation results and discussion

A key part of the design process is to explore the parametric variations prior to building a prototype

UAV, thus reducing the design and development costs. Therefore, three simulations are processed for each selected engine with different initial SOC: $SOC_A(t=0)=50\%$, $SOC_B(t=0)=75\%$ and $SOC_C(t=0)=100\%$. Engines have three fundamental operating modes: (a) the electric mode, (b) the ideal mode and (c) the maximum power mode. Mode conversions are triggered by the SOC. In this paper, the high threshold is set as 80% and the low threshold is set at 20%. Namely, when the SOC is beyond 80%, the system will switch into the electric mode, while if the SOC is below 20%, the system will switch into the maximum power mode. Moreover, this system incorporates a gap, which results in obtaining an extra 10% SOC during the charging process. If batteries were in the charging mode, the system will be switched back to the ideal mode at 90% SOC instead of 80%. This setting has dual purposes, which not only guarantees the power output, but also protects batteries.

Figure 6 shows the SOC curve of each simulation. When simulations start with a full SOC_c, all simulations began from the electrical mode. Gradually, when the SOC drops below 80%, the differences of various engines began to show up by the altered discharging rate. Amongst them, RT600XE is the most powerful engine and firstly recharged back to 80% SOC. Since its ideal power output is about 1.4 times of the average power demand, the SOC stays in 80%–90% area for most of the flight. RT600LCR engine recovers to 80% SOC as well but at a slower rate than RT600XE. RT600JET outputs just the right power as demanded at its ideal operating point. The SOC stays stable during the cruise mode. RT300XE and RT300LCR cannot provide enough power even for the average power demand for the specific UAV parameters. Their SOC dropped below 20% and jumped to maximum power mode. The fuel consumption rate during the maximum power mode is not as good as the ideal mode, but they are powerful to generate electricity and guaranteed that batteries are not fully depleted.

With an initial 75% SOC_B and 50% SOC_A, small engines can easily drop below 20% and trigger the maximum power operating mode. The SOC for RT300LCR was nearly 0 in its third simulation, which shows that although it was in maximum power mode, it cannot stop SOC decrease during a

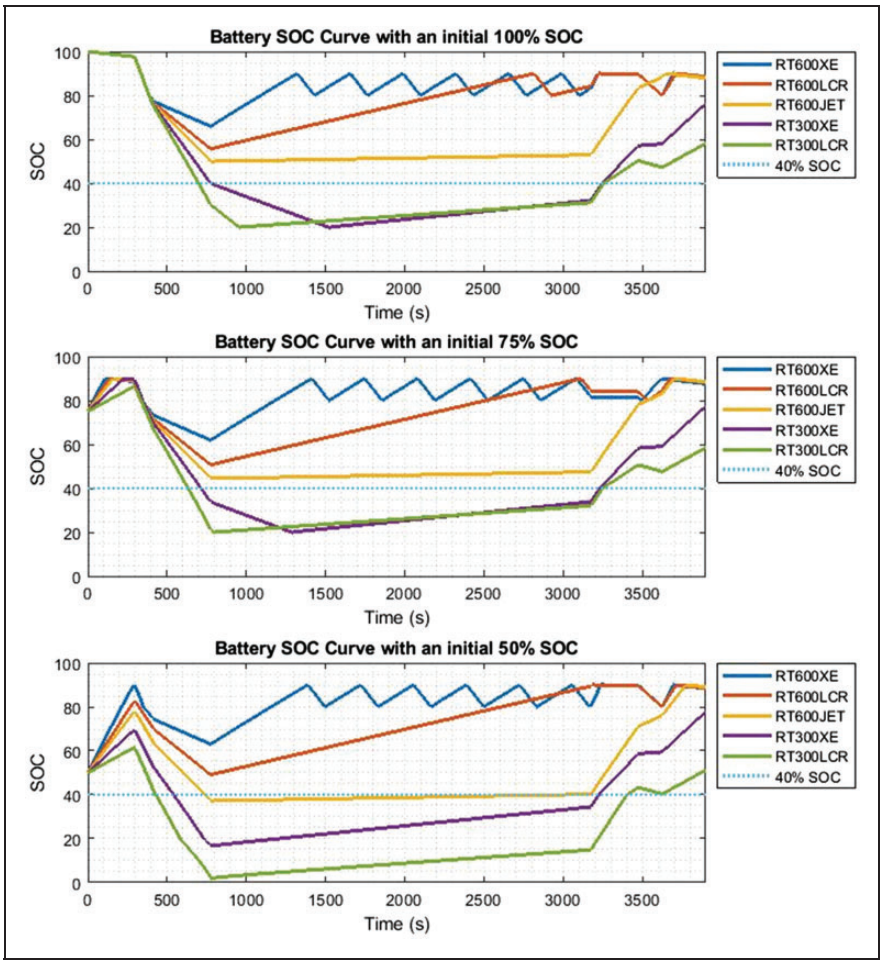

Figure 6. Batteries SOC curves.
SOC: state-of-charge.

high-powerful requirement. In addition, it can be seen that RT600JET, RT600LCR and RT600XE have three similar SOC curve. For these three engines, no matter how much is the initial SOC, batteries have a similar performance. An alternative hybridisation factor $HF_{realtime}$ is introduced to estimate the ratio of power which comes which relates to batteries power P_B and motor output P_{EM}.

$$HF_{realtime} = 1 - \frac{P_B}{P_{EM}} \tag{7}$$

While the system is running, the $HF_{realtime}$ is calculated to show the 'degree of electrification' and the importance of electricity by second. These results are summarised in Figure 7 and Table 3.

From these results, it can be seen that RT 600JET is operating at ideal conditions and its final SOC is the same as RT600LCR and RT600XE. RT600JET avoids the frequent mode conversions and can achieve a high SOC at the end of the mission. Therefore, if the vehicle is not specially designed for an electric mode, it is not necessary to have a big engine.

Figure 8 illustrates the length of time remaining under 40% SOC during each simulation. From this figure, it can be observed that SOC of RT600XE and RT600LCR have not been to a value under 40%. The SOC of RT600JET was once under 40% SOC when $SOC_A(t = 0) = 50\%$. But from Figure 6, it can be determined that the SOC is around 40% and the lowest SOC value is about 38%. It has not dropped to the low boundary of 20% SOC. For the other two small engines, although the initial SOC is different,

Table 3. Simulation results.

	50% SOC_A ($t = 0$)	75% SOC_B ($t = 0$)	100% SOC_C ($t = 0$)
RT600XE			
Electric mode	1305 s	1462 s	1648 s
Ideal mode	2595 s	2438 s	2252 s
Max power mode	0	0	0
Average $HF_{realtime}$	73%	77%	69%
RT600LCR			
Electric mode	631 s	851 s	1081 s
Ideal mode	3269 s	3049 s	2819 s
Max power mode	0	0	0
Average $HF_{realtime}$	85%	84%	77%
RT600JET			
Electric mode	124 s	382 s	642 s
Ideal mode	3776 s	3518 s	3258 s
Max power mode	0	0	0
Average $HF_{realtime}$	85%	84%	80%
RT300XE			
Electric mode	0	116 s	386 s
Ideal mode	1407 s	1840 s	1789 s
Max power mode	2493 s	1944 s	1725 s
Average $HF_{realtime}$	84%	80%	77%
RT300LCR			
Electric mode	0	0	386 s
Ideal mode	1078 s	1449 s	1215 s
Max power mode	2822 s	2451 s	2299 s
Average $HF_{realtime}$	80%	77%	73%

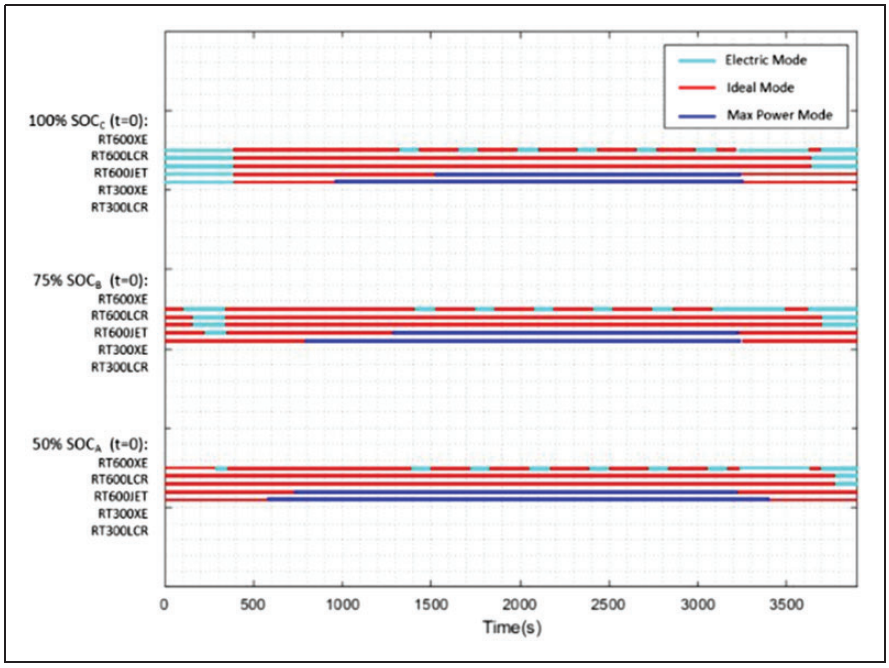

Figure 7. Operating modes during flight scenario.

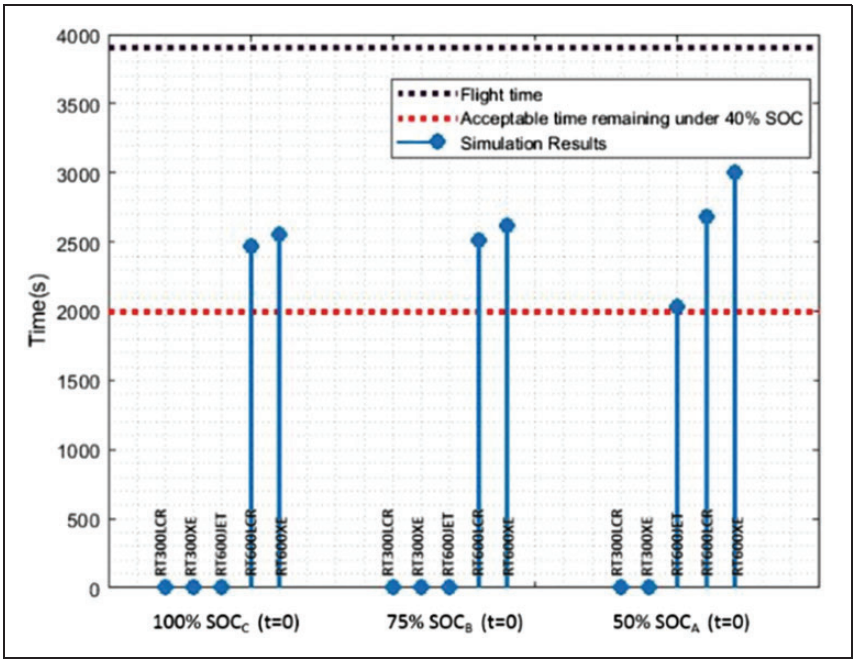

Figure 8. The length of time remaining under 40% SOC.
SOC: state-of-charge.

the length of time remaining under 40% SOC is similar. Because SOC_B and SOC_C tests have a charging procession at the beginning of the flight, they performed similarly. However, due to the difference of the result of SOC_A and SOC_B being small, it can be deduced that the initial SOC has lesser influence for a system operating, and the engine size indeed influences the system performance. The HEPS requires an engine, which can provide equal amount of energy of the average value of power demand at its lowest fuel consumption rate point.

Conclusions

The UAV simulations were repeated for three cases: SOC_A, SOC_B, SOC_C with initial battery pack state-of-charge $SOC_A(t=0) = 50\%$, $SOC_B(t=0) = 75\%$ and $SOC_C(t=0) = 100\%$ respectively for the defined UAV mission flying scenario. For each one of the three SOC five combustion power sizes (RT600XE, RT600LCR, RT600JET, RT300LCR, RT300XE) were simulated to explore if the SOC will enter the range of less than 40%, which is considered as the acceptance criterion.

From all the results presented, the five different power pack options performed well; however, two did not meet the minimum SOC criterion: LT300LCR and RT300XE. Clearly, using the proposed approach the design team can select for different flight scenarios and range of engine packs (five in this case) the best option for a range of initial preflight battery pack SOC. The design sizing approach is effective because it links the combustion engine power pack operation and choice of size with the battery pack and also the power pack initial conditions.

The next step of research is to optimise the entire propulsion system design by using genetic algorithms. Each subsystem would be selected according to the total system weight and the estimated fuel consumption. Furthermore, a trade-off study of fuel efficiency and emissions will be conducted, and an intelligent controller with configurability will also be designed.

Declaration of Conflicting Interests

The author(s) declared no potential conflicts of interest with respect to the research, authorship, and/or publication of this article.

Funding

The author(s) received no financial support for the research, authorship, and/or publication of this article.

ORCID iD

S Wang http://orcid.org/0000-0002-3064-4347
JT Economou http://orcid.org/0000-0002-3627-4949
A Tsourdos http://orcid.org/0000-0002-3966-7633

References

1. Koster J, Velazco A and Munz C. Hyperion UAV: an international collaboration. In: *50th AIAA aerospace sciences meeting including the new horizons forum and aerospace exposition, aerospace sciences meetings*, Nashville, TN, USA, January 2012.
2. Glassock R, Hung J and Gonzalez L. Multimodal hybrid powerplant for unmanned aerial systems (UAS) robotics. In: *Twenty-fourth Bristol international unmanned air vehicle systems conference*, Bristol, UK, March 2009.

3. Ausserer J and Harmon F. Integration validation and testing of a hybrid-electric propulsion system for a small remotely piloted aircraft. In: *10th international energy conversion engineering conference*, Atlanta, GA, USA, 2012.
4. Xie Y, Savvaris A and Tsourdos A. Modelling and control of a hybrid electric propulsion system for unmanned aerial vehicles. In: *2018 IEEE aerospace conference*, Big Sky, MT, USA, 2018.
5. Talbert T. *The EcoEagle*. Washington DC: National Aeronautics and Space Administration, 2012.
6. Siemens, Diamond Aircraft and EADS. World's first serial hybrid electric aircraft to fly at Le Bourget, Siemens, Diamond Aircraft and EADS, Munich, 2011.
7. Friedrich C and Robertson PA. Hybrid-electric propulsion for aircraft. *J Aircraft* 2015; 52: 176–189.
8. National Aeronautics and Space Administration. Overview of subsonic fixed wing project: technical challenges for energy efficient, environmentally compatible subsonic transport aircraft. In: *3rd NASA Glenn propulsion control & diagnostics workshop*, Cleveland, OH, USA, 2012.
9. Welstead J and Felder JL. Conceptual design of a single-aisle turboelectric commercial transport with fuselage boundary layer ingestion. In: *54th AIAA aerospace sciences meeting*, AIAA SciTech Forum, California, USA, 2016.
10. Moore MD. Distributed electric propulsion (DEP) aircraft. Washington DC: National Aeronautics and Space Administration, 2014.
11. Bradley MK and Droney CK. *Subsonic Ultra Green Aircraft Research Phase II: N+4 advanced concept development*. Washington DC: National Aeronautics and Space Administration, 2012.
12. Siemens, Airbus and Rolls-Royce. Airbus, Rolls-Royce, and Siemens team up for electric future, London, 2017.
13. Yang H, Lu L and Zhou W. A novel optimization sizing model for hybrid solar-wind power generation system. *Solar Energy* 2007; 81: 76–84.
14. Seeling-Hochmuth GC. A combined optimisation concept for the design and operation strategy of hybrid-PV energy system. *Solar Energy* 1997; 61: 77–87.
15. Zou Y, Sun F and Hu X. Combined optimal sizing and control for a hybrid tracked vehicle. *Energies* 2012; 5: 4697–4710.
16. Deere KA, Viken JK and Viken S. Computational analysis of a wing designed for the X-57 distributed electric propulsion aircraft. In: *35th AIAA applied aerodynamics conference*, AIAA Aviation Forum, 2017. Reston, VA: AIAA.
17. Stoll AM, Bevirt J and Moore MD. Drag reduction through distributed electric propulsion. In: *14th AIAA aviation technology, integration, and operations conference*, AIAA Aviation Forum, 2014. Reston, VA: AIAA.
18. Papathakis KV. NASA Armstrong Flight Research Center Distributed Electric Propulsion Portfolio, Safety and Certification Considerations, 2017.
19. Brelje BJ and Martins JRRA. Development of a conceptual design model for aircraft electric propulsion with efficient gradients. In: *2018 AIAA/IEEE electric aircraft technologies symposium (EATS)*, Cincinnati, OH, USA, 2018.
20. Wheeler PW, Clare JC, Trentin A, et al. An overview of the more electrical aircraft. *Proc IMechE, Part G: J Aerospace Engineering* 2013; 227: 578–585.
21. Naayagi RT. A review of more electric aircraft technology. In: *2013 international conference on energy efficient technologies for sustainability*, Nagercoil, India, 2013.
22. Hafez AAA and Forsyth A. A review of more-electric aircraft. In: *13th international conference on aerospace sciences and aviation technology*, ASAT-13, Cairo, Egypt, 2009.
23. Dunne A. *Aerodynamic analysis and optimization of the Aegis UAV*. MSc Thesis, UK, 2012.
24. Friedrich C and Robertson PA. Design of hybrid-electric propulsion systems for light aircraft. In: *14th AIAA aviation technology, integration, and operations conference*, AIAA Aviation Forum, 2004. Reston, VA: AIAA.
25. Lukic SM and Emadi A. Effects of drivetrain hybridization on fuel economy and dynamic performance of parallel hybrid electric vehicles. *IEEE Trans Veh Technol* 2004; 53: 385–389.

Appendix

Notation

A	wing area (m^2)
C_D	drag coefficient
C_L	lift coefficient
D	aerodynamic drag (N)
EF	engine factor
HF	hybridisation factor
HF_{opt}	HF using P_{E_opt}
$HF_{realtime}$	real-time hybridisation factor
m	maximum take-off weight (kg)
P	power (W)
P_{req}	required power (W)
P_{EM_max}	maximum power of the motor (W)
P_{E_max}	maximum power of the engine (W)
P_{E_opt}	engine power at its most efficient point (W)
P_{req_av}	average value of power requirement (W)
P_B	battery output power (W)
P_{EM}	motor output power (W)
SOC	state of charge
v	aircraft airspeed (m/s)
ρ	air density (kg/m^3)